The University Of Sheffield.

Investigating the role of a dynamin-actin interaction

By:

Sarah Elizabeth Palmer

A thesis submitted in partial fulfilment of the requirements for the degree of Doctor of Philosophy

The University of Sheffield
Faculty of Science
Department of Biomedical Science

November-2015

Abstract

Endocytosis is a fundamental cellular process which facilitates the uptake of lipids and proteins from the plasma membrane. During endocytosis, the plasma membrane is internalised through the formation of an invagination, which is then pinched off to form a vesicle. Endocytosed vesicles are then able to fuse with endosomal compartments allowing cargo to be sorted within the endo-lysosomal system. One of the most well characterised forms of endocytosis is clathrin mediated, which takes place in distinct stages. These include coat and clathrin recruitment, membrane invagination and finally scission which releases the vesicle into the cytoplasm. Cells require many different molecules to orchestrate each stage including the GTPase dynamin and cytoskeletal protein actin. Dynamin facilitates the scission stage of endocytosis where it oligomerises around the vesicle neck and, through the hydrolysis of GTP, enables scission. Furthermore dynamin-1 has been reported to bind directly to actin. In *Saccharomyces cerevisiae* (yeast) actin is essential to endocytic invagination in order to overcome turgor pressure. Yeast contain a dynamin-like protein Vps1 which acts during endocytic scission and has orthology with dynamin-1. In this thesis the direct interaction between Vps1 and actin was explored to elucidate how this interaction may be required during endocytosis. It is understood that both dynamin and actin are involved in other cellular processes and therefore the knowledge gained from investigating this interaction during endocytosis may well provide new insight into how these two molecules work together in other molecular systems. Thus, mutations found to perturb the Vps1-actin interaction were created in human dynamin-1 and preliminary results suggest this could have an effect on mammalian cell endocytosis and cell migration.

This project has identified a novel Vps1-actin interaction which is required for the scission stage of yeast endocytosis. It also describes a point mutation in Vps1 E461K, which has been found to cause an early stage endocytic defect.

Acknowledgements

I would like to take this opportunity to thank everyone who has helped me complete this thesis whether it be through your teaching, advice or support. Every single one of you have aided my progression through the great times, and the not so great times, to make this a very memorable and enjoyable few years.

Firstly I would like to extend my immense thanks to Kathryn Ayscough who has supervised this project, taught and guided my ideas. She has always had time for me, even during the busiest of weeks and I am very grateful for her support. I would like to thank Steve Winder who has also supervised this project, taught me cell culture techniques and put up with me randomly turning up in his office to ask him questions out of the blue.

My advisors Andy Furley and Liz Smythe have also been invaluable to my experience at this university. Not only for helping with my PhD progression but also with advice for my future career. They have taken the time to encourage and support my future plans and have been instrumental to my development throughout this degree.

I would like to thank everyone in the Ayscough/Winder labs for making my time at Sheffield enjoyable both in and out of the lab. Specifically, I would like to thank Ellen Allwood and Iwona Smaczynska-de Rooij for teaching me so many different techniques, to Ellen for being there to troubleshoot experiments (amongst other things!) and to Iwona for all your help with the publications. I would also like to especially thank Chris Marklew and Laura Jacobs for keeping me going and discussing ideas, Joe Tyler, Kate Collins-Taylor and Daniel Leocadio Victoria for many chats and lots of fun. To Aga Urbanek for your excellent attitude and never putting up with any rubbish! And to Lemya Abugharsa, Laila Moushtaq, Emma Hoffman, Tracy Emmerson and Katja Vogt-who is continuing this project- I will miss you all. Thanks is also due to Rob Piggott who guided me through my nervous first year and introduced me to PhD life. Since leaving the lab Rob has taken the time to proof read my thesis and provide excellent feedback and for that I am very grateful.

Thanks to the ‘Unkillable Clerics’ Wezz Booth, Dave Pickthall, Ryan O’Conner, Diz Carberry and Ash Tuck for introducing me to post-rock music and getting me back in to ‘cello playing. Thanks also to Dom Kolarova and Craig Fishwick for all those hikes in the peaks and trips to the pub which provided me with many well needed breaks from work.

Finally I would like to thank my family, Mum, Dad, Helen, Steph and my Grandad Arthur for putting up with me disappearing for four years to complete this project. You have always believed I could do it even when I didn’t, thanks for always being there. Similarly I would like to thank Sid Dongre. You have given me the confidence to complete this thesis and your continual support means the world to me.

Contents

List of figures

List of Abbreviations

Abp1	Actin Binding Protein 1
ADP	Adenosine DiPhosphate
ANTH	AP180-N Terminal Homology domain
AP	Adapter Protein
ATP	Adenosine TriPhosphate
BAR	Bin–Amphiphysin–Rvs domain
BSE	Bundle Signalling Element
CD	Circular Dichroism
CIE	Clathrin Independent Endocytosis
CME	Clathrin Mediated Endocytosis
CPY	CarboxyPeptidase Y protein
Dlp	Dynamin-like protein
DNA	DeoxyriboNucleic Acid
E.coli	*Escherichia coli*
ECM	ExtraCellular Matrix
EDTA	EthyleneDiamineTetraacetic Acid
EGFR	Epidermal Growth Factor Receptor
EGTA	Ethylene Glycol Tetraacetic Acid
EM	Electron Microscopy
ENTH	Epsin-N Terminal Homology domain
F- BAR	FCH Bin-Amphiphysin-Rvs
FACS	Fluorescence-Activated Cell Sorting
F-Actin	Filamentous Actin
FBP17	Formin Binding Protein (17)
FBS	Fetal Bovine Serum
FEME	Fast Endophilin Mediated Endocytosis
FLIM	Fluorescence Lifetime Imaging Microscopy
G-Actin	Globular Actin
GAK	G-Associated protein Kinase
GAPDH	Glyceraldehyde 3-phosphate dehydrogenase

GED	GTPase Effector Domain
GST	Glutathione Sepharose Transferase
GTP	Guanosine TriPhosphate
HEPES	4-(2-HydroxyEthyl)-1-PiperazineEthaneSulfonic acid
Hsc70	Heat shock cognate protein 70
IRSp53	Insulin Receptor tyrosine kinase Substrate protein of 53 kDal
KME	Potassium Magnesium EDTA
mAbp1	mammalian Actin binding protein 1
mCPY	mature CarboxyPeptidase Y protein
MxA/B	Myxovirus resistance proteins A/B
OD	Optical Density
Pa	Pascals
PBS	Phosphate-Buffered Saline
pCPY	precursor CarboxyPeptidase Y protein
PDBu	Phorbol 12,13-DiButyrate
PH	Pleckstrin Homology
PIP2	Phosphatidylinositol 4,5 phosphate / PtdIns(4,5)P2
PRD	Proline Rich Domain
RNA	RiboNucleic Acid
RT	Room Temperature
SD	Standard Deviation
SDM	Site Directed Mutagenesis
SDS-PAGE	Sodium Dodecyl Sulphate Polyacrylamide Gel Electrophoresis
SEM	Standard Error of the Mean
SH3	Src Homology 3 domain
Sla1/2	Synthetically lethal with Abp1 1/2
TIRF	Total Internal Reflection Fluorescence microscopy
Vps1	Vacuolar protein sorting 1
WASP	Wiskott–Aldrich Syndrome Protein
WCL	Whole Cell Lysate
WT	Wild type

Chapter 1

Introduction

By maintaining the integrity of different cellular compartments, a cell is able to carry out distinct and varied chemical reactions whilst maintaining cell homeostasis. This enables cells to respond to extracellular signalling cues, to process molecules for energy production and compartmentalise gene expression, all of which define life for eukaryotic organisms.

Membrane traffic refers to the organised movement of molecules in membrane bound vesicles as they bud away from one membrane and fuse onto another, a complex, regulated process which maintains the integrity of each respective compartment or organelle. This extensive membrane exchange happens continually within cells with different molecular markers and lipids distinguishing each compartments identity. Extracellular molecules can be taken up at the plasma membrane and encased into vesicles in a process called endocytosis (figure 1A). Once encased at the plasma membrane, cargo can then be trafficked to different compartments. This includes movement to endosomes, and then to the lysosome for degradation (figure 1B), to the Golgi network (figure 1C), or into recycling endosomes (figure 1D), which return back to the plasma membrane by exocytosis (reviewed in Scott et al. 2014).

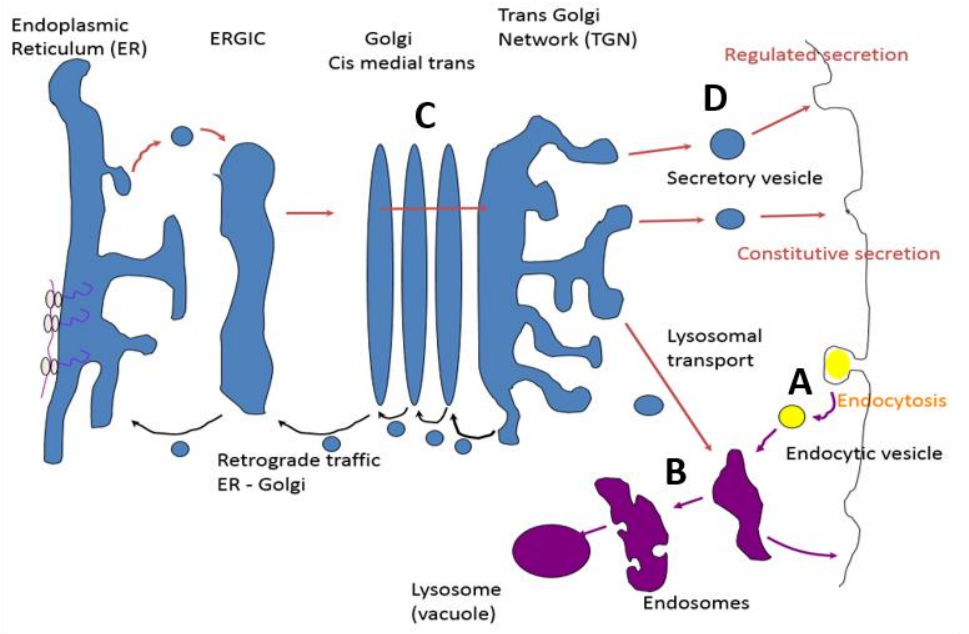

Figure 1. Membrane trafficking pathways within cells. A) Endocytosis, molecules are taken from the plasma membrane and distributed for degradation or recycling. B) Vesicles are trafficked to the late endosomes to be delivered to the lysosome/vacuole for degradation. C) ER-Golgi traffic where vesicles are moved through ER to Golgi or from the Golgi back to ER (retrograde traffic). D) Vesicle cargo can be secreted from recycling endosomes to the plasma membrane via exocytosis.

Within this system, the integrity of the plasma membrane and its associated proteins is essential for cell survival. Endocytosis is imperative to this process, as it facilitates the regulation of cell signalling, the uptake of nutrients and the uptake and degradation of pathogens.

1.1 Endocytosis

Endocytosis describes the uptake of molecules into a cell by means of plasma membrane invagination and vesicle release from the cell surface. Examples of molecules taken up by endocytosis include hormones, nutrients and receptors. The uptake of these molecules can occur in many different ways which can be both constitutive and regulated, depending on the cargo and processes involved. Some of the different endocytic processes understood to take place in mammalian cells and *Saccharomyces cerevisiae* (subsequently referred to as yeast), are shown in figure 2 and described in table 1. The most well characterised form of endocytosis is clathrin mediated which has been extensively researched in both yeast and mammalian cells (Mukherjee et al. 1997; Freeman & Grinstein 2014; Robinson 2015).

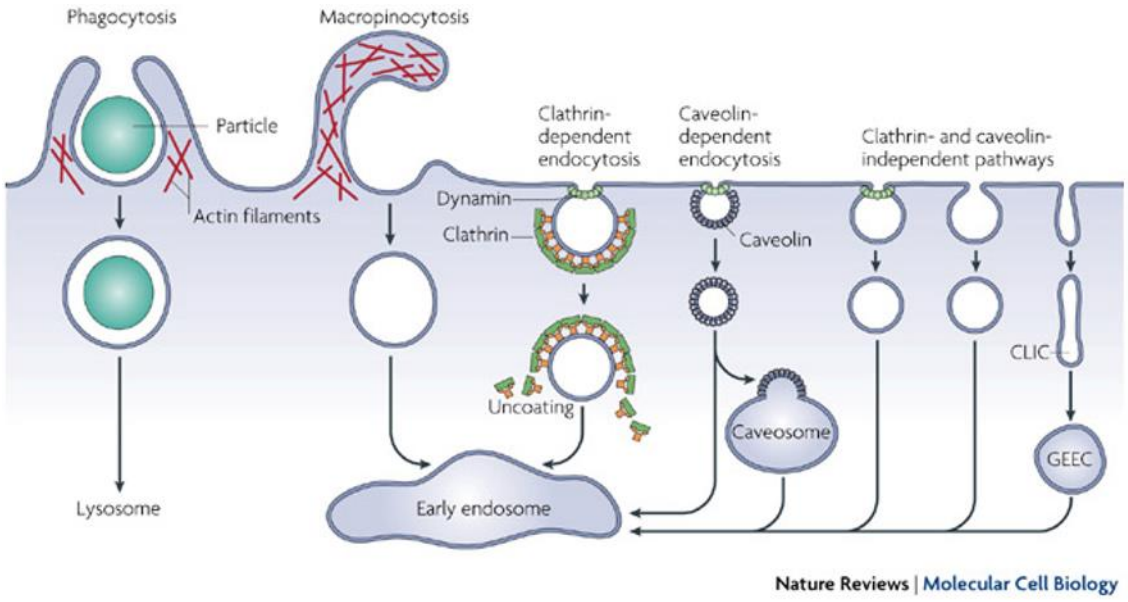

Figure 2. Pathways of endocytosis in cells This figure reproduced from Mayor et al., 2007 with permission from Nature Publishing Group, and describes diagrammatically different endocytic pathways in cells with a simplified indication of the subsequent traffic of vesicles after release from the plasma membrane. A description of these pathways can be found in Table 1. The clathrin and caveolin independent pathways for the purposes of this thesis include FEME, Ultrafast endocytosis, Rho dependent endocytosis and CIE pathways. CLIC stands for clathrin and dynamin independent carriers and GEEC indicates glycosyl phosphatidylinositol-anchored protein enriched early endosomal compartments. These indicate compartments, similar to the caveosome, to which some endocytosed vesicles traffic to first before the early endosome.

Table 1. Pathways of endocytosis

	DESCRIPTION	REFERENCES
CLATHRIN MEDIATED ENDOCYTOSIS (CME)	Clathrin dependent 'canonical' endocytic pathway that functions in eukaryotic cells.	(Kirchhausen et al. 2014; Merrifield & Kaksonen 2014; Boettner et al. 2012; Weinberg & Drubin 2012)
CLATHRIN INDEPENDENT ENDOCYTOSIS (CIE)	This describes a number of different clathrin independent endocytic uptake pathways. Uptake into vesicles by CIE can be both stimulated and constitutive and is regulated by molecules such as the GTPase Arf6 and Src kinase.	(Donaldson et al. 2009; Eyster et al. 2009; Mayor & Pagano 2007)
FAST ENDOPHILIN MEDIATED ENDOCYTOSIS (FEME)	CIE which requires the F-BAR protein endophilin, actin and dynamin.	(Renard et al. 2014; Boucrot et al. 2014)
ENDOCYTOSIS OF LIPID RAFT/CAVEOLAE	Lipid rafts and caveolae can form invaginations in the cell surface. Caveolae are formed by the protein caveolin, and can be stimulated to undergo endocytosis when stimulated by factors, such as the Simian Virus 40 (SV40).	(Parton & Simons 2007; Pelkmans et al. 2001)
PHAGOCYTOSIS	The uptake of large particles and bacteria by immune cells (such as macrophages). This process forms actin rich protrusions which encapsulate the particle to be taken into the cell.	(Freeman & Grinstein 2014; Aderem & Underhill 1999)
MACROPINOCYTOSIS	A process in which fluid is taken up into a cell. This process relies on actin ruffles which then form invaginations of fluid from outside the cell. This can be constitutive in some cells like macrophages for example.	(Lim & Gleeson 2011)
ULTRAFAST ENDOCYTOSIS	CIE in neuronal cells which occurs in fractions of a second to recycle receptors. Requires both dynamin and actin to take place.	(Watanabe et al. 2013)
ACTIN BINDING PROTEIN 1 DEPENDENT ENDOCYTOSIS	In yeast an Abp1 dependent endocytic pathway has been described which can function when CME is blocked.	(Aghamohammadzadeh et al. 2014)
RHO DEPENDENT ENDOCYTOSIS	A CIE process which in yeast requires Rho1 and formin Bni1. There is a similar pathway in mammalian cells which requires RhoA and dynamin-1 function.	(Prosser et al. 2011; Lamaze et al. 2001)

1.1.1 Clathrin mediated endocytosis

Through clathrin mediated endocytosis (CME) molecules and receptors are taken up from the cell surface in clathrin coated vesicles. CME is particularly important for the recycling of receptors after synapse firing in the brain (reviewed in Saheki & De Camilli 2012) and this process happens to such a high extent in neuronal cells that clathrin coated vesicles are most easily purified from brain tissue (Kadota & Kadota 1973).

The discovery of clathrin began in 1964 when vesicles, covered in a cage like coat, were observed by way of electron microscopy (EM) (Roth & Porter 1964). Upon isolation of these vesicles clathrin was identified and purified (Pearse 1976). Subsequent studies revealed that clathrin molecules form a triskelion, made from three clathrin heavy chains bound to clathrin light chains, which were able to make a net or cage around a vesicle (reviewed in Kirchhausen 2000; Kirchhausen et al. 2014). The most well characterised function of clathrin is during CME, however clathrin also functions in other intracellular trafficking events for example during endosome to Golgi trafficking (Saint-Pol et al. 2004) and other types of endocytosis such as during the phagocytosis of different types of bacteria (Veiga et al. 2007). In yeast, clathrin has been described to be recruited to flat membranes which then undergo actin dependent invagination (Kukulski et al. 2012) indicating that its recruitment happens in the early on in the endocytic process. This has been supported by a recent publication which combined fluorescence and EM in human melanoma cells (SK-MEL-2), showing clathrin coated pits being created from flat clathrin lattices (Avinoam et al. 2015).

The initiation of an endocytic pit requires the assembly of Adaptor Proteins (AP's) which link the clathrin coat to the endocytic patch (Pearse & Bretscher 1981). There are 5 AP's that have been discovered, AP1, 2, 3, 4 and 5. Each AP protein has four subunits which are involved in membrane trafficking events (reviewed in Robinson 2004; Hirst et al. 2013). AP2 is the most abundant adaptor protein and is involved in cargo binding in CME and for that reason it has been extensively researched. To begin its role during CME, AP2 first binds PtdIns(4,5)P_2 (PIP2) which causes a conformational change to link the AP2 complex to cargo at the membrane (Jackson et al. 2010). The binding of AP2 to PIP2 and cargo, stimulates its binding to clathrin (Rapoport et al. 1997) which initiates the assembly of clathrin triskelions and a clathrin coated pit.

1.1.2 Yeast clathrin mediated endocytosis

Our current understanding of yeast CME has arisen from decades of research using yeast genetic screens, fluorescently marking endocytic proteins and live *in vivo* imaging of fluorescently marked patches (reviewed in Weinberg & Drubin 2012). Yeast genetic screens have been invaluable for the identification of proteins that are essential or involved in CME (Raths et al. 1993; Wendland et al. 1996) and more than 60 different proteins have now been identified to play a role in CME, including the important discovery that actin is essential for yeast endocytosis (Munn et al. 1995; Kübler & Riezman 1993). Fluorescence tagging and live cell imaging has provided insight into the stages of yeast endocytosis and a detailed view of the mechanism of CME (Kaksonen et al. 2003; Kaksonen et al. 2005). These findings in turn have been invaluable for understanding the dynamics of mammalian CME which is only recently becoming similarly well defined (Taylor et al. 2011).

During CME there are three defined stages. First there is the non-motile coat assembly phase in which cargo is bound and nucleation of the clathrin coat is established. This is followed by the slow movement phase in which the clathrin pit is invaginated into the cell. Finally there is the fast movement phase during which the vesicle is pinched off by the membrane and is trafficked into the cell (figure 3A,B). There are many proteins found to function in CME and many of these have mammalian orthologues. Some of these are listed in table 2 for reference during the following descriptions of the current understanding of yeast CME.

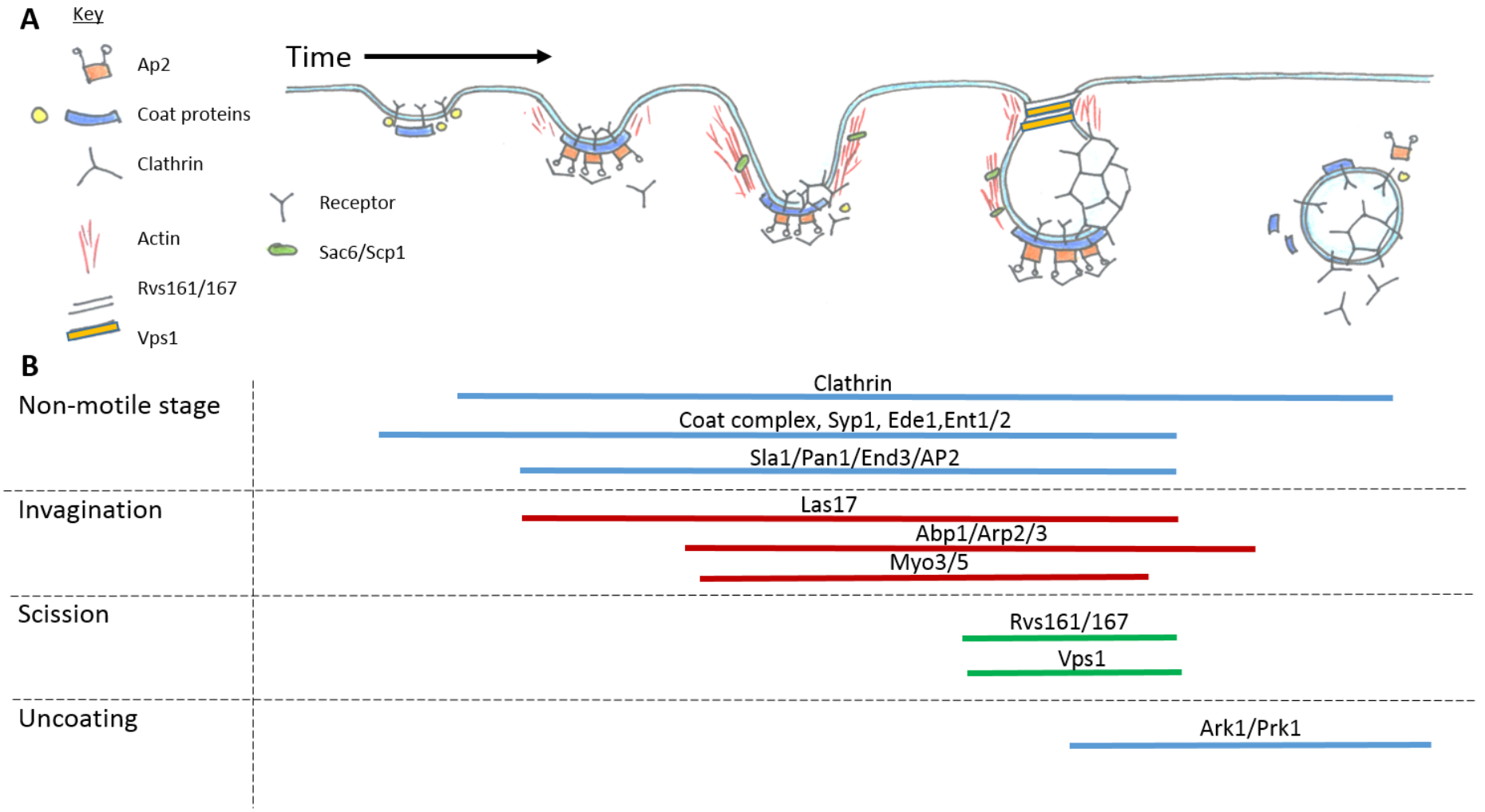

Figure 3. Yeast clathrin mediated endocytosis. A) A diagram of the stages of vesicle endocytosis in yeast over time, with a simplified key of the components required for this process. B) A breakdown of the different stages with the key components described in each section. The bold lines indicate a rough lifetime for these molecules as they accumulate and are disassembled from the endocytosed vesicle over time.

Table 2.[1] **Yeast endocytic proteins and their mammalian orthologues**

	YEAST PROTEINS	MAMMALIAN ORTHOLOGUE	REFERENCES[2]
COAT ASSEMBLY PHASE	Clathrin heavy chain	Clathrin heavy chain	*(Payne & Schekman 1985)* (Newpher & Lemmon 2006)
	Clathrin light chain	Clathrin light chain	*(Siverira et al. 1990)* (Huang et al. 1997)
	Syp1	FCHo1	*(Reider et al. 2009)* (Boettner et al. 2009)
	Ede1	Eps15	*(Gagny et al. 2000)* (Stimpson et al. 2009)
	Ent1/2	Epsin	*(Wendland et al. 1999)*
	Sla2	Hip1R	*(Engqvist-Goldstein et al. 1999)* (Gourlay et al. 2003)
	Sla1	CIN85	*(Stamenova et al. 2004)* (Gourlay et al. 2003)
	Pan1	Eps15	*(Wong et al. 1995)* (Wendland & Emr 1998)
	AP-2	AP-2	*(Barlow et al. 2014)* (Chapa-y-Lazo et al. 2014)
INVAGINATION	Las17	WASP	*(Li 1997)* (Urbanek et al. 2013)
	Arp2/3	Arp2/3	*(Winter et al. 1997)* (Moreau et al. 1997)
	Sac6	Fimbrin	*(Adams et al. 1991)* (Gheorghe et al. 2008)
	Scp1	Transgelin	*(Goodman 2003)* (Gheorghe et al. 2008)
	Abp1	mAbp1/Hip-55	*(Kessels et al. 2000)* (Kaksonen et al. 2005)
SCISSION	Rvs161/167	Amphiphysin	*(David et al. 1994)* (Friesen et al. 2006)
	Vps1	Dynamin	*(Obar et al. 1990)* (Smaczynska-de Rooij et al. 2010)
UNCOATING	Ark1	AAK1/Akl1	*(reviewed in Smythe & Ayscough 2003)* (Sekiya-Kawasaki et al. 2003)
	Prk1	AAK1/GAK	*(reviewed in Smythe & Ayscough 2003)* (Sekiya-Kawasaki et al. 2003)
	Sjl1,2 and 3	Synaptojanin	*(Srinivasan et al. 1997)* (Singer-Krüger et al. 1998)

[1] Other tables comparing yeast endocytic proteins and their mammalian homologues can be found in the following publications; Merrifield & Kaksonen 2014, Weinberg & Drubin 2012 and Robertson et al. 2009.

[2] References in italics are linked to data indicating the yeast proteins are homologous to the named mammalian proteins, otherwise the references are connected to the role of the yeast proteins in endocytosis.

1.1.2.1 Stage 1: Coat assembly and nucleation of a clathrin coated pit

At the initiation of an endocytic event, coat proteins accumulate and are brought together with adapter proteins and clathrin. This stage is shown diagrammatically in figure 3A,B and indicates that there are proteins recruited which initiate membrane curvature, including actin, which leads into the following invagination stage of endocytosis as described in section 1.1.2.2.

The earliest proteins seen to accumulate during an endocytic event are Syp1 and Ede1. Syp1 contains an F- BAR (Bin-Amphiphysin-Rvs) domain which can bind and bend membranes (Peter et al. 2004), and binds directly to Ede1 therefore facilitating Ede1 arrival at a site of endocytosis (Boettner et al. 2009; Stimpson et al. 2009; Reider et al. 2009). Ede1 is a scaffold protein and contains an EH (Epsin15 Homology) domain known to be found in many endocytic accessory proteins (Gagny et al. 2000; Santolini et al. 1999). Therefore Syp1 and Ede1 are thought to create an environment to which other endocytic proteins can bind and membrane bending can begin.

The epsins Ent1/2 accumulate after Syp1 and Ede1 and act as clathrin adapters linking the coat to the lipid vesicle. Ent1/2 can bind clathrin, actin and phosphoinositides the latter of which is carried out through the Epsin-N Terminal Homology domain (ENTH) (Wendland et al. 1999).

Initiation of an endocytic site then provides an environment for the accumulation of adaptor proteins to bind. Cargo adaptor binding protein AP2 is a protein complex made of four subunits in yeast and whilst AP2 is extremely important for CME in mammalian cells, in yeast AP2 is not essential. Deleting yeast AP2 was found to have no effect on the uptake of the lipid dye FM4-64 or the pheromone α factor (Carroll et al. 2009) but there are defects in pheromone response and polarisation (Chapa-y-Lazo et al. 2014). Yeast AP2 has been shown to bind the protein Mid2, a cell wall stress sensor, which is the first cargo identified for yeast AP2 binding (Chapa-y-Lazo et al. 2014). Clathrin recruitment also takes place during this early stage of CME in yeast. During yeast CME clathrin is not essential but is thought to stabilise the coat proteins (Carroll et al. 2012; Newpher & Lemmon 2006). Its assembly is dependent on clathrin heavy chain binding clathrin light chain (Huang et al. 1997) and the recruitment of clathrin requires Ent1/2 localisation (Newpher et al. 2005).

During clathrin recruitment, other coat proteins are localised to the endocytic site including Sla2, Sla1, Pan1 and End3 (Kaksonen et al. 2005). Sla2 has been found to localise to an endocytic patch before Sla1 and the localisation of the latter is dependent on the presence of End3 (Warren et al. 2002; Gourlay et al. 2003). Sla1 and Sla2 were identified by a synthetically lethal genetic screen with Abp1 and were therefore names Synthetically Lethal

with Abp1 (Sla) (Holtzman et al. 1993). Sla2 is the mammalian Hip1R orthologue which can bind PIP2 by its AP180-N Terminal Homology domain (ANTH) as well as actin and clathrin (Wesp et al. 1997; Sun et al. 2005). It has been suggested that Sla2 ANTH domain and the early endocytic protein Ent1 ENTH domain work in synergy as they co-assemble on PIP2 lipids *in vitro* to form a lattice. This lattice can both bind actin and clathrin so that Sla2 and Ent1 act as clathrin adapter and a molecular bridge linking the force from actin polymerisation to the tubulation of the endocytic vesicle (Skruzny et al. 2015; Skruzny et al. 2012).

Sla1 is known to localise to actin patches and is required for actin patch organisation and structure (Ayscough et al. 1999). Like Sla2, Sla1 binds clathrin and it has been found, through a yeast two hybrid experiment, that Sla1 and Sla2 can interact with each other (Gourlay et al. 2003; Di Pietro et al. 2010) suggesting a synergy between these two proteins during an endocytic event - perhaps to aid the link between membrane, actin and clathrin during endocytosis. Sla1 is also been found to bind Pan1, Abp1 and Las17 which are three proteins known to activate the Arp2/3 complex (Tang et al. 2000; Warren et al. 2002). The Arp2/3 complex forms actin branches by binding to existing actin filaments and then nucleating actin side branch polymerisation to create F-actin network to aid endocytic invagination (Rodal et al. 2005; Moreau et al. 1997). Sla1 has therefore been suggested to be involved in the organisation of actin during the early to invagination stages of endocytosis (Warren et al. 2002).

Pan1, as briefly mentioned, is known to bind actin and is required for actin organisation at an endocytic site (Wendland & Emr 1998; Tang & Cai 1996). This function is also required for the invagination/slow moving stage of endocytosis. Therefore the involvement of Sla2 with Ent1, Sla1 with Sla2, Pan1 and Las17 at these early stages contribute to the next stage of the endocytic event where membrane bending and actin dynamics form a membrane invagination.

The recruitment of early stage endocytic proteins has been described to be highly flexible rather than each protein assembling at a site in a specific temporal manner. It was found that deletions of some of the early stage markers described above (eg *ede1, syp1*) did not prevent endocytosis but did disrupt cargo recruitment which suggested that cargo binding could be a checkpoint for early to late stage endocytosis (Brach et al. 2014).

1.1.2.2 Stage 2: Invagination of a clathrin coated pit

Once the coat proteins have assembled the invagination stage takes place (figure 3A,B). In yeast this is actin dependent and relies on a number of different actin regulatory proteins. Las17 (mammalian orthologue WASP) is involved in actin regulation during invagination but is found to be recruited to the site before this stage and stays localised to the endocytic patch through to scission (Kaksonen et al. 2003; Kaksonen et al. 2005). Las17 can

bind and activate the actin nucleation factor Arp2/3 and in addition, is able to bind and nucleate actin filaments directly (Urbanek et al. 2013). Las17 has been found to be negatively regulated by Syp1 during the early stages of endocytosis. Membrane bending is thought to release Syp1 from the endocytic patch (Boettner et al. 2009) thus contributing to the activation of Las17 to regulate actin dynamics directly and indirectly. Deleting Las17 from the yeast genome causes temperature sensitivity and defects in cortical actin patches (Li 1997; Winter et al. 1999) indicating its importance in regulating the actin cytoskeleton. The deletion of the Las17 Arp2/3 binding site however, has relatively subtle defects in the late stages of endocytosis (Galletta et al. 2008) indicating that the Arp2/3 independent and dependent functions of Las17 may be temporally distinct.

Type 1 myosins, Myo3 and Myo5, are both motor proteins which, when removed from the genome separately, are not found to cause a defective phenotype. However, a double deletion of both Myo3 and Myo5 was found to cause growth defects and disorganisation of the actin cytoskeleton (Goodson et al. 1996). Furthermore, this double deletion of Myo3/5 prevented the internalisation of an endocytic vesicle (Sun et al. 2006; Geli & Riezman 1996), providing evidence that Myo3 and 5 are required as actin motors to drive inward invagination after an F-actin structure has been established.

A number of other actin regulatory proteins are also known to interact with actin during invagination such as Sac6, Scp1 and Abp1. Sac6 and Scp1 bundle actin filaments and it is thought that this increases the force provided by actin to aid in invagination (Gheorghe et al. 2008; Winder et al. 2003). The actin binding protein 1 (Abp1) is recruited a few seconds before invagination and remains with the vesicle until uncoating (Kaksonen et al. 2005). As its name suggests, Abp1 binds to actin and localises with actin patches (Lappalainen et al. 1998; Drubin et al. 1988) it may be required for linking the actin cytoskeleton to the endocytic patch and during the recruitment of the uncoating proteins Ark1 and Prk1 during the vesicle release stage of endocytosis (Robertson et al. 2009).

1.1.2.3 Stage 3: Scission and vesicle release

After invagination has occurred the vesicle then undergoes scission to release the vesicle into the cytoplasm whilst retaining the integrity of the plasma membrane (figure 3A,B). In yeast, this scission process is primarily facilitated by the proteins Rvs161, Rvs167 and Vps1. Rvs161/167 contain BAR domains which bend membranes or sense membrane curvature (Peter et al. 2004). Rvs167/161 act as a heterodimer *in vivo* and have been shown to bind lipid vesicles *in vitro* and were, until recently, proposed to act alone during endocytic scission in yeast (Friesen et al. 2006; Kaksonen et al. 2005; Colwill et al. 1999). Rvs167 localises to actin patches and this localisation is not disrupted when actin polymerisation is blocked (by the drug

latrunculin) indicating that it functions alongside, but is not dependent on, actin (Colwill et al. 1999). The SH3 domain in Rvs167 is known to bind a number of different proteins including Abp1 and Las17 (Colwill et al. 1999; Bon et al. 2000) which could indicate a role of Rvs167 in the switch between invagination and scission during CME.

Vps1, one of three dynamin like proteins in yeast, functions at the scission stage of endocytosis with Rvs167, not unlike mammalian amphiphysin-2 and dynamin (Meinecke et al. 2013). This GTPase is known to be able to bind and tubulate lipids and co-localises with endocytic markers Sla1 and Rvs167 (Smaczynska-de Rooij et al. 2010; Smaczynska-de Rooij et al. 2012). Vps1 was also shown to bind directly to Sla1 which further supports a role for Vps1 in endocytosis (Yu & Cai 2004). During the same study it was found that the deletion of *VPS1* causes a defect in the actin cytoskeleton. The function of actin in the scission stage of yeast endocytosis has not been investigated and is explored during the course of this thesis.

In the final stages of CME, vesicles are uncoated and sorted through different membrane trafficking compartments depending on the type of cargo each vesicle contains. Uncoating of vesicles in both yeast and mammalian endocytosis is known to require Ark1 and Prk1 protein kinases (reviewed in Smythe & Ayscough 2003). This was discovered by the observation of *ark1* and *prk1* deletion strains which contained vesicles in the cytoplasm that were positive for endocytic proteins such as Sla2, Abp1, Ent1 and Pan1 indicating that the endocytic vesicle coats were unable to disassemble, couldn't fuse with endosomes and therefore accumulate in the cytoplasm (Cope et al. 1999; Sekiya-Kawasaki et al. 2003). The phospholipid PIP2 is known to be required throughout endocytosis and during internalisation it is dephosphorylated by synaptojanin-like proteins Sjl1, 2 and 3 causing release of the PIP2 binding proteins such as epsins and Sla2 from the coated vesicle (Toret et al. 2008; Stefan et al. 2002). Deletion of *Sjl1* and *Sjl2* (triple deletion is not viable) produced long invaginations stretching into the cell. These invaginations co-localised with endocytic proteins thought to be continuously assembling at abortive endocytic sites due to incorrect localisation of PIP2 (Sun et al. 2007; Singer-Krüger et al. 1998).

1.1.3 Mammalian CME

In this section the various stages of CME in mammals are described and compared briefly with that of yeast endocytosis. Overall, mammalian cells CME is thought to happen in a very similar way to that of yeast endocytosis with sequential assembly and disassembly of coat components at an endocytic site. There are however differences, including a reduced necessity for actin, where the cytoskeleton appears to facilitate endocytosis rather than be an absolute requirement for it. There are cases where actin is required during mammalian CME, this

includes situations where a cell may have increased plasma membrane tension (Boulant et al. 2011) for example after polarisation of epithelial cells (see section 1.3.2).

Each stage of mammalian CME will be described, as with the yeast CME section, beginning with a description of the molecules involved in the initiation of an endocytic site, followed by the invagination of a clathrin pit, ending with how scission is understood to occur.

During the initiation of an endocytic site FCHo1/2 proteins, orthologous to the yeast Syp1, are known to be recruited. FCHo1/2 are F-BAR domain proteins which can bend lipid membranes and interestingly bind directly to Eps15, an orthologue of the yeast Ede1 (Uezu et al. 2007). Yeast CME initiation includes the binding of Syp1 to Ede1 and therefore this mechanism may have been evolutionarily conserved, taking place in mammalian endocytosis between the FCHo1/2 Eps15 interaction. Hip1R (Sla2 orthologue) is also recruited at this stage and binds directly to clathrin, facilitating clathrin recruitment to the endocytic patch (Engqvist-Goldstein et al. 2001). Also similar to yeast, the initiation of a clathrin coated pit corresponds with the presence of phosphoinositide PIP2 and, in mammals, this is stabilised by the F-BAR protein FCHo1/2 (Cocucci et al. 2012; Henne et al. 2010; Sun & Drubin 2012). In mammals the presence of PIP2 is required for AP2 cargo binding (Jost et al. 1998) in the first few seconds of CME (figure 4). When AP2 binds to PIP2 it is then able to associate with clathrin (Rapoport et al. 1997) which then can assemble to nucleate a clathrin coated pit (figure 4).

It has been suggested that there is a molecular checkpoint which regulates whether the coat assembly will be aborted or continue to invagination. In yeast it has been suggested that this involves cargo binding (Carroll et al. 2012; Brach et al. 2014) and this has also been hypothesised for mammalian cell CME (Ehrlich et al. 2004). Recently a new report has suggested that both AP2 and dynamin in mammalian cells act as a molecular checkpoint for endocytosis (Aguet et al. 2013) and that this checkpoint could even dictate which isoform of dynamin is involved in CME (Skruzny et al. 2015).

After initiation of a clathrin pit and adaptor protein recruitment, the membrane undergoes invagination. Most mammalian cells tested in *in vitro* tissue culture do not require actin for invagination, unless their plasma membrane is under tension (Boulant et al. 2011), although it is generally accepted that actin is present during all CME events (see section 1.3.2). The role of actin during this stage is still under investigation however it is known that there are proteins required for invagination such as FBP17. FBP17 is a Formin Binding Protein (17) which is recruited to the membrane during invagination (Taylor et al. 2011). Formin proteins are primarily actin nucleators and FBP17 has been reported to be able to activate other actin nucleating proteins such as WASP during cell migration (Tsujita et al. 2015). Furthermore, FBP17 is known to be able to bend membranes and co-localise with transferrin receptors in

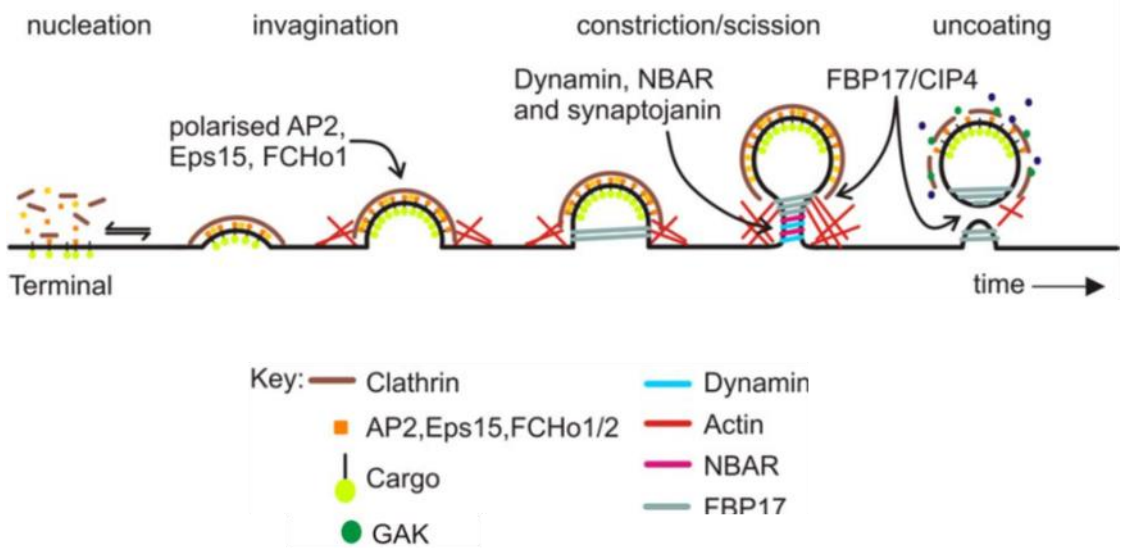

Figure 4. Stages of mammalian endocytosis This diagram has been modified from Taylor et al., 2011. It shows a simplified version of our understanding of mammalian clathrin mediated endocytosis from nucleation to scission. The key below indicates the different molecules represented in the diagram above. This includes actin which is present but, unlike yeast, is not always required.

cells and has been reported to be involved in the invagination stage of endocytosis (Kamioka et al. 2004).

After invagination, vesicles undergo scission from the membrane (figure 4). This is facilitated by the protein dynamin. It is understood that dynamin proteins are recruited to the vesicle neck where they bind the lipid membrane, polymerise into a coil and through GTPase hydrolysis facilitate vesicle release (Cocucci et al. 2014) (reviewed in Ferguson & De Camilli 2012). Dynamin proteins also function alongside amphiphysin proteins not unlike the yeast Vps1 with Rvs167 (Meinecke et al. 2013). There are a number of other BAR-domain containing proteins involved during scission (reviewed in Daumke et al. 2014). BAR domain containing proteins are thought to aid in vesicle scission by surrounding the vesicle neck thereby allowing dynamin GTPase function. SNX9, endophilin and amphiphysin are all BAR domain proteins which have been shown to recruit dynamin to the neck of an endocytic vesicle and increase the ability of dynamin to facilitate scission. This suggests a close functional relationship between these BAR domain containing proteins and dynamin during this process (Lundmark & Carlsson 2004; Meinecke et al. 2013; Andersson et al. 2010).

Finally, clathrin-coated vesicle uncoating in mammalian cells is aided by the two proteins auxillin (or auxilin-like protein GAK which is similar to the yeast protein Prk1) and Hsc70 (figure 4). Hsc70 is an ATPase which was found to function in clathrin coat disassembly (Rothman & Schmid 1986). Hsc70 has been found to clamp onto the heavy chain of clathrin and through ATPase hydrolysis aid clathrin lattice disassembly (Xing et al. 2010; Böcking et al.

2011). Auxilin is proposed to be brain specific protein which activates and associates Hsc70 with clathrin to aid in vesicle uncoating (Ungewickell et al. 1995). In all other non-neuronal cells it is widely accepted that the G-Associated protein Kinase (GAK) works in the same way as auxilin and it has a similar structure. GAK is known to be able to activate Hsc70 and phosphorylate adaptor proteins to release the clathrin coat (Umeda et al. 2000; Lee et al. 2006; Greener et al. 2000).

In conclusion, the yeast and mammalian CME have many similarities indicating an evolutionarily conserved cellular function which relies on the orchestration of many different proteins. One difference between them is the absolute necessity for actin during yeast endocytosis whereas in mammalian endocytosis, actin is present but not always required.

1.2 Actin

Actin is a fundamental, highly conserved protein found in all eukaryotes. It exists as a monomer which can polymerise to form filaments and this function is essential for its role in cell migration, cell shape and to form tracks, along which molecules can be moved within a cell. It propensity to polymerise is such that is requires a high level of regulation. In a cell, this regulation is achieved through association with actin binding proteins. Actin function *in vivo* can be hijacked by invading pathogens (reviewed in Welch & Way 2013) and also altered to further cancer cell metastasis (reviewed in Stevenson et al. 2012; Gross 2013). Therefore understanding how actin is regulated is extremely important for medical research.

Actin was discovered in 1942 by Brunó Ferenc Straub in Albert Szent-György's laboratory and, after a year's work, it was described to occur in two forms, a globular G- form in the absence of salt and a filamentous F- form upon addition of salt (reviewed in Szent-Györgyi 2004). The purification of actin can be most easily achieved from skeletal muscle where it is found in great abundance, playing a pivotal role in muscle contraction with myosin. A 42 kDa ATPase, actin is found in all eukaryotic organisms and is highly conserved, with mammalian actin sharing 85% similarity with its yeast orthologue. Actin is not known to occur in bacteria however there are a number of actin-like proteins which have been described (Popp & Robinson 2011). These proteins include MreB and MamK which can both form filaments and have a very similar structure to that of eukaryotic actin (Derman et al. 2009; Ozyamak et al. 2013; Jones et al. 2001).

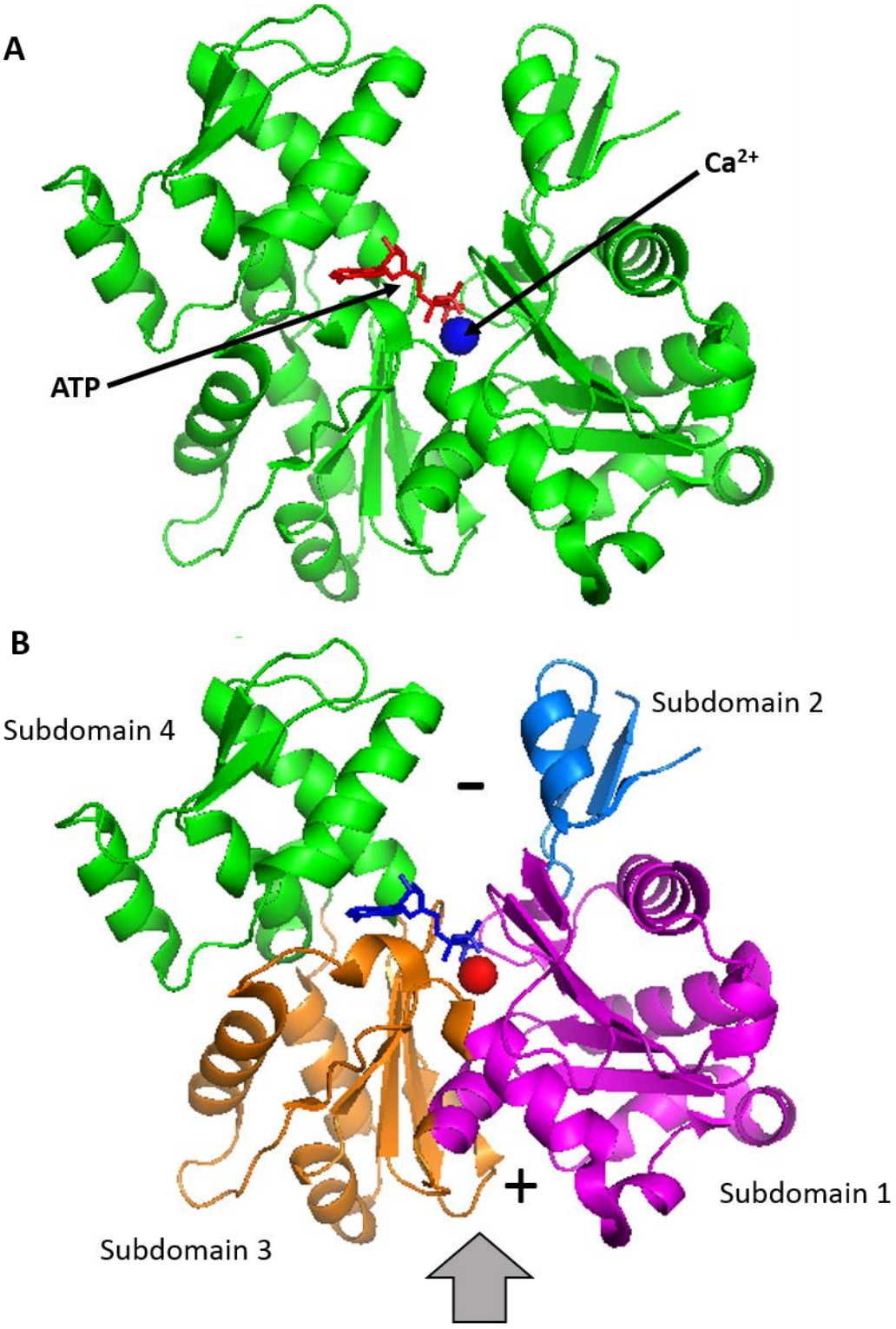

Figure 5. The crystal structure of G-actin A) G-actin monomer bound to ATP and calcium, created using PyMol Molecular Graphics software (Version 1.2r3pre, Schrödinger, LLC) and the crystal structure PDB 3HBT (Wang et al., 2010). Red molecule is ATP blue atom indicates calcium. B) G-actin monomer, purple- subdomain 1, blue- subdomain 2, orange-subdomain 3 and green indicates subdomain 4. Grey arrow indicates the barbed end of an actin monomer where other actin monomers bind to form an actin filament.

1.2.1 G-actin structure

Globular actin was first crystallised in 1990 bound to the protein DNAase1. The binding of DNAase1 stabilised G-actin so it could be crystallised and its structure determined (Kabsch et al. 1990). It wasn't until 2010 that a crystal structure of G-actin was achieved without G-actin binding proteins. However overall, the structure was found to be similar to those which had been previously reported (Wang et al. 2010a). G-actin contains four subdomain domains, 1-4, of which domains 1 and 2 are part of one major domain as are 3 and 4 creating a cleft between them where ATP and Mg^{2+} or Ca^{2+} can bind (figure 5A). G-actin is structurally polar due to subdomain 2 being smaller in mass, giving rise to a 'pointed' end and a 'barbed' end in each G-actin monomer (figure 5B). The barbed end is indicated by a plus symbol figure 5B, and is where actin monomers are added at a faster rate than at the pointed end. The pointed end, is where actin monomers generally disassemble more readily, is shown as a minus symbol in figure 5B.

1.2.2 F-actin structure

Ever since its discovery, it has been known that actin can form filaments in the presence of salt. The filamentous actin (F-actin) structure was first modelled in 1990 (Holmes et al. 1990) and shows that F-actin forms a right helical structure where actin monomers twist around each other with thirteen molecules per helical turn (figure 6A). This model was well received as the structure was modelled using the G-actin crystal structure published by the same group. However, a more recent study has shown in F-actin the conformation of the G-actin monomers is in fact altered by 20^{o} (Oda et al. 2009). In this model the slight twist in G-actin is straightened in the filament so that some G-actin binding proteins, such as DNAse1 (Wang et al. 2010a), can no longer bind making the affinity specific to G-actin (figure 6B). In fact, the conformation of an actin filament is not fixed and can change upon the binding of regulatory proteins and the tension on the filament (McGough et al. 1997; Hayakawa et al. 2011). Due to this and the fact F-actin cannot be crystallised, recent investigations have turned to cryo-electron microscopy to decipher the structure of F-actin at a near-atomic level (Galkin et al. 2015). This methodology provides a new way of investigating the different states of F-actin as modulated by regulatory proteins or mechanical tension.

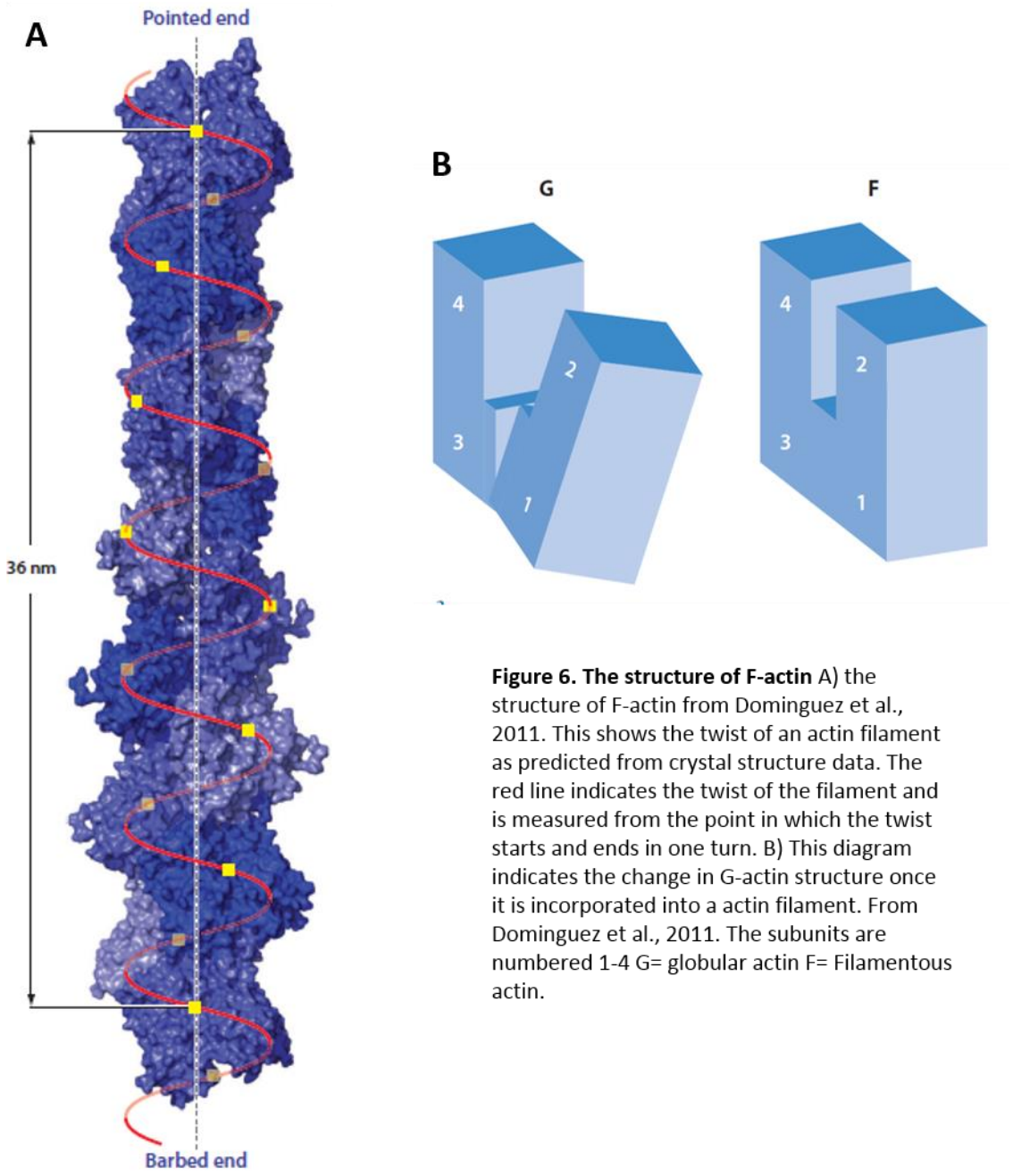

Figure 6. The structure of F-actin A) the structure of F-actin from Dominguez et al., 2011. This shows the twist of an actin filament as predicted from crystal structure data. The red line indicates the twist of the filament and is measured from the point in which the twist starts and ends in one turn. B) This diagram indicates the change in G-actin structure once it is incorporated into a actin filament. From Dominguez et al., 2011. The subunits are numbered 1-4 G= globular actin F= Filamentous actin.

1.2.3 Actin polymerisation

The polymerisation of G-actin into F-actin *in vitro* can be described in three distinct phases, nucleation, elongation and tread milling (Steinmetz et al. 1997). The nucleation of a filament begins by the dimerisation and tetramerisation of G-actin monomers. These steps are energetically unstable and therefore constitute the rate limiting step of polymerisation. Once a nucleus of G-actin monomers has been formed then polymerisation is energetically favourable and elongation can occur. Actin filaments grow from both the pointed and barbed ends however filament growth is faster at the barbed end than the pointed end (Kuhn & Pollard 2005). As this rapid elongation takes place the number of free actin monomers decreases which limits F-actin formation. This precedes F-actin tread-milling, where the number of

monomers which bind to the filament matches the depolymerisation so that the overall amount of F:G actin is not affected and the pool of G and F-actin is constantly being recycled. When the polymerisation is plotted over time this gives rise to a sigmoidal curve (figure 7). G-actin monomers are incorporated into a filament bound to ATP. As the F-actin filament grows ATP is hydrolysed to ADP and phosphate which forms a stable F-actin filament. The release of phosphate destabilises the filament causing depolymerisation at the pointed end and release of G-actin bound to ADP (Korn et al. 1987).

The polymerisation of actin relies on hydrogen bonds being created between each monomer. The factors that promote this include the presence of salt (>50 mM KCl, Mg^{2+}) slightly acidic pH, increased temperature and the concentration of G-actin in solution, called the critical concentration (reviewed in Carlier 1990).

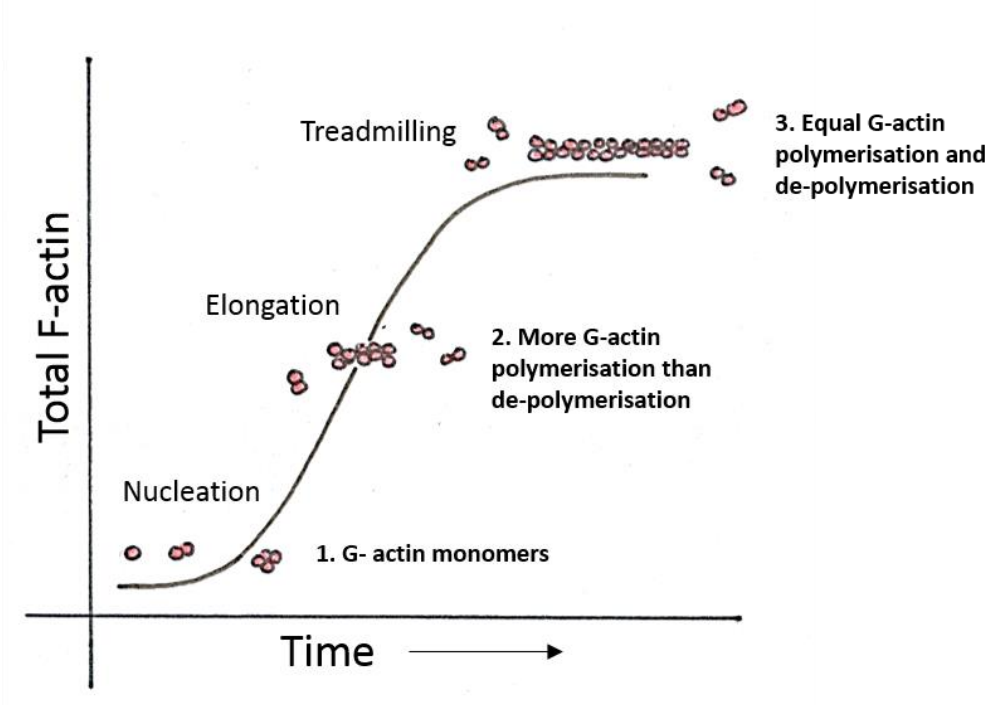

Figure 7. Actin polymerisation over time Modified from Molecular Biology of the Cell (Garland Science 2008). This diagram indicates how actin polymerisation happens over time. 1. First actin nucleation is unfavourable resulting in a lag phase. 2. This is followed by energetically favourable polymerisation. 3. Finally the number of G-actin being bound and lost is equal resulting in F-actin treadmilling.

1.2.4 Actin structures in yeast

Saccharomyces cerevisiae, is commonly known as budding yeast as, during asexually reproduction, daughter cells are able to bud off from the mother cell. This takes place in different stages which each require different types of actin structures. These different structures include actin patches, which are sites of endocytosis, actin cables and an actin ring formed during cytokinesis. To analyse these structures F-actin can be stained using rhodamine

phalloidin, a chemical that has been used for over three decades to visualise the yeast actin cytoskeleton (Adams & Pringle 1984; Amberg 1998). In order to understand how actin has been analysed in yeast studies and how it has been linked to endocytic events, the different forms of actin during a budding yeast cycle will first be explained.

Actin cables are stable actin bundles formed by the binding of both tropomyosin and Abp140 (Liu & Bretscher 1989; Yang & Pon 2002). These cables are found to polarise in cells during cell division between the mother and bud (Adams & Pringle 1984) (figure 8) and are required for vesicle traffic and mitotic spindle orientation (Pruyne et al. 1998; Yin et al. 2000).

Actin is also required to form a contractile ring with myosin (Myo1) during cytokinesis. Actin patches are found to accumulate at the midpoint between mother and bud (Kilmartin & Adams 1984) and reorganise to form a ring structure which acts in the cell division step (Young et al. 2010).

Actin patches are found at the periphery of cells in all stages of the cell cycle and are found to be more prevalent in the bud in comparison to the mother (figure 8). These patches have been investigated by EM and found to consist of a large network of branched and bundled actin filaments (Young et al. 2004). A number of different endocytic proteins localise to actin patches such as Arp2/3, Sla2, and Rvs167 (Raths et al. 1993; Munn et al. 1995; Moreau et al. 1997) demonstrating that these are sites of endocytosis.

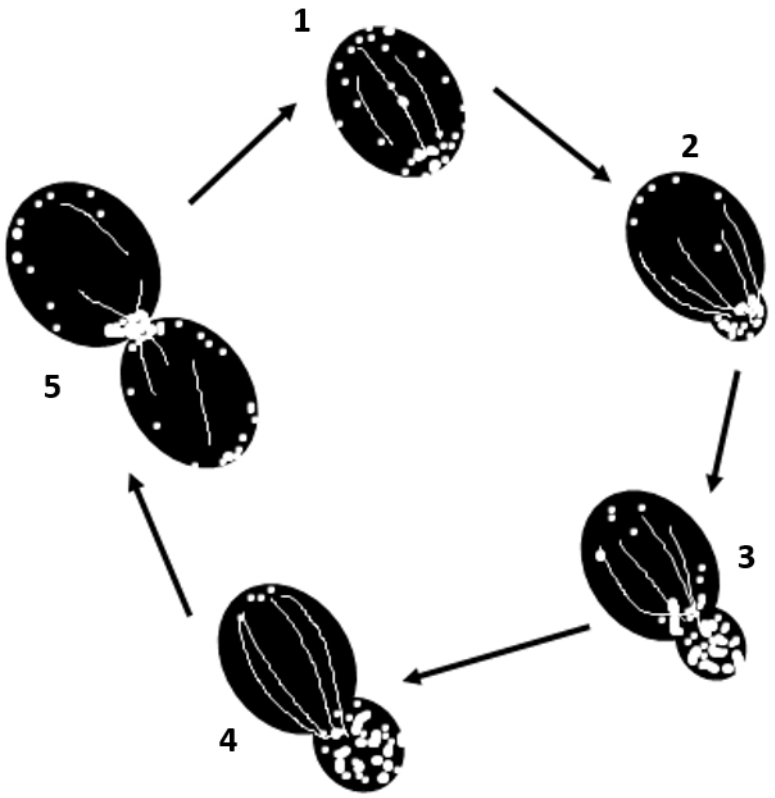

Figure 8. The cycle of actin patches and cables in budding yeast cell division
Modified from Amberg et al., 1998. 1. Yeast cells beginning division have some actin patches localised to the site where budding will occur. 2. As bud appears from mother actin patches localise to the bud. 3/4. Bud increases in size and actin cables link actin patches from mother to bud. 5. During cell division actin ring forms to function during cytokinesis and the mother and bud separate.

1.3 Actin in endocytosis

Endocytic patches in yeast are found to localise with actin during initiation through to the released vesicle moving into the cell (Huckaba et al. 2004). Actin is understood to function during CME from initiation of a endocytic patch to scission and its role in yeast endocytosis has been extensively studied and compared with that of mammalian CME (Mooren et al. 2012; Smythe & Ayscough 2006; Aghamohammadzadeh & Ayscough 2010). Electron microscopy studies in mammalian cells have identified actin filaments associated with coated pits which suggest that the growing barbed end is localised towards the membrane (Salisbury et al. 1980) however the role of these filaments have yet to be fully defined as actin is not always required for mammalian CME. In contrast, actin is essential for yeast endocytosis to occur, however its role during scission has yet to be fully defined.

1.3.1 Actin requirement in yeast CME

Yeast endocytosis was found to require actin through genetic screens for endocytic mutants (end mutants). During these screens the actin gene ACT1 was found (end7) along with proteins that bound to actin such as Sla2 (end4) and proteins that localise actin to an endocytic site Rvs167 (end6) (Raths et al. 1993; Munn et al. 1995). By blocking actin polymerisation using drugs such as latrunculin or making mutations in the actin gene endocytic defects were found, suggesting that actin is required for endocytosis in yeast (Ayscough et al. 1997; Ayscough 2000; Kübler & Riezman 1993). Fluorescently tagging endocytic markers and tracking them using live cell imaging has provided a clear temporal order to the endocytic process (Kaksonen et al. 2003; Kaksonen et al. 2005). From these investigations it has been found that just before invagination, a number of actin regulatory proteins are recruited to the site of endocytosis. This begins with the recruitment of WASP orthologue Las17 which generates actin filaments and recruits Arp2/3 and type 1 myosins to initiate invagination (Urbanek et al. 2013). These proteins are proposed to be involved with stimulating actin polymerisation and coupling it to invagination of an endocytic pit. Las17 and Arp2/3 are followed by the recruitment of actin modulating proteins such as Sac6 and Scp1. Sac6 (ortholog of mammalian fimbrin) works alongside Scp1 (transgelin) to organise and bundle actin. Without these proteins endocytic invaginations are found to have reduced inward movement and it suggests that the actin bundling process increases the force generated aiding invagination (Kaksonen et al. 2005; Winder et al. 2003; Gheorghe et al. 2008).

Actin may also have a role during yeast endocytic scission, however its role in this mechanism has not yet been clarified. During scission the BAR domain containing proteins Rvs167/161 bind together encircling the membrane to facilitate scission with the yeast

dynamin Vps1 (Smaczynska-de Rooij et al. 2012; Peter et al. 2004; Kaksonen et al. 2005; Navarro et al. 1997) but it is not known if these proteins require actin function.

From these data it is clear that actin is required for endocytosis. The reason why this was the case for yeast and not mammalian cells was discovered in 2009. During this study it was found that reducing the turgor pressure of a yeast cell by the addition of sorbitol reduced a yeast cells requirement for actin during endocytosis. This suggested that actin is required as a force generator to overcome membrane tension and create inward movement of the membrane during invagination. Furthermore, having reduced membrane tension by sorbitol, disrupting the actin cytoskeleton by latrunculin was found to cause a reduction in the number of scission events in comparison to cells treated only with sorbitol (Aghamohammadzadeh & Ayscough 2009). This suggests that there may be a role for actin during endocytic scission as well as during invagination.

1.3.2 Actin in mammalian CME

The presence of actin during mammalian CME has been visualised by EM of tissue culture cells, which showed clathrin coated pits with filaments of actin surrounding them (Salisbury et al. 1980). However, actin is not always absolutely required for CME and for this reason, evidence of a role for actin in CME was less straightforward than in yeast studies where actin is clearly required for CME events. This situation has been further confounded as initial studies using the drugs such as latrunculin, that block actin polymerisation, were found to have varied responses on CME depending on the cell type (Fujimoto et al. 2000). For example in mice fibroblast cells, latrunculin caused clathrin coated pits to form wider necks suggesting actin is required for the progression of CME potentially by functioning with BAR domain proteins in narrowing the lipid invaginations (Ferguson et al. 2009). However CME still took place indicating actin was not essential. Other cell types such as COS-7 (a fibroblast like monkey kidney cell line) and K562 (an erythroleukemic cell line) still take up transferrin receptor at normal levels when treated with latrunculin suggesting that they do not require actin for CME.

There are a number of different proteins known to function in mammalian CME which can bind and modulate actin polymerisation such as Hip1R (Sla2 in yeast) and mAbp1. Hip1R binds both clathrin and actin and reducing Hip1R by RNAi causes accumulation of actin at an endocytic site suggesting it is involved in actin regulation (Engqvist-Goldstein et al. 2004). By overexpressing the SH3 domain of mAbp1 in COS-7 it was found that transferrin uptake was reduced, again indicating a role for actin during CME (Kessels et al. 2001). This lead to a more in depth analysis of whether actin was localise to CME in mammalian cells.

Total Internal Reflection Fluorescence microscopy (TIRF) was utilised to visualise the localisation of actin at sites of CME. From these analyses actin was found to accumulate transiently after a burst of dynamin localisation at clathrin pits (Merrifield et al. 2002). Furthermore, using the same TIRF technique, the Arp2/3 complex along with WASP proteins were found to associate at endocytic sites furthering the evidence for a non-essential role of actin during CME and also indicated that actin was present for all stages of the endocytic process (Merrifield et al. 2004; Yarar et al. 2005). Since then new techniques have been developed which can temporally follow CME events by use of a pH sensitive probe which is able to identify invaginations from the membrane separately from closed internalised endocytic pits. Using this technique, it was found that there was a reduction in scission events after the cells were treated with latrunculin (Merrifield et al. 2005). This therefore indicates that that actin may play a role at the scission stage of endocytosis, however how this is orchestrated has yet to be defined. Most recently, it has been reported that by increasing the membrane tension in mammalian cell by either polarisation or mechanical stretching, actin is recruited for endocytic events (Boulant et al. 2011). This suggests that, like yeast, actin is required for mammalian CME to overcome membrane tension by providing the force necessary to drive invagination.

It is becoming clear that actin is required during endocytic invagination to overcome membrane tension in both yeast and mammalian cells. There is evidence to suggest that the role of actin during CME also extends into endocytic scission events. If this is the case then actin would be expected to interact, and be regulated by, proteins required for endocytic scission events. As discussed, there are many proteins which interact with actin during both yeast and mammalian CME. Studies have suggested that the actin binding proteins Sla2 and Ent function to link the actin cytoskeleton to the membrane during invagination (Skruzny et al. 2015) however other proteins may be required to link the force of actin to the scission stage of endocytosis. In 2010 it was discovered that the scission protein dynamin-1 can also bind actin (Gu et al. 2010) however the role of a dynamin-actin interaction during endocytosis has not been fully elucidated. In order to determine whether the involvement of actin in mammalian CME is mediated through dynamin it is important to understand the characteristics of dynamin itself.

1.4 Dynamin

Dynamin was first discovered in 1989, having been purified from bovine brain, and was subsequently analysed *in vitro*. These first experiments indicated that dynamin could bind and bundle microtubules and was thought to hydrolyse ATP (Shpetner & Vallee 1989). Shortly after these observations it was discovered that this protein was a orthologue of the *Drosophila shibire* gene (van der Bliek & Meyerowitz 1991; Chen et al. 1991) and in fact functions as a GTPase. Temperature sensitive mutations in the *shibire* gene cause paralysis at 29^{o}C in *Drosophila* which is reversible. It was found that this paralysis caused an increase in coated membrane invaginations in *Drosophila* neuronal cells and therefore this gene was described to be required for synaptic vesicle recycling (Kosaka & Ikeda 1983). The fact that the protein encoded by the *shibire* gene was an orthologue of dynamin was the first link to the idea that dynamin is involved in endocytosis. Subsequent structural analysis *in vitro* showed coils of dynamin binding to and tubulating lipids and, in the presence of GTP, forming vesicles pinched off from the lipid tubes (Sweitzer & Hinshaw 1998; Takei et al. 1998). This suggested a role for dynamin in endocytosis whereby the mechanochemical protein binds to lipids, oligomerises into a coil around a vesicle neck, and through its GTPase activity, facilitates scission (McNiven 1998; Cocucci et al. 2014). In order to understand this mechanism, the structure of dynamin and its different functional domains must first be described.

1.4.1 Domains of dynamin

Dynamin proteins have been described either as classical dynamin proteins which include mammalian dynamin-1,2,3 or other dynamin proteins which are described in the literature as either dynamin-like proteins or dynamin-related proteins. For the purpose of this thesis the term dynamin-like proteins will be used. These describe Dlp1 (Smirnova et al. 2001), and OPA1 (Alexander et al. 2000) which are involved in mitochondrial fission and fusion respectively, and the myxovirus resistance (Mx) proteins which are interferon inducible and act as antivirals within the cell reducing infection and viral replication (Liu et al. 2013). Dynamin-like proteins in humans such as the antiviral proteins MxA/B and the mitochondrial fission/fusion proteins OPA1/Dlp1 contain three regions of their structure found in all dynamin proteins. These are the GTPase, middle and GTPase effector domains (GED). These regions are also found in the yeast dynamin-like proteins Dnm1, Mgm1 and Vps1 (see section 1.6).

Classical dynamins contain five main protein domains, a GTPase domain, GTPase effector domains or GED domains, middle coiled coil region, a pleckstrin homology domain, and a proline rich C terminus (reviewed in Ramachandran 2011; Ferguson & De Camilli 2012). The crystal structure of dynamin was published in 2011 (Ford et al. 2011; Faelber et al. 2011).

This structure excluded the proline rich C terminus but for the first time showed how the domains fold into the tertiary structure of dynamin (figure 9A). Each domain (marked in bold) is discussed in turn below. Dynamin molecules can occur as a monomer, dimer, tetramer and higher order ring oligomer. For clarity when discussing dynamin higher order structures, the term oligomer will mean ring formation and any other quaternary structure will be referred to by name when appropriate.

The **GTPase domain** (figure 9A,B) of dynamin is at the N terminus of the protein and functions in a similar way to small GTPases such as Ras in which two switch regions form hydrogen bonds with the γ-phosphate of the GTP molecule which then change conformation upon GTP hydrolysis (Vetter & Wittinghofer 2001). Dynamin has a low affinity for GTP 10-100 μM and a turnover of around 1.4 min^{-1} (Praefcke & McMahon 2004; Leonard et al. 2005). However this turnover is increased up to 100 fold after oligomerisation (Warnock et al. 1996) due to the dimerisation between GTPase domains which stabilise the switch regions and GTP binding pocket (Chappie et al. 2010).

The **GTPase effector domain (GED)** (figure 9A,B) is an alpha helical bundle made of three distinct sections of dynamin primary structure. As seen in figure 9B the sections that combine to create this domain contain bundle signalling elements (BSE) and these are found at the N and C terminus of the GTPase domain and at the C terminus of the middle domain. In the tertiary structure of dynamin each of the BSE sections are organised to form the GED (Faelber et al. 2011; Chappie et al. 2009). It was discovered that the GTPase domain could not be purified without the presence of the GED domain indicating the close structural relationship between these domains (Chappie et al. 2009). Mutations in this GED domain have been found to impair GTPase activity (Sever et al. 1999) and mutations such as I690K prevent dynamin oligomerisation (Song et al. 2004). This indicated a role for the GED domain in both GTPase domain structure and higher order oligomerisation.

The **middle coiled-coil domain** (figure 9A,B) within dynamin has been found to be required for oligomerisation and actin binding (Ramachandran et al. 2007; Gu et al. 2010). A full investigation of where these two mechanisms lie on the crystal structure is described in chapter 3 section 3.1.1 and detail into the direct actin interaction is described in section 1.5.1. It was found that the middle domain had a more conserved N terminus 301-350 than C terminus 350-520 (Warnock & Schmid 1996) and as the described C terminus covers the actin binding region (399-444), this may suggest altered mechanisms of function between different dynamin proteins and actin. The middle coiled-coil domain has been structurally mapped to form dynamin dimers and oligomers from both the crystal structure data and in vitro EM re-construction (Ford et al. 2011; Faelber et al. 2011; Chappie et al. 2011) indicating this region to be extremely important in dynamin self-assembly.

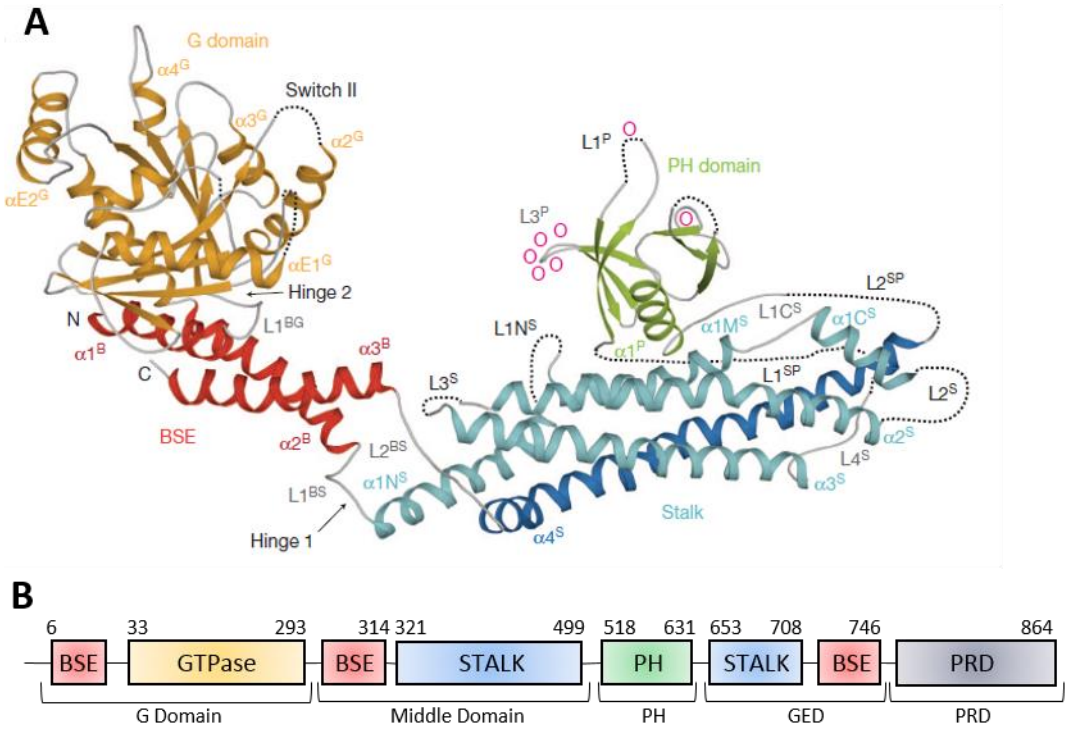

Figure 9. The crystal structure of dynamin-1 A) The crystal structure of dynamin-1 from Faelber et al., 2010 PDB 3SNH reproduced with permission from Nature Publishing Group. Each domain is indicated and the PRD is not present as it was not able to be crystallised with the rest of the structure due to its high flexibility. B) A diagram of the domains of dynamin with the amino acid numbers indicated above each section and the main sections described below.

Dynamin can bind and tubulate lipids (Sweitzer & Hinshaw 1998; Takei et al. 1998) and can bind the phosphoinositide PIP2 through its **Pleckstrin Homology (PH) domain** (Salim et al. 1996; Zheng et al. 1996) (figure 9A,B). It was found that mutations to the PH domain of dynamin, or removing it entirely from the protein, prevented PIP2 binding and transferrin uptake indicating the PH domain was required for dynamin function in receptor mediated endocytosis (Lee et al. 1999; Achiriloaie et al. 1999; Vallis et al. 1999). Dynamin lipid binding has been found to cause clustering of PIP2 at the neck of a forming endocytic vesicle which was hypothesised to be aiding vesicle scission (Bethoney et al. 2009). Moreover dynamin-1, as well as binding to lipids, has also been found to be able to induce membrane curvature (Ramachandran et al. 2009). This function however, seems to be specific to dynamin-1 PH domain, as the ubiquitously expressed dynamin-2 isoform cannot aid in membrane curvature (Liu et al. 2011b). Interestingly, the lipid binding ability of dynamin requires dynamin oligomerisation (Klein et al. 1998) and therefore without higher order structure, lipid binding does not take place indicating a close relationship between dynamin oligomerisation and lipid binding. This could be presumed to aid in the orchestration of vesicle scission or may indicate that the lipid binding ability of dynamin is weak and therefore multiple molecules are required to strengthen this interaction.

Classical dynamin proteins contain a fifth domain which is the **Proline Rich Domain (PRD)** (figure 9A,B). Due to the high number of proline residues this C terminal domain is very flexible and therefore was removed before dynamin was crystallised. This domain is known to bind Src Homology 3 (SH3) domain containing proteins such as amphiphysin, endophilin, sorting nexin 9 and syndapin (Grabs et al. 1997; Anggono et al. 2006; Lundmark & Carlsson 2004). The PRD domain is required for the recruitment of dynamin to clathrin coated pits and therefore without this domain endocytosis is reduced (Shpetner et al. 1996; Okamoto et al. 1997).

1.4.2 Dynamin function at the scission stage of endocytosis

Dynamin has many roles in a cell, however its most characterised function is at the scission stage of endocytosis. There have been many studies carried out to identify how dynamin functions during scission. It is known that dynamin forms rings around lipids *in vitro* (Hinshaw & Schmid 1995; Carr & Hinshaw 1997) and upon addition of GTP these lipids can be pinched off into vesicles (Sweitzer & Hinshaw 1998). It is also known that dynamin oligomerisation leads to an increase in GTP hydrolysis (Warnock et al. 1996) and therefore it was proposed that the GTPase action of dynamin causes a conformational change to bring lipids together. This was analysed by EM and crystal structure data and it was concluded that dynamin rings cause a GTP dependent power stroke to bring the membranes together (Chappie et al. 2011; Ford et al. 2011; Faelber et al. 2011). Recent *in vivo* studies using live cell imaging and quantitative fluorescence measurements have indicated that a single ring of dynamin is required for scission (Cocucci et al. 2014; Grassart et al. 2014). This suggests that after one ring of dynamin is formed the dimerisation of one set of GTPase domains can cause the power stroke to constrict the ring so the next two GTPase domains can bind and this continues to facilitate scission (Cocucci et al. 2014).

There is evidence however, to suggest that the force from dynamin GTPase hydrolysis on a membrane would not be enough to stimulate scission on its own. An *in vitro* experiment with liposomes in solution or lipids tethered under tension (by use of kinesins) indicated that scission by dynamin could only occur when the membrane was held under tension (Roux et al. 2006). A subsequent study has determined that the difference in angle of invagination to that of the plasma membrane also contributes to the force required to release a vesicle (Morlot et al. 2012). These experiments indicate that while dynamin is an important contributor for scission to occur there are likely to be other force-providing proteins that function alongside dynamin to facilitate vesicle scission *in vivo*. In light of the possible role of actin during scission,

this additional force could be provided by actin and therefore scission may be mediated by a dynamin-actin interaction.

1.4.3 Dynamin isoforms 1, 2 and 3

In mammals there are three isoforms of dynamin which are encoded for by separate genes, namely dynamin-1,2 and 3. Most of the studies into dynamin function during endocytosis have been carried out with dynamin-1 and dynamin-2. In order to understand how these isoforms differ and how this may affect each one interacting with actin, the three classical dynamin proteins are discussed in turn.

Historically it is understood that dynamin-1,2 and 3 are expressed at higher levels in different tissues therefore their differing roles are thought to be tissue specific. Dynamin-1 is found highly expressed in neuronal tissues (Nakata et al. 1991), dynamin-2 is ubiquitously expressed (Cook et al. 1994) and dynamin-3 is highly expressed in the brain and testes (Cook et al. 1996; Nakata et al. 1993). However, new evidence has suggested that the differences in expression may not be as clear as previously thought. For example, dynamin-1 is highly expressed in neuronal tissue and enriched at the synapse however transcriptional analysis shows similar levels of mRNA for both dynamin-1 and dynamin-2 in most tissues (Reis et al. 2015). The differences between the cellular roles of dynamin-1 and 2 highlighted by the isoform specific mutations which cause disease. Mutations in dynamin-2 have been found to cause the muscle wasting and peripheral nervous system diseases Charcot-Marie-Tooth and centronuclear myopathy (Tanabe & Takei 2012; Kenniston & Lemmon 2010). Whereas mutations in dynamin-1 have been linked to epileptic phenotypes in both mice models and humans (Boumil et al. 2010; Asinof et al. 2015). This indicates how important dynamin-1 is in neuronal cell function and that dynamin-2 mutations may have a more global effect in developmental disease. In this section each dynamin isoform is described with the current understanding of how they function.

1.4.3.1 Dynamin-1

Dynamin-1 is known to function primarily in neuronal tissue and in endocytosis of receptors in the brain (reviewed in Saheki & De Camilli 2012). Dynamin-1 plays a role in a number of different types of endocytosis in neurons including CME, bulk endocytosis and ultrafast endocytosis (Clayton et al. 2010; Watanabe et al. 2013).

The role of dynamin-1 in neuronal cell endocytosis is regulated by phosphorylation at serine 774 and 778 which inactivates dynamin function (Clayton et al. 2010). S774 is not conserved in dynamin-2 and recently this phosphorylation site in dynamin-1 was found to regulate dynamin-1 function in non-neuronal cells. It has been suggested that endosomal

signalling can activate dynamin-1 in non-neuronal cells to trigger rapid and dysregulated CME (Reis et al. 2015). Dynamin-1 has been found to be able to bend membranes whereas dynamin-2 can only sense membrane curvature (Liu et al. 2011b). This difference may be important for up-regulating CME in non-neuronal cells and facilitating fast endocytosis to recover receptors in neuronal cells. This indicates a role for both dynamin-1 and dynamin-2 in all cell types.

In 2010, the Sever lab demonstrated that dynamin-1 is able to bind directly to actin and by perturbing this interaction, stress fibre production in kidney podocyte cells was reduced (Gu et al. 2010). This report also indicated that dynamin-1 is also highly expressed in podocytes, the reason for which has yet to be fully elucidated. The dynamin-1-actin interaction has been suggested as a new therapeutic target for kidney disease, by the same group, who were able to pharmacologically promote dynamin oligomerisation which increases actin polymerisation. This is thought to increase actin stress fibres in podocytes and it was found to improve the renal health in animal models of chronic kidney disease (Gu et al. 2010; Schiffer et al. 2015).

There are also other cellular functions that dynamin-1 has been shown to play a role in such as in filopodia outgrowth and in actin comet tails (Yamada et al. 2013; Lee & De Camilli 2002). Moreover, filopodia outgrowth has been found to be affected by perturbing the dynamin-1-actin interaction (Chou et al. 2014) suggesting that there are further functions of dynamin-1 with actin which have yet to be analysed. Therefore dynamin-1 has an important role in neuronal endocytosis however this is not the limit of its functions and future investigations into this protein are likely to show it playing a role in a number of other cellular processes possibly in cell migration and invasion.

1.4.3.2 Dynamin-2

Dynamin-2 is ubiquitously expressed and is known to have a major role in CME. Its ubiquitous expression has led to it being used for most recent live cell imaging of dynamin function in CME. Recent investigations include the fluorescent tagging of dynamin-2 to calculate the precise number of dynamin molecules involved in a scission event as well as dynamin-2 and actin interplay during CME (Cocucci et al. 2014; Grassart et al. 2014; Taylor et al. 2012). As mentioned above dynamin-2 has been found to be able to sense curved membranes but not induce them and is thought to play a role in slower constitutive forms of endocytosis in neuronal cells (Liu et al. 2011b; Tanifuji et al. 2013). Dynamin-2 is known to function in forms of endocytosis other than CME including Fast Endophilin Mediated Endocytosis (FEME), phagocytosis and internalisation of caveolae (Boucrot et al. 2014; Di 2003; Henley et al. 1998).

Dynamin-2 also functions in cellular processes distinct from endocytosis including lamellipodial formation, actin comet tail formation, and cell invasion (Menon et al. 2014; Lee & De Camilli 2002; McNiven et al. 2000; Ochoa et al. 2000) these are described in more detail in section 1.5 and indicates that dynamin and actin function together in many cellular processes (reviewed in Menon & Schafer 2013). Dynamin-2 has also been found to function in intracellular vesicle traffic where expression of dynamin-2 GTPase mutant caused tubulation of the Golgi membranes which were unable to be detached into the cytoplasm (Kreitzer et al. 2000).

Dynamin was first described as a microtubule binding protein and since then dynamin-2 has been found to be implicated in microtubule dependent cellular functions such as during the formation of the mid-body during cytokinesis (reviewed in Konopka et al. 2006). Dynamin-2 has been found to localise to the spindle mid-zone and a knockdown of dynamin-2 reduces the speed of fibroblast cytokinesis (Thompson et al. 2002; Liu et al. 2008) however the function of dynamin-2 during cytokinesis has yet to be fully defined and may well require the direct dynamin-actin interaction.

Overall dynamin-2 is the most abundant dynamin isoform in mammalian cells taking part in endocytosis and other cellular processes such as cell migration. It is currently believed that dynamin-2 functions in all cell types but may play a more restricted role in, for example, neuronal cells where the role of dynamin-1 dominates.

1.4.3.3 Dynamin-3

Dynamin-3 is traditionally thought to function in the testis where it has high expression and has been hypothesised to function in spermogenesis (Nakata et al. 1993; Vaid et al. 2007). However it is also known to have a similar expression profile to dynamin-1 and is found upregulated in synapse production suggesting a role in neuronal development (Cook et al. 1996; Arnold et al. 2003). Dynamin-3 was found to play a role in the post-synapse (Gray et al. 2003) as well as in the pre-synapse organising the uptake of stimulus specific neurotransmitters. Dynamin-3 was found to function in bulk endocytosis after a neuronal stimulus however, this role was usurped by dynamin-1 in high frequency neuronal firing (Tanifuji et al. 2013). This suggested a slow kinetic function for dynamin-3 in replenishing the Readily Releasable Pool of neurotransmitters in the pre-synapse.

Dynamin-3 has also been implicated in the production of platelets as it has found to be required for the production of megakarayoctes, cells which produce platelets (Reems et al. 2008). Furthermore by blocking dynamin-3 function using the dynamin drug dynasore (Macia et al. 2006) platelet production was reduced (Nürnberg et al. 2012) and this suggests a role for dynamin-3 in regulating platelet size (reviewed in Cantor 2012).

1.5 Dynamin and actin in cellular processes

The role of dynamin during endocytosis is well defined however the link between this function and its ability to directly bind actin has not been investigated in detail. In order to understand how dynamin may work with actin during this process it is important to outline what is known about the different cellular processes within which both dynamin and actin are known to play a role. Dynamin functions in a number of ways in a cell distinct from endocytosis as described, including cell migration and cell invasion through tissues. All of these processes also require actin and it is becoming increasingly clear that dynamin and actin have a close interplay and sometimes interact directly, to orchestrate these cellular processes, reviewed in Menon & Schafer 2013. In this section, the direct dynamin-actin interaction is explained followed by how these two proteins are currently understood to function in endocytosis and other cellular roles. Figure 10 provides a diagram of all these cellular processes.

1.5.1 The direct dynamin-actin interaction

Dynamin-1 has been found to bind directly to actin through its middle coiled-coil region between amino acids 399-444 (Gu et al. 2010). By mutating positively charged basic residues within this area to negatively charged acidic residues (K/E) the affinity between dynamin and actin was reduced indicating these basic residues are required for this interaction. Interestingly, swapping acidic residues within this region for basic amino acids (E/K) actually increased the affinity between dynamin and actin. In the same study it was found that the K/E mutations causes a reduction in the number of stress fibres in kidney podocyte cells suggesting this direct interaction is required for actin organisation *in vivo*. *In vitro* analysis showed that dynamin oligomerises in the presence of short actin filaments which therefore increased the GTPase action of the protein (see section 1.4.1). Moreover dynamin was found to increase the polymerisation of actin through displacement of the actin capping protein gelsolin (Gu et al. 2010). This data provides insight into the regulation of both dynamin and actin in cellular processes.

The effect of actin on dynamin oligomerisation has been followed in cells using a quantitative Fluorescence Lifetime Imaging Microscopy (FLIM) to follow the creation of dynamin oligomers in cells (Gu et al. 2014). During this study the mutation K/E was used to analyse whether a reduction in actin binding prevents higher order oligomerisation in COS-7 and podocyte cells. It was found that the K/E mutation prevented actin dependent dynamin oligomerisation in cells and also that there was more oligomerised dynamin found overall in COS-7 cells in comparison to kidney podocyte cells. This indicates that actin binding was required for dynamin oligomerisation in cells and that dynamin oligomerisation is more highly

regulated in podocyte cells. Variation in oligomeric dynamin from one cell type to the next may be indicative of differing roles of dynamin in different tissues, possibly linked to which dynamin isoform is most highly expressed.

1.5.2 Dynamin and actin in endocytosis

During the initial study into the direct dynamin-actin interaction (Gu et al. 2010) endocytosis of transferrin was tested in HeLa cells to determine whether a reduction in actin binding (by K/E mutations in the actin binding site) reduced endocytic uptake. It was found that this mutation did not affect endocytic uptake of transferrin and therefore it was concluded that the direct dynamin-actin interaction was not required for its function in endocytosis (Gu et al. 2010). However it is understood that in mammalian cells actin is not required during endocytosis unless there is membrane tension to overcome (Boulant et al. 2011). As HeLa cells are not known to require actin for endocytosis a role of the direct dynamin-actin interaction during endocytosis cannot be ruled out entirely based on this evidence alone.

1.5.2.1 The function of dynamin and actin in CME

Prior to the discovery of the direct dynamin-actin interaction there was evidence that dynamin plays a role in integrating actin dynamics with endocytosis. It is known that dynamin can bind actin regulatory proteins involved in endocytosis such as cortactin and mAbp1 and therefore is involved in actin regulation during CME (McNiven et al. 2000; Kessels et al. 2001). Dynamin has also been shown to accumulate at stages of CME earlier than scission suggesting it could play a role in the invagination stages potentially to orchestrate actin dynamics (Ehrlich et al. 2004; Merrifield et al. 2002).

Live cell fluorescence imaging of dynamin and actin in murine NIH3T3 fibroblasts has indicated that dynamin and actin act in a feedback loop throughout an endocytic event. By tracking fluorescently tagged dynamin and actin in TIRF the localisation of each molecule can be analysed temporally with each CME event. Data from this technique indicated that there is a low amount of actin at a site of CME which is followed by the recruitment of dynamin molecules, which then stimulates the polymerisation of actin. The F-actin then in turn stimulates the oligomerisation of dynamin (Taylor et al. 2012). The oligomerisation of dynamin was seen as a burst of fluorescence (Merrifield et al. 2002; Merrifield et al. 2005) and this burst was not observed when actin polymerisation was blocked by the addition of latrunculin (Taylor et al. 2012). Quantitative fluorescence studies have supported this data by indicating that 2-4 dynamin monomers are recruited early in endocytosis and that this precedes actin recruitment which in turn promotes dynamin oligomerisation (Grassart et al. 2014). This indicates a close

relationship between dynamin and actin during endocytosis which begins before scission and orchestrates the scission event (figure 4,10).

1.5.2.2 Dynamin and actin in clathrin independent endocytosis

There are other types of endocytosis that do not require clathrin, some of which utilise both dynamin and actin. It is not known if these mechanisms require the direct interaction between dynamin and actin but, the identification of both proteins at clathrin independent endocytic (CIE) events (outlined below), provides evidence to suggest that their direct association could be important for CIE in mammalian cells.

Recently, a new endocytic pathway was described in which the BAR domain protein endophilin A2 is implicated in the scission stage of endocytosis in what is known as Fast Endophilin Mediated Endocytosis (FEME) (Renard et al. 2014; Boucrot et al. 2014). Using *in vitro* experiments it was found that endophilin A2 can bend the membrane but cannot form vesicles without additional force. It was found that both dynamin and actin function with endophilin during the scission stage of FEME. Uptake by FEME was only perturbed however if all three proteins (endophilin, dynamin and actin) were knocked out of the system and it was therefore concluded that each one can function independently (Renard et al. 2014). However these experiments were not carried out in cells which require actin for endocytic events and if they had been, perhaps more of a dependency between dynamin and actin would have been found.

Another fast endocytic mechanism has been described to occur in neurons whereby cells are able to uptake receptors for recycling within tens of milliseconds. This has been named ultrafast endocytosis and was discovered through the use of a new EM technique, whereby mouse hippocampal neurons were stimulated and snap frozen within a fraction of a second then imaged by EM (Watanabe et al. 2013). This showed vesicles being pinched off which, in previous experiments, may have been assumed to be vesicle 'kiss and run' events. The group found that this CIE was dependent on both dynamin and actin. This is interesting as neurons are polarised and therefore would have a higher membrane tension than unpolarised cells. As polarisation of cells has been found to stimulate the requirement of actin during endocytosis (Boulant et al. 2011) this may indicate an in vivo example of actin dependent endocytosis which could also require a direct dynamin interaction.

Dynamin has also been described as playing a role in phagocytosis as it localises to the tip of phagocytic protrusions and the GTPase mutation K44A is found to prevent phagocytic cup closure (Gold et al. 1999; Di 2003). Whether the direct interaction between dynamin and actin is required for this function has not been investigated however it could act to remodel actin filaments during closure of a phagocytic cup. There has been evidence to suggest that

actin is not essential for this cellular mechanism however and it could be that dynamin functions in this process simply to recycle vesicles and lipids from the membrane (Tse et al. 2003; Di 2003).

1.5.3 Interactions of dynamin with actin binding proteins

Dynamin binds a number of SH3 domain containing proteins, through its PRD (section 1.4.1), a number of which bind and regulate actin filament organisation. By understanding these interactions potential indirect actin binding partners may be identified which may also function during endocytic events and specifically at scission. Therefore a selection of actin binding proteins and their role with dynamin and actin are described below.

Dynamin is known to interact with actin binding proteins such as cortactin (McNiven et al. 2000), profilin (Witke et al. 1998), and mAbp1 (Kessels et al. 2001), as well as actin regulatory proteins FBP17 (Kamioka et al. 2004), syndapin (Qualmann et al. 1999) and SNX9 (Lundmark & Carlsson 2003; Soulet et al. 2005). Below, the role of cortactin, FBP17 and SNX9 with dynamin are described as an indication of the role of dynamin with actin binding and regulatory proteins within the cell.

Cortactin binds F-actin and is localised to cortical actin structures (Wu et al. 1991; Wu & Parsons 1993). Cortactin can also bind and activate the actin branching molecule Arp2/3 to form branched actin networks (Weaver et al. 2001) in both cell migration and the formation of invadosomes (Clark et al. 2007; Kowalski et al. 2005). These cell processes also require dynamin which has been shown to directly bind the SH3 domain in cortactin. Disrupting this association causes a reduction in stress fibre production within cells (McNiven et al. 2000). The direct dynamin-cortactin interaction has also been found to regulate the organisation of actin at membranes and to stabilize actin in neuronal growth cone dynamics (Schafer et al. 2002; Kurklinsky et al. 2011; Yamada et al. 2013).

Dynamin can also bind directly to the Formin Binding Protein 17 (FBP17) a protein required for endocytosis in the formation of invaginations (Kamioka et al. 2004). FBP17 is found in the brain and testis which is similar to the distribution of the isoform dynamin-1 and 3 in tissues (Nakata et al. 1991; Nakata et al. 1993; Cook et al. 1996) and recruits actin regulatory proteins Arp2/3, WASP and WIP to regulate actin structures (Tsuboi et al. 2009; Tsujita et al. 2015). FBP17 has been found to be required for the development of hippocampal neurones in the rat brain and this requires its SH3 domain (Wakita et al. 2011). Interestingly FBP17 can also recruit dynamin-2 along with WASP/WIP proteins in order to form podosomes and phagocytic cups in macrophage tissue invasion and phagocytosis (Tsuboi et al. 2009). Most recently it has been discovered that FBP17 recruits actin modulating proteins to aid in cell migration, only when membrane tension is increased. However above a certain level of membrane tension

FBP17 function is inhibited which indicates FBP17 may form a molecular link between membrane tension and actin dynamics within a cell (Tsujita et al. 2015). This is interesting as it could indicate that dynamin function with actin is also regulated in this process during the orchestration of membrane dynamics.

SNX9 is BAR domain containing protein (Howard et al. 1999) that can bind to lipids, and other proteins through its SH3 domain and functions during endocytic scission (reviewed in Lundmark & Carlsson 2009). It can bind directly to dynamin (Lundmark & Carlsson 2003; Soulet et al. 2005) and is required for dynamin recruitment to an endocytic site appearing before dynamin recruitment (Lundmark & Carlsson 2004; Taylor et al. 2011). TIRF and *in vitro* work found that SNX9 arrives at an endocytic site and stimulates dynamin GTPase activity (Soulet et al. 2005). Furthermore, SNX9 can also bind actin regulatory proteins such as WASP and Arp2/3 (Shin et al. 2008) and therefore it was hypothesised that SNX9 may act to bridge actin and dynamin function to aid scission (Shin et al. 2008; Lundmark & Carlsson 2009). Interestingly however, the appearance of SNX9 at an endocytic site has been found to peak after scission suggesting that SNX9 main role may be linked to post scission events (Taylor et al. 2011).

1.5.4 The role of dynamin and actin in cell migration

Cell migration requires an orchestration of actin remodelling for membrane protrusion, signal transduction, recycling of adhesion structures as well as contraction and relaxation of the whole cell during directional movement. Dynamin can act in this process by orchestrating actin dynamics in lamellipodia or filopodia formation with actin regulatory proteins or by direct interactions with actin (Menon et al. 2014; Chou et al. 2014) figure 10.

Dynamin-2 has been found to localise at lamellipodia in mouse fibroblasts and US-O2 cells (human bone cancer cell line) (McNiven et al. 2000; Menon et al. 2014). Its direct interaction with cortactin has been found to localise it to lamellipodia and this association is required for the formation of cortical ruffles during cell migration (McNiven et al. 2000; Schafer et al. 2002; Krueger et al. 2003). This indicated that dynamin could have an indirect interaction with actin, where it functions with cortactin to regulate actin dynamics at the site of lamellipodial formation and cell extension. This may also suggest that cortactin binding is required to localise dynamin to actin where dynamin can then bind actin filaments. A study in 2014 utilised the newly discovered actin binding site mutations (K/E) (Gu et al. 2010) to investigate if the direct interaction also has an effect on lamellipodia dynamics. This study identified that a reduction in the dynamin-2-actin interaction reduced the localisation of dynamin to lamellipod and reduces lamellipodia outgrowth (Menon et al. 2014). It also

demonstrated that dynamin-2 function has an impact on downstream actomyosin contractility. This indicated that dynamin is a part of lamellipodial actin dynamics for both orchestration of filaments and downstream signalling in migrating cells.

Filopodia are actin rich protrusions which precede a lamellipodial outgrowth from a cell. These structures are thought to be required for initiation of cell adhesions and to link contractile force from the lamellipodia back to the main cell body (Xue et al. 2010). Dynamin-1 has been reported to be required for the formation and stability or growth cone filopodia by forming stable actin bundles with cortactin in a GTPase dependent manner (Yamada et al. 2013). In a more recent study dynamin-1 was also found to directly interact with Insulin Receptor tyrosine kinase Substrate protein of 53 kDal (IRSp53) which is activated by Cdc42 and is required for filopodia formation. By knocking out dynamin-1 filopodia formation was reduced and this could not be rescued by the actin binding mutation K/E suggesting that the direct interaction between dynamin and actin is required during filopodia formation in neuroblastoma cells (Chou et al. 2014).

These data suggest that dynamin is required for actin organisation during cell migration and that its role is dependent on interactions with actin regulatory proteins cortactin and IRSp53. Moreover dynamin-1 and 2 requires its ability to hydrolyse GTP and directly bind to actin to function in lamellipodia and filopodia formation.

1.5.5 Dynamin and actin in podosomes and invadopodia

Podosomes and invadopodia are highly dynamic, actin rich structures that protrude from a cell and form attachments with the extracellular matrix (ECM). They contain a dense filamentous actin core surrounded by an actin cloud (consisting of short filaments of actin) and can form singly or combine to create structures called rosettes (Luxenburg et al. 2007). Their role is to facilitate a cells movement through tissues and they do so through attachments to the ECM and the secretion of proteases, such as the transmembrane matrix metalloprotease MT1-MMP (Poincloux et al. 2009), to break down the ECM in order to move through it (reviewed in Linder et al. 2011).

The term ‘podosome’ was initially coined due to its attachment to the ECM which formed structures appearing to be cell feet (Tarone et al. 1985). The differentiation between podosomes and invadopodia has been debated, however it is now generally accepted that invadopodia are more invasive due to a higher ECM degradation ability, they are longer lived and are mainly present in cancer cells, created for metastasis (Artym et al.; Linder et al. 2011). Podosomes however are mainly found in healthy cell processes are smaller in size and have a shorter lifetime. Overall podosomes and invadopodia are similar and when talking about

characteristics of both structures the name 'invadosome' will be used, a term now widely used in most literature on the subject (reviewed in Linder 2009).

Dynamin has been found to localise to invadopodia and is required for their organisation (Ochoa et al. 2000; Baldassarre et al. 2003; Destaing et al. 2013) figure 10. It was found that by knocking down dynamin expression in cells the invasiveness of invadopodia was reduced suggesting it is required for efficient invadosome function (Baldassarre et al. 2003). This reduction in invasiveness was also seen when dynamin was depleted directly by a photo-activated 'killer red' protein which provided a direct knockdown mechanism in mouse fibroblasts. This study also found that the removal of dynamin function caused the invadosomes to become disordered suggesting a role for dynamin in actin organisation within these structures (Destaing et al. 2013). Moreover by removing dynamin GTPase function by the mutation K44A it was found that the actin turnover at podosomes was reduced suggesting that actin organisation within podosomes requires a functional dynamin enzyme (Ochoa et al. 2000). The formation of podosomes was prevented by the removal of the PRD domain of dynamin suggesting that interactions with SH3 domain containing proteins is required for invadosome formation (Baldassarre et al. 2003). It is probable that dynamin functions with cortactin in invadosome formation and actin organisation. Cortactin is known to be required for invadosome maturation and in the secretion of metalloproteases and is regularly used as a marker for these structures (Clark et al. 2007; Oser et al. 2009). Therefore the need for a direct dynamin-cortactin interaction could be the reason why dynaminΔPRD causes a reduction in invadosome function (Baldassarre et al. 2003).

These data indicate that dynamin is required for the formation and function of invadosomes. There is evidence that this is due to its role in actin organisation however whether this requires a direct dynamin-actin interaction has yet to be determined.

1.5.6 Dynamin in actin comet tails

A number of bacterial pathogens are known to hijack actin for entry and proliferation in cells. For example *Listeria* are known to propel themselves through the cell cytoplasm using actin comet tails. These can also be used to push the bacteria from one cell into another to avoid immune detection (reviewed in Ireton et al. 2014). Both dynamin-1 and 2 have been found to localise to actin comets made by *Listeria* and also comets formed by the overexpression of PIP kinase (type 1-PIPK1γ) (Lee & De Camilli 2002; Orth et al. 2002; Henmi et al. 2011) figure 10. PIP kinase increases the amount of PIP2 in a cell so that the vesicles are PIP2 rich, preventing the disassembly of actin regulatory proteins after endocytic scission and inducing an actin comets to propel the vesicles through the cell (Rozelle et al. 2000).

Overexpression of PIP kinase therefore provides a way of testing the components of an actin comet without the requirement for *Listeria* infection. It was found that dynamin requires its PRD domain in order to be recruited to actin comets, and without dynamin recruitment the speed of vesicle movement by actin comets was reduced (Lee & De Camilli 2002; Orth et al. 2002). Interestingly the removal of the PRD domain in dynamin-2 was found to reduce actin tail formation in HeLa cells (Lee & De Camilli 2002) but increase actin tails in rat fibroblasts (Orth et al. 2002) (both were tested using actin comets induced by the overexpression of PIP kinase). It is known that dynamin-1 can displace gelsolin from actin to increase actin polymerisation (Gu et al. 2010) and therefore this could be that the removal of PRD in rat fibroblasts does not effect this function however in Hela cells other mechanisms may override this ability of dynamin reducing the actin comet.

The function of dynamin in actin comets requires its GTPase activity as mutations which prevent this (K44A) cause a reduction in actin comet length and a reduced speed (Lee & De Camilli 2002; Orth et al. 2002; Henmi et al. 2011). It could be that this function is required when forming complexes with cortactin which can directly impact actin filaments however, it was found that dynamin-2 knockdown, but not cortactin knockdown, reduced actin tail formation (Henmi et al. 2011). This provides evidence that dynamin-2 may influence the actin network independently of cortactin however whether this is through its direct actin binding ability has yet to be determined.

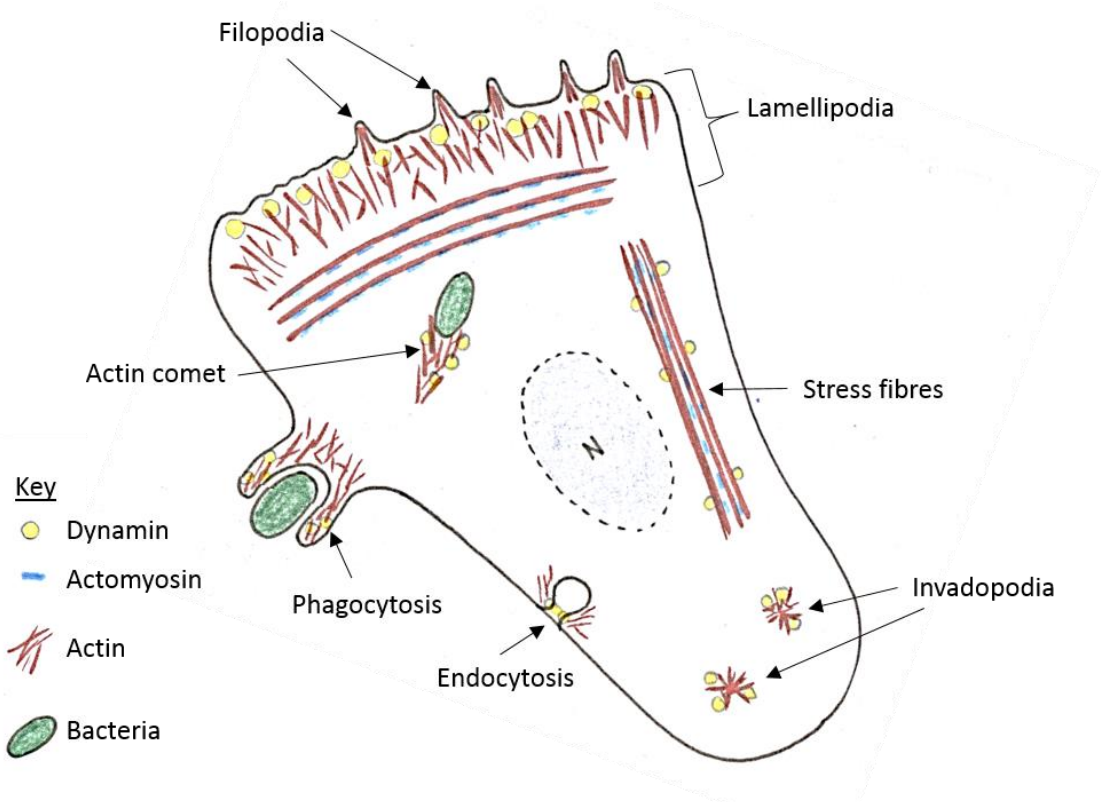

Figure 10. Cellular processes in which both dynamin and actin take part. This diagram has been modified from Menon and Schafer 2013. It shows the various cellular processes which involve both dynamin and actin.

In conclusion, the direct dynamin-actin interaction has yet to be fully investigated in mammalian cellular processes, including endocytosis. There is an understanding that during endocytic events both actin and dynamin are present and that dynamin is fundamental to the scission process, but how they may interact directly during CME has not been elucidated. Therefore this project set out to investigate the direct dynamin-actin interaction and its function during endocytosis. The role of actin during the scission stage of CME in both yeast and mammals has yet to be fully defined and this is further complicated when studying a mammalian cell system as the reliance on actin for endocytic events changes depending on cell type and how they may be responding to the environment around them. In yeast however, actin is always required and therefore using *Saccharomyces cerevisiae* as a model organism provides an opportunity to identify more easily how actin may function during endocytic events right up to and including scission. Moreover, yeast contain a dynamin-like protein, Vps1, which has been shown to act during endocytic scission events (Smaczynska-de Rooij et al. 2010). Vps1 shares amino acid sequence orthology with dynamin-1 and investigating how Vps1 and actin may function together during yeast CME could identify new ways in which mammalian dynamin-1 and actin function together *in vivo*.

1.6 Vps1

Vps1 stands for Vacuolar Protein Sorting-1 and it was discovered, along with a large number of other proteins, during genetic screens to identify genes required for trafficking proteins to the vacuole (equivalent to the mammalian lysosome) in yeast. Investigations into vacuolar protein sorting molecules began in the mid to late 1980's including genetic screens which isolated both Vacuolar Protein Targeting (*VPT*) and Vacuolar Protein Localising (*VPL*) genes (Bankaitis et al. 1986; Robinson et al. 1988; Banta et al. 1988; Rothman & Stevens 1986). In 1989 it was collectively decided that all of the genes isolated as involved in vacuole protein localisation/targeting were to be re-named as Vacuolar Protein Sorting (*VPS*) for clarity (Rothman et al. 1989).

In 1990 *VPS1* was isolated, sequenced and found to be orthologous with the anti-viral MxA protein and rat dynamin-1 (Obar et al. 1990; Rothman et al. 1990). It was understood at that time that classical dynamin proteins bound to microtubules and therefore it was predicted that Vps1 would also function with microtubules during its role in Golgi to vacuole trafficking. However, yeast cells treated with the microtubule binding drug nocodazole (which prevents microtubule polymerisation) showed no defect in vacuole protein miss-localisation

and therefore it was concluded that the role of Vps1 *in vivo* was not microtubule dependent (Vater et al. 1992).

Since the early studies, Vps1 has been shown to share orthology with dynamin-like proteins as it harbours a GTPase domain, a middle coiled-coil region and a GTPase effector domain (GED). This is shown diagrammatically in figure 11B and is compared with mammalian dynamin (figure 11A). Vps1 has been shown to be able to bind and tubulate lipids (Smaczynska-de Rooij et al. 2010) despite not containing a PH domain which, in dynamin, has been shown to facilitate lipid binding. Vps1 also does not contain a proline rich domain required in classical dynamins to bind SH3 domain containing proteins. Vps1 does however, have an insert A and insert B regions found in the GTPase domain and N terminus of the middle domain respectively (figure 11B). The role of the insert A region has yet to be established however the insert B region has been demonstrated to bind SH3 domain containing proteins (Smaczynska-de Rooij et al. 2012).

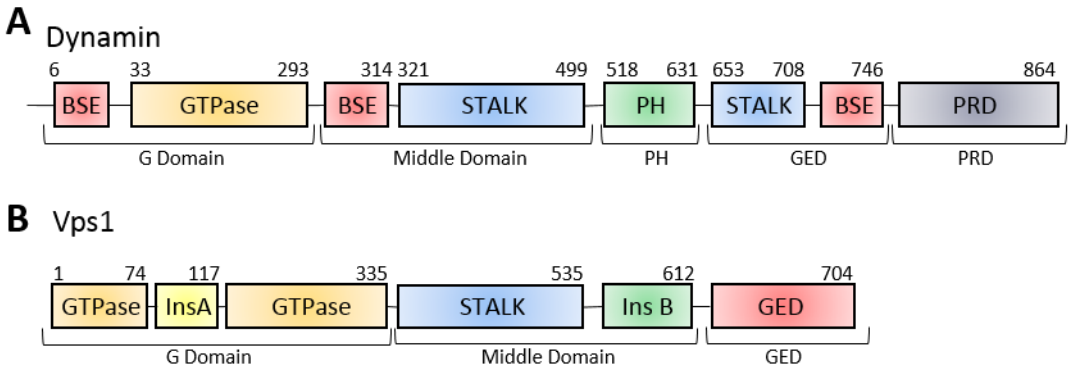

Figure 11. Domain structure of both Vps1 and dynamin-1 A) The domains found within dynamin-1. B) The domains within Vps1. Please note the additional insert A and B coloured yellow and green respectively. The amino acids are indicated above each diagram.

Vps1 is one of three dynamin-like proteins in yeast. Dnm1 and Mgm1 also share orthology with mammalian dynamin proteins (reviewed in Williams & Kim 2014). Mitochondrial genome maintenance 1 (Mgm1) is an inner mitochondrial membrane protein which is required fusion of inner mitochondrial membranes. Mgm1 can hydrolyse GTP, self-assemble and bind lipids and all three characteristics are required for its membrane fusion ability (Abutbul-Ionita et al. 2012; Meglei & McQuibban 2009). Mgm1 is orthologous to the mammalian protein OPA1 (Alexander et al. 2000) which is also required for mitochondrial membrane fusion indicating Mgm1 function is evolutionarily conserved.

Dnm1 is a dynamin-like protein which is involved in mitochondrial fission and without Dnm1 yeast cells form elongated mitochondria to create a mitochondrial 'net' like structure (Bleazard et al. 1999). Dnm1 is orthologous to the dynamin like protein Dlp1 (Smirnova et al.

1998) and structural changes within Dnm1 enable its function in mitochondrial fission (Mears et al. 2011). Dnm1 also functions in peroxisomal fission as described in section 1.6.4.

1.6.1 The role of Vps1 in endocytosis

Vps1 has been shown to function in endocytosis (Yu & Cai 2004; Smaczynska-de Rooij et al. 2010). It was found that, of the three dynamin-like proteins in yeast (Dnm1, Mgm1 and Vps1), only the deletion of the *VPS1* gene caused an endocytic defect where the uptake of the pheromone receptor Ste3 was delayed and Sla1 was miss-localised (Yu & Cai 2004). Sla1 functions at the early stages of endocytosis (figure 3) and it was suggested by co-immunoprecipitation that Vps1 could bind Sla1. During the same study it was found that *vps1* null cells have a disrupted actin cytoskeleton where cortical actin patches are unpolarised throughout the mother and bud of a yeast cell.

The removal of *VPS1* from cells causes an increase in the lifetimes of fluorescently tagged endocytic proteins such as Sla2-GFP, Abp1-GFP and Las 17-GFP. Furthermore Vps1-GFP has been reported to co-localise with Sla1-GFP (Smaczynska-de Rooij et al. 2010). By tracking the accumulation of these endocytic markers *in vivo* it was discovered that Vps1 GTP hydrolysis and the corresponding GED domain are both required for efficient endocytic uptake (Nannapaneni et al. 2010). Moreover, it was discovered that Vps1 can bind and tubulate lipids *in vitro* indicating that this protein functions like classical dynamins at the scission stage of endocytosis (Smaczynska-de Rooij et al. 2010). Oligomerisation of Vps1 has been reported to be prevented by the mutation I649K which is orthologous to the I690K mutation, reported to prevent higher order oligomerisation of the classical dynamin-1 (Song et al. 2004). The presence of I649K in Vps1 was found to inhibit the ability of Vps1 to tubulate lipids *in vitro* however, *in vivo* this mutation was found to cause the creation of long invaginations (Mishra et al. 2011). This suggests that the role of Vps1 is more involved at the point of scission rather than during invagination and that there could be other proteins involved enhancing the tubulation at this site. An obvious candidate for this is the BAR domain protein Rvs161/167 which functions at the scission stage of endocytosis and is able to tubulate lipids (Friesen et al. 2006; Colwill et al. 1999). It could be that without the ability of Vps1 to oligomerise for scission the tubulation of Rvs167/161 continues creating long tubules into the cell.

The BAR domain containing protein Rvs167 has been found to bind directly to Vps1 by yeast two hybrid and biomolecular fluorescence complementation assay (BiFC) (Smaczynska-de Rooij et al. 2012). During the same study it was hypothesised that Vps1 may bind Rvs167 through its insert B region. This region was selected as Vps1 does not have a proline rich domain like classical dynamins however does contain a proline motif in insert B which was predicted to bind SH3 domains. To test this a point mutation was made P564A. Expression of

this in yeast increased the lifetimes of Las17 and Sla2, not unlike *vps1* null cells, and decreased the lifetime of Rvs167-GFP at an endocytic site which suggested that by reducing Rvs167 binding this reduced endocytic scission. Correspondingly, this P564A mutation creates long invaginations into the cell indicating a scission defect (Smaczynska-de Rooij et al. 2012). This was similar to the I649K mutation (Mishra et al. 2011) which could suggest that the interaction between Vps1 and Rvs167 requires oligomerised Vps1 *in vivo*. It was also discovered that Rvs167 caused disassembly of Vps1 from lipid tubules *in vitro* a function which did not take place when the mutation P564A was present. This suggests a negative feedback mechanism between Rvs167 and Vps1 which, when disrupted, causes the development of long tubules into the cell presumably by oligomerised Vps1.

1.6.2 Vps1 in Vacuole morphology

Initial genetic screens identified *VPS* genes which, when deleted, hindered the maturation of the carboxypeptidase Y protein (CPY) from the Golgi to the vacuole (Rothman et al. 1989). Fluorescence studies of the vacuole morphology subsequently identified three classes of vacuole phenotype (A-C) when *VPS* genes were deleted (Banta et al. 1988). To do this, yeast cells were exposed to a fluorescent dye (FITC) which was taken up into the vacuole and provided a mechanism by which the vacuole morphology could be assessed by microscopy. The three initial classes were then increased to six (A-F) after an in depth analysis of these vacuole phenotypes found further differences between vacuole morphologies when different *VPS* genes were deleted (Raymond et al. 1992). Mutating the *VPS1* gene caused the vacuole morphology to be fragmented with one large vacuole surrounded by smaller vacuole structures which is described as Class F phenotype (Raymond et al. 1992). This suggested that Vps1 was required for the correct morphology of the vacuole and this is potentially due to a role of Vps1 in vacuole fusion. Vacuole fusion is known to require SNARE (Soluble *N*-ethylmaleimide-sensitive-factor Attachment protein REceptor) proteins and it has been recently discovered that the self-assembly of Vps1 is involved in the formation of these SNARE protein complexes (Kulkarni et al. 2014). Vps1 was also found to directly bind the v-SNARE (vesicle-SNARE) Vam3 and stimulate v and t-SNARE (target-SNARE) complex for vacuole fusion. Interestingly this was prevented when cells were exposed to the dynamin drug dynasore (Macia et al. 2006) suggesting the GTPase activity of Vps1 is required for its function in vacuole fusion (Alpadi et al. 2013). However dynasore (Macia et al. 2006) is known not only to block dynamins GTPase function, but to also have a number of off target effects (Park et al. 2013) therefore the role of Vps1 GTPase in vacuole fusion still requires further investigation. This model suggests that Vps1 is involved in SNARE protein accumulation and function in vacuole membrane fusion.

1.6.3 The role of Vps1 in Golgi membrane trafficking

The protein carboxypeptidase Y (CPY) is required for breaking down proteins in the yeast vacuole. It is synthesised in the endoplasmic reticulum as an inactive protein (Hasilik & Tanner 1978) and trafficked to the Golgi as this precursor (pCPY) for further modifications. pCPY is then trafficked from the Golgi to the vacuole where it is cleaved to become an active mature CPY (mCPY). Accumulation of pCPY in comparison to mCPY indicates a defect in CPY trafficking (Rothman et al. 1989). When *VPS1* is deleted there is an accumulation of pCPY and CPY also gets secreted from the cell (Rothman et al. 1989) indicating that Vps1 is required for Golgi-vacuole traffic.

Vps1 has also been described to be involved in endosome to Golgi traffic in the localisation of the endoprotease Kex2. Kex2 is involved in the production of the α factor pheromone and shuttles from the endosomes to Golgi. Mutations to Vps1 miss-localises Kex2 from Golgi to the vacuole which leads to a reduction in α factor secretion (Wilsbach & Payne 1993). From this data it was concluded that Vps1 function acts to retain proteins in the Golgi, however it may also be linked to the role of Vps1 in endosome to Golgi trafficking as it was found that without Vps1, Kex2 is re-directed to the plasma membrane rather than the Golgi and reaches the vacuole by endocytosis (Nothwehr et al. 1995).

1.6.4 The role of Vps1 in peroxisomal fission

Peroxisomes are membrane bound organelles required for β-oxidation during fatty acid metabolism (van der Klei & Veenhuis 1997) and the breakdown of reactive oxygen species such as hydrogen peroxide (reviewed in Gabaldón 2010). Peroxisomes undergo fission, so as to distribute the organelle between the mother and bud cells in yeast division, and this was found to be dependent on Vps1. Upon deletion of *VPS1*, cells form long peroxisomes which are less able to undergo scission, a phenotype which was not observed when *dnm1* or *mgm1* were deleted (Hoepfner et al. 2001). The double deletion *vps1 dnm1* cells show a more marked elongated peroxisome phenotype and interestingly this can be rescued by an overexpression of Dnm1 (Motley & Hettema 2007). This suggests that Vps1 and Dnm1 can both function to facilitate peroxisome fission.

1.6.5 The role of Vps1 in endosome recycling

Vps1 has been implicated in both early endosome to Golgi traffic as well as late endosome to vacuole traffic (Hayden et al. 2013; Nannapaneni et al. 2010). It has been discovered that when *VPS1* is deleted from the genome, endosomes marked with the lipid dye FM4-64, took a longer time to reach the vacuole in comparison to WT *VPS1* cells. This is also the case when Vps1 harboured GTPase mutations and when actin was disrupted (Nannapaneni et al. 2010). There is also an increase in the number of endosomes in the cytoplasm and Vps1 was found to co-localise with the late vacuole suggesting that it is required for late endosome to vacuole traffic (Hayden et al. 2013). Endosome recycling is important for the regulation of proteins at the plasma membrane such as Snc1 which is a v-SNARE protein involved in the exocytosis of vesicles. After an exocytic event Snc1 is recycled back into the cytoplasm to be re-used for another exocytosis event (Lewis et al. 2000). Without Vps1, Snc1 is found to accumulate in the cytoplasm (Lukehart et al. 2013; Smaczynska-de Rooij et al. 2010) indicating that Vps1 is required for Snc1 recycling back to the plasma membrane.

1.7 Summary

Our understanding of dynamin function in cells has been, until recently, heavily focused on its role during endocytic scission. However dynamin proteins, especially dynamin-2, have other functions in a cell and many of these roles are also dependent on actin. The discovery that dynamin can bind directly to actin has indicated that there are new levels of regulation and signalling in these processes that are now open to be investigated. In order to understand these, model organisms, such as yeast, will be invaluable to gain a detailed insight into the interaction between dynamin and actin in processes such as endocytosis. Our understanding of yeast endocytosis has provided data into how actin is required to overcome turgor pressure, however it is unclear whether the role of actin is also required to facilitate scission. The yeast dynamin Vps1 is present at this stage and may provide a tool to assess if the dynamin-actin interaction may be evolutionarily conserved and if it is required during multiple cellular processes. Vps1 is not essential for endocytosis and its role in this process is still being elucidated. By investigating a Vps1-actin interaction this could uncover processes in yeast which require both Vps1 and actin as well as create a more defined description of the role of Vps1 in yeast endocytosis.

1.8 Project Aims

This project aims to test the following hypotheses:

1. The actin-dynamin interaction is evolutionarily conserved.
2. The direct Vps1-actin interaction is required for membrane remodelling functions in vivo including endocytosis.
3. There are residues within the middle domain of Vps1 that are required for actin binding and these can be more specifically assigned to an actin binding region within the protein.
4. Specific orthologous residues (identified in number 3) can be used to define the actin binding site of human dynamin-1 more clearly.
5. The residues described in 4, are required for actin binding and dynamin-1 cellular functions including endocytosis.

Chapter 2

Materials and Methods

Unless otherwise stated all materials were obtained from the following suppliers: Sigma, Fischer Scientific, Gibco or BDH Chemicals. Tables of plasmids, oligonucleotides, yeast strains and antibodies used can be found in section 2.7.

2.1 Bacterial methods

2.1.1 Bacterial growth conditions

Escherichia coli (E.coli) strains DH5α, BL21 (DE3), C43/C41(DE3) (Lucigen) and XL-10 Gold (Stratagene) were grown at 37°C, in 5 ml liquid 2xYT media (1% (w/v) yeast extract, 1.6% (w/v) tryptone, 0.5% (w/v) NaCl + 2% (w/v) agar for solid media) with either ampicillin (100 µg/ml) or kanamycin (30 µg/ml) as required for selection.

2.1.2 Bacterial transformation

25 µl of competent bacteria[3] and 80-150 ng of the plasmid required for transformation were incubated on ice for 30 minutes to 1 hour. For plasmid DNA purification DH5α or XL-10 Gold (Stratagene) *E.coli* were used, and for protein purification BL21 (DE3) or C41/43 (DE3) *E.coli* (Lucigen) were used. After incubation, the bacteria were then moved to 42°C for 40 seconds before being returned to ice for 2 minutes. 0.5 ml of non-selective medium (2xYT or, for XL-10 Gold cells, NZY$^+$ broth as per manufacturer's direction) were added before the cells were left to recover for 1 hour in a shaking incubator at 37°C. The bacteria were then harvested by centrifugation (3000*g,* 3 minutes), the non-selective medium was then removed, and the bacteria were re-suspended in 200 µl of non-selective media before plating on agar with the required antibiotic for selection (see 2.1.1) and incubated overnight at 37°C.

[3] Competent *E.coli* were made in house through incubation with ice-cold 0.1 M $CaCl_2$. The *E.coli* were then re-suspended with additional 10% (v/v) glycerol and stored at -80°C.

2.1.3 Glycerol stocks of bacterial cultures

E.coli glycerol stocks were made of *E.coli* cultures in order to store plasmids for future use. Bacteria were transformed with the required plasmid (2.1.2) and from the plated bacteria a single colony was selected and grown overnight (2.3.1). 750 µl of this bacterial culture was mixed with 750 µl of 50% (v/v) glycerol and stored at -80^{o}C in a cryovial.

2.2 Molecular biology

2.2.1 Plasmid purification by Mini or Maxi prep

All DNA plasmids were transformed into *E.coli* DH5α as described (2.1.2) and grown in the appropriate volume of media. The plasmids were then purified using either a Mini or Maxi prep kit (QIAGEN) according to the manufacturer's protocol. Briefly, cells were lysed using detergent based alkaline solution, and DNA was bound to either a silica anion exchange membrane or silica resin for Mini and Maxi preps respectively. The purified DNA was then eluted into sterile deionised water (preceded by isopropanol precipitation in the case of the Maxi prep procedure). Plasmid concentrations were analysed using either a spectrophotometer (Jenway 7315) at 260 nm in a quartz cuvette (10 mm path length) or using NanoDropLite (Thermo Scientific) before being stored at -20^{o}C for future use.

2.2.3 Site directed mutagenesis

Site directed mutagenesis (SDM) was carried out using the QuikChange® Lightning kit (Stratagene). The following mixture was made;

5 µl of 10x reaction buffer
10-50 ng/µl of dsDNA plasmid
125 ng Forward primer
125 ng Reverse primer
1 µl dNTP mix
1.5 µl Quik solution
1 µl *PfuTurbo* DNA polymerase (2.5 U/µl)

Made up to 50 µl with sterile deionised water.

This was then exposed to the following PCR reaction;

Order	Cycles	Temperature	Time
1	1	95°C	2minutes
2	16	95°C	20 seconds
		60°C	10 seconds
		68°C	30 seconds/kb plasmid length
3	1	68°C	5 minutes
4	1	4°C	10 minutes/Hold

To remove any remaining template plasmid, 2 µl of the enzyme Dpn1 (10 U/µl) were added to the resulting PCR product for 10 minutes at 37°C. Following this, 2 µl of the reaction was then transformed into XL-10 Gold cells, which came as part of the SDM kit, as per the manufacture's instruction. The resulting colonies that were found growing on the appropriate antibiotic plate were then grown up in selective medium and purified via Mini prep (2.2.1). Plasmids were then analysed by restriction digest (2.2.4) before being sent to DNA sequencing and services at the University of Dundee for sequence analysis to confirm the incorporation of the correct mutation.

2.2.4 Restriction enzyme digest of plasmid DNA

Before sending plasmids away for sequencing they were analysed by restriction enzyme digest. Restriction enzymes from New England BioLabs were used, along with the provided buffers and required plasmid DNA in the following mixture;

0.2 µl BSA
2 µl 10 x Reaction Buffer
0.5 µl enzyme (volume modified depending on the activity of the enzyme required)
1 µl dsDNA (50-100 ng)
Made up to 20 µl with sterile deionised water

This mixture was then incubated at 37°C for 2 hours before being analysed by agarose gel electrophoresis (2.2.5).

2.2.5 Agarose gel electrophoresis

DNA samples and restriction digest products were mixed with loading buffer (1x stock; Orange G 0.035% (w/v), 3% (v/v) glycerol) at a ratio of 10:1. Each sample was loaded into separate wells of a 0.8% (w/v) agarose gel containing ethidium bromide (0.5 mg/ml) alongside 5 µl of Hyper Ladder 1 size marker (Bioline). The gel was run at 100 V in 1xTAE buffer (10 mM Tris-acetate pH 7.5, 1 mM EDTA pH 7.5) until the loading dye had run to the desired distance. The gel was then imaged on a UV trans-illuminator (UVitec with Mitsubishi P91 printer).

2.3 Protein methods

2.3.1 Growth conditions of E.coli used for recombinant protein expression

Plasmids containing the required recombinant protein for expression were transformed into either BL21(DE3) or C41/C43 *E.coli*, as described in 2.1.2. The resulting colonies were scraped from the plate into 1 L of sterile 2xYT media containing ampicillin (100 µg/ml) and grown overnight at 37^{o}C (30^{o}C for expression of 6xhis-tagged Vps1) in a shaking incubator set at 175 rpm. Protein expression was induced via the addition of isopropyl β-D-1-thiogalactopyranoside (IPTG) to a final concentration of 1 mM and the *E.coli* culture was left in the shaking incubator for a further 6 hours (for 6xhis tagged Vps1 this step was also carried out at 30^{o}C rather than 37^{o}C). The 1 L cultures were then centrifuged at 6000 rpm for 12 minutes at 4^{o}C in a Beckman Coulter® Avanti J-26 XP centrifuge in a fixed angle JLA 8.1 rotor and the supernatant was removed. The resulting pellet was stored at -20^{o}C until further use and, in the case of Vps1 purifications, never left at -20^{o}C for longer than one month.

2.3.2 Preparation of E.coli cell lysates for protein purification

The appropriate cell pellets were thawed from -20^{o}C and re-suspended in 10 ml 1xPhosphate-Buffered Saline (PBS) (13.7 mM NaCl, 2.7 mM KCl, 10 mM Na_2HPO_4, 1.76 mM KH_2PO_4) with 200 µl 25x protease inhibitor cocktail (Roche). The cells were then lysed by cycles of 30 second sonication (Sanyo Soniprep 150 at amplitudes between 10-15 µm) and a 30 second rest in ice, repeated up to 6 times. The lysate was then spun at 21,000*g* in a Sigma 4K15 centrifuge (rotor 12169-H) for 40 minutes. The supernatant was then passed through 0.2 µM filters (Minisart) and then the filtrate was used for the appropriate protein purification technique as described 2.3.3 and 2.3.4.

2.3.3 6xhis tag purification

Recombinant 6xhis tagged Vps1 was expressed from plasmid pKA 850 (and all mutations introduced into this plasmid) in *E.coli*, lysed (2.3.1) and purified using a his trap column (HisTrap™ GE Healthcare) as described previously (Smaczynska-de Rooij et al. 2010). Briefly, bacterial cell lysate (as prepared in 2.3.2) was passed through the 6xhis trap column, washed and eluted with imidazole (500 mM imidazole in Start buffer: 20 mM NaH_2PO_4, 0.5 M NaCl, 20 mM imidazole pH 7.4). Unless otherwise stated, the recombinant purified Vps1 was then buffer exchanged using a PD-10 column (GE Healthcare) into F-buffer (2 mM Tris, 0.2 mM CaCl, 10 mM Imidazole (pH 7.2), 1 mM EGTA, 2 mM EDTA, 150 mM KCl) without MgCl in order to prevent Vps1 oligomerisation as much as possible. Buffer-exchanged recombinant Vps1 was then either used at this stage, or pre-spun to remove any oligomerised protein in an ultra-centrifuge at 90,000*g* for 15 minutes at 4°C. Unless otherwise stated, purified recombinant Vps1 used in the *in vitro* assays came from the resulting supernatant, the concentration of which was usually between 1-5 µM (as estimated by a Bradford assay 2.3.10.1). Un-spun Vps1 protein concentrations ranged between 8-12 µM. Recombinant Vps1 protein was only used in an assay on the same day as its purification.

2.3.4 Glutathione-S-transferase (GST) tag purification

E.Coli were lysed as described in 2.3.2. Afterwards, 0.05 mg/ml of lysozyme was added with the necessary co-factors $MgCl_2$ and $MnCl_2$ (added to a final concentration of 10 mM and 1 mM respectively) and incubated at 4°C for 10 minutes before centrifugation (see 2.3.2). The supernatant was then mixed with 300-500 µl glutathione Separose beads (GE Healthcare) which had been washed prior to this step in 15 ml 1xPBS three times. The lysate and bead slurry was incubated at 4°C for at least 1 hour with rotation. The beads were then washed three times in 1xPBS + 1% (v/v) Triton and 300 mM NaCl, three times in 1xPBS and then twice in buffer A (20 mM HEPES pH 7.4, 150 mM NaCl, 1 mM DTT see 2.3.7). The GST-fusion protein was kept on beads at 4°C and used within 24 hours.

In this thesis, this purification technique was used to purify the recombinant SH3 domain of amphiphysin-2 onto glutathione Sepharose for dynamin affinity purification (see 2.3.7). Therefore, this protocol did not require cleavage of the purified protein from the GST beads.

2.3.5 Purification of rabbit actin

Preparation of rabbit skeletal muscle acetone powder (Spudich & Watt 1971)

As much of this protocol as possible was carried out in a 4°C room with all required buffers, deionised water and equipment pre-chilled to this temperature. The hind leg muscles from 2-4 freshly killed rabbits (from either the University of Sheffield animal house or from Woldsway Food Ltd., Spilsby, Lincs., UK) were removed and quickly stored in ice. Fat and connective tissues were removed and the muscle passed twice through a Porkert mincer before being mixed with 3 volumes of Guba Straub buffer (300 mM NaCl, 100 mM NaH_2PO_4, 50 mM $NaHPO_4$, 1 mM NaN_3, 1 mM $MgCl_2$, 1 mM $Na_4P_2O_7$, 0.05 mM PMSF, 2 mM ATP pH 6.5) and stirred for 15 minutes so that the binding of ATP removes myosin. This was then centrifuged at 3000*g* for 20 minutes and the supernatant removed. The pellet was then re-suspended in 1 L of Buffer I (0.04% (w/v) $NaHCO_3$, 0.01 mM $CaCl_2$) plus 9 L of deionised water and stirred again for 15 minutes. The muscle residue was then filtered through two layers of cheesecloth and re-suspended in 1 L Buffer II (10 mM $NaHCO_3$, 10 mM Na_2CO_3, 0.1 mM $CaCl_2$), stirred for 10 minutes, and filtered again through cheesecloth. The residue was then re-suspended in 10 volumes of deionised water and quickly filtered through cheese cloth, as muscle swells at low ionic strength causing G-actin to be lost in solution. The muscle residue was then then re-suspended in 2.5 litres of Acetone (Fisher Scientific). This mixture was then stirred and left to stand for 15 minutes before filtration through two layers of cheesecloth. The acetone washing step was repeated until the filtrate was clear. After this stage the muscle residue was spread evenly across filter paper (Whatman 3 mm) and left to dry overnight in a fume hood. The resulting acetone powder was collected, weighed and stored at -80°C.

Actin purification from acetone powder

This protocol is based on the actin purification method published in Spudich & Watt 1971 and Winder et al. 1995. 5 g of acetone powder was re-suspended in 100 ml G-Buffer (2 mM Tris-HCl (pH 8), 0.2 mM $CaCl_2$, 1 mM NaN_3, 0.5 mM DTT, 0.2 mM ATP) and stirred slowly on ice for 30 minutes. The solution was then centrifuged at 20,000*g* for 30 minutes before filtering the supernatant through glass wool, followed by 0.45 µm and 0.2 µm filters (Minisart). The actin was then polymerised with the addition of $MgCl_2$ and KCl to a final concentration of 2 mM and 800 mM respectively. The solution was stirred slowly at room temperature (RT) and then at 4°C for 30 minutes each. The resulting F-actin solution was centrifuged at 35,000 rpm (Beckman Coulter Optima L-90K) in a Ti45 rotor at 4°C for two hours. The supernatant was then removed and the pellet carefully re-suspended in G-buffer with a glass-teflon homogeniser and loaded into dialysis tubing. The actin was dialysed in G-buffer refreshed 3 times a day for at least 2 days. To remove any remaining F-actin the solution was centrifuged

once more at 35,000 rpm (Beckman Coulter OptimaMax 130K) in an MLA80 rotor for 2 hours at 4°C. The clear supernatant was removed (leaving the last 1 ml behind) and was gel filtered on a Sephacryl S300 gel filtration column (Amersham XK26) with G-buffer. Actin was collected in 3-5 ml fractions using an Amersham LKB RediFrac collector. The concentration of these actin fractions was determined via spectrophotometry (taken at 290 nm so as to avoid read out at 280 nm from ATP absorbance). G-actin was stored at 4°C and used within 1 month of preparation.

2.3.6 Purification of yeast actin

This method followed the protocols described in Goode et al. 1999 and Goode 2002. Briefly, commercially available baker's yeast (*Saccharomyces cerevisiae*) (Sainsbury's) was lysed with a cell disrupter (Constant systems) and frozen, drop-wise, in liquid nitrogen before being stored at -80°C. The lysis step was carried out by Dr. Ellen Allwood. When required, 100*g* yeast lysate was thawed in 100 ml G-buffer (2 mM Tris-HCl, 0.2 mM $CaCl_2$, 1 mM NaN_3, 0.5 mM DTT, 0.2 mM ATP) and spun at 21,000*g* for 30 minutes in a Sigma 4K15 centrifuge (rotor 12169-H). The rest of the protocol took place at 4°C. The supernatant was loaded on to a DNAse 1 column[4] with the use of a peristaltic pump (Gilson Minipuls3) at 5 ml/minute. This is washed with G-buffer for 1 hour at either the same speed or reduced slightly to 2 ml/minute, then washed with the following (in order):

- 5% (v/v) formamide
- 5% (v/v) formamide, 0.2 M NH_4Cl
- G-buffer
- Elute 50% (v/v) formamide in 5 ml fractions

The eluate was then dialysed overnight in G-buffer and the concentration of G-actin was determined by gel electrophoresis. Finally, the purified G-actin solution was split into aliquots, snap frozen in liquid nitrogen, and stored at -80°C.

[4] Making the DNAse 1 column: 200 mg DNAse 1 dissolved in 10 ml coupling buffer (0.1 M HEPES pH 7.2, 80 mM CaCl2, 1 mM PMSF) was dialysed overnight in coupling buffer. 25 ml Affigel-10 resin (BioRad) was washed five times with ice cold deionised water, then twice with ice cold coupling buffer before being added to DNAase 1 solution. This was incubated with rocking for 3 hours at 4°C before being poured into an XK16 Pharmacia Biotech column. The resin was then washed with 15 column volumes of coupling buffer and pre-equilibrated with 5 volumes of G-buffer.

2.3.7 Dynamin purification

Human dynamin-1 (pKA 1108 table 2.8.1) was expressed via transient transfection of SF21 cells and then purified either by affinity purification with the amphiphysin-2 SH3 domain alone (Chappie et al. 2009) or (in later preps) with the addition of a nickel bead binding step to increase purity (see chapter 6 section 6.2).

2.3.7.1 SF21 cell growth and transfection

SF21 insect cells were grown at 27°C in SF900™ III SFM media (Gibco) with 5% (v/v) Foetal Bovine Serum (FBS) in suspension culture and passaged every other day from $2x10^6$ cells/ml to $0.5x10^6$ cells/ml. On the day of transfection around 200 ml of cells at $1x10^6$ cells/ml were moved into serum-free media and transfected by adding transfection reagent[5] containing 200 µg DNA and transfection medium[6] to the cell suspension. This was then left for 48 hours before the cells were harvested by centrifugation at 3000*g* for 30 minutes and flash frozen in liquid nitrogen. Cell pellets were stored at -80°C until required for protein purification.

2.3.7.2 Amphiphysin-2 SH3 affinity purification

An SF21 cell pellet was thawed and cells were re-suspended in 10 ml Buffer A (20 mM HEPES pH 7.4, 150 mM NaCl, 1 mM DTT) containing protease inhibitor cocktail (Roche) at a working concentration of 0.5x with 2.5 µM Pepstatin, 25 µM Leupeptin and 2 µM phenylmethanesulfonylfluoride (PMSF). The cells were then lysed by being passed twice through a French press (Thermo Electron Corporation Cat No. FA-078A 120 VAC 60 Hz) with 40,000 psi, 1 inch diameter pressure cell at 1500 psi. The resulting lysate was then centrifuged at 21,000*g* in a Sigma 4K15 centrifuge (rotor 12169-H) for 40 minutes at 4°C and the

[5] Transfection reagent: Before transfection, Maxi-prepped DNA constructs were incubated with the transfection medium[6]. To do this, two sterile tubes each containing 10 ml SF900™ III SFM media (serum free) were prepared. To one of these tubes 200 µg DNA were added and to the other 1 ml transfection medium were added drop wise and slowly. Then the diluted DNA was slowly transferred into the transfection medium and the two solutions were mixed carefully and incubated at RT for 20 minutes. Then the 20 ml transfection reagent were added to the SF21 cells.

[6] Transfection medium: for one transfection, 80 µl of a 25 mg/ml stock solution of 1:1 DOTAP:DOPE lipids (Avanti) in chloroform were dried down in a glass vial with nitrogen gas. The dried lipids were then washed once with chloroform, dried once more, then washed with ether and dried. The lipids were then left to dry in a fume hood for up to one hour. Afterwards, the dry lipids and 1 ml transfection buffer (20 mM MES pH 6.5, 150 mM NaCl filter sterilised) were heated to 60°C and then mixed. The lipid solution was incubated, with intermittent vortexing, at 60°C for a further hour. Then the lipids were frozen and thawed 4-5 times with liquid nitrogen and kept at 4°C for up to one week before use.

supernatant was then removed and incubated with amphiphysin-2 SH3 GST beads (see section 2.3.4) at 4°C for 1 hour. The beads were then washed 4 times in buffer A by centrifugation and transferred into a BioRad empty gravity flow column. Dynamin was eluted from the amphiphysin-2 SH3 GST beads in 1 ml fractions using buffer B (20 mM PIPES pH 6.2, 1.2 M NaCl, 10 mM $CaCl_2$ 1 mM DTT). The fractions containing protein were determined using Bradford reagent (BioRad) and the main fractions were pooled and dialysed overnight in freezing buffer (20 mM HEPES pH 7.4, 150 mM KCl, 1 mM EDTA, 1 mM EGTA, 1 mM DTT). The pooled dynamin fractions were then aliquoted and snap frozen in liquid nitrogen and stored at -80°C until use. The concentration of dynamin was subsequently determined by gel densitometry using actin standards (see section 2.3.10.2).

2.3.7.3 Increasing the purity of dynamin using the inclusion of nickel bead binding

An additional purification step took advantage of the 6xhis-tag also present on the recombinant dynamin-1 protein. 600 µl Nickel beads (GM Healthcare) were washed with buffer A and incubated with the same buffer for 1 hour at 4°C. After cell lysis and centrifugation, the supernatant was incubated with these beads with rolling for 1 hour at 4°C. The beads were then washed with buffer A, followed by buffer A containing 60 mM Imidazole. Finally dynamin was eluted from the beads by incubation at 4°C for 15 minutes with 10 ml buffer A containing 500 mM imidazole. The resulting eluate was then added to amphiphysin-2 SH3 GST beads and the protocol continued as described in 2.3.7.2.

2.3.8 Protein separation by Sodium Dodecyl Sulphate Polyacrylamide Gel Electrophoresis (SDS-PAGE)

Modified from (Weber & Osborn 1969). Protein samples were prepared for SDS-PAGE by addition of an equal volume of 2x sample buffer (20% (v/v) glycerol, 100 mM Tris-HCL pH 6.8, 4% (w/v) SDS, 0.2% (w/v) bromophenol blue, 2% (v/v) beta mecaptoethanol) and heating to 100°C for 3 minutes. The samples were then cooled, vortexed and spun down in a bench top centrifuge before loading into a mini gel, either made in the laboratory (Resolving gel: 10% (v/v) acrylamide, 380 mM Tris pH 8.8, 0.1% (w/v) SDS, 0.1% (v/v) ammonium persulfate 0.04% (v/v) TEMED. Stacking: 5% (v/v) acrylamide, 125 mM Tris pH 6.8, 0.01% (w/v) SDS, 0.01% (v/v) ammonium persulfate, 0.1% (v/v) TEMED) or pre-cast (BioRad Mini-PROTEAN® TGX™ 12 well 20 µl/well any KD). For experiments with large sample numbers to be analysed alongside each other 18 or 26 well pre-cast gels were used (Criterion™ TGX™ 1 mm thick any KD). Gels were then either processed for western blotting (2.3.9) or stained with Coomassie safe stain (80 mg Coomassie brilliant blue G250, 35 mM HCL in 1 L deionised water) or methanol stain

(Methanol 50% (v/v), Acetic acid 10% (v/v), 1% (w/v) Coomassie G250). Images of stained gels were recoded with a Chemidoc machine (Bio-RAD) and analysed using Image Lab software version 3.0 build 11 (BioRad).

2.3.9 Western blotting

Protein SDS-PAGE gels were transferred onto 0.2 µM PVDF membrane (BioRad) using a Trans-Blot Turbo™ (Bio-RAD) with the mixed MW 7 minute transfer protocol (constant 1.3 A and up to 25 V). The membrane was then blocked with 5% (w/v) milk in 1xTBST (50 mM Tris pH 7.5, 150 mM NaCl, 0.5% (v/v) Tween 20) for 1 hour. The membrane was washed three times with 1xTBST over 30 minutes and incubated with the appropriate primary antibodies in 1% (w/v) milk made up in 1xTBST in a sealed bag and left at 4°C overnight. The membrane was then washed a further three times with 1xTBST before being incubated with horseradish peroxidase (HRP) conjugated secondary antibodies in 1% (w/v) milk with 1xTBST. The membrane was developed using enhanced chemi-luminescence (ECL). ECL solution 1 (2.5 mM Luminol (Fluka), 0.4 mM p-calmaric acid, 100 mM Tris pH 8.5) was mixed with ECL solution 2 (20% (v/v) H_2O_2, 100 mM Tris pH 8.5) in a 1:1 proportion and gently washed over the membrane for 30 seconds. The membrane was then placed in a Chemidoc machine (Bio-RAD) and luminescence was detected every 30 seconds for up to 30 minutes.

2.3.10 Protein concentration analysis

2.3.10.1 Bradford assay

The concentration of purified protein was calculated using a Bradford assay developed from 'Short Protocols in Molecular Biology' 2nd edition (Ausubel 1993) using BSA as a standard. Dilutions of 0, 2.5, 5, 7.5 and 10 µg of BSA were made in duplicate alongside the protein solutions to be assayed, also in duplicate, at dilutions of both 1:10 and 1:100. These were all made up to 100 µl, with 0.15 M NaCl, before the addition of 1 ml Coomassie brilliant blue solution (0.1 mg/ml Coomassie brilliant blue G-250, 4.5% (v/v) ethanol, 8.5% (v/v) phosphoric acid). The solutions were then vortexed and transferred into 1 cm path length polystyrene cuvettes and the absorbance at 595 nm recorded by spectrophotometer (7315 model Jenway). The readings for the BSA concentrations were used to create a standard curve from which the concentration of the unknown solutions were calculated.

2.3.10.2 SDS-PAGE gel analysis

Bradford assays were not always an appropriate method of concentration analysis if there were other proteins present that were contaminating the preparation. In order to analyse only the purified protein of interest a second method of calculating protein concentration was utilised. G-actin standards were used at concentrations of 0, 0.1, 0.5, 1, 1.5, 2, 5 and 10 µM and run alongside protein solutions to be assayed on a 10% (w/v) SDS-PAGE gel (see section 2.3.8). The resulting gel was then stained with Coomassie safe stain, de-stained in deionised water, and imaged via Chemidoc machine (Bio-RAD). The concentration of the protein in question was determined by densitometry analysis of the standards verses the unknown sample using Image Lab software version 3.0 build 11 (BioRad).

2.3.10.3 BCA assay

The BCA assay was used to determine the overall protein concentration in a mammalian cell lysis sample. A BCA assay kit (Thermo Scientific) was used according to the manufacturer's instruction. Briefly, 0.5 ml of each BSA standard (0, 0.5, 1, 2.5, 10, 20, 40 and 200 µg/ml) and 0.5 ml of lysates diluted 1:10 were added to 0.5 ml of working reagent (as stated in kit: 25 parts reagent MA, 24 parts MB and 1 part MC). The samples were then incubated away from direct light at 60^{o}C for 1 hour. The tubes were cooled to RT, transferred into 1-cm path length polystyrene cuvettes and the absorbance at 595nm recorded by spectrophotometer (7315 model Jenway). The absorbance readings for the BSA concentrations were used to create a standard curve from which the concentration of the lysates were calculated.

2.3.10 Preparation of lipids

Folch lipids (Avanti) at 25 mg/ml in chloroform were dried with nitrogen and then air dried at RT for 15 minutes. The lipids were then re-hydrated in liposome buffer (20 mM HEPES pH 7.2, 100 mM KCl, 2 mM $MgCl_2$, 1 mM DTT) to a final concentration of 5 mg/ml. These were then left at 60^{o}C for 1 hour and vortexed 4-5 times during this incubation to re-suspend the liposomes. The lipids were then freeze thawed in liquid nitrogen 4-5 times before being stored at 4^{o}C for use within one week, or snap frozen in liquid nitrogen and stored long-term at -20^{o}C.

2.3.11 Co-sedimentation assays

Vps1 assays

Purified pre-spun Vps1 in F-buffer (2.3.3) was mixed with purified rabbit F-actin (2.3.11), which had been previously polymerised for 1 hour at RT with 1x KME buffer pH 8 (500 mM KCl, 10 mM $MgCl_2$, 10 mM EGTA, 100 mM Imidazole pH 8.0), and incubated overnight at 4^{o}C. Vps1 and actin were incubated for 15 minutes at RT (21^{o}C) and then pelleted by centrifugation in a Beckman table top ultracentrifuge in a TLA-100 rotor for 15 minutes. For high speed pelleting assays the samples were centrifuged at 90,000 rpm and for low speed pelleting the samples were centrifuged at 10,000 rpm (TL100 rotor). The resulting supernatant and pellet were separated and processed for SDS-PAGE as described previously (2.3.8). Quantification from the gel images was performed by relative densitometry using the Bio-Rad software Image Lab^{TM} 3.0 build 11.

For lipid binding, prepared lipids (2.3.10) at 1 mg/ml were incubated with 1.5 µM Vps1 for 15 minutes before high speed centrifugation (90,000 rpm TL100 rotor) and separation by SDS-PAGE as described above.

Dynamin-1 assays

Purified dynamin-1 was thawed on ice and kept in HEPES buffer (2.3.7) during the experiment. Therefore an addition of KME buffer was required in the dynamin only sample so as to ensure salt levels were similar to that when F-actin was added. Similarly in the actin only control the same volume of HEPES buffer (that would be present with addition of dynamin-1) was added to ensure the buffer conditions did not affect the assay. Otherwise, the co-sedimentation assay protocol was the same as the high speed (90,000 rpm TL100 rotor) assay above.

2.3.12 Falling ball assays

This method was performed as described in Winder et al. 1995; and MacLean-Fletcher & Pollard 1980. Briefly, Vps1 and actin were prepared as described in sections 2.3.3 and 2.3.5 respectively. Vps1 at 0.5, 1 or 1.5 µM was added to 3 µM G-actin then, following the addition of KME buffer, the mixture was taken up and sealed in a 100 µl capillary tube (Corning Pyrex 100 µl micro pipettes) and left to polymerise at RT for 20 minutes before being stored overnight at 4^{o}C. The next morning each tube was placed upright in a holder so that marked cm distances were visible down the length of the capillary. A 0.6 mm stainless steel ball bearing (Precision Ball and Gauge Company) was then placed on the meniscus of the liquid and gently pushed into the liquid with a needle. The time it took for the ball to fall 6 cm was measured using a stopwatch and the speed calculated as required.

2.3.13 GTPase assays

Vps1 was purified in HEPES (Melford) buffer (20 mM HEPES pH 7.2, 0.5 M NaCl, 20 mM imidazole) with 1 mM DTT. The intrinsic GTPase activity of Vps1 was measured by changes in phosphate levels and therefore the purification preparation was modified to remove background phosphate from the assay. Vps1 was then buffer exchanged into GTPase buffer (20 mM HEPES-KOH pH 7.5, 150 mM KCl, 2 mM $MgCl_2$, 1 mM DTT). GTP (Calbiochem) was added from 0.2 mM up to 1.5 mM and the stopped assay experiment carried out as described in (Leonard et al. 2005). Briefly, a standard curve was made in a 96 well plate with K_2HPO_4 at concentrations of 0, 5, 10, 20, 30, 50, 60, 80 µM (in triplicate with 10 µl 0.5 M EDTA) to a total volume of 50 µl. GTP at various concentrations (0.2-1.5 mM in triplicate) in micro-centrifuge tubes were then added to Vps1 at a concentration of 0.5 µM to a total volume of 200 µl and incubated at 37^{o}C. Every 5 minutes 40 µl of each reaction was added into separate wells of the 96 well plate which contained 10 µl of 0.5 M EDTA to stop the reaction. After 30 minutes the reaction was complete and 200 µl of Malachite green solution[7] was added to all wells left for 5 minutes at RT then the absorbance of each well was taken using a 96 well plate spectrophotometer (Biochrom Asys Expert Puls microplate reader). The rate of reaction was calculated for each concentration of GTP and plotted using Graphpad Prism software. The Malachite green was a gift from Professor Elizabeth Smythe.

2.3.14 Circular dichroism (CD)

Vps1 was purified as described in 2.3.5 and buffer exchanged into 20 mM NaH_2PO_4 pH 7.4 before use. The rest of this protocol was carried out by Dr. Chris Marklew as described in Palmer et al. 2015a. Briefly, CD spectra were recorded on a Jasco J-810 spectropholarimeter with a buffer only baseline correction. Recordings were taken at a scan speed of 50 nm/minute with a 1 second response time in a 1 mm path length quartz cuvette. This was run three times for each condition and the average of these scans plotted.

[7] Malachite green solution: 34 mg Malachite green was dissolved in 40 ml 1N HCl. In a separate tube 1 g Ammonium molybdate tetrahydrate was dissolved in 14 ml 4N HCl. Each solution was vortexed and then missed together (the solution was then yellow in colour). This was then adjusted to 100 ml by the addition of deionised water and was store at 4^{o}C in the dark. The solution was filtered before use.

2.4 Yeast methods

2.4.1 Yeast growth conditions

Yeast were grown in liquid media with shaking at 30°C in either YPD media (1% (w/v) yeast extract, 2% (w/v) Bacto-peptone, 2% (v/v) glucose and 40 µg/ml adenine) or synthetic (drop-out) media (0.67% (w/v) yeast nitrogen base, 2% (v/v) glucose) and supplemented with amino acids as required for selection as directed by the supplier (Uracil and Histamine were added to a final concentration of 76 mg/L). All media and supplements were purchased from ForMedium.

2.4.2 Yeast transformations

Yeast transformations were carried out using cells in stationary phase using the method described in (Chen et al. 1992). Briefly, transformation buffer (0.1M DTT, 0.2M LiAc, 40% (v/v) PEG 3000) and short chain herring sperm DNA were mixed with a pellet from 200 µl of an overnight culture and heat shocked at 45°C for 30 minutes before plating on synthetic medium with appropriate amino acid selection (see list of yeast strains, table 2.8.3). Yeast were then left to grow for 24-48 hours, before colonies were re-streaked and grown for later stage applications.

2.4.3 Growth analysis in liquid and on solid media

Overnight cultures (5 ml of cell culture in 20 ml container) were diluted as appropriate for each growth assay. For growth curve analyses in liquid media, yeast were refreshed to an OD_{600} of 0.1 units and incubated at 30°C. Yeast cell growth was analysed via optical density OD_{600} every hour for 7 hours using a Jenway 7315 spectrophotometer. The results were plotted against time using Graphpad Prism 6 software. For growth analyses on solid media an overnight culture was diluted to an OD_{600} of 0.5 units, then serially diluted 1:10 a further 4-5 times. 5 µl of each dilution were then transferred by a multi-pipette onto an agar plate made of the appropriate amino acid selection, with the addition of 1M sorbitol if required. The plates were left to dry, sealed and grown at 30°C for 16-24 hours. The resulting growth patterns were imaged and recorded as appropriate.

2.4.4 Yeast whole cell lysates

Yeast whole cell lysates were obtained by mixing a cell pellet, from 1 ml of cell culture at an OD_{600} of 2 units, with glass beads and 2x sample buffer (20% (v/v) glycerol, 100 mM Tris pH 6.8, 4% (w/v) SDS (Melford), 0.2% (w/v) bromophenol blue, 2% (v/v) mercaptoethanol). The mixtures were boiled for 3 minutes at 100°C and then lysed using a cell disrupter (Scientific industries) for a further 3 minutes. The resulting lysate could then be processed by an SDS-PAGE gel (2.3.8), transferred onto a PVDF membrane for western blotting and probed for proteins with the appropriate antibodies. For Vps1 detection, anti-Vps1 antibodies were used (rat antibodies at a dilution of 1:20,000) and developed using horseradish peroxidise (HRP) (2.3.9).

2.4.5 Carboxypeptidase Y assay (CPY)

As described in Smaczynska-de Rooij et al., 2012. Cells were grown to log phase (OD_{600} 0.7 units per ml) then centrifuged at 3000 rpm in a Hettich 1619 rotor using a C28 Boeco centrifuge for 3 minutes. Pellets were re-suspended in drop out Ura media with 0.05 mg/ml cyclohexamide and incubated at 30°C for 30 minutes. After this a total of 2 units of cells (OD_{600}) were washed with sterile deionised water and pelleted by centrifugation. Whole cell lysates were then obtained (see 2.4.4) and probed by western blotting (see 2.3.9). Pre-cleaned CPY antibodies (Chemicon international AB1817) were used at 1:1000 dilution and membrane developed with Enhanced chemiluminescence (ECL) solution.

2.5 Yeast cell Microscopy techniques

Unless otherwise specified, all microscopy techniques were imaged using an Olympus IX81 microscope (Mazurek) with a 100x oil objective and a CoolSnapHQ^2 camera, using FRAP A1 metamorph software for image capture and Autoquant X2 software for deconvolution. At the point of imaging, 3-5 µl of culture, grown in synthetic medium or prepared as described below, was applied directly to an uncoated slide and covered with a coverslip before inverting for microscopy, images were all recorded at RT (21°C).

2.5.1 FM4-64 vacuole staining in yeast

5 ml yeast culture in liquid media at an OD_{600} of 0.5-0.7 units were pelleted at 3000 rpm in a Hettich 1619 rotor using a C28 Boeco centrifuge and re-suspended in 500 µl YPD media. The cells were then transferred from the 15 ml universal tube into a micro-centrifuge tube and incubated with FM4-64 (Invitrogen), at a final concentration of 16 µM, for 15 minutes at RT. Cells were washed with synthetic media plus uracil before incubation for a further hour

with rotation at RT. Cells were then centrifuged at 700*g* for 3 minutes in Eppendorf centrifuge 5424 and re-suspended in the appropriate selection media before imaging.

2.5.2 Lucifer yellow uptake in yeast

5 ml yeast culture grown to an OD_{600} of 0.5-0.7 units were pelleted at 3000 rpm in a Hettich 1619 rotor using a C28 Boeco centrifuge, and then incubated in 500 µl YPD media with Lucifer yellow (stock solution 40 mg/ml in deionised water, Sigma) in a micro-centrifuge tube at a final concentration of 13 mg/ml for 15, 30, 60 or 90 minutes at either RT (21^{o}C) or 30^{o}C. Cells were then pelleted at 700*g* for 3 minutes in Eppendorf centrifuge 5424, and washed in succinate azide buffer (50 mM succinate, 20 mM NaN_3 pH 5.0) three times. The final pellet was re-suspended in 10-20 µl succinate azide buffer before imaging.

2.5.3 Snc1 localisation

Snc1 is a Vesicle membrane receptor protein or v-SNARE and was used previously when fused to GFP to demonstrate endocytic recycling defects (Burston et al 2009). Mutations of Vps1 were expressed in the integrated Snc1-GFP strain (KAY 1462 table 2.8.3) and grown to an OD_{600} of 0.7 units before being imaged.

2.5.4 Observation of peroxisome morphology

To visualise peroxisomal fission the yeast strain containing a plasmid borne GFP tagged Peroxisomal targeting signal 1 (PTS1) was utilised (Hoepfner et al. 2001). This strain was transformed (KAY 1096 table 2.8.3) with the appropriate Vps1 plasmids and grown in solution overnight. Overnight cultures were then diluted (0.5 ml culture in 4.5 ml selection media) and grown to an OD_{600} of 0.5-0.7 units before imaging.

2.5.5 Lifetimes and intensity readings of endocytic markers Sla1, Sla2, Abp1 and Rvs167

Yeast with integrated Sla1-GFP, Sla2-GFP, Abp1-mCherry and Rvs167-GFP, which were all *vps1* null (see table 2.8.3) were transformed with different Vps1 plasmids and grown from an overnight culture to an OD_{600} of 0.5-0.7 units. For experiments including Sla1-GFP, Abp1-mCherry and Rvs167-GFP images were taken with a 1 s time-lapse and 0.5 s exposure on a Mazurek Olympus IX81 microscope. Abp1-mCherry was also imaged at a 60 ms exposure with a frame interval of 0.11 s for a total of 60 s using a Nikon Eclipse Ti microscope with a 1003 oil objective lens and an Andor Zyla sCMOS camera. Imaging was performed using the NIS

Elements 4.20.01 software. Finally dual colour Sla1-GFP and Abp1-mCherry microscopy was performed by Dr. Iwona Smaczynska-de Rooij on a DeltaVision RT Restoration Microscope using a 100x 1003 1.40 numerical aperture oil objective and Photometrics Coolsnap HQ camera. Image capture was performed using SoftWoRxTM (Applied Precision Instruments) with a time-lapse of 1.5 sec with 0.25 sec exposure for both for up to 90 seconds.

2.5.6 Total Internal Reflection Fluorescence (TIRF) microscopy

TIRF microscopy was carried out using a Nikon TIRF microscope with a 1003 oil objective and a Photometrics Evolve EMCCD camera. Image capture used NIS Elements 4.20.01 software and capture settings were 60 s with 2-s interval. All images were deconvolved before analysis.

2.5.7 Preparation of samples for electron microscopy

Vps1 was prepared as described (section 2.3.3) and either analysed alone or 1 µM of Vps1 was mixed with pre polymerised actin at 1.5 µM. Samples were incubated at RT for 15 minutes before being loaded onto carbon coated grids at a dilution of 1:10. Proteins were visualised following negative staining with uranyl formate and imaged using a Gatan MultiScan 794 charge-coupled device (CCD) camera on a Philips CM 100 electron microscope. Grid loading and imaging were performed with the help of Wesley I. Booth and Dr. Christopher J. Marklew.

Preparation of yeast cells for electron microscopy

This procedure was carried out at Durham University by Dr. Martin Goldberg, Dr. Ritu Mishra and Dr. Simeon Johnson. Full experimental procedures can be found in Palmer et al. 2015a and Fiserova & Goldberg 2010.

2.5.8 Statistical analysis

Images were analysed using ImageJ software (Schneider et al. 2012) to investigate lifetimes, peak intensity and intensity profiles of endocytic reporter proteins. Statistical analyses were carried out using GraphPad Prism 6 software (GraphPad Software, San Diego, CA). To determine if the differences in the lifetimes or intensity of endocytic markers were statistically significant either a two-tailed *t*-test or a one-way ANOVA analysis with Tukeys multiple comparison test were used. These tests were used to compare two values together or multiple values respectively.

2.6 Mammalian cell culture techniques

2.6.1 Cell culture techniques

A431 cells (Giard et al. 1973) were maintained in Dulbecco's modified eagle medium (DMEM) media (Gibco) plus 4.5 g/L D-Glucose, L-Glutamine and Pyruvate. MDA-MB-231 cells (Cailleau et al. 1978; Brinkley et al. 1980) were maintained in RPMI media (Gibco) with L-Glutamine. Both media were supplemented with 10% (v/v) FBS. A431 and MDA-MB-231 cells were grown in either T-75 or T175 plastic culture flasks, 10 cm dishes, or 6/12 well plates (Greiner Bio-One) and incubated at 37^{o}C with 5% CO_2. Cells were passaged using 1% (v/v) trypsin-EDTA solution (Sigma), followed by centrifugation in an 11030 rotor (Sigma) at 80*g* for 3 minutes before re-suspension in growth media. Cells were then seeded at the required density for either future cell growth or specific experiments.

2.6.2 Preparation of cell lysates

6 well dishes of cells were placed on ice, washed in ice-cold 1xPBS and then lysed with 100 µl per well RIPA buffer (50 mM Tris pH 7.5, 150 mM NaCl, 1 mM EGTA, 1 mM EDTA, 1% (v/v) Triton-X, 0.5% (w/v) sodium deoxycholate, 0.1% (w/v) SDS, 1 mM sodium azide) with protease inhibitors (200 µl 25x protease inhibitor cocktail, Roche). The cells were then scraped off to ensure removal of cells from surface and collected into a 1.5 ml micro-centrifuge tube. The samples were then sonicated to fragment DNA (Sanyo Soniprep 150 at amplitudes between 10-15 µm) for 10 seconds on ice. Finally the samples were centrifuged at 18,000*g* for 15 minutes at 4^{o}C using a Sigma 1-15K benchtop centrifuge and the supernatant removed as the whole cell lysate fraction. Lysates were analysed for protein concentration by BSA assay (see 2.3.10.3), then mixed 1:1 with sample buffer before either SDS-PAGE and western blotting (see 2.3.9) or storage at -20^{o}C.

2.6.3 Transfection of cells using the electroporation technique

Electroporation was performed using the Invitrogen Neon® Transfection system with the MPK 5000 electroporator and 100 µl pipette transfection kit. Conditions for A431 electroporation were optimised as discussed in chapter 6, section 6.5 and conditions for MDA-MB-231 cells were based on the online Neon transfection cell protocol and cell line data (http://www.lifetechnologies.com/uk/en/home/life-science/cell-culture/transfection/transfection---selection-misc/neon-transfection-system.html).

Cells were grown to the appropriate density then the media was removed before trypsinisation (trypsin-EDTA solution, Sigma) and centrifugation in an 11030 rotor (Sigma) at 80*g* for 3 minutes to remove trypsin. The cells were washed once in 1xPBS, then re-suspended

in 1xPBS and counted using a haemocytometer (Weber Scientific Ltd). The appropriate number of cells and mass of DNA (see table below) were then incubated at RT for 5 minutes before electroporation at the appropriate conditions (see table below). Once transfected, cells were placed in the appropriate cell culture dish with media pre-warmed to 37^{o}C and incubated for 24 hours at 37^{o}C with 5% CO_2. For cell fixation and microscopy work, glass coverslips (Merienfeld GmbH and Co.) were added to the cell culture dishes for cells to adhere to.

Cell line	**Number of cells per 100 µl**	**µg DNA per 100 µl cells**	**Cell culture dish size**	**Electroporation conditions**
A431	$1x10^6$	5	10 cm dish	1200 volts, 30 ms width, 1 pulse
A431	$2.5x10^5$	2.5	1 well in 6 well dish	1200 volts, 30 ms width, 1 pulse
MDA-MB-231	$5x10^5$	5	2-3 wells in 12 well dish	1450 volts, 10 ms width 4 pulses

2.6.4 Transferrin uptake assay

A431 cells were transfected and seeded onto 10 cm dishes as described in section 2.6.3. Due to the toxicity of the dynamin-1 overexpression multiple cell transfections were combined to get enough cells for FACS analyses. For the untransfected condition $1x10^6$ cells were used, GFP expressing cells $2x10^6$ cells were used and for WT and KK418-9EE $4x10^6$ cells were required. The cells requiring transferrin uptake were removed from their 10 cm dishes with 2 ml trypsin-EDTA solution (Sigma) then centrifuged at 80*g* for 3 minutes using an 11030 rotor (Sigma) and re-suspended in media with 25 µg/ml transferrin. The cells were then incubated for 10 minutes at 37^{o}C in a water bath before removal of transferrin containing media. The cells were then washed in ice-cold 1xPBS then incubated for 5 minutes with 5 ml acid wash (50 mM glycine-HCL pH 3.0) to remove surface-bound transferrin. Cells were then washed in 10 ml 1xPBS and then fixed in 1ml 10% (v/v) formadehyde in 1xPBS for 10 minutes. Once fixed, cells were washed in 1xPBS twice and re-suspended in 1 ml 1xPBS for analysis by FACS (see section 2.6.5).

2.6.5 Fluorescence Activated Cell Sorting (FACS) analysis

Fixed cell analysis

Fixed cells were prepared as described (section 2.6.4) and analysed using a Dakocytomation flow cytometer by Dr. Mark Jones in Prof. Peter Andrews lab. Dr. Jones ran the samples and, with the use of Sommet Software gated the populations for granularity, size and doublets before collecting the data for both Texas red and GFP fluorescence.

Live cell sorting

Live and transfected A431 cells were prepared in solution by trypsinisation. Cells were then washed and re-suspended in growth media before sorting for GFP fluorescence. This was performed by Dr. Jones with the use of a FACS Jazz machine (BD Biosciences) and BD FACS™ software. The samples were gated for granularity, size and doublets and then single fluorescent cells were collected for further experiments.

2.6.6 Rhodamine phalloidin and 4',6-diamidino-2-phenylindole (DAPI) staining

Cells were transfected, grown and seeded at the required density on coverslips. They were then placed on ice and washed with 1xPBS before being fixed in 3.7% (v/v) formaldehyde for 10 minutes at RT. The fixative was removed and the cells were permeabilised with 0.05% (w/v) saponin in 1xPBS for 1 minute before being washed once more in 1xPBS and transferred to a humid chamber where they were incubated for 1 hour with 20 µl blocking buffer (5% (v/v) FCS, 1% (v/v) BSA in 1xPBS). Then the coverslips were dried and transferred onto 20 µl rhodamine phalloidin stain at 1:200 (v/v) in blocking buffer for 1 hour (Rhodamine phalloidin from Molecular probes, dissolved in methanol to a final concentration of 6.6 µM). Finally, the coverslips were washed three times in 1xPBS, dried, and mounted on slides with mounting media with DAPI (hydromount™, 1% (v/v) DABCO, 0.02% (w/v) DAPI from stock 1 mg/ml solution). Slides were then left overnight at 4°C to set and imaged by fluorescence microscopy. Slides were stored at 4°C for up to 6 months.

2.6.7 Scratch wound assay

Cells were transfected and grown to the required cell density before live cell sorting for GFP (see section 2.6.5). Cells were then plated in a fibronectin covered 24 well plate (see section 2.6.10) at $2x10^5$ cells per well and incubated at 37°C and 5% CO_2 overnight to adhere. The next day, media was removed and a scratch made with a pipette tip down the centre of each well. The cells were washed in 1xPBS before media was added to the cells. The plate was moved to the microscope and left to adjust in the chamber (temperature and CO_2 level 37°C and 5% respectively), before imaging took place for 16 hours using a 10x objective (see section 2.6.11).

2.6.8 Single cell migration assay

MDA-MB-231 cells were transfected at a density of $5x10^5$ cells/100 µl and seeded in a fibronectin covered (see section 2.6.10) 24 well plate. Transfected cells were split into 3 wells and diluted to reflect the viability of the transfections. Specifically, untransfected cells were seeded $1.25x10^5$ cells per well after electroporation, cells with GFP vector were seeded at a density of $1.67x10^5$ and for both WT dynamin-1 GFP and KK418-9EE GFP these cells were seeded after electroporation at a density of $2.5x10^5$. The cells were left for 4-6 hours before being moved to the microscope and let to adjust. Images and movies were then taken over the course of 16 hours.

2.6.9 Phorbol 12,13-dibutyrate (PDBu) treatment of cells

MDA-MB-231 cells were transfected at $5x10^5$ cells/100 µl and seeded onto 2 coverslips in a 6 well plate, coated in poly-l-lysine, and incubated at 37°C and 5% CO_2 overnight to adhere and express the desired protein. The following day cells were stimulated to form podosomes by the addition of 2.5 µM PDBu at in 1xPBS for 30 minutes. The cells were then placed on ice and stained for actin as described in 2.6.6.

2.6.10 Preparation of coated dishes

Fibronectin was prepared at a concentration of 5 µg/ml in 1xPBS and pipetted into each well in a 24 well plate. This was incubated overnight at 4°C then removed before washing in 1xPBS. The prepared plates were used within 1 hour of preparation.

Poly-L-lysine was prepared at a concentration of 5 µg/ml in 1xPBS and pipetted on to each well of a 6 well plate, containing coverslips as required. The 6 well place was incubated at RT for 30 minutes and the poly-l-lysine removed before the immediate addition of cells.

2.7 Mammalian cell microscopy techniques

2.7.1 Fluorescence microscopy

Images of fixed cells were taken with a Leica DMIREZ fluorescence microscope powered by a Leica CTRMIC controller. Images were obtained using a 63x oil objective or 20x air objective. Image acquisition was performed using Leica QFluoro software on a Leica Q550FW Pentium II computer and analysed using ImageJ.

2.7.2 Live cell imaging

Images and subsequent movies for single cell and scratch wound experiments were taken in both bright field and GFP channels every 5 minutes for 16 hours on a Nikon Eclipse Ti microscope with a 10x air objective and an Andor Zyla sCMOS camera. Image capture was performed using NIS Elements 4.20.01 software set up by Dr. Darren Robinson using equipment in the Light Microscope facility. Movies were analysed using ImageJ and the Chemotaxis plugin (Ibidi).

2.7.3 Statistical analysis

Statistical analyses for cell size, shape and other mammalian cell techniques were carried out using GraphPad Prism 6 software (GraphPad Software, San Diego, CA). To determine if the differences in cell size and shape were statistically significant either a two-tailed *t*-test or a one-way ANOVA analysis with Tukeys multiple comparison was used. These tests were used to compare two values together or multiple values respectively.

2.8.1 Table 1 Plasmids

PKA	DESCRIPTION	SOURCE
677	YCp with *VPS1* under its own promoter *in vivo* expression, *URA3*	(Smaczynska-de Rooij et al. 2010)
544	*URA* marked empty plasmid	E. Hettema (University of Sheffield)
943	pKA 677 with RR457-8EE, *URA3*	(Palmer et al. 2015a)
944	pKA 677 with RR457-8EE+K453E, *URA3*	(Palmer et al. 2015a)
945	pKA 677 with E461K, *URA3*	(Palmer et al. 2015a)
946	pKA 677 with E473K, *URA3*	(Palmer et al. 2015a)
850	pCRT7-NT TOPO with His tagged *VPS1* WT	(Smaczynska-de Rooij et al. 2012)
969	pKA 850 with *VPS1 RR457-8EE*	(Palmer et al. 2015a)
1096	pKA 850 with *VPS1 RR457-8EE+K453E*	(Palmer et al. 2015a)
1025	pKA 850 with *VPS1 E461K*	(Palmer et al. 2015a)
1095	pKA 850 with *VPS1 E473K*	(Palmer et al. 2015a)
910	GFP-PTS1 under *TPI1* promoter, *LEU2*	E. Hettema (University of Sheffield)
1070	pVPS1-VPS1-GFP EcoR1-Pst1 from pKA 836	(Smaczynska-de Rooij et al. 2012)
1101	pKA 1070 with *VPS1* RR457-8EE	(Palmer et al. 2015a)
1108	pIEX-6 with human Dynamin-1 for *in vitro* expression	Gift from Prof. Sandra Schmid
1133	pKA 1108 with A408T	This study
1178	pKA 1108 with KK418-9EE	This study
1109	pGEX-2T with SH3 domain of Amphiphysin-2	Gift from Prof. Sandra Schmid
1141	pEGFP-N1 with human Dynamin-1	Pietro De Camilli (Addgene # 22163)
1179	pKA 1141 with KK418-9EE	This study
1177	pEGFP-N1	S. Winder (University of Sheffield)

2.8.2 Table 2 Oligonucleotides

OKA	SEQUENCE	DESCRIPTION
1100	GTTTTAGTTAAACAGCAAATTGAAGAGTTTGAAGAACCATCTCTACG	Vps1 RR457-8EE 5’
1101	CGTAGAGATGGTTCTTCAAACTCTTCAATTTGCTGTTTAACTAAAAC	Vps1 RR457-8EE 3’
1102	GCAAATTAGAAGATTTGAAAAACCATCTCTACGTTTAG	Vps1 E461K 5’
1103	CTAAACGTAGAGATGGTTTTTCAAATCTTCTAATTTGC	Vps1 E461K 3’
1104	CTCTGGTGTTTGATAAACTTGTTCGTATGC	Vps1 E473K 5’
1105	GCATACGAACAAGTTTATCAAACACCAGAG	Vps1 E473K 3’
1106	GCTTTTGAAGTTTTAGTTGAACAGCAAATTGAAGAG	Vps1 K453E 5’
1107	CTCTTCAATTTGCTGTTCAACTAAAACTTCAAAAGC	Vps1 K453E 3’
1331	CCATTGTGAAAAAGCAGGTGGAGGAGATCCGAGAACCGTGTCTC	Dyn-1 KK418-9EE 5’
1332	GAGACACGGTTCTCGGATCTCCTCCACCTGCTTTTTCACAATGG	Dyn-1 KK418-9EE 3’
1293	CACAATGGTCTCAAAGGTCATGTCTGGGGTAAACA	Dyn-1 A408T 5’
1294	TGTTTACCCCAGACATGACCTTTGAGACCATTGTG	Dyn-1 A408T 3’

2.8.3 Table 3 Antibodies

ANTIBODY	PRIMARY (P) OR SECONDARY (S)	RAISED IN	WESTERN BLOT DILUTION	SOURCE
ANTI-VPS1	P	Mouse	1:2000	(Smaczynska-de Rooij et al. 2010)
ANTI - CPY	P	Rabbit	1:1000	Chemicon International Cat# A-6428
ANTI-DYNAMIN-1	P	Rabbit	1:1000	Abcam Cat# ab52611
ANTI-ACTIN	P	Mouse	1:500	Abcam Cat# ab14128
ANTI-GAPDH	P	Mouse	1:2500	Thermo Scientific Cat# MA5-15738
ANTI- HIS TAG	P	Mouse	1:1000	BD Biosciences Cat# 51-9000012
ANTI-GFP	P	Mouse	1:500	Roche Cat# 11814460001
ANTI-MOUSE HRP	S	Rabbit	1:10,000	Sigma Cat# A4416
ANTI-RABBIT HRP	S	Goat	1:19,000	Sigma Cat# A0545

2.8.4 Table 4 Yeast strains

KAY	GENOTYPE	SOURCE
302	*MATα ura3-52, leu2, 3-112, his3Δ200, trp1-1*	KA lab
389	*Mat a, ura3-52, leu2, 3-112, his3Δ200, trp1-1, lys2-801*	KA lab
1095	*MATα his3Δ1, leu2Δ0, lys2Δ, ura3Δ0 Δvps1::KanMx*	E.Hettema (Univ of Sheffield)
1096	*MATα his3Δ1, leu2Δ0, lys2Δ, ura3Δ0 Δdnm1::KanMx Δvps1::HIS5*	E.Hettema (Univ of Sheffield)
1459	*MATα SLA2-GFP::HIS3, his3Δ1, leu2Δ0, met15Δ0, ura3Δ0, Δvps1::LEU2*	(Smaczynska-de Rooij et al. 2010)
1337	*MATα Rvs167-GFP::HIS3, his3Δ1, leu2Δ0, met15Δ0, ura3Δ0 Δvps1::LEU2*	(Smaczynska-de Rooij et al. 2010)
1462	*MATα his3Δ1, leu2Δ0, lys2Δ, ura3Δ0, GFP-Snc1-SUC2 URA3, Δvps1::KanMx*	(Smaczynska-de Rooij et al. 2010)
1664	*MATα/α vps1::LEU2/vps1::KanMx, ABP1/ABP1-mCherry::HIS3, SLA1-GFP::HIS3/SLA1, his3Δ1/his3Δ1, leu2Δ0/ leu2Δ0, met15Δ/MET15,LYS2/lys2Δ, ura3Δ/ura3Δ*	(Palmer et al. 2015a)
1756	*vps1Δ::URA in KAY 389*	(Palmer et al. 2015a)
1793	*VPS1E461K in KAY 389*	(Palmer et al. 2015a)
1794	*VPS1RR457-8EE in KAY 389*	(Palmer et al. 2015a)
1806	*VPS1K453E, RR457-8EE in KAY 389*	(Palmer et al. 2015a)
1807	*VPS1E473K in KAY 389*	(Palmer et al. 2015a)
1466	*MATα his3Δ1, leu2Δ0, lys2Δ, ura3Δ0, Abp1-mCherry::HIS*	(Palmer et al. 2015a)
1621	*RVS167-VC::TRP1 in KAY 389*	(Palmer et al. 2015a)
1832	*VPS1-VN::HIS3 in KAY 389*	(Palmer et al. 2015a)
1833	*VPS1E461K-VN::HIS3 in KAY 389*	(Palmer et al. 2015b)
1834	*VPS1RR457-8EE-VN::HIS3 in KAY 389*	(Palmer et al. 2015a)
1849	*Pil1mRFP in KAY 389 (Vps1 WT)*	(Palmer et al. 2015a)
1850	*Pil1mRFP in KAY 1793 (Vps1 RR-EE)*	(Palmer et al. 2015a)

Chapter 3

Bioinformatic study of the actin binding region in dynamins

3.1 Introduction

During the course of this study a number of comparisons were made between the yeast Vps1 and human dynamin-1. This was done initially to identify evolutionarily conserved residues to test the direct Vps1-actin interaction. Once these residues were identified they were then used to more precisely map and refine the conserved actin binding region in human dynamin-1. As the project continued, it became evident that there are differences between dynamin-1 actin binding region in comparison to dynamin-2 and 3. Moreover, different species (rat and mouse) harbour differences in their dynamin-1 actin binding region in comparison to human dynamin-1. This could suggest that the dynamin-actin interaction may be altered in different dynamin proteins and across different species so as to orchestrate its role more precisely *in vivo*. The reporting of the laboratory based aspects of the project will therefore be preceded by an analysis of the amino acids required for dynamin-1 actin binding, a comparison of these with Vps1 and a description of the specific residues predicted to be required for Vps1-actin interaction. This is then followed by a comparison between amino acids making up the actin binding region in the human dynamin genes and between in rat and mouse dynamin genes.

3.1.1 The middle coiled-coil region of dynamins

Dynamin and dynamin-like proteins all contain a middle alpha helical coiled-coil region. This has been described to be involved in the oligomerisation of dynamin (Ramachandran et al. 2007) and to be required for actin binding (Gu et al. 2010). Certain mutations have been found to reduce the ability of dynamin to oligomerise such as R361S, R399S and I690K (Ramachandran et al. 2007; Song et al. 2004). These lie either side of the actin binding region reported for dynamin-1 (residues 399-444) and have been found to reduce the ability of dynamin to form tetramers from dimers therefore preventing higher order oligomerisation (Ramachandran et al. 2007; Sever et al. 2006). There is a chance that residues involved in actin binding within dynamin-1 are also involved in dynamin-1 self-

assembly, though it has been reported that dynamin-1 was able to self-assemble after charged residues involved in actin binding were mutated (Gu et al. 2010). Conversely, one disease mutation reported, A408T, is within the reported actin binding region and is known to affect dynamin oligomerisation (Boumil et al. 2010). The A408T mutation was found in mice to cause an epileptic phenotype and this residue lies just upstream from the charged residues reported to be involved with dynamin-actin interaction. A408T was found to reduce transferrin uptake in COS-7 cells and be defective in higher order oligomerisation suggesting that this residue can affect dynamin oligomers as well as potentially affecting actin binding (Boumil et al. 2010). The ability of dynamin-1 A408T to bind actin was investigated in this study and preliminary results are described in chapter 6 (section 6.3).

In 2011 the crystal structure of full length dynamin was published by two separate groups (Ford et al. 2011; Faelber et al. 2011). Both reports indicated how dynamin dimers and higher order oligomers may form and which area of the middle domain alpha helices were responsible for this interaction. Mutation of residues 395-399 (IHGIR-AAAAA) resulted in dynamin that was unable to oligomerise, and using this mutation dynamin crystals were generated (Faelber et al. 2011). Interestingly this stretch of amino acids lies just outside the main stretch of the actin binding region and includes residue R399 which was previously reported to be required for oligomerisation (Ramachandran et al. 2007). The second report described three interfaces between dynamin monomers which were predicted to be involved in dynamin oligomerisation. Interface 2 is proposed to be involved in dimerisation of dynamin monomers whereas interfaces 1 and 3 are thought to be required in higher order oligomers (Ford et al. 2011; Reubold et al. 2015). Figure 1 shows a comparison between the residues in interface 2, known to be required for dynamin dimerisation.

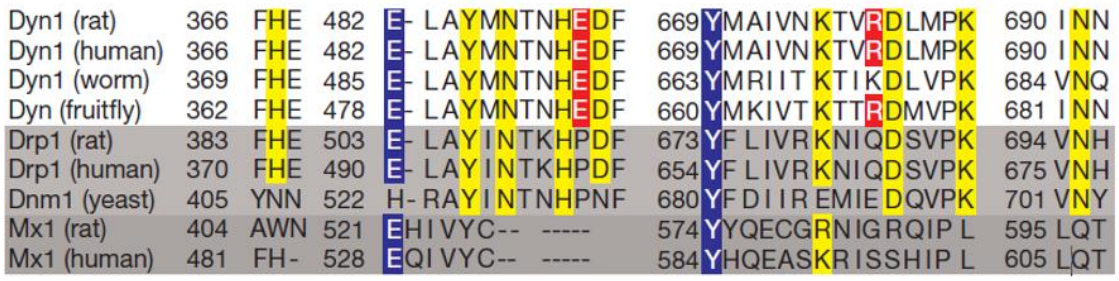

Figure 1. Comparing middle domain residues in interface 2 of dynamin proteins. From Ford et al., 2011 reproduced with permission from Nature Publishing Group. Sequence showing the residues predicted to be required for dimerization of dynamin proteins namely interface 2. The yellow residues indicate conserved residues in dynamin and Drp proteins. Blue are conserved residues in most dynamin and dynamin-like proteins and red indicate conserved residues in dynamin proteins only.

These residues are compared between dynamin and dynamin-like proteins and none of the residues shown to be required for dimerisation lie within the proposed actin binding region (Ford et al. 2011; Gu et al. 2010). Interface 1 and 3 are at the tip and distal ends of the middle domain alpha helices respectively and are thought to interact with other dynamin monomers when forming tetramers (Reubold et al. 2015) and higher order structures (figure 2A). Each of the residues involved in dimerisation and predicted higher order oligomerisation were plotted onto the crystal structure of dynamin (PDB 3SNH) using PyMol Molecular Graphics software (Version 1.2r3pre, Schrödinger, LLC). As seen in figure 2B and C, each region predicted to be involved in higher order dynamin structure borders the actin binding region. The actin binding alpha helix does extend down close to interface 3 and therefore mutations in this area could affect oligomerisation, however the majority of the actin binding region residues are predicted to project away from neighbouring helices in the complex and would be found on the outside of a dynamin ring.

In this chapter the actin binding region within dynamin-1 were compared with those of Vps1. This was to identify a specific number of residues that were orthologous, and potentially evolutionarily conserved, that can describe a more refined characterisation of the actin binding region in Vps1 and other dynamin proteins. The middle domain and actin binding region were also compared with other dynamin isoforms. These data describe and identify the residues selected for the Vps1-actin investigation and will begin to discuss differences in Vps1 and dynamin isoform actin binding regions. These differences could indicate varying cellular roles for which yeast Vps1 and mammalian dynamin function with actin.

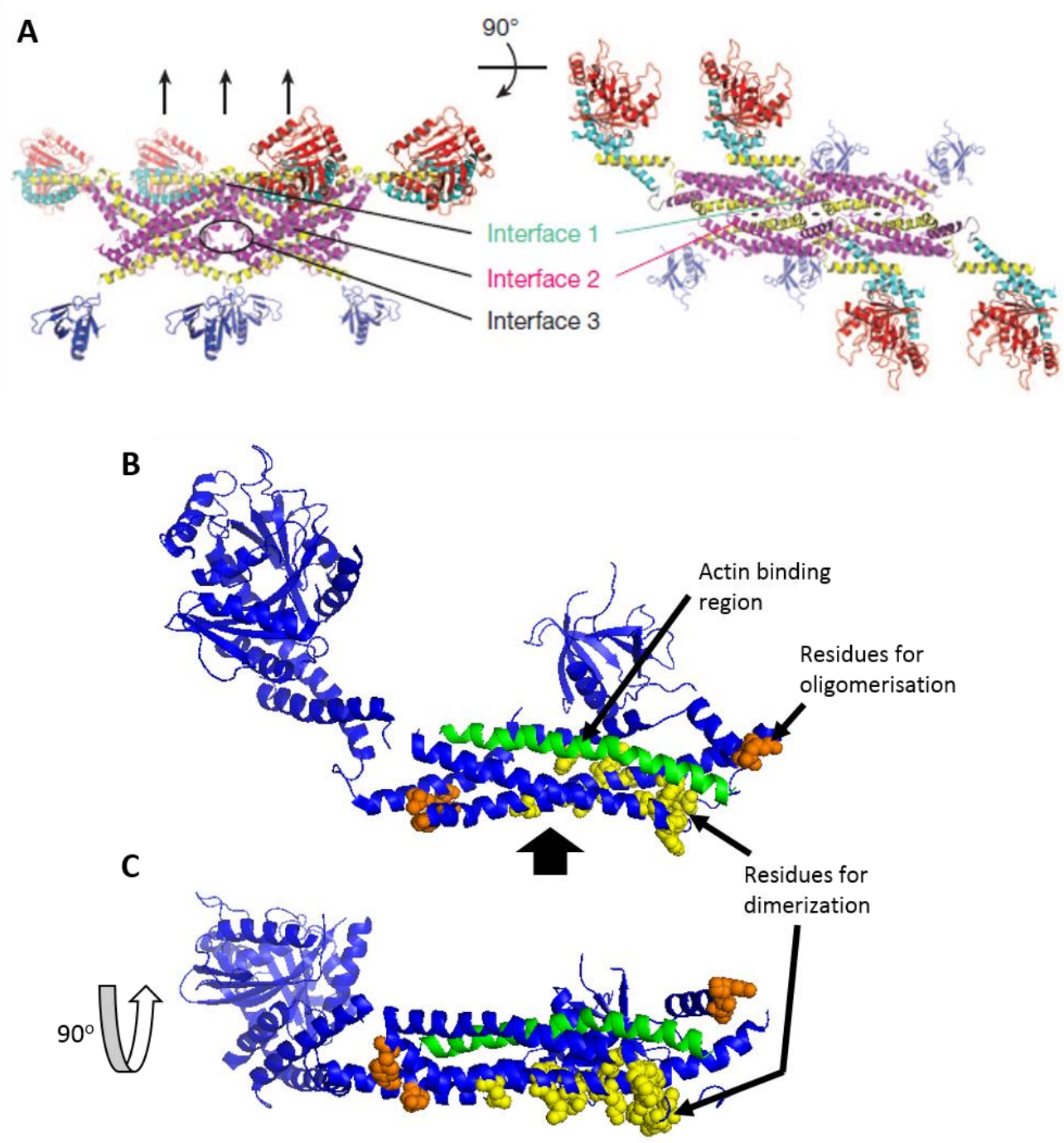

Figure 2. Mapping the actin binding and oligomerisation regions in dynamin-1 A) Diagram from Ford et al., 2011 reproduced with permission from Nature Publishing Group. This shows the predicted three interfaces between dynamin monomers from the crystal structure of dynamin-1 that are involved in dimerization (interface 2) or oligomerisation (interface 1,3). B) PyMol diagram of dynamin crystal structure (PDB 3SNH) in blue, showing the actin binding region in green, residues required for dimerization in yellow and residues required for oligomerisation in orange as described in Ford et al., 2011 and Faelber et al 2011. C) A 90º rotation of B so as to show the residues labelled from another angle. The black arrow in B indicates the field of view seen in C.

3.2 Identification of key residues to mutagenise in the Vps1-actin study

3.2.1 Conserved residues within the actin binding region of dynamin-1 and Vps1

Vps1 has sequence orthology with mammalian dynamin-1 as well as dynamin-like proteins MxA and Drp1 (Obar et al. 1990; Rothman et al. 1990; Imoto et al. 1998; Smaczynska-de Rooij et al. 2010). Therefore it was hypothesised that Vps1 could have conserved charged residues in its middle domain which could bind to actin in a similar way to dynamin-1 (Gu et al. 2010).

In order to compare the actin binding region of dynamin-1 (residues 399-444) with that of Vps1 (residues 438-483) the whole canonical dynamin-1 sequence (UniProt Q05193) was aligned with Vps1 (UniProt P21576) by Clustal Omega sequence alignment software (version 1.2.1, McWilliam et al. 2013) and it was found that the two sequences share 44.51% identity (figure 3). The actin binding region, as reported previously (Gu et al. 2010), is indicated by a red box figure 3. Interestingly dynamin-1 has 13 charged residues within its actin binding region and 57% of these charged residues are conserved in Vps1. This is shown in figure 4, where magenta coloured residues indicate positively charged amino acids and blue coloured residues indicate negatively charged ones. There are five positively charged residues found both in Vps1 and dynamin-1 (white arrows) which are thought to be involved with binding between dynamin-1 and actin. There are also three residues found in both dynamin-1 and actin which are negatively charged (black arrows) and it was predicted that changing these to positively charged residues would increase the affinity between Vps1 and actin (as previously shown with dynamin-1, Gu et al. 2010). These similarities suggest that there may be a direct interaction between Vps1 and actin.

3.2.2 Selecting charge residues to test the Vps1-actin binding region

The affinity between dynamin-1 and actin was reportedly altered when charge residues within the defined actin binding region are mutated (Gu et al. 2010). The actin binding region has been described to stretch between amino acid residues 399-444 in mammalian dynamin-1 and there are eight conserved charged residues in the yeast Vps1 protein (figure 4). It is known that, in dynamin-1, by removing positively charged residues from this area and swapping them for negative charges reduces the affinity between dynamin-1 and actin and by changing the negative residues to positive ones increases this affinity. The initial study into dynamin-actin interaction created one mutated form of dynamin-1 where five lysines were

```
DYN1_HUMAN      MGNRGMEDLIPLVNRLQDAFSAIG--QNADLDLPQIAVVGGQSAGKSSVLENFVGRDFLP 58
VPS1_YEAST      MD----EHLISTINKLQDALAPLGGGSQSPIDLPQITVVGSQSSGKSSVLENIVGRDFLP 56
                *.    *.**. :*:****::.:*  .:: :*****:***.**:********:*******

DYN1_HUMAN      RGSGIVTRRPLVLQLVN------------------------------------------- 75
VPS1_YEAST      RGTGIVTRRPLVLQLINRRPKKSEHAKVNQTANELIDLNINDDDKKKDESGKHQNEGQSE 116
                **:*************:*

DYN1_HUMAN      -ATTEYAEFLHCKGKKFTDFEEVRLEIEAETDRVTGTNKGISPVPINLRVYSPHVLNLTL 134
VPS1_YEAST      DNKEEWGEFLHLPGKKFYNFDEIRKEIVKETDKVTGANSGISSVPINLRIYSPHVLTLTL 176
                  . *:.****  **** :*:*:* **  ***:***:*.***.******:******.***

DYN1_HUMAN      VDLPGMTKVPVGDQPPDIEFQIRDMLMQFVTKENCLILAVSPANSDLANSDALKVAKEVD 194
VPS1_YEAST      VDLPGLTKVPVGDQPPDIERQIKDMLLKYISKPNAIILSVNAANTDLANSDGLKLAREVD 236
                *****:************* **:***:::::* *.:**:*..**:******.**:*:***

DYN1_HUMAN      PQGQRTIGVITKLDLMDEGTDARDVLENKLLPLRRGYIGVVNRSQKDIDGKKDITAALAA 254
VPS1_YEAST      PEGTRTIGVLTKVDLMDQGTDVIDILAGRVIPLRYGYIPVINRGQKDIEHKKTIREALEN 296
                *:* *****:**:****:***. *:* .:::*** *** *:**.****: ** *  **

DYN1_HUMAN      ERKFFLSHPSYRHLADRMGTPYLQKVLNQQLTNHIRDTLPGLRNKLQSQLLSIEKEVEEY 314
VPS1_YEAST      ERKFFENHPSYSSKAHYCGTPYLAKKLNSILLHHIRQTLPEIKAKIEATLK---KYQNEL 353
                ***** .****   *.  ***** * **. * :***:*** :: *::: *    *  :*

DYN1_HUMAN      KNFRPDDPARKTKALLQMVQQFAVDFEKRIEGSGDQIDTYELSGGARINRIFHERFPFEL 374
VPS1_YEAST      INLGPETMDSASSVVLSMITDFSNEYAGILDGEAKELSSQELSGGARISYVFHETFKNGV 413
                 *: *:     :..:*.*: :*: ::   ::*...::.: ********. :*** *   :

DYN1_HUMAN      VKMEFDEKELRREISYAIKNIHGIRTGLFTPDMAFETIVKKQVKKIREPCLKCVDMVISE 434
VPS1_YEAST      DSLDPFDQIKDSDIRTIMYNSSGSAPSLFVGTEAFEVLVKQQIRRFEEPSLRLVTLVFDE 473
                 .::  ::    :*   : *  *  ..**.   ***.:**:*::::.**.*: * :*:.*

DYN1_HUMAN      LISTVRQCTK--KLQQYPRLREEMERIVTTHIREREGRTKEQVMLLIDIELAYMNTNHED 492
VPS1_YEAST      LVRMLKQIISQPKYSRYPALREAISNQFIQFLKDATIPTNEFVVDIIKAEQTYINTAHPD 533
                *:  ::*  .  * .:** *** :.. .  .:::    *:* *: :*. * :*:** * *

DYN1_HUMAN      FIGFANAQQRSNQMNKKKTSGNQDEILVIRKGWLTINNIGIMKGGSKEYWFVLTAENLSW 552
VPS1_YEAST      LL-----------------KGSQAMVMVEEKLHPRQVAVDPKTG---------------- 560
                ::                 .*.*  ::* .*       :.  .*

DYN1_HUMAN      YKDDEEKEKKYMLSVDNLKLRDVEKGFMSSKHIFALFNTEQRNVYKDYRQLELACETQEE 612
VPS1_YEAST      ------KPLPTQPSSSKAPVMEEKSGFFG-----GFFSTKNK-------------KKLAA 596
                      *      * .:  : : :.**:.     .:*.*:::             :.

DYN1_HUMAN      VDSWKASFLRAGVYPERVGDKEKASETEENGSDSFMHSMDPQLERQVETIRNLVDSYMAI 672
VPS1_YEAST      LESPPPVLKATGQMTER--------ETMET-----------------EVIKLLISSYFSI 631
                ::*  . :  :*  .**        ** *.                 *.*: *:.**::*

DYN1_HUMAN      VNKTVRDLMPKTIMHLMINNTKEFIFSELLANLYSCGDQNTLMEESAEQAQRRDEMLRMY 732
VPS1_YEAST      VKRTIADIIPKALMLKLIVKSKTDIQKVLLEKLYGKQDIEELTKENDITIQRRKECKKMV 691
                *::*: *::**::*  :* ::*  * . ** :**.  * : * :*.    ***.*  :*

DYN1_HUMAN      HALKEALSIIGDINTTTVSTPMPPPVDDSWLQVQSVPAGRRSPTSSPTPQRRAPAVPPAR 792
VPS1_YEAST      EILRNASQIVSSV----------------------------------------------- 704
                . *::* .*:..:

DYN1_HUMAN      PGSRGPAPGPPPAGSALGGAPPVPSRPGASPDPFGPPPQVPSRPNRAPPGVPSRSGQASP 852
VPS1_YEAST      ------------------------------------------------------------


DYN1_HUMAN      SRPESPRPPFDL 864
VPS1_YEAST      ------------
```

Figure 3. A comparison between dynamin-1 and Vps1 amino acid sequence. Human dynamin-1 from UniProt Q05193 was lined up with Vps1 amino acid sequence (UniProt P21576) by Clustal Omega sequence alignment software (version 1.2.1). The red box indicates the amino acids involved in dynamin-1 actin binding. * Indicates identity, : Indicates strong similarity between amino acids and . Indicates weak similarity.

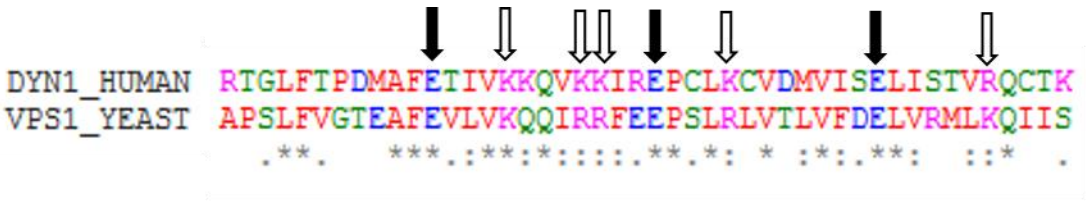

Figure 4. A comparison between dynamin-1 and Vps1 actin binding region Human dynamin-1 from UniProt Q05193 actin binding region with Vps1 actin binding region (UniProt P21576) aligned by Clustal Omega sequence alignment software (version 1.2.1). * Indicates identity, : Indicates strong similarity between amino acids and . Indicates weak similarity. Black arrows indicate acidic residues mutated in the initial study (Gu et al., 2010) and white arrows indicate basic residues mutated. Key Blue= acidic Purple = basic Red= small/hydrophobic Green =hydroxyl/sulphydryl/amine/glycine.

replaced with aspartic acid residues, and one form where two aspartic acid residues were changed to lysines. These residues were chosen as they were conserved between dynamin-1 and 2 and were within amino acids 399-444. To identify the orientation of these residues on the structure of dynamin-1 each amino acid mutated was plotted as space filling models on the crystal structure of dynamin (PDB 3SNH) using the structural software PyMol (Ford et al. 2011; Faelber et al. 2011). This indicated that the residues occupy an alpha helix on the outside of the dynamin structure and were orientated away from the main body of the protein (figure 5). Therefore changes to these residues are unlikely to affect the overall structure of the protein.

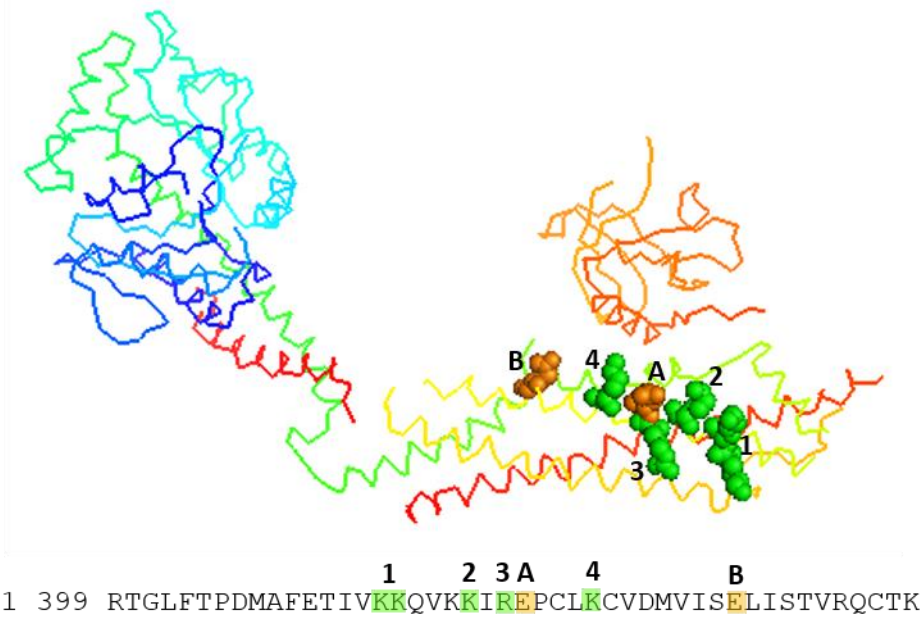

Figure 5. Mapping the charge mutations onto the crystal structure of dynamin-1. Crystal structure of dynamin-1 (PDB 3SNH) showing the charge mutations made in the initial dynamin-actin study (Gu et al., 2010). Each mutation is shown on the structure and labelled with a number (basic changes) or letter (acidic changes). Green indicates basic residues and orange acidic.

The Vps1-actin interaction was hypothesised to require conserved charged amino acids described in figure 4. By identifying these residues within a more specific region than previously reported, the actin binding region may be more precisely identified in the Vps1 study. With this knowledge, the refined actin binding region could then be examined in mammalian dynamin once more to identify the specific residues within amino acids 399-444 in dynamin-1 which are required for actin binding. Within the actin binding dynamin-1 alpha helix there are eight charged residues which are orthologous in Vps1 indicated by arrows (figure 6). It was hypothesised that basic amino acids were required for the Vps1-actin interaction, as it was demonstrated for the direct dynamin-actin interaction (Gu et al. 2010). Therefore three basic amino acids were chosen to be mutated in Vps1 namely RR457-8 and K453 (KK418-9 and K414 in dynamin-1). It was decided that all three of these would be mutated together to negatively charged glutamic acid residues to assess how they are involved in the Vps1-actin interaction (KRR-EEE). As a separate test, the two arginine residues which reside next to each other would be mutated separately (RR-EE) for two reasons. One because the creation of the triple mutation would have to take place in two steps, first creating the RR-EE mutation then adding the final K-E mutation in a separate reaction and therefore the RR-EE could easily be tested alongside the KRR-EEE mutant. Secondly the creation of the RR-EE alone would test a more specific site so as to further define a more precise actin binding region in Vps1.

It was also hypothesised that changing negatively charged amino acids to positively charged residues would increase the affinity of Vps1 for actin. In order to test this two glutamic acid residues were identified for mutation. The first was the residue E461 in Vps1 (E422 in dynamin-1), the second lies further downstream to the E461/422 residue, E473 in Vps1 (E434 in dynamin-1). Both residues were chosen due to their involvement in the original dynamin-1 actin binding study. The E461 and E473 residues were mutated to lysine residues separately to test if either of these single point mutations could increase the affinity of Vps1 for actin.

There are other conserved and charged residues within the predicated actin binding region of Vps1 which were not mutated during this study. This was to restrict investigation to a more specific actin binding region in Vps1. In the future a full analysis of the *in vitro* and *in vivo* effects of mutating each charged residue separately as well as all together would provide a

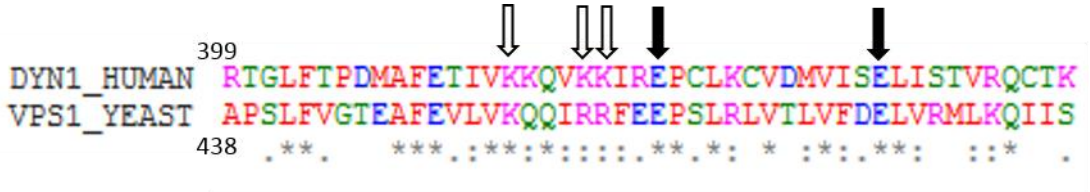

Figure 6. Mutations made in the predicted actin binding region of Vps1 This diagram indicates the residues selected for mutation in the Vps1 study. White arrows indicate basic to acidic changes and black arrows indicated acidic to basic mutations.

more in depth analysis of the predicted actin binding region in Vps1. This was deemed beyond the scope of this thesis and therefore the four mutations were the focus for this project.

So far, the crystal structure of Vps1 has not been reported. Therefore, for clarity, the crystal structure of dynamin (Ford et al. 2011; Faelber et al. 2011) was used to map the location and space filling models of the chosen of these charged amino acids for mutagenesis. As shown in figure 7, the charged residues project away from the structure of the protein. Therefore, assuming the actin binding region is similarly structured within Vps1, changing residues RR457-8, K453, E461 and E473 were predicted to not have a detrimental effect on overall structure of the protein and therefore could be used to specifically test the Vps1-actin interaction.

In conclusion, four mutations were selected for the Vps1 study, RR457-8EE, RR457-8EE+K453E, E461K and E473K. Both *in vitro* and *in vivo* analysis of these mutations in Vps1 is outlined in detail in chapters 4 and 5.

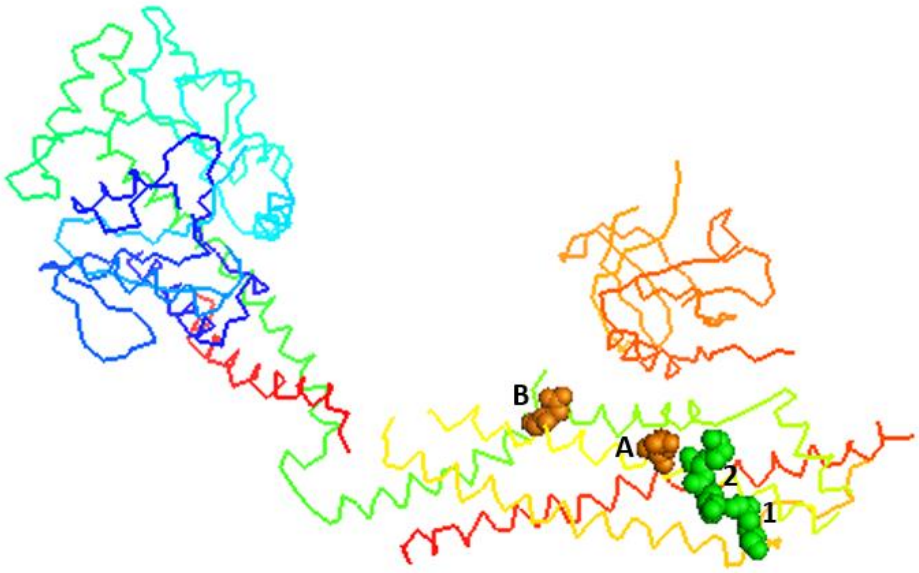

Figure 7. Selected mutations for Vps1 study mapped onto the crystal structure of dynamin-1. The crystal structure of dynamin-1 (PDB 3SNH) with the residues selected for Vps1-actin study highlighted in green for basic residue changes (numbers 1 and 2) and orange for acidic residue changes (letters A and B).

3.3 Analysis of conserved charged residues in the actin binding region of dynamin-1

3.3.1 Conserved residues in the actin binding helix in dynamin-1,2 and 3

There are three types of dynamin known to function in mammals: dynamin-1, 2 and 3. These are discussed in chapter 1 section 1.4.2. The initial study into the dynamin-actin interaction identified differences between dynamin-1 and 2 and therefore the actin binding regions were compared between the canonical human dynamin-1, 2 and 3 to identify any differences between them which could indicate a difference in function with actin. To do this the actin binding region from dynamin-1, 2 and 3 were aligned using Clustal Omega sequence alignment software (version 1.2.1, McWilliam et al. 2013, UniProt sequences Q05193, P050570 and Q9UQ16) and the orthologue residues chosen for the Vps1 study are indicated by arrows figure 8.

The dynamin-2 actin binding region shares 80.43% identity to the actin binding region of dynamin-1 and contains four of the five charged residues chosen for the Vps1 study. The residue at site 418 is a lysine in dynamin-1 and a valine in dynamin-2 (figure 8). This difference could suggest that dynamin-2 binds actin in a different way or that the extra lysine is not required for this interaction in the dynamin-2 isoform.

Dynamin-3 actin binding region shares 71.74% identity with the actin binding region of dynamin-1 and contains three of the five charged residues chosen for the Vps1 study. Similar to dynamin-2 it also does not have a charged residue at site 418 instead harbouring a valine at this point. In fact, the dynamin-3 actin binding region has 82.61% sequence homology with that of the dynamin-2 actin binding region. This suggests that the function of dynamin-2 and 3 could be similar and the interaction between dynamin-1 and actin could be to tailor dynamin-1 to cellular functions within neuronal cells. One interesting difference is seen at site 422 which

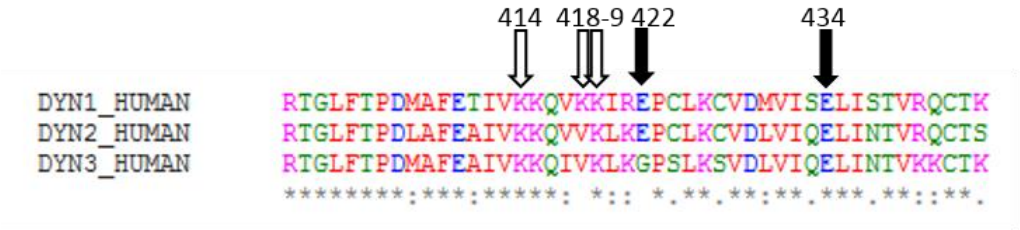

Figure 8. Comparing dynamin-1 actin binding region to dynamin-2 and 3. Canonical dynamin-1,2 and 3 actin binding regions. UniProt sequences, dynamin-1 Q05193 dynamin-2 P050570 and dynamin-3 Q9UQ16 aligned by Clustal Omega sequence alignment software (version 1.2.1). * Indicates the same amino acid. : Indicates strong similarity between amino acids and . Indicates weak similarity. Black arrows indicate acidic residues chosen for mutation in Vps1 study and white arrows indicate basic residues mutated. Key Blue= acidic Purple = basic Red= small/hydrophobic Green =hydroxyl/sulphydryl/amine/glycine

is a glutamic acid in dynamin-1,2 and Vps1 however in dynamin-3 this is a glycine (figure 8). This suggests a difference in function for this charged residue in dynamin-1 and 2 to that of dynamin-3. Due to the fact that glutamic acid residues are negatively charged whereas glycine residues are flexible, a change at this point in dynamin could affect both the way in which dynamin-3 binds to actin and how it oligomerises. This alteration could dictate how dynamin-3 interacts with actin which may be different to both dynamin-1 and 2, although this has yet to be investigated.

3.3.2 Conserved residues in the actin binding helix between species

During this study the specific residues identified to be required for Vps1 actin binding were then re-tested in dynamin-1 to see if they alone can affect dynamin-1 actin binding. For this study the use of recombinant rat dynamin-1 tagged with cerulean was kindly gifted by Professor Elizabeth Smythe and Professor Mike Cousin. In previous studies mouse dynamin (Liu et al. 2011a) and rat dynamin (Wang et al. 2010b; Anggono et al. 2006) have been used for investigations and therefore the rat dynamin-1 was considered to be appropriate. Because the dynamin-1 actin interaction has only been reported for human dynamin-1 the sequences of both human and rat canonical dynamin-1 were compared (UniProt Q05193 and P21575 respectively). This showed a 98.03% similarity between the two. However, there were 17 amino acid differences 14 of which were found within the actin binding region (red box figure 9). This suggests that this alpha helix may be markedly different between dynamin-1 in humans in comparison to rats.

The proposed actin binding region was found to vary between the three dynamin isoforms (figure 8) and therefore the differences between dynamin-1 from humans to rats may also be the case when comparing dynamin-2 and 3. To analyse this, the canonical human, rat and mouse dynamin-1,2 and 3, actin binding regions were compared and a phylogenetic tree was created using Clustal Omega online software (McWilliam et al. 2013) and the dynamin sequences from figure 8. From the phylogenetic tree data it was found that Vps1 sequence is most similar to that of dynamin-1 mammalian sequence and that the mouse and rat sequences are more comparable to each other than the human dynamin isoforms (figure 10A). From the sequence analysis a number of observations were made. Firstly at site 413-4 there are two charged lysine residues found in human, rat and mouse dynamin-1,2 and 3 (number 1 figure 10B). However in Vps1 there is only one residue present at the equivalent site to amino acid 414 (453 in yeast Vps1). This suggests that the requirement for two basic residues at this site is not evolutionarily conserved and could indicate a potential increase in actin binding ability of mammalian dynamin proteins that was not required in yeast cellular functions. The two lysine

Figure 9. A comparison between human and rat canonical dynamin-1. Human dynamin-1 aligned with rat dynamin-1 by Clustal Omega sequence alignment software (version 1.2.1). The UniProt references are next to each line. The red box indicates the amino acids involved in dynamin-1 actin binding. * Indicates the same amino acid. : Indicates strong similarity between amino acids and . Indicates weak similarity.

residues at site 418-419 are only seen in dynamin-1 isoforms in human and mouse canonical sequences (number 2 figure 10B). This double positive charge is also found in Vps1 at an equivalent site 457-8 however they are arginine residues rather than lysine. This could suggest that Vps1 may function with actin in a similar way to dynamin-1 if these charged residues are found to be important in a direct Vps1-actin interaction. Interestingly, the residue E422 in dynamin-1 and 2 is a glycine in all dynamin-3 human, mouse and rat genes (number 3 figure 10B). Vps1 has a glutamic acid at this residue (E461) suggesting that dynamin-3 may have evolved this difference so as to carry out a specific role in mammalian tissues. Finally, the residue E434 is conserved throughout the dynamin genes in humans, rats and mice (number 4 figure 10B). This is also conserved in yeast (E473) and therefore is likely to be an important residue for dynamin and dynamin-like proteins.

Figure 10. Comparing the actin binding region found in human, rat and mouse. A) Canonical dynamin-1,2 and 3 UniProt sequences, rat P21575, P39052, Q08877, mouse P39053, P39054, Q8BZ98 and Vps1 P21576 full length sequences aligned as a phylogenetic tree using Clustal Omega sequence alignment software (version 1.2.1). B) The actin binding region from canonical human dynamin-1,2 and 3 compared with rat and mouse canonical dynamin-1,2 and 3.* Indicates the same amino acid. : Indicates strong similarity between amino acids and . Indicates weak similarity. Key Blue= acidic Purple = basic Red= small/hydrophobic Green = hydroxyl/sulphydryl/amine/glycine. Numbers correspond to text.

From the Vps1 study the residues RR457-8 were found to be required for effective actin binding. Having identified this specific region within Vps1 actin binding region this was then tested in dynamin-1 (chapter 6). With the understanding of the differences between dynamin-1 proteins between species the study in chapter 6 focused on the human dynamin-1 aa isoform (described as the canonical sequence, accession number NP004399.2) as it has been used in previous studies of dynamin-actin function (Ochoa et al. 2000) and contains two charge residues orthologous with the Vps1 RR457-8 (namely KK418-9). Dynamin-1 was chosen for further investigation over dynamin-2 and 3 isoforms due to the direct dynamin-actin interaction having first been defined in dynamin-1 (Gu et al. 2010). Using dynamin-1 there is also scope to test the effects of disrupting this interaction through mutation on documented cellular processes, such as endocytosis and migration. With regards to this point, the dynamin-1 isoform is also more likely to function with actin during certain forms of endocytosis, as there is evidence for actin requirement in polarised neuronal cells for ultra-fast endocytic uptake (Watanabe et al. 2013). Finally, by using the dynamin-1 isoform the mutation A408T can be analysed. This mutation in murine dynamin-1, as previously mentioned, was found to cause an epileptic phenotype. As this mutation lies within the actin binding region it was also tested for its ability to bind actin as described in chapter 6 section 6.3.

3.3.3 The location and conserved nature of A408 in dynamin-1

A spontaneous murine mutation of alanine to threonine was found to cause an epileptic phenotype and was therefore named ‘fitful’ (Boumil et al. 2010). The A408T mutation was found near to the beginning of the actin binding region and when plotted on the crystal structure of dynamin-1 (figure 11A) was shown to reside at the start of the alpha helix, close to the area understood to be involved with creating higher order dynamin oligomers (figure 2B,C). Therefore it is unsurprising that the original report into this mutation found that dynamin-1 A408T was less able to form higher order structures and reduces transferrin uptake in COS-7 cells (Boumil et al. 2010). The residue A408 is extremely well conserved throughout dynamin isoforms in humans, rats and mice as well as yeast (Vps1 A447T) (figure 11B). Furthermore, this mutation is within the actin binding region of dynamin-1 and therefore could have an effect on actin binding. If this is the case it could provide further insight into the dynamin-1-actin interaction and its function in normal neuronal cell signalling and disease.

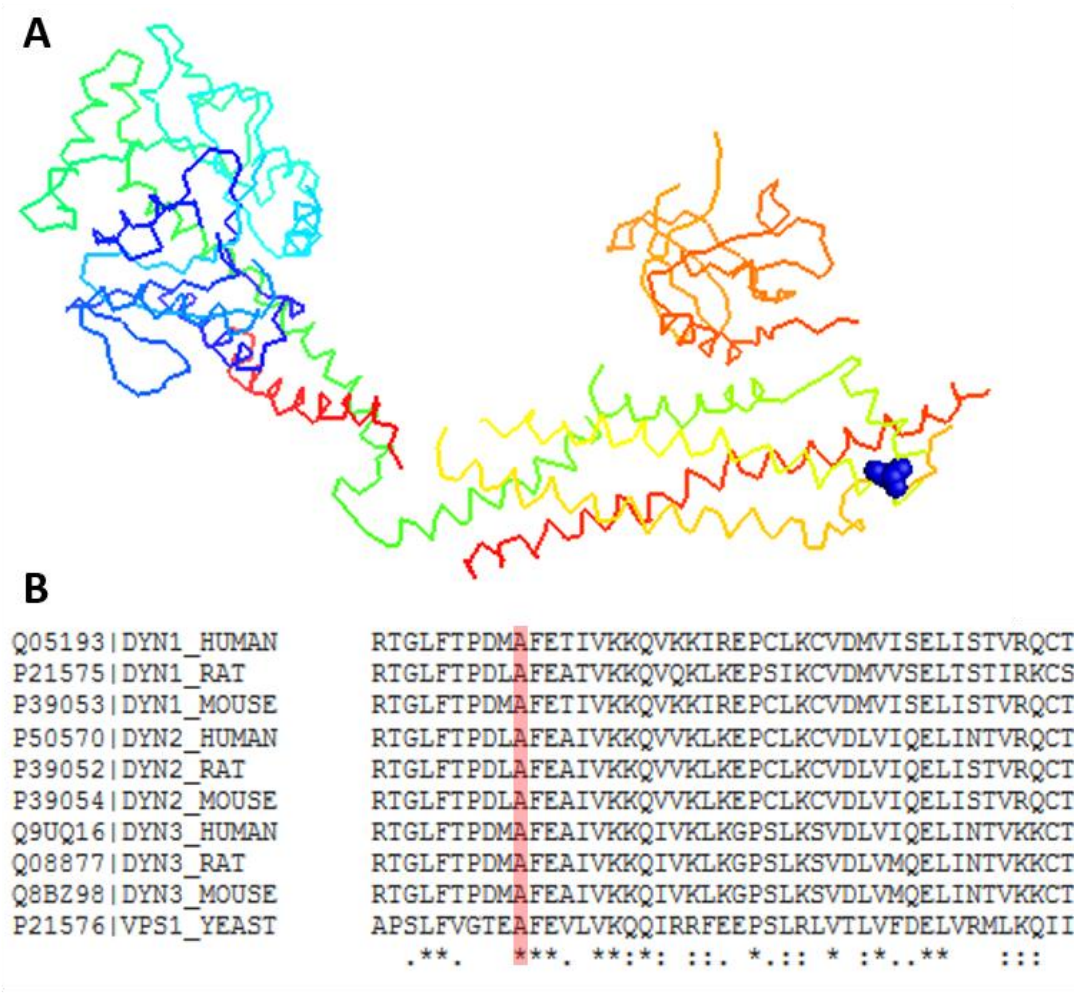

Figure 11. The conserved A408 residue A) The A408 residue plotted in blue as a space filling atomic model onto the crystal structure of dynamin-1 (PDB 3SNH) using PyMol software. B) Human, rat and mouse dynamin-1,2 and 3 aligned with Vps1 sequence by Clustal Omega sequence alignment software (version 1.2.1). A408 (447 in yeast) residue is highlighted in red. Unitprot reference numbers are to the left of each dynamin. * Indicates the same amino acid. : Indicates strong similarity between amino acids and . Indicates weak similarity.

3.4 Discussion

In this chapter the residues predicted to be required for actin binding in dynamin-1 were compared with Vps1 to select residues for the Vps1-actin study. This analysis has selected three positively charged residues in Vps1 which are conserved in dynamin-1 and predicted to be required for a Vps1-actin interaction. In addition, two acidic residues were chosen to see if the addition of positively charged residues within the actin binding alpha helix increases actin binding. Each residue mutated projects away from the main structure of dynamin-1 and were considered unlikely to affect overall Vps1 structure.

By comparing the predicted actin binding regions of dynamin isoforms and Vps1 it is clear that there are conserved charged residues. This suggests that the middle domain of Vps1

could also be involved in a direct actin interaction as has been reported for dynamin-1 (Gu et al. 2010). Dynamin-1 is a classical dynamin whereas Vps1 is a dynamin-like protein. Conserved charged residues in the middle domains of both dynamin and Vps1 suggests that the actin binding ability of dynamin-like proteins may be evolutionarily conserved. This could suggest that dynamin-like proteins interact with actin in a similar way to classical dynamins but use this affinity in very different cellular processes. For example the mitochondrial fission dynamin-like proteins OPA1 in mammals, Mgm1 in yeast, may also require a direct actin interaction to carry out mitochondrial fission.

The publication of the dynamin crystal structure also postulated how single dynamin molecules could form dimers and higher order oligomers. This was done using the single molecule structure and with the knowledge of certain residues and regions, found biochemically, to affect dynamin oligomerisation. This data provides an indication of how dynamin monomers bind to form a dimer and how dimers may create a ring structure. However, these interactions are possibly ambiguous due to probable differences between lattice dynamin crystal structures and oligomeric ring structures created *in vivo*. The ring model based on the crystal structure suggests that the middle domain actin binding helix would be available for binding actin with key residues pointing away from the areas of dimerisation or oligomeric structure (Faelber et al. 2011) (figure 2).

Cryo-EM studies of lipid bound dynamin spirals have provided insight into the orientation of each dynamin monomer within a more physiologically relevant ring (Chappie et al. 2011). These experiments were obtained using dynamin without the flexible proline rich domain (ΔPRD) bound to a non-hydrolysable GTP molecule, GMPPCP (Guanosine 5' β,γ-methyleno triphosphate), which was allowed to form around lipid tubules *in vitro*. It is known that GTP hydrolysis causes destabilisation of dynamin oligomers, releasing them from the membrane and for this reason a non-hydrolysable GTP was used to visualise dynamin in its GTP bound state which would otherwise be very transient (Danino et al. 2004; Pucadyil & Schmid 2008). Cryo-EM analysis of these structures have shown that, when dynamin is locked into this helical structure, the lipid binding domain is in the inside of the ring with the middle domain aiding in oligomerisation and the GTPase domains forming dimers between layers around the outside of the dynamin tubule. As shown in figure 12 this suggests that the GTPase dimers would shield the middle domain potentially impeding actin binding from the outside of the ring (Chappie et al. 2011). Since this data was published, studies using fluorescently bound dynamin in cells have indicated that for scission to occur only one full ring of dynamin is created (Cocucci et al. 2014). This has lead on to the hypothesis that one dynamin ring then forms dimers with the GTPase domains of the next ring causing hydrolysis which in turn causes a conformational change to pull the dynamin ring together. This would suggest that whilst *in*

vitro data has shown that a number of coils can form around a lipid tubule, this may be due to the conditions used such as the using a non-hydrolysable GTP. Therefore if only one ring is required for constriction in cells then there is a possibility that the middle actin binding region would be less shielded by GTPase domains and still be free to bind actin around the dynamin ring. A separate hypothesis would be that the actin filaments could lie on the top of the ring of dynamin perpendicular to the direction of endocytic invagination, although how this could be utilised in such a system has yet to be investigated.

There is possibility that the actin binding region functions as both actin binding and oligomerisation. Dynamin rings are known to change shape due to GTP hydrolysis and this could change the role of the residues in the middle domain from actin binding to oligomerisation. Ideally a structural description of the involvement of all residues at different stages of dynamin oligomer would be required to identify if residues involved in actin binding are also required for the constricted state of a dynamin ring.

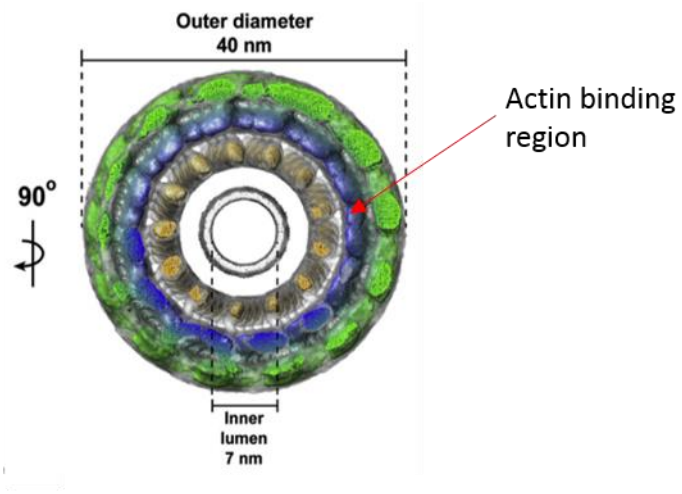

Figure 12. A reconstruction of lipid bound dynamin tubules. Image from Chappie et al., 2011 reproduced with permission from Elsevier. This figure indicates the different domain structure within a dynamin coil, green indicates the GTPase domains, blue is the middle coiled-coil domain and orange indicates the PH lipid binding domain.

Chapter 4

The direct Vps1-Actin interaction in yeast endocytosis

4.1 Introduction

Saccharomyces cerevisiae (subsequently referred to as yeast) have been invaluable for understanding eukaryotic cell systems due to the ease of genetically manipulating them and how evolutionarily conserved they are. During this study yeast are utilised as a model organism within which the Vps1-actin interaction is investigated to indicate if it is evolutionarily conserved and to test whether this interaction is required during yeast cellular processes including endocytosis. Yeast require actin for every endocytic event and therefore were an ideal model organism to analyse this direct interaction with regards to CME.

4.1.1 Vps1 in endocytosis

Vps1 is one of three dynamin-like proteins in yeast which include Dnm1 and Mgm1. Vps1 was first defined as a Vacuolar Protein Sorting molecule as its deletion caused a vacuole morphology defect (Raymond et al. 1992). Since Vps1 was discovered it has been found to function in a number of membrane trafficking events within yeast cells. These include: the trafficking of endosomes to the vacuole (Chi et al. 2014), the correct fission of peroxisomes to ensure inheritance from mother to bud (Hoepfner et al. 2001), the trafficking of proteins from the Golgi to the vacuole (Robinson et al. 1988), and the scission stage of endocytosis (Smaczynska-de Rooij et al. 2010). During endocytosis Vps1 can tubulate lipids (Smaczynska-de Rooij et al. 2010), bind directly to the coat protein Sla1 (Yu & Cai 2004) as well as the amphiphysin orthologue Rvs167 (Smaczynska-de Rooij et al. 2012).

Vps1 is known to be required for efficient scission events during CME *in vivo* (Smaczynska-de Rooij et al. 2010). Removing the *VPS1* gene was found to cause longer endocytic invaginations to occur, indicating a delay in scission, and caused disruption of the actin cytoskeleton (Smaczynska-de Rooij et al. 2010; Yu & Cai 2004). This could suggest that

Vps1 and actin may function together *in vivo*. As Vps1 has many function in a cell including during peroxisomal fission and vacuolar protein sorting, its potential interaction with actin could impact all aspects of its cellular function.

Vps1 has sequence orthology with the mammalian dynamin proteins. Moreover, the middle domain of Vps1 harbours orthologous charged residues, which are reported to be required for the dynamin-actin interaction (Gu et al. 2010). In this chapter the orthologous charged residues in Vps1 are tested to see if their mutation causes defects to Vps1 function in cells. Due to the similarity between the Vps1 and dynamin-1 actin binding sites, the fact that Vps1 functions during endocytosis, and that actin is required for every endocytic event in yeast, there is a strong possibility that Vps1 can bind directly to actin and that this interaction may be required during endocytosis.

4.1.2 The role of actin during endocytosis

The requirement for actin during endocytosis in yeast was first identified by testing mutations to the actin gene. By blocking actin function, through point mutations, a reduction in the uptake of the fluid phase marker Lucifer yellow was observed, suggesting a role for actin during endocytosis (Kübler & Riezman 1993). During this study this method of analysing endocytic uptake is used to analyse how Vps1 may require a direct actin interaction for efficient CME in yeast. Furthermore, there are a number of proteins required for endocytosis which bind to, and function with, actin during endocytosis such as Sla2 (Raths et al. 1993; McCann & Craig 1997) and Abp1 (Drubin et al. 1988; Kaksonen et al. 2003). This chapter uses these markers along with others and analyses their function when mutations in Vps1 are expressed *in vivo*.

Actin is required during the invagination stage of endocytosis. Prior to invagination, the WASP orthologue Las17 has been shown to recruit and polymerise actin (Urbanek et al. 2013). Actin filaments can then be bundled by proteins, such as Sac6 (Adams et al. 1991), and the force generated by actin polymerisation stimulates invagination to occur by overcoming yeast cell turgor pressure (Aghamohammadzadeh & Ayscough 2009). However, how actin may be involved in the scission stage of CME has yet to be defined.

The initial aim of this study was to determine whether there is a direct Vps1-actin interaction and, if so, whether this can be affected by specific charge mutations in the predicted actin binding site. Using this knowledge the study then focused on testing how these mutations affect the function of Vps1 *in vivo* and investigate what this may indicate for the function of dynamin and actin during endocytosis.

4.2 The direct Vps1-actin interaction

4.2.1 Vps1 binding to F-actin

Mammalian dynamin-1 has been demonstrated to bind directly to F-actin, an interaction mediated by an alpha helical region within the middle domain of the protein. The actin binding region described in dynamin-1 is homologous to other mammalian dynamin proteins, such as dynamin-2, as well as dynamin proteins in other species: namely, *Drosophila* shibire, *Caenorhabditis elegans* dynamin-1, and *Saccharomyces cerevisiae* Vps1 (Gu et al. 2010). The potential direct actin interaction of these dynamin-like proteins has not been fully investigated. Vps1 has been shown to function during endocytosis (Smaczynska-de Rooij et al. 2010), a cellular function that in yeast (as described previously) requires actin. In this study the orthologous middle region in the yeast dynamin Vps1 was investigated, to identify if the dynamin-actin interaction was evolutionarily conserved and if so, this would precede an investigation into the role of this interaction during endocytosis.

The interaction between mammalian dynamin-1 and actin was tested in a centrifugal based binding assay (Gu et al. 2010). In order to address if the yeast dynamin Vps1 can interact with actin, a similar centrifugal assay was designed. In this assay F-actin was incubated with soluble Vps1 and centrifuged at a high speed (90,000 rpm TL100 Beckman rotor). F-actin will sediment at this speed, whereas soluble Vps1 should not. The supernatant and pellet fractions were then separated, and then analysed by SDS-PAGE gel and Coomassie staining. Any increase in the proportion of Vps1 in the pellet fraction following incubation with actin would then suggest a direct interaction.

Vps1 was expressed in *Escherichia coli* (*E.Coli*) and affinity purified by its 6xhis tag, as described in chapter 2 section 2.3.3 (Smaczynska-de Rooij et al. 2012). Purified Vps1 was then pre-spun and the soluble protein in the supernatant retained for the assay. The concentration of Vps1 in the assay was set at 1.5 µM (by Bradford assay) as each Vps1 purification and pre-spinning step (carried out on the day of experimentation) was almost always guaranteed to provide enough protein for this concentration to be used. Rabbit muscle actin (purified as described 2.3.5) was used in this assay due to its extremely high purity and concentration, and because its polymerisation activity can be checked regularly (using pyrene actin assays Urbanek et al. 2013). The actin concentration was set at 3 µM to provide an excess binding partner for Vps1.

F-actin was pre-polymerised and incubated with Vps1 for 15 minutes at RT before centrifugation at high speed to separate F-actin and bound Vps1 from G-actin and unbound soluble Vps1. When incubated with actin there was an increase in the amount of Vps1 in the

pellet fraction in comparison to the Vps1-only control (figure 1A). This suggests that Vps1 can bind F-actin as predicted (Palmer et al. 2015a).

To calculate the binding affinity between Vps1 and rabbit muscle F-actin, a binding curve was generated. This was done by taking the proportion of Vps1 bound to F-actin, as assessed by densitometry, then plotting these for a range of Vps1 concentrations (figures 1B,C (Palmer et al. 2015a). Four independent experiments indicated a K_d of rabbit actin for Vps1 at 0.92 ± 0.31 µM, (figure 1B) which is similar to the estimated K_d calculated for actin to dynamin-1 of 0.42 µM (Gu et al. 2010). This interesting as it suggests that the affinity of Vps1 for actin is similar to that of dynamin-1 and other actin binding proteins, such as cortactin, which has an calculated K_d of ~0.4 µM (van Rossum et al. 2003).

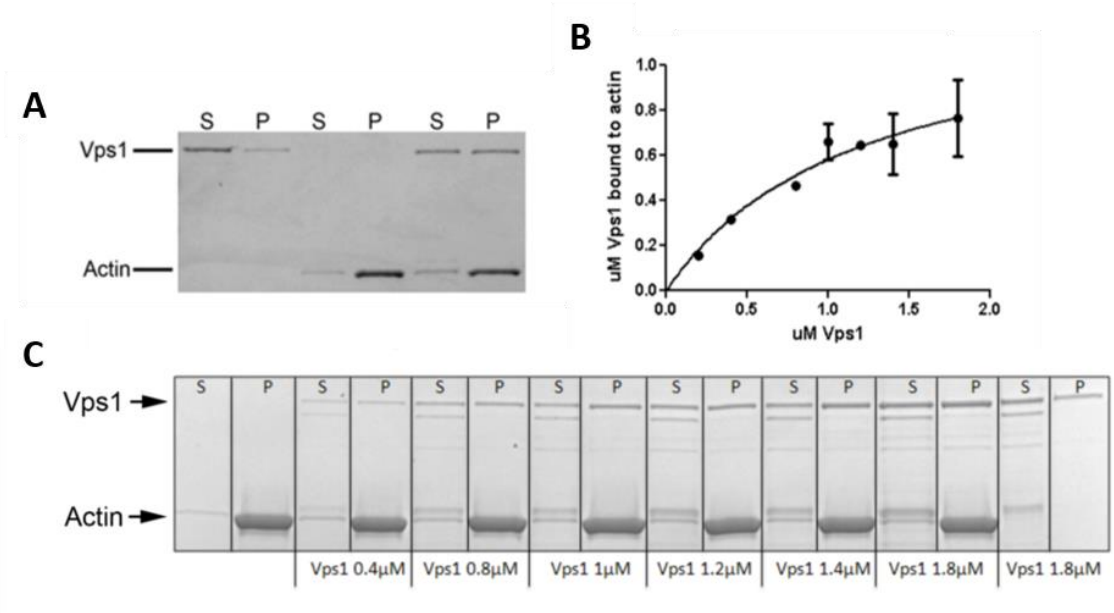

Figure 1. Vps1 binds rabbit F-actin A) Coomassie stained SDS-PAGE gel showing a co-sedimentation assay between 1.5 µM Vps1 and 3 µM F-actin. S= supernatant, P= pellet. B) Binding curve generated by increasing concentrations of Vps1 from 0.2-1.8 µM in the presence of 5 µM F- actin. Error bars are Standard Error of the Mean (SEM). C) Example Coomassie stained gel from which densitometry was carried out to calculate the amount of bound Vps1 to actin shown graphically in B).

These data demonstrated a direct interaction between Vps1 and actin. However, in order to verify the physiological relevance of this result, the experiment was also performed with yeast actin. Yeast actin was purified from 100 g of commercially available bakers yeast lysate using a DNAse 1 affinity column (Chapter 2 section 2.3.6). The K_d of bovine DNAse 1 for skeletal muscle G-actin is reported to be 0.05 nm (Mannherz et al. 1980) and this strong binding affinity is utilised in this yeast actin purification. To elute the yeast actin from DNAse 1 a 50% (v/v) solution of formamide was used. Formamide is known to denature and depolymerise actin (Zechel 1980; Zechel 1981) and therefore had to be dialysed away from the yeast actin as soon as possible following elution from the DNAse 1 column. Following dialysis

the yeast actin was polymerised and incubated with Vps1 at final concentrations of 3 µM and 1.5 µM respectively. Following centrifugation and processing on SDS-PAGE gels as described above, Vps1 was found to co-sediment with actin indicating a direct interaction (figure 2A). Further densitometry analyses using increasing Vps1 concentrations with actin yielded a K_d of yeast actin for Vps1 of 1.9 ± 0.36 µM (figure 2B,C Palmer et al. 2015a). This is similar to the binding affinity calculated for rabbit F-actin indicating that the use of rabbit F-actin yields similar results to that of yeast F-actin. As the skeletal rabbit muscle preparations yielded a higher purity and activity, without the use of formamide, this source of F-actin was continued to be used for subsequent *in vitro* analyses of the Vps1 actin interaction.

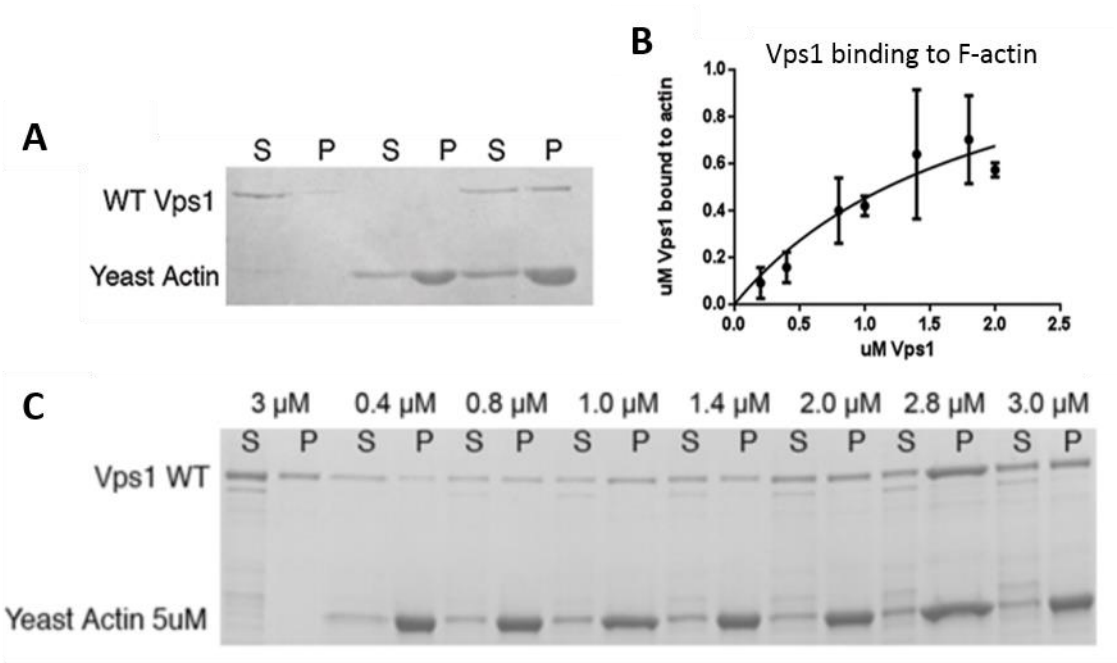

Figure 2. Vps1 binds yeast F-actin A) Coomassie stained SDS-PAGE gel showing a co-sedimentation assay between 1.5 µM Vps1 and 3 µM yeast F-actin. B) binding curve calculated from densitometry shown in C) Increasing concentrations of Vps1 from 0.4-3 µM, in the presence of yeast actin. Error bars are SEM.

4.2.2 GTPase activity of Vps1 with and without actin

Dynamin-1 is a large GTPase and its ability to hydrolyse GTP has been well documented. When dynamin-1 is at a concentration of 0.5 µM its basal Kcat or turnover of GTP has been calculated as 1.44 ± 0.026 min^{-1} and this can increase up to 100 fold when dynamin-1 is in the presence of lipids (Leonard et al. 2005). Moreover it has been reported that the GTPase activity of dynamin-1 can increase up to ~3.5 fold in the presence of short actin filaments (Gu et al. 2010). It is well documented that Vps1 is a GTPase however its activity has not been fully documented. This project therefore set out to confirm the ability of Vps1 to hydrolyse GTP (Vater et al. 1992) and see if this hydrolysis is affected by the presence of actin.

A colourimetric assay was used to monitor GTPase activity, at a temperature of 37^{o}C, in which the GTPase action of Vps1 is stopped at various time points by the addition of EDTA to chelate and sequester the magnesium ions required for GTP hydrolysis. The amount of phosphate released was analysed by the addition of an acidic malachite green and ammonium molybdate solution. Malachite green is an organic compound which reacts with ammonium molybdate bound to inorganic phosphate to produce a green colour.

To investigate the basal rate of Vps1 GTP hydrolysis, Vps1 was purified in phosphate free buffer (HEPES see chapter 2 section 2.3.14) and pre-spun to reflect the conditions of the co-sedimentation assays. The concentration of Vps1 was adjusted to 0.5 µM during the assay and either tested alone, or combined with 0.25 µM F-actin, with concentrations of GTP ranging from 0-1.5 mM. The GTPase activity of Vps1 was predicted to be similar to that of dynamin-1 and to increase in the presence of F-actin. Four independent experiments were performed in the presence and absence of actin (figure 3A). The data from these experiments, whilst preliminary, indicated that actin does not have an effect on the GTPase action of Vps1. From these data, the GTPase rate (Vmax), turnover (Kcat) and affinity (Km) of Vps1 for GTP was calculated. As seen in the table below, the turnover of GTP for pre-spun Vps1 is similar to that reported for dynamin-1 as predicted.

The oligomeric state of dynamin-1 is known to affect its ability to hydrolyse GTP (Chappie et al. 2010). Therefore, in order to test if oligomeric Vps1 causes an increase GTP hydrolysis, alone or in the presence of actin, this experiment was repeated on one occasion with Vps1 that had not been pre-spun. Oligomeric Vps1 was predicted to slightly increase GTP hydrolysis, as the basal rate of spun Vps1 protein has a turnover similar to that of dynamin-1. Similarly the addition of actin was not predicted to have much of an effect due to the Vps1 in the assay being already oligomerised. The ability of Vps1 to bind to GTP (Km) was hypothesized to stay the same as this should not be affected by the oligomeric state of Vps1. This initial investigation indicated a large increase in rate as well as the turnover of GTP hydrolysis by oligomerised Vps1 in comparison with pre-spun Vps1 (figure 3B) and this was not affected by the presence of actin. As seen in the table below figure 3, the affinity of Vps1 for GTP was unaffected by the oligomeric state of Vps1.

These preliminary experiments suggests that the oligomeric state of Vps1 does indeed influence the rate of GTP turnover and that the basal GTPase hydrolysis of Vps1 is greater than that of dynamin-1. The presence of actin does not affect the ability of Vps1 to hydrolyse GTP. However in future studies it would be imperative to repeat this with short-capped fragments of actin as only short actin filaments have been reported to increase the ability of dynamin-1 to hydrolyse GTP (Gu et al. 2010).

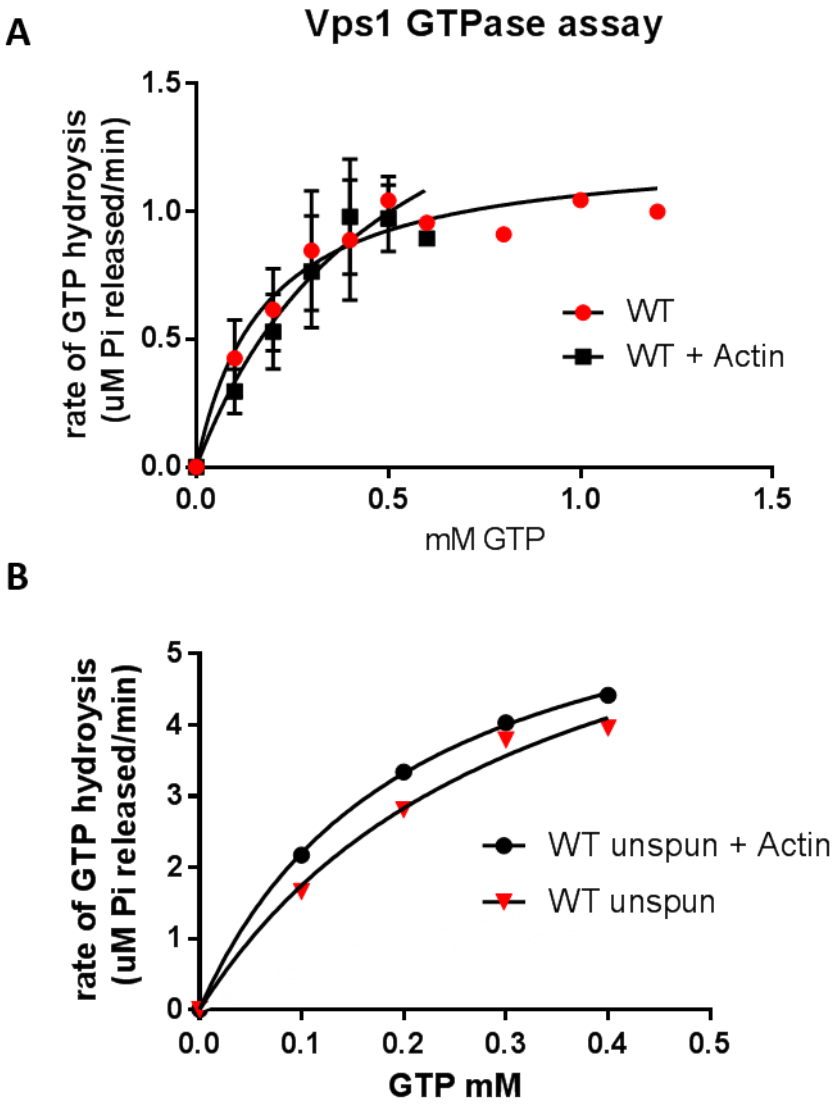

Figure 3. The presence of actin does not effect Vps1 GTPase activity A) The rate of GTP hydrolysis for pre-spun WT Vps1 was tested in four independent experiments and this was compared with four independent experiments with the addition of 0.25 µM F-Actin. This yielded preliminary results that F-actin does not affect the GTPase action of Vps1. B) The rate of GTPase hydrolysis for unspun WT Vps1 alone and with actin from one experiment.

Vps1	**Vmax** µM Phosphate min^{-1}	**Km** µM	**Kcat** min^{-1}
Spun WT	1.25 ± 0.13	0.18 ± 0.056	2.46 ± 0.26
Spun WT + 0.25 F-Actin	1.99 ± 0.59	0.50 ± 0.254	3.98 ± 1.19
WT	7.46 ± 1.11	0.33 ± 0.09	14.90 ± 2.22
WT + 0.25 F-Actin	6.75 ± 0.14	0.21 ± 0.01	13.50 ± 0.28

4.2.3 Identification of mutations in the predicted actin binding site of Vps1

Having identified that Vps1 interacts with actin, and that this seems to have little effect on the GTPase action of the enzyme, this project moved on to analyse the predicted actin binding site. The actin binding site in dynamin-1 has been identified as being between amino acids 399-444, which form an alpha helix within the middle domain. By creating charge mutations within this region, the affinity of dynamin-1 for actin was either enhanced (by the addition of basic residues) or reduced (by the addition of acidic residues) (Gu et al. 2010). In this study, the orthologous region in Vps1 (amino acids 439-483) was analysed to determine whether there are specific charged residues that are critical for actin binding in yeast. This analysis found five charged residues in the predicted actin binding site of Vps1 that were chosen to be mutated. These were RR457-8 and K453, created as two separate mutations (RR-EE and KRR-EEE) and the point mutations E461K and E473K. From the published dynamin-1 study it was predicted that the change in residues from acidic to basic would increase the affinity between Vps1 and actin and basic to acidic mutations would cause a decrease in this affinity. The location of these residues are shown and discussed in chapter 3 section 3.2.2 figure 7.

4.2.4 Effects of charge mutations on the actin binding ability of Vps1

Having identified the four charged mutations to be analysed, the relevant mutants were then created for recombinant expression in a plasmid with 6xhis-tagged Vps1 (pKA 850) by site directed mutagenesis (SDM). Each mutation was then expressed in *E.coli* and purified, when required, on the day of experimentation. The purification of each Vps1 mutation was similar to that of Vps1 Wild Type (WT), with similar yields and purity for every preparation (data not shown).

The first experiment to be carried out was the analysis of whether the four mutations affect the ability of Vps1 to bind actin. This was carried out using the same high speed sedimentation assay with rabbit skeletal F-actin as described earlier. The E-K mutations were predicted to increase actin binding whereas K/R-E mutations were expected to reduce this interaction. The E461K mutation did not significantly affect actin binding, as compared with WT (figure 4A,B). The binding ability was also similar to that of WT Vps1 when KRR-EEE mutation was present which was surprising as this mutant introduces three negative residues in this region. The E473K and RR-EE mutations however both significantly reduce the ability of Vps1 to bind to actin (one way ANOVA $F=11.87$ d.f. 4,25 $p < 0.0001$) (figure 4B). A similar result with yeast F-actin has also been described (Palmer et al. 2015a) indicating that this result is physiologically relevant.

The E473K is acting in an opposite manner to what was predicted and it is interesting that this single residue is so critical to the Vps1-actin interaction. The Vps1 RR-EE mutation was predicted to reduce actin binding and it does indeed reduce the ability of Vps1 to bind actin and be pulled into the pellet fraction. Whereas the RR-EE mutation can reduce Vps1 actin binding, the addition of the K453E mutation seems to reduce this effect. It should be noted that none of these mutations completely abolish the ability of Vps1 to bind to actin and the rescuing effect of the K453E mutation indicates that there may be other contributors in this region, or indeed other areas of the Vps1 molecule that may be modified structurally or electrostatically, when the additional K453E mutation is present, which may strengthen the Vps1-actin interaction.

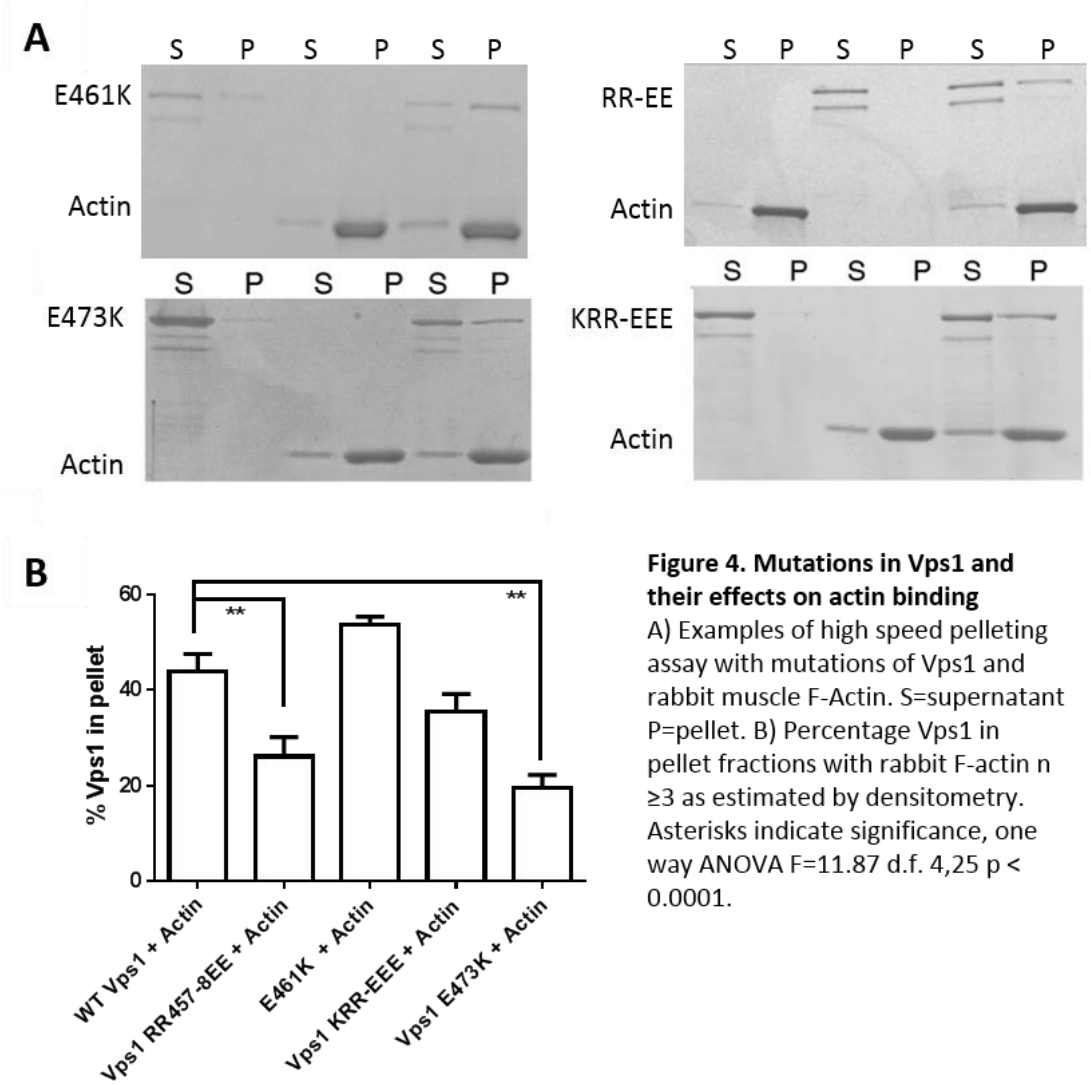

Figure 4. Mutations in Vps1 and their effects on actin binding
A) Examples of high speed pelleting assay with mutations of Vps1 and rabbit muscle F-Actin. S=supernatant P=pellet. B) Percentage Vps1 in pellet fractions with rabbit F-actin n ≥3 as estimated by densitometry. Asterisks indicate significance, one way ANOVA $F=11.87$ d.f. 4,25 $p < 0.0001$.

Mammalian dynamin proteins are known to function during endocytosis by binding to lipids, oligomerising into a coil at the vesicle neck, and facilitating scission by GTP hydrolysis. Dynamin proteins also contain a proline rich C terminus which can bind SH3 domain containing

proteins, such as amphiphysin-2, that aids in the regulation of an endocytic event (Meinecke et al. 2013). The alpha helix in the actin binding site within the middle domain between the GTPase and lipid binding regions of dynamin. There is a possibility that charge mutations within the actin binding site may affect the ability of dynamin to oligomerise, bind to lipids and protein SH3 domains as well as affect its ability to hydrolyse GTP. As previously discussed, each of the charge mutations are orientated away from the centre of dynamin and therefore the effects on other functions of this protein are likely to be small. Vps1 is known to bind to lipids, interact with Rvs167 and hydrolyse GTP (Smaczynska-de Rooij et al. 2012). Therefore it would be ideal to test each of these functions with every one of the four charge mutations. Whilst a full *in vitro* investigation into the effects of site-directed mutagenesis on all of the functions of Vps1 was beyond the scope of this project, the effect on lipid binding of each mutation and on GTPase action of two of these mutations was chosen for analysis. These investigations are described in the next two sections.

4.2.5 Effects of charge mutations on the lipid binding ability of Vps1

Dynamin proteins harbour a pleckstrin homology (PH) domain, which is reported to facilitate lipid binding (Salim et al. 1996; Mehrotra et al. 2014). Vps1 is known to be able to bind directly to and tubulate lipids (Smaczynska-de Rooij et al. 2010), although there is not a defined lipid binding region known to facilitate this function. There is, however, a region within the molecule identified as insert B, which is in a similar position to the PH domain in mammalian dynamins that could be involved with the lipid binding in Vps1. This has yet to be fully investigated but there is potential for any mutations made within Vps1 to modify the tertiary structure and reduce or affect the ability of Vps1 to bind to lipids. This could then cause defects *in vivo* that could be incorrectly associated with changes to the actin binding site. The four mutations identified and tested in this thesis are not nearby the insert B region and, if this region is involved in lipid binding, would therefore be unlikely to affect the interaction between Vps1 and lipids. However, to test if this indeed the case a high speed centrifugation assay was utilised and modified to include the addition of lipids.

Vps1 WT and the E461K, E473K, RR-EE and KRR-EEE mutations were purified separately and incubated with Folch lipids (Avanti): a mixture of different types of lipids to which Vps1 is known to bind (Smaczynska-de Rooij et al. 2010). The Vps1 and lipids were then centrifuged at high speed, then the supernatant and pellet fractions were run on an SDS-PAGE gel, followed by staining with Coomassie. As each of the mutations are in the middle domain of Vps1 it was predicted that they would not affect Vps1 lipid binding. As seen in figure 5A each of the mutations are found in the pellet fraction when incubated with lipids indicating they can

all bind lipids like the WT as hypothesised. By densitometry analysis, the proportion of Vps1 E461K, E473K, RR-EE or KRR-EEE found in the pellet upon incubation with Folch lipids was not significantly different to that of Vps1 WT ($n \geq 2$ one way ANOVA $F=2.362$ d.f. 3,10 p 0.157). These data indicate that the mutations are not affecting the ability of Vps1 to bind lipids and are therefore not involved in lipid binding.

In a number of cases it was found that a second, faster migrating band of Vps1 (which did not pellet or bind to actin) could be seen in the Coomassie stained gels. It was important to check that this was a breakdown product of Vps1 rather than a contaminant as a contaminant could be affecting the binding results described above. Western blot analysis, using anti Vps1 antibodies, revealed that this faster migrating band was indeed Vps1 (figure 5B Palmer et al. 2015a). If the structure of Vps1 is similar to that of dynamin, then its tertiary structure is reliant on several intramolecular interactions between various domains within the protein.

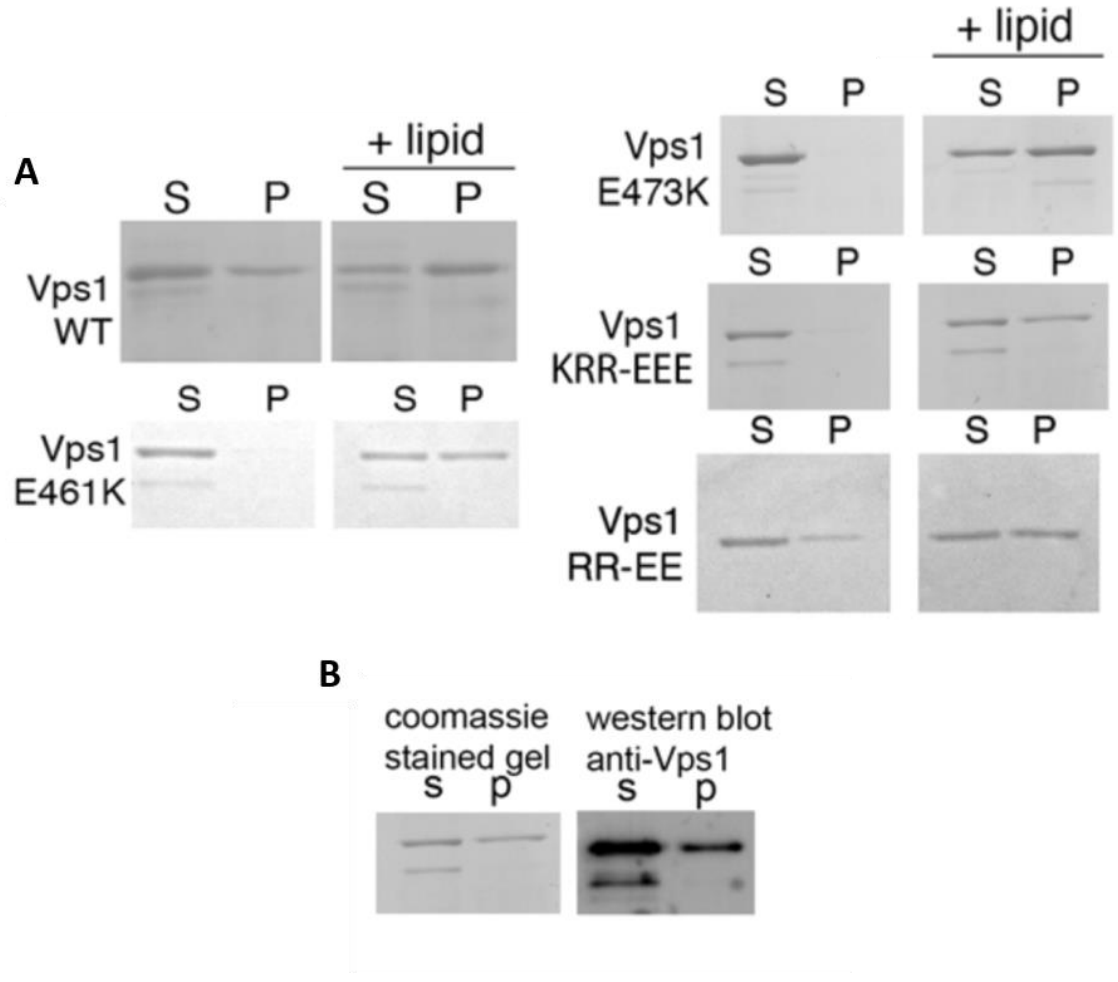

Figure 5. Vps1 actin binding mutations do not affect lipid binding. A) Examples of high speed pelleting assay with mutations of Vps1 and Folch lipid fraction S= supernatant P=pellet. B) Coomassie stained gel compared with western blot of S and P from a pelleting assay with Vps1. This indicates the second band in the Coomassie gel is a Vps1 breakdown product.

Therefore a truncation of Vps1 would lose part of these domains and therefore prevent proper folding of the tertiary structure of the whole protein. This could give rise to an unfolded potentially soluble truncated protein that is unable to interact with actin.

4.2.6 Effects of charge mutations on the ability of Vps1 to hydrolyse GTP

Mutating the alpha helix in the middle domain of dynamin or Vps1 could change the ability of the protein to hydrolyse GTP. Therefore, in order to test the effects of the charge mutations on the ability of Vps1 to hydrolyse GTP, a stopped GTPase assay was carried out as described previously. The GTPase assay was only undertaken for two of the four mutations, RR-EE and E461K, due to the complexity of the assay and limitations on time. These mutations were not expected to change the ability of Vps1 to hydrolyse GTP significantly.

Vps1 RR-EE and E461K were purified and pre-spun before being added to the assay at 0.5 µM with concentrations of GTP from 0-1.5 mM. Two replicates of the stopped assay were performed for Vps1 RR-EE and three separate occasions for E461K. The results from these experiments were compared with WT Vps1 GTPase data (figure 3, 4.2.2). The average phosphate by each mutant released was plotted against the concentration of GTP (figure 6). The curve for Vps1 E461K was not considerably different from WT Vps1 indicating little difference in GTP turnover, rate of hydrolysis, or affinity for GTP (Kcat, Vmax and Km respectively). However, the average turnover of GTP (see table below) calculated for the RR-EE mutant was notably different from WT Vps1 suggesting that the RR-EE mutation slightly reduces the ability of Vps1 to hydrolyse GTP. However, the reproducibility of these results was extremely variable from one Vps1 preparation to another. The low number of repeats meant that these results were preliminary and it was deemed beyond the scope of this project to continue with the enzymatic profiling of Vps1. Overall, this data indicates that the RR-EE and E461K mutations are not affecting the ability of Vps1 to hydrolyse GTP.

0.5 µM protein in assay	**Vmax** µM Phosphate min^{-1}	**Km** µM	**Kcat** min^{-1}
WT	1.25 ± 0.13	0.18 ± 0.06	2.50 ± 0.26
RR457-8EE	0.78 ± 0.07	0.36 ± 0.09	1.6 ± 0.13
E461K	0.99 ± 0.24	0.23 ± 0.19	1.98 ± 0.47

In conclusion, these *in vitro* results reveal that of the four mutations RR-EE and E473K reduce the ability of Vps1 to bind to actin and none of the mutations significantly increase the affinity of this interaction. To understand the cellular effects of reduced actin binding mutations RR-EE and E473K, and to analyse if there are *in vivo* effects of the E461K and KRR-EEE mutations, these mutations were expressed *in vivo.*

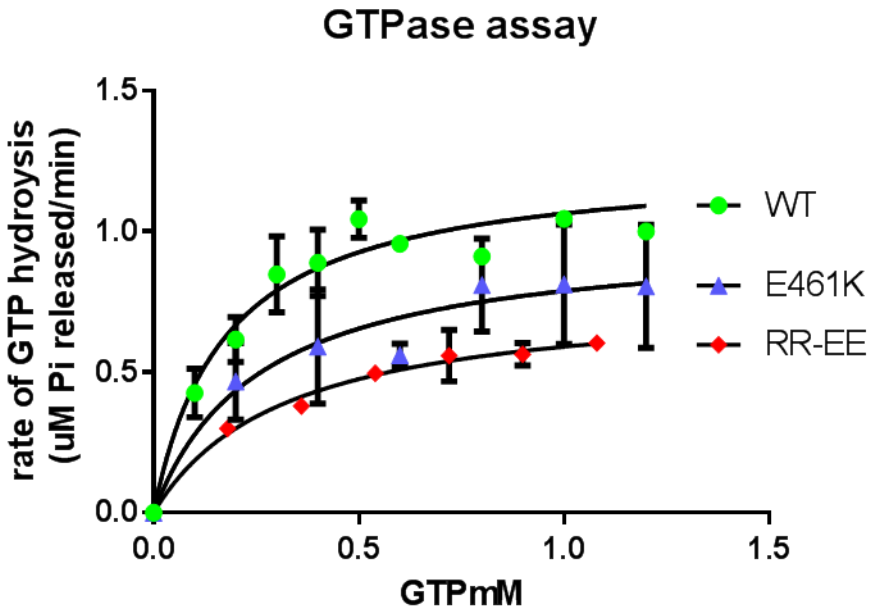

Figure 6. Mutations RR-EE and E461K do not affect Vps1 GTPase activity. This graphs shows the average rate of GTP hydrolysis for WT (n=4), RR-EE (n=2) and E461K (n=3).

4.3 The effect of Vps1 mutations on cellular functions requiring Vps1

4.3.1 The expression of Vps1 actin binding mutations in vivo

Each of the actin binding site mutations were created in the *in vivo* expression plasmid pKA 677 by site directed mutagenesis (chapter 2 section 2.2.3 and tables 2.8.1/2). This plasmid expresses Vps1 under its own promoter and therefore should express Vps1 to a similar level to wild type yeast. WT Vps1, along with the four mutations described, were transformed into *vps1* null yeast strains (KAY 1095) and grown in selective media. Initially, the expression levels of the Vps1 mutations were assessed by western blot of whole cell lysate fractions and compared with WT expression. To do this cells were grown overnight and a 1 ml sample was taken and adjusted to an optical density (OD_{600}) of 2. These cells were then pelleted by centrifugation, lysed with glass beads and SDS sample buffer then run on a SDS-PAGE gel. This gel was transferred onto a PVDF membrane and probed for using Vps1 antibodies. The membrane was then developed using enhanced chemi-luminescence and this showed a band of Vps1 in the whole cell lysate of *vps1* null cells transfected with the Vps1 WT plasmid, as expected. Conversely, there is no Vps1 band in the lysate fraction of *vps1* null cells transfected with the plasmid vector alone (figure 7). Western blots of whole cell lysates from cells expressing Vps1 RR-EE, E461K and E473K indicate similar levels of Vps1 in comparison to the

WT protein. Interestingly, there is a reduction in the overall amount of Vps1 KRR-EEE in the whole cell lysate fraction in comparison to WT and the other three expressed mutations of Vps1 (figure 7). This suggests that the KRR-EEE is less stable than WT Vps1 and may break down in the cytosol, or that it may be more toxic to yeast cells than the other mutations, and therefore more readily degraded.

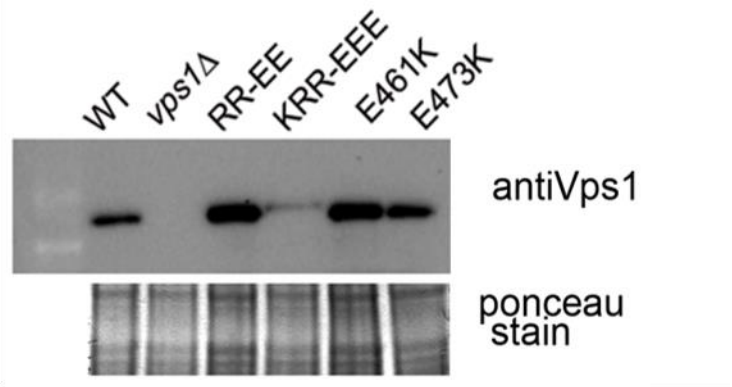

Figure 7. The expression of Vps1 actin binding mutations *in vivo*
Western blot of whole cell lysates expressing Vps1 mutations with corresponding Ponceau stain of membrane as a loading control. Note that the KRR-EEE mutation results in a noticeably reduced level of protein relative to the WT strain.

4.3.2 Growth analyses in both liquid and solid media of Vps1 actin binding mutations

It is known that the null *vps1* strain yeast grows slowly and are temperature sensitive (Smaczynska-de Rooij et al. 2010). It is possible that the expression of the actin binding mutations also cause a similar phenotype when expressed *in vivo*. To test if this is the case, a growth analysis in liquid media was performed. An overnight culture of budding yeast was adjusted to an OD_{600} of 0.1 and tracking the increase in optical density (or absorbance) at 600 nm over time to provide an indication of cell growth. KRR-EEE and E473K expressing cells had a growth phenotype similar to that of the null strain (figure 8A). For yeast expressing the Vps1 KRR-EEE this is not surprising as the expression of this mutation (figure 7) is much lower than that of WT Vps1, and therefore yeast expressing this were expected to have a phenotype similar to that of the *vps1* null strain. The expression of Vps1 RR-EE and E461K was able to rescue the growth rate of *vps1* null yeast to WT levels (figure 8A). By fitting an exponential growth curve to this data the average doubling time for each strain was calculated (GraphPad Prism software). This indicated a doubling time for the WT Vps1 strain of 2.40 hours, and this was similar to those of the RR-EE and E461K strains, which were 2.33 and 2.32 hours respectively. The doubling time for the *vps1* null strain was 2.71 hours a phenotype reflected in Vps1 KRR-EEE and E473K strains which had doubling times of 2.76 and 2.70 hours respectively.

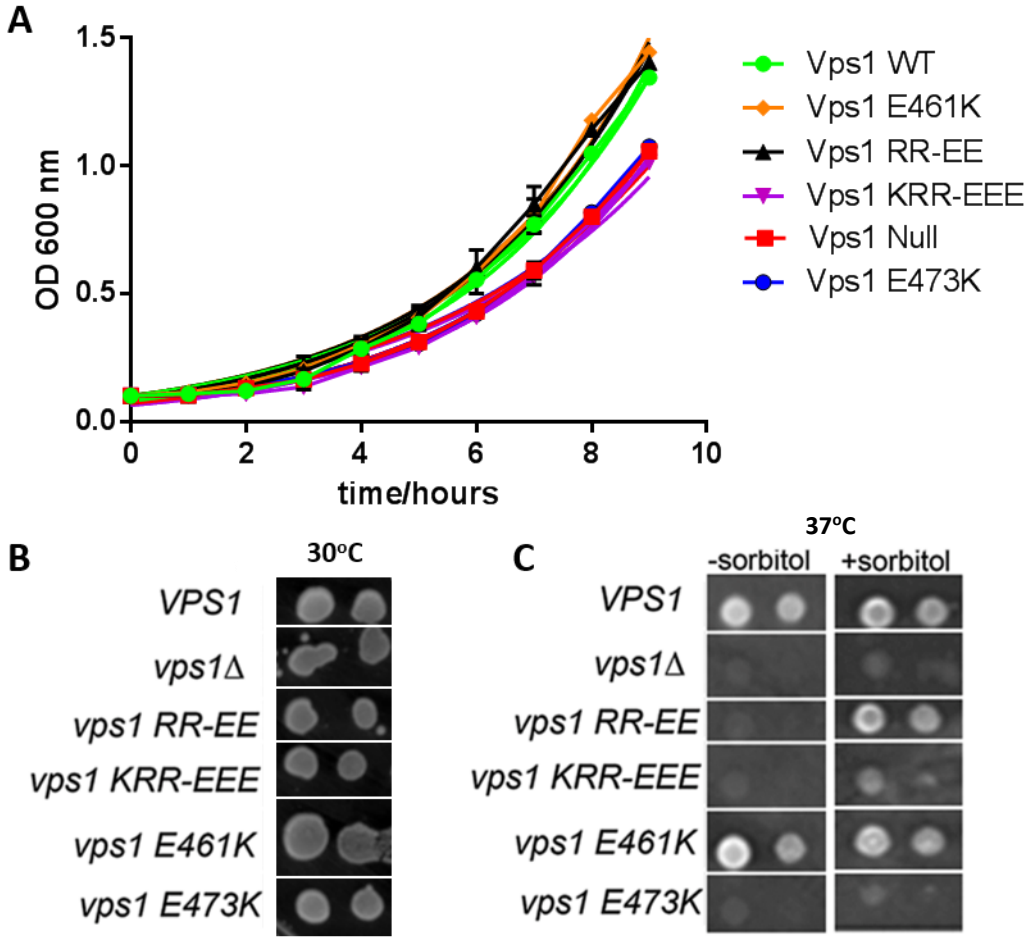

Figure 8. Growth analyses of cells expressing Vps1 actin binding mutations. A) A Growth curve tracked over 9 hours for Vps1 and actin binding mutations n= 2. B) An example of Vps1 and actin binding mutations grown on solid media at 30°C. C) An example of Vps1 and actin binding mutations grown on solid media at 37°C with and without the addition of sorbitol. The temperature sensitivity of yeast cells expressing Vps1 RR-EE is shown to be rescued by the addition of sorbitol.

These results indicate that the KRR-EEE and E473K mutations of Vps1 cause a null growth phenotype in yeast. Therefore, as *vps1* null cells are temperature sensitive, it was likely that the KRR-EEE and E473K strains were also temperature sensitive. This phenotype was also predicted to be rescued by the expression of either WT Vps1, RR-EE or E461K. In order to test this hypothesis, overnight liquid cultures of each of the yeast strains were adjusted to an OD_{600} of 0.5 and plated in 5 µl spots on to plates of selective soft agar. The plates were then dried and incubated at either 30°C or 37°C for up to 24 hours. As seen in figure 8B all strains grew at 30°C, including the *vps1* null strain. However, when the strains were grown at 37°C, only the Vps1 E461K strain rescued the *vps1* null temperature sensitive phenotype. This is interesting, as the RR-EE strain was predicted to rescue temperature sensitivity, but instead it reduced growth at 37°C.

The temperature sensitivity of the RR-EE mutation may indicate a reduction in the ability of Vps1 to function in endocytosis. This may not be the only reason why this mutation shows temperature sensitivity however, the fact that it has a reduced ability to bind actin, and that actin is required for yeast endocytosis, could indicate how this mutation is affecting Vps1 function in cells. It is understood that yeast require actin during endocytosis to overcome turgor pressure and this pressure can be reduced by growing yeast cells on sorbitol media, thus decreasing the requirement for actin-dependent force generation during an endocytic invagination (Aghamohammadzadeh & Ayscough 2009). Therefore, if the reduction in the ability of RR-EE to bind actin is causing a defect in endocytosis, by removing the requirement for the actin should reverse the growth defect observed on solid media. As hypothesised, when the cells were grown on media containing sorbitol the temperature sensitivity of the RR-EE mutation was rescued (figure 8C). This supports the hypothesis that the RR-EE mutation could be causing a defect in the function of Vps1 at an endocytic invagination due to its reduced actin binding ability.

4.3.3 The effect of Vps1 actin binding mutations on vacuole morphology

It is understood that Vps1 functions during endocytosis (Smaczynska-de Rooij et al. 2010) however Vps1 also has a role in vacuolar morphology (Raymond et al. 1992), endosome trafficking (Chi et al. 2014), peroxisomal fission (Hoepfner et al. 2001), and Golgi to vacuole trafficking (Robinson et al. 1988). By changing the actin binding site, and therefore the middle domain of Vps1, its role in any of these cellular process may well be disrupted. In order to test if the actin binding mutations were having a detrimental effect on the function of Vps1 *in vivo* each of these cellular processes were analysed in turn. The results from these studies are described over the next four sections.

Vps1 stands for vacuole protein sorting 1 and, as discussed in the introduction (section 1.6) was named along with other genes which are required for sorting proteins to the vacuole (Rothman & Stevens 1986; Rothman et al. 1989). *vps1* null cells were found to exhibit vacuoles with a class F phenotype, which is defined by the presence of a large vacuole surrounded by smaller, fragmented vacuole structures, or simply collection of fragmented vacuole structures clustered together. As the mutations KRR-EEE and E473K exhibit a null phenotype in growth assays these mutations were also predicted to cause disruption to the vacuole morphology, a phenotype that was hypothesised to be rescued by the expression of Vps1 E461K and RR-EE.

In order to test whether the actin binding mutations cause a class F phenotype of vacuole, overnight cultures of cells expressing Vps1 actin binding mutations were adjusted to

an OD_{600} of 0.7 and exposed to the dye FM4-64. FM4-64 is lipophilic dye which, when bound to a lipid membrane, fluoresces more brightly than when in solution. This provided a useful tool whereby lipids could be visualised by fluorescence microscopy. The cells were exposed to this dye for up to 15 minutes by which time the stained vacuole could be seen by fluorescence microscopy. After analysing over 100 cells from two separate experiments it was found that over 80% of cells expressing KRR-EEE or the E473K mutation harboured the class F vacuole morphology similar to that of *vps1* null cells (figure 9). This phenotype was rescued by the expression of Vps1 WT, E461K or RR-EE as predicted (figure 9). This indicates that the two mutations E461K and RR-EE do not affect the morphology of the vacuole and therefore are likely to function as the WT in this cellular role of Vps1.

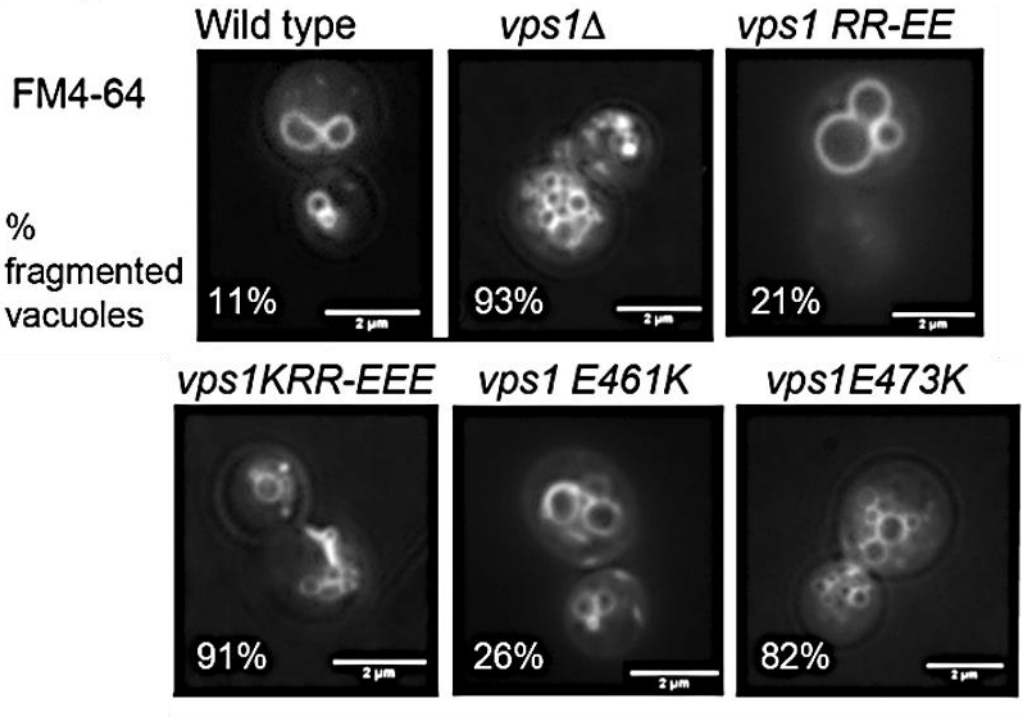

Figure 9. The morphology of the vacuole in cells expressing Vps1 mutations. Examples of cells with vacuole staining by the lipophilic dye FM4-64. The percentage of cells indicating fragmented vacuole morphology (class F) is indicated on each image. Scale bar is 2 µm.

4.3.4 The effect of Vps1 actin binding mutations on Snc1 recycling

Vps1 is known to function in the recycling of endosomes (Chi et al. 2014) and in order to analyse the effects of Vps1 mutations on this process the localisation of Snc1 was analysed. Snc1 is involved in the exocytosis of vesicles after which it is rapidly endocytosed and recycled back to the plasma membrane (Lewis et al. 2000). Therefore a GFP-tagged Snc1 was used to visualise endosomal trafficking from and to the cell membrane. Disruption to the recycling of Snc1-GFP results in a reduction of membrane and punctate staining within yeast cells (Burston

et al. 2009; Lewis et al. 2000). In the absence of Vps1, the Snc1-GFP signal is found to be dispersed with a reduction of membrane staining, indicating a disruption of endosomal trafficking (Smaczynska-de Rooij et al. 2010). The Vps1 KRR-EEE and E473K were predicted to have similar Snc1-GFP localisation to the null cells, with the RR-EE and E461K mutants rescuing this phenotype.

In order to analyse the localisation of Snc1-GFP in yeast the strain KAY 1462 (table 2.8.4) was used, which contains an integrated Snc1-GFP-SUC2. The addition of the enzyme invertase (SUC2) can be used for a different endosomal recycling assay method not undertaken during the course of this study (Burston et al. 2009). The different Vps1 mutations were transformed into KAY 1462 yeast and grown to an OD_{600} of 0.7. The bud of yeast cells (where endocytosis and membrane recycling occurs at a faster rate) were then analysed for Snc1 localisation by fluorescence microscopy. As shown in figure 10 over 90% of cells expressing KRR-EEE and E473K have a diffuse Snc1 localisation indicating a defect in endosomal recycling as seen in *vps1* null cells. This is, as predicted, rescued by the expression of the WT, RR-EE and E461K mutations. This suggests that the RR-EE and E461K mutations are less likely to be causing defects in the ability of Vps1 to function in the recycling of endosomes.

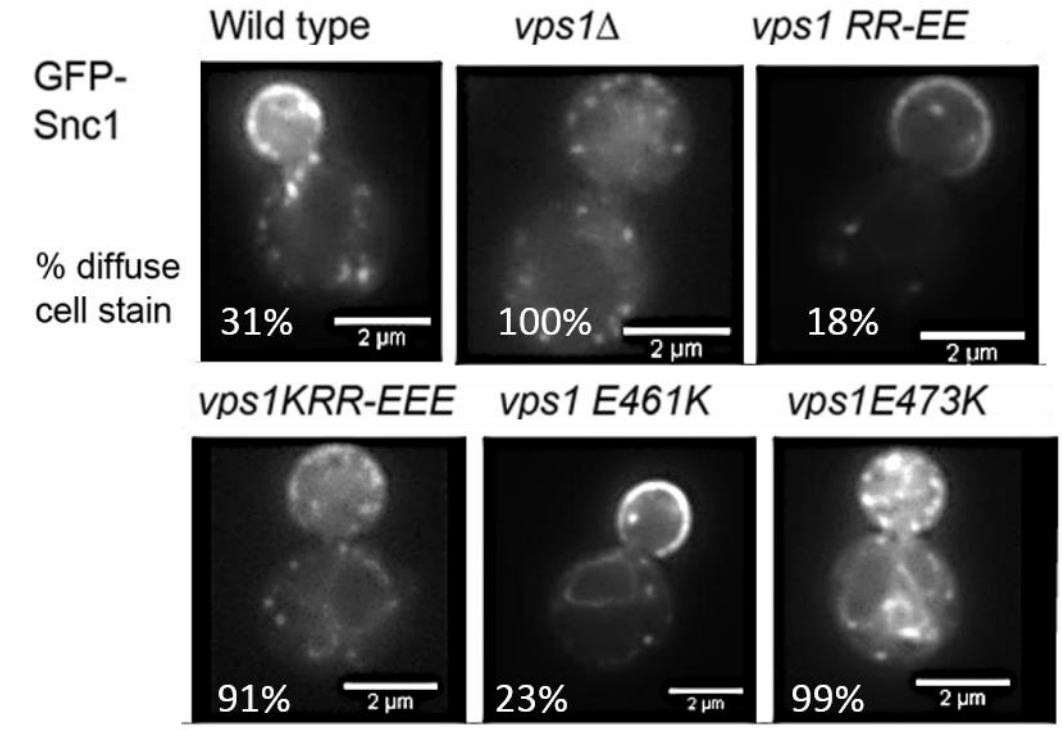

Figure 10. The localisation of Snc1 in cells expressing Vps1 mutations. Examples of cells expressing Snc1-GFP. The percentage of cells in each condition which show dispersed Snc1 localisation is indicated in each image. Membrane and puncta localisation of Snc1 in the bud is seen as normal WT phenotype. Scale bar is 2 µm.

4.3.5 The effect of Vps1 actin binding mutations on peroxisomal fission

The peroxisome organelle is required for fatty acid metabolism (van der Klei & Veenhuis 1997) and during yeast cell growth peroxisomal fission is required to separate this organelle between the mother and new budding cell. Peroxisomal fission is delayed in the absence of Vps1, resulting in elongated peroxisomes stretching between the mother and bud of a dividing cell (Hoepfner et al. 2001). This phenotype is even more prevalent when the yeast dynamin-like protein Dnm1 is removed (Kuravi et al. 2006) suggesting that both Vps1 and Dnm1 are required for peroxisomal fission. In order to test the role of Vps1 mutations in peroxisomal fission the yeast strain KAY 1096 was used, which has both *VPS1* and *DNM1* removed from its genome. Therefore, the expression of Vps1 mutations should rescue the enlongated peroxisome phenotype in budding cells if they are able to function like the WT. It was predicted that expression of the KRR-EEE and E473K mutations would result in the presence of long peroxisomes, as seen with the *vps1* null condition. The formation of elongated peroxisomes by delayed fission was predicted to be rescued in budding yeast cells by the expression of Vps1 WT, RR-EE or E461K.

In order to visualise the peroxisomal morphology of yeast cells expressing the Vps1 mutations the peroxisomal marker PTS-1 tagged with GFP was utilised. PTS-1 is a peptide (Hettema et al. 1998) which localises to the peroxisome so that their morphology can be analysed. PTS-1 GFP was expressed from a plasmid (pKA 910) in the KAY 1096 cell line (*dnm1* and *vps1* null) along with the Vps1 mutations. Elongated peroxisomes in budding yeast cells were counted and the percentage of cells showing an elongated peroxisome morphology was calculated (figure 11). The elongated peroxisome phenotype was rescued upon expression of Vps1 WT, RR-EE and E461K as predicted. The expression of the KRR-EEE and E473K mutants indicated a null phenotype whereby the fission of peroxisomes from mother to bud is delayed. This supports the conclusion that the RR-EE and E461K mutations are functioning as the WT in this cellular process.

Even without Vps1 and Dnm1 peroxisomes still go through fission at a slow rate. This is thought to be due to their transport along actin cables by myosin2 (Hoepfner et al. 2001). Therefore if they are stretched long enough they will undergo spontaneous fission. This indicates a close mechanism between peroxisome and actin. This study suggests a Vps1 actin binding mutations do not cause elongated peroxisome phenotype suggesting that the direct Vps1-actin is not required during this fission mechanism. This could be due to the peroxisome membranes not being under pressure like plasma membrane and therefore there is less of a requirement for extra force during fission so that the action of Vps1 GTPase action may be enough during this process.

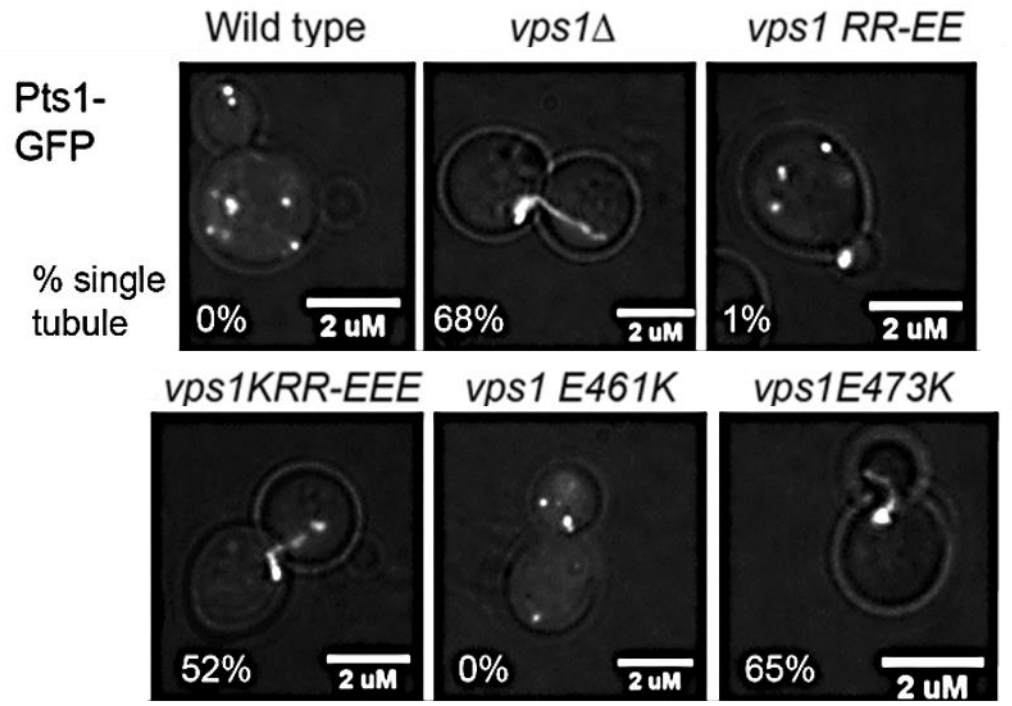

Figure 11. The morphology of peroxisomes in cells expressing Vps1 mutations. Examples of cells expressing PTS1-GFP peptide. The percentage of cells showing elongated peroxisome between the mother and bud is indicated in each image. Scale bar is 2 µm.

4.3.6 The effect of Vps1 actin binding mutations on the trafficking of carboxypeptidase Y (CPY)

Vps1 is known to function in the trafficking of proteins from the Golgi apparatus to the vacuole. This was first discovered due to the abnormal secretion of the carboxypeptidase Y protein (CPY) upon deletion of the *VPS1* gene. CPY is an enzyme that is made as a precursor protein (pCPY) in the endoplasmic reticulum (ER) and trafficked to the vacuole where it gets cleaved into its mature form (mCPY). If the trafficking process is disrupted then pCPY accumulates in the Golgi, indicating a defect in trafficking (Hasilik & Tanner 1978). The deletion of *VPS1* was found to increase the amount of pCPY in cells indicating a defect in its trafficking from the Golgi to the vacuole (Rothman et al. 1989).

In order to test if Vps1 mutations are preventing the delivery of CPY to the vacuole, yeast expressing each of the four mutations were grown to an OD_{600} of 0.7 and then pelleted by centrifugation. The cell pellets were then re-suspended in media with cyclohexamide to prevent protein synthesis and therefore prevent expression of CPY which may hinder the ability to differentiate between the amounts of mCPY in comparison to pCPY. Following the 30 minute incubation, cells were lysed and lysates were resolved on SDS-PAGE gels, transferred onto a PVDF membrane, before western blotting with anti-CPY antibodies. The presence of a

slower migrating band (pCPY ~64 KDa) above the expected faster migrating band (mCPY ~60 KDa) indicates the presence of pCPY that has accumulated due to a defect in Golgi to vacuole trafficking. It was predicted that the KRR-EEE and E473K mutants would result in the presence of a pCPY band, whereas the RR-EE and E461K mutations were predicted to act like the WT and rescue this defect in trafficking. As hypothesised there is no pCPY band present in cells expressing Vps1 WT, RR-EE or E461K mutations (figure 12). This band is present in *vps1* null cells, KRR-EEE and E473K mutant cells indicating these two mutations are unable to function in Golgi to vacuole trafficking. There seemed to be less CPY in general when Vps1 was not present or in the RR-EE cells analysed (in comparison to the GAPDH loading control). This could suggest that the amount of CPY being secreted is increased upon loss of functional Vps1, however this was not tested during this project. This would be a useful test to be performed in the future however for the purpose of this study it was deemed enough to conclude that when RR-EE, E461K and WT were present there was not an accumulation of pCPY in the cells, in comparison to *vps1* null, KRR-EEE and E473K where miss-localised pCPY was visible (figure 12).

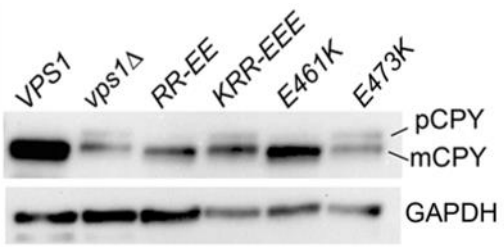

Figure 12. The effect of Vps1 mutations on the trafficking of CPY Carboxypeptidase Y is trafficked to the vacuole from the Golgi where it is cleaved into its mature form shown here as mCPY. If trafficking of this protein is disrupted then there is a build up of precursor CPY (pCPY). As is seen in this western blot Vps1 null, KRR-EEE and E473K mutations cause an increase in pCPY. GAPDH is a loading control.

4.3.7 The effect of Vps1 actin binding mutations on fluid phase endocytic uptake

The final cellular role tested was the ability of the Vps1 mutant proteins to function in endocytosis. This was first investigated by following the uptake of a fluid phase endocytic marker: Lucifer yellow. Lucifer yellow is a water soluble fluorescent dye, which is normally taken up by yeast and trafficked to the vacuole. Due to its fluorescence, its passage into yeast cells can be tracked from the membrane to intracellular punctate structures (endosomes) and subsequently to the vacuole, where it accumulates.

Each of the Vps1 mutations were tested to see if the accumulation of Lucifer yellow was slower in any of the strains, suggesting a defect in endocytic uptake. It was predicted that *vps1* null, KRR-EE and E473K would have defects in endocytic uptake and therefore would show fewer cells with Lucifer yellow dye taken up to the vacuole. The RR-EE and E461K mutations were hypothesised to take the fluorescent Lucifer yellow dye up into the vacuole to the same extent as the WT as these two mutations have showed no defects in other *in vivo* roles of Vps1 such as peroxisomal fission and endosomal recycling.

To test this hypothesis, Vps1 mutants were expressed in the *vps1* null strain KAY 1095 and grown in liquid culture to an OD_{600} of 0.7. Lucifer yellow was then added to the media at a concentration of 13 mg/ml for 90 minutes at 30^{o}C and then visualised using a fluorescence microscope. Up to 200 cells were analysed over two experiments and categorised depending on whether the dye was seen predominantly the membrane, in punctate endosomal structures, or in the vacuole (figure 13A). After incubation with Lucifer yellow for 90 minutes at 30^{o}C a large proportion of the dye would be expected to have been taken up into the vacuole. This initial experiment indicated that the KRR-EEE and E473K mutants were slower at trafficking the Lucifer yellow dye into the vacuole, a phenotype which is also reflected by the *vps1* null strain (figure 13B). This result supports the idea that the E473K and KRR-EEE mutations prevent Vps1 to function efficiently in all its cellular roles. The endocytic phenotype for the KRR-EEE mutation may also be due to its lower expression level as discussed earlier. Interestingly, in cells expressing the RR-EE and E461K mutants there was a slight increase in the number of cells showing punctate staining in comparison to the WT (figure 13B). This could suggest that these two mutations are also reducing a cells ability to take up this dye over time. This would be unexpected having found that all other Vps1 functions are similar to the WT when these two mutations are present. However, this could indicate a more subtle defect caused by these mutations.

The uptake of Lucifer yellow dye in a WT cell condition at 30^{o}C would be expected to have moved primarily into the vacuole by a 90 minute time point. The result obtained following a 90 minute incubation suggested that there could be defect in endocytic uptake of this dye in the presence of Vsp1 RR-EE and E461K mutations. If this were the case then testing a shorter incubation with Lucifer yellow may exhibit a clearer difference when these two mutations of Vps1 are expressed in cells. To test this, a single experiment was undertaken whereby the uptake of Lucifer yellow was visualised after 30 minutes and the localisation of the dye was analysed in 100 cells per condition (figure 13C). At the 30 minute time point, cells expressing RR-EE exhibited a marked reduction in the number of cells where the dye had reached the vacuole (figure 13C). There was also an increase in the number of cells with endosomal punctate and plasma membrane staining. This suggests that the RR-EE mutation is

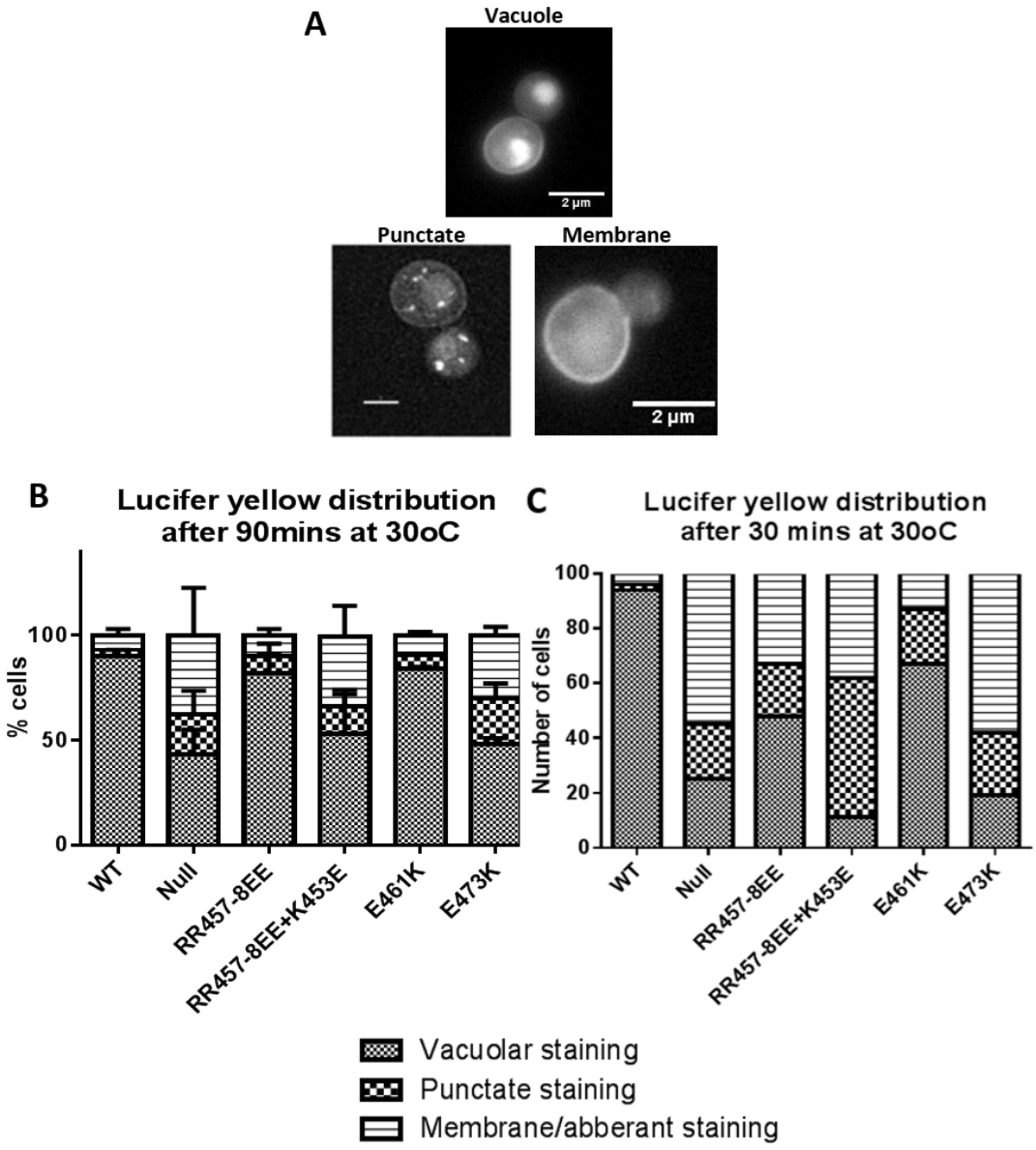

Figure 13. The fluid phase uptake of Lucifer yellow dye in cells expressing Vps1 mutations.
A) Example of cells counted as vacuole, punctate and membrane staining. B) The distribution of Lucifer yellow in cells expressing Vps1 mutations after 90 minutes of exposure to the fluorescent dye at 30ºC. This was calculated from 200 cells over two experiments. C) The distribution of Lucifer yellow in 100 cells expressing Vps1 mutations. This was carried at 30ºC after 30 minutes of exposure.

specifically affecting the uptake of the fluid phase marker Lucifer yellow and no other known functions of Vps1, such as peroxisomal fission or CPY trafficking. The mutation KRR-EEE was found to have more punctate endosomal staining than the null *vps1* strain suggesting that this mutation is reducing uptake as well as potentially affecting the trafficking of the dye to the vacuole (figure 13C). However, as this mutation was found to express at levels much lower than the WT this may be an artefact and would require further clarification by repeating this assay.

The E461K mutation was the second mutation found to act like the WT strain in all other functions of Vps1. However, when testing the uptake of Lucifer yellow at an earlier time point, the E461K mutant data seemed to indicate a defect in fluid phase uptake due to more cells exhibiting membrane and endosomal staining (figure 13C). This difference was not as marked as the other mutations, suggesting that the influence of the E461K mutation on the uptake of Lucifer yellow is mild. However, it was interesting to find that, despite having a WT phenotype in all other aspects of Vps1 *in vivo* functions, the E461K mutation could be having a negative impact on endocytosis. Finally, the E473K mutation was predicted to act like the null strain, and exhibited a similar number of cells with vacuole, membrane and punctate staining as *vps1* null cells after 90 minutes. This confirms that this charge change mutation prevents the function of Vps1 *in vivo*.

These results suggest that all four of the Vps1 mutations are defective in fluid phase uptake of Lucifer yellow. This was confirmed by assays conducted at the 30 minute time point, which in future work would need repeating to confirm that this result is robust. This however was not undertaken during the course of this project as confirmation of this result was indicated when the four mutations were integrated into the genome and tested once again for fluid phase uptake. This is described in more detail in section 4.5. For clarity, this report will focus on the rest of the work undertaken with the plasmid borne Vps1 mutations up until section 4.5 where the results of the integrated mutations are discussed.

The E461K mutation rescues *vps1* null phenotypes, such as defects in vacuole and peroxisomal morphology, Golgi to vacuole trafficking and endosomal sorting (figures 9-12). However, this mutation does cause a slight delay in the uptake of the fluid phase marker relative to WT Vps1 (figure 13C). This indicates that the E461K mutation has a specific endocytic defect in the function of Vps1 in cells. *In vitro* the E461K mutation was not found to increase the ability of Vps1 to bind to actin (figure 4) as was predicted by the introduction of a basic residue. Therefore in order to analyse how this point mutation is affecting endocytosis specifically, a further, in-depth analysis was planned to analyse the effects of this mutation on markers of endocytosis. This study is described in detail in chapter 5.

When expressed *in vivo,* the RR457-8EE mutation was found to have a specific defect in fluid phase endocytic uptake (figure 13C) and was temperature sensitive (figure 8C). This temperature sensitivity was rescued by the addition of sorbitol, which is interesting because sorbitol alleviates the effects of turgor pressure which causes a reduction in the requirement for actin during endocytosis. This raised the question, is the rescue of growth by sorbitol when the RR-EE mutation is expressed directly linked to the reduced requirement for actin during endocytosis? The mutation RR457-8EE was found to significantly reduce, but not block, the

ability of Vps1 to bind actin (figure 4). Therefore this reduction in actin binding could be linked to the specific endocytic defect seen in cells harbouring this mutation.

Therefore, the project subsequently focused on the following question: how does a reduction in the ability of Vps1 to bind to actin affect endocytosis? In order to address this, the RR457-8EE mutation was investigated in detail to determine how it may affect different stages of endocytosis and how this could be linked to the actin binding ability of Vps1.

4.4 The endocytic effects of reducing the Vps1-actin interaction

4.4.1 Presence of Vps1 RR457-8EE at the site of endocytosis

During the previous section the delay of the Vps1 mutation RR-EE on the uptake of the fluid phase dye Lucifer yellow was described. This phenotype may be due to a miss-localisation of Vps1 RR-EE, whereby the mutation prevents its accumulation at an endocytic site. In order to test if this is the case, the co-localisation between Abp1-mCherry and GFP-tagged Vps1 RR-EE was tested using Total Internal Reflection Fluorescence (TIRF) microscopy (chapter 2 section 2.5.6). In order to achieve this, RR-EE was created by site directed mutagenesis of the Vps1-GFP plasmid, pKA 1070. This was then transfected into the yeast strain KAY 1466, which has an mCherry-tagged version of Abp1 integrated onto the genome. Abp1 is actin binding protein 1, which is known to function during the invagination stage of endocytosis in yeast and is frequently used as a marker of endocytosis (Kaksonen et al. 2003; Kaksonen et al. 2005). The co-localisation between Abp1-mCherry and Vps1-GFP was then analysed in transfected cells. TIRF microscopy was chosen as a method for visualisation as this provides a way to select for the accumulation of Abp1 and Vps1 at the membrane and to reduce the chance of visualising endosomes. Using this method it was found that there was co-localisation between Abp1-mCherry and WT Vps1-GFP (number of patches 24 ± 4.1% are co-localised) and between Abp1-mCherry and Vps1 RR-EE (21.5 ± 5.1%) figure 14A,B (Palmer et al. 2015a). This low percentage may reflect the problems with tagging Vps1 with GFP (Chi et al. 2014). It is known that Vps1-GFP is not fully functionally active and therefore would be less likely to become incorporated with a functional endocytic patch. Despite this, the observed co-localisation found was similar previously published findings (Smaczynska-de Rooij et al. 2010). This result suggested that the RR-EE localises to an endocytic patch to the same amount as the WT. Therefore any differences between WT and RR-EE during endocytosis is unlikely to be due to a difference in accumulation of the proteins during endocytosis.

The localisation of WT and RR-EE Vps1 at an endocytic site has been further verified with the use of a biomolecular fluorescence complementation assay (BiFC) in which half a fluorescent protein was tagged to Vps1 and half to Rvs167 within the genome (KAY 1832 and KAY 1621 respectively) . The presence of fluorescence in both WT and RR-EE Vps1 indicated localisation at an endocytic site (Palmer et al. 2015a). These results suggest that both WT and RR-EE Vps1 both localise to endocytic patches at the membrane, suggesting that the defect in endocytosis is not due to abnormal recruitment.

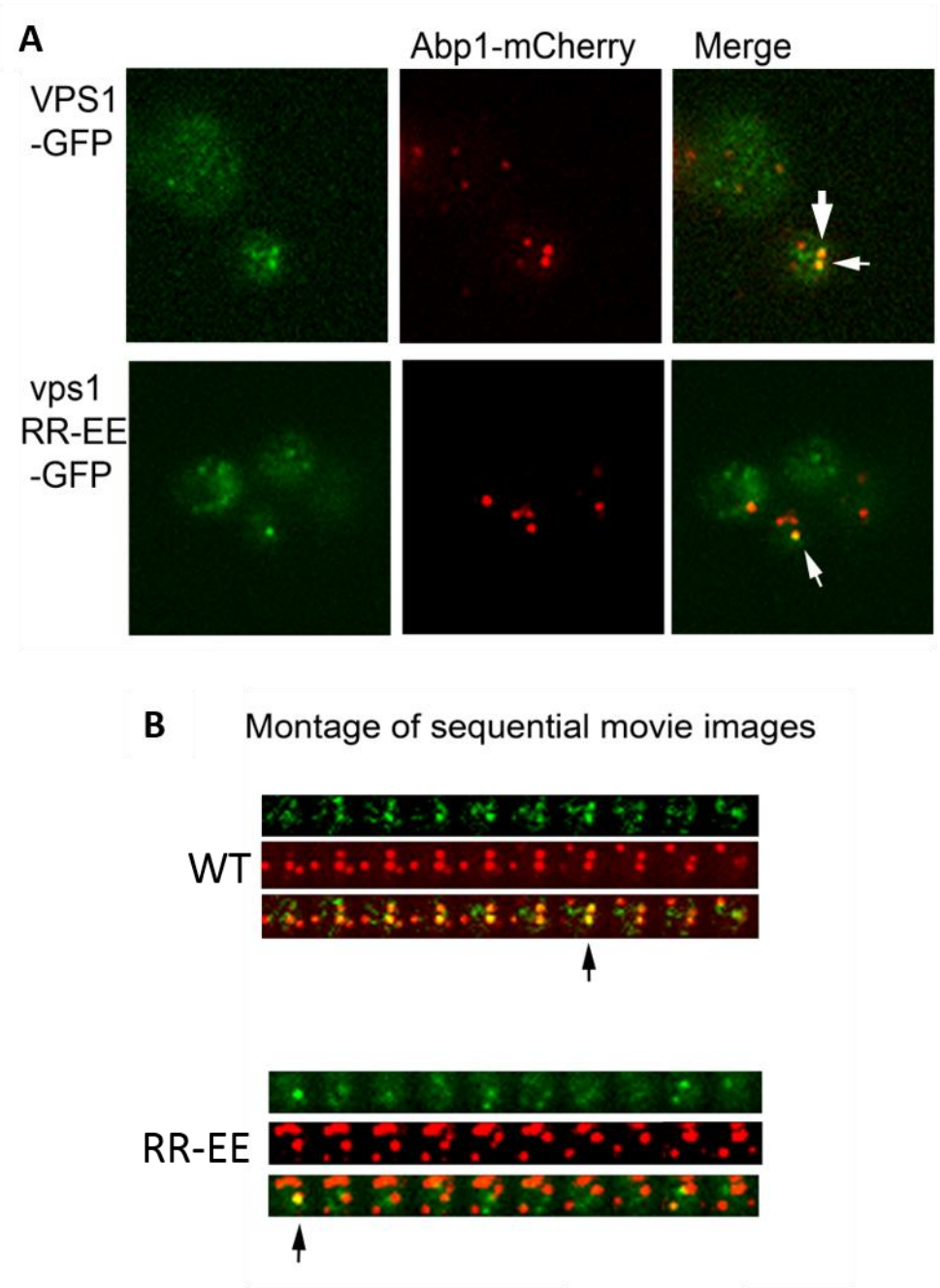

Figure 14. TIRF microscopy of co-localisation between Abp1-mCherry and Vps1-GFP (Palmer et.al., 2015a) A) example TIRF images of plasmid borne Vps1-GFP (under its own promoter) and Abp1 tagged with mCherry (integrated). Arrows indicate co-localisation. B) montage of sequential images from live cell movies indicate the appearance of the same patch over time. Black arrows indicate the time point at which the picture from A was taken.

4.4.2 RR457-8EE Vps1 and its effect on the accumulation of Sla1, Sla2 and Abp1 during endocytosis

Yeast and mammalian endocytosis progresses in distinct stages: coat protein assembly, invagination, and then scission of the vesicle and release into the cytoplasm. By fluorescently tagging different proteins involved in each of these stages, molecules could be seen arriving at an endocytic site and then timed to see when they disappear into the cell and their movements at the membrane during this event. This produced a temporal view of the molecular mechanisms orchestrating an endocytic event (Kaksonen et al. 2003; Kaksonen et al. 2005). This method enables a specific analysis of the proteins involved at each stage of endocytosis from the initiation through to invagination and scission. Therefore this was chosen as a way of analysing these stages in turn which, in contrast to a fluid phase uptake assay, would provide further more detailed insight to find out at which point the RR-EE mutation in Vps1 was affecting endocytosis.

Initially, in order to analyse early stage endocytic events, a yeast strain containing Sla1 tagged with GFP and Abp1 tagged with mCherry was used (KAY 1664 table 2.8.4). Sla1 functions at the initiation stage of endocytosis and binds clathrin and is involved in the organisation of actin patches (Di Pietro et al. 2010; Ayscough et al. 1999). Sla1 has also been reported to bind Vps1, as tested by co-immunoprecipitation, which could suggest a role for Vps1 at the early coat stages of endocytosis (Yu & Cai 2004). Abp1 binds actin and arrives a few seconds prior to invagination, remains with the vesicle until after scission (Kaksonen et al. 2005; Lappalainen et al. 1998). By analysing these two markers at once the coat accumulation and invagination stages of endocytosis could be tracked at the same time.

The Sla1-GFP Abp1-mCherry strain was transfected with plasmids containing Vps1 WT and RR-EE. These were then grown in liquid media to an OD_{600} of 0.7 prior to live fluorescence microscopy. Live cell movies were then analysed to track the sequential initiation of endocytosis marked by the appearance of Sla1-GFP, maturation and co-localisation with Abp1, then invagination which is marked by the presence of Abp1-mCherry alone. Cells expressing Vps1 WT and RR-EE both show co-localisation between the Sla1-GFP and Abp1-mCherry fluorophores (figure 15A).

Vps1 RR-EE has been found to reduce fluid phase uptake specifically and does not affect other functions of Vps1 in the cell. This could be due to the mutation disrupting recruitment to Sla1-postive endocytic patches or reducing its stability at an endocytic patch. If Sla1 recruitment is being disrupted then this could lead to Sla1 instability at an endocytic patch leading to it being lost and therefore a reduction in Sla1 lifetime would be predicted. A reduction in the ability of RR-EE to bind actin may conversely have an effect on the localisation

of Abp1 whereby a reduction of actin recruitment could delay invagination which would be predicted to result in a longer lifetime of Abp1 at an endocytic site.

To analyse any changes in the behaviour of these proteins the intensity and lifetimes of proteins at endocytic patches showing accumulation of Sla1, subsequent co-localisation with Abp1, and Abp1 invagination were recorded. The live cell recordings for these particular dual colour microscopy were taken by Dr. Iwona Smaczynska-de Rooji. From the recordings, the patches were tracked using ImageJ software (Schneider et al. 2012), which analysed the number of frames per track (lifetime) and intensity of the patch (pixel intensity). The data from six separate endocytic events were combined to indicate an average accumulation and disappearance of Sla1 and Abp1 at the cell membrane. The two fluorophores have different intensities when imaged and therefore to compare them together the data was normalised so as to show all data within the same scale. Strains expressing Vps1 WT indicated a clear accumulation of Sla1-GFP, followed by co-localisation with Abp1-mCherry and disappearance of both fluorophores with invagination (figure 15E). Kymographs are a way of displaying this data whereby all fluorescence data from a single track is accumulated together and shown over time and distance into the cell (figure 15E). The kymographs from Vps1 WT indicate clear patch accumulation and movement into the cell. The average lifetimes of Abp1-mCherry and Sla1-GFP are 22.40 ± 0.9 sec and 17.74 ± 0.78 sec respectively, which are slightly less than has been previously reported for the lifetimes of these markers (Smaczynska-de Rooij et al. 2010) (figure 15B). In comparison to the WT strain the *vps1* null strain exhibited aberrant movements of the endocytic markers as shown by kymographic analysis (figure 15C). This was also reflected by the average intensity recordings for Sla1-GFP and Abp1-mCherry with Abp1-mCherry being recruited for longer (average lifetime 20.34 ± 0.89 sec) as previously reported (Smaczynska-de Rooij et al. 2010). Both Sla1-GFP and Abp1-mCherry reporter intensities were much more variable than the WT condition (figure 15C) and the average lifetime for Sla1-GFP in the *vps1* null condition was 21.58 ± 0.99 sec. When Vps1 RR-EE was expressed in these cells the dual reporter kymographs once again indicated aberrant movements at the plasma membrane (figure 15E). This was less apparent when the intensity of six patches were compared over time (figure 15D). This suggested that there were endocytic events which recruited Sla1-GFP and Abp1-mCherry similar to that of the WT. The average lifetimes of these markers in the presence of RR-EE was found to be 19.29 ± 0.80 sec and 14.49 ± 0.68 sec for Sla1-GFP and Abp1-mCherry respectively.

The lifetime of both Sla1-GFP and Abp1-mCherry at endocytic patches was reduced in cells expressing Vps1 RR-EE in comparison with the WT condition. This suggested that Vps1 RR-EE mutant strain were causing effects prior to scission. This data also indicated that the appearance of Sla1-GFP followed by Abp1-mCherry was similar to that of the WT (figure 15D)

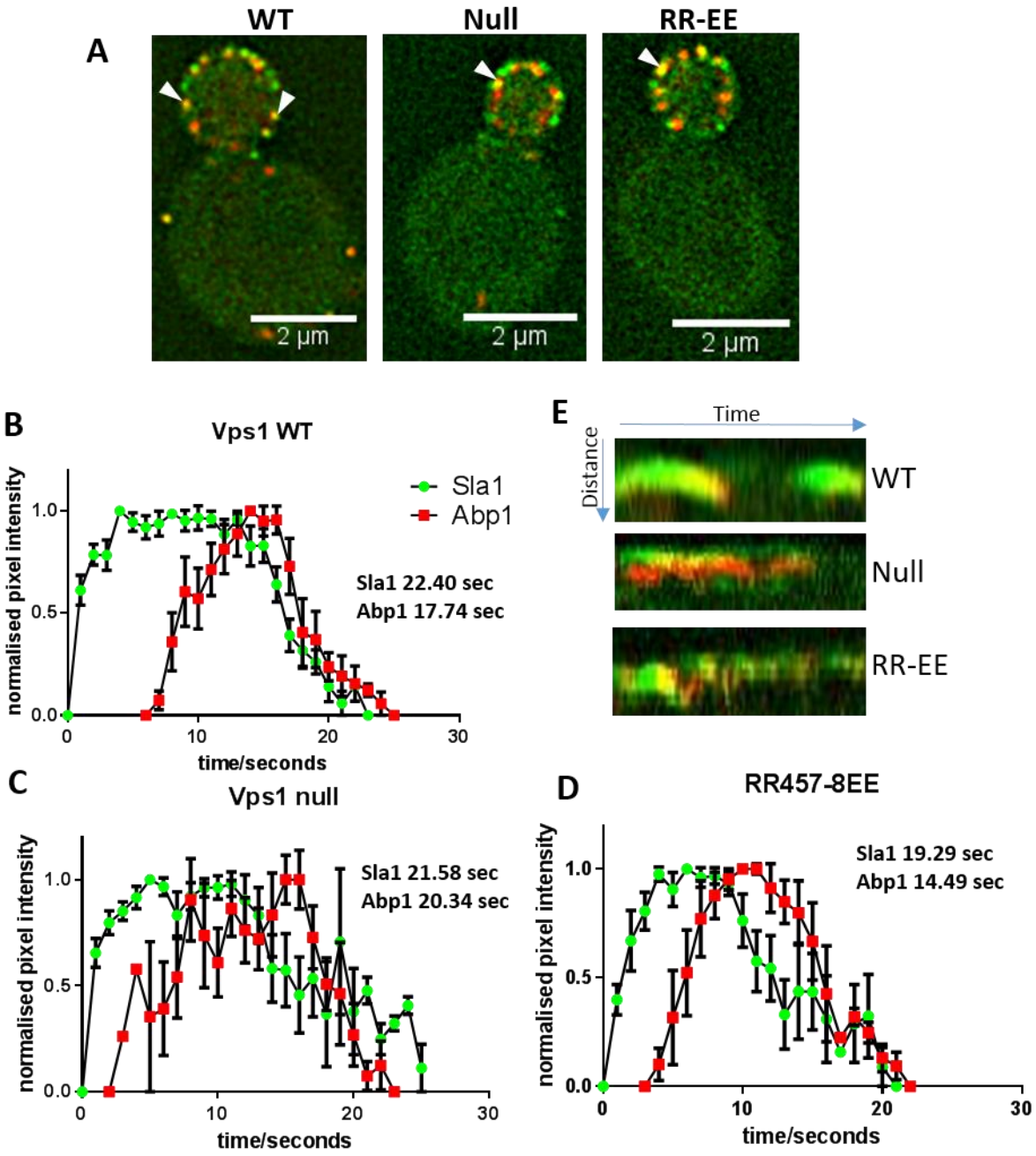

Figure 15. Sla1-GFP and Abp1-mCherry at endocytic patches in cells expressing Vps1 RR-EE.
A) an example of cells imaged by Dr. Iwona Smaczynska-de Rooij with co-localisation of Sla1 and Abp1 indicated with white arrow heads. B-D) normalised intensity graphs of 4-6 patches tracked showing the accumulation of both Sla1-GFP and Abp1-mCherry. Average lifetimes of clear endocytic events are show to the right of each graph. E) Examples of kymographs taken from live cell images WT normal invagination, Null indicating aberrant scission and RR-EE showing a retraction of the patch back to the membrane.

that is to say that their temporal accumulation at a site of endocytosis does not seem to be affected. However, the kymographs suggest that the patches of Sla1-GFP and Abp1-mCherry in cells expressing RR-EE can retract back to the cell membrane and act differently to that of the WT cell condition. The reason why this occurs is not reflected in the intensity over lifetime data and could be due to the reduced number of patches analysed for this data (5-6 separate patches). Similarly the recording of the lifetimes were taken from clear endocytic events and therefore the overall phenotype of patch movements were not fully reflected.

In order to address these concerns the behaviour of patches was assessed and counted so as to identify the average phenotype of endocytic patch events. For this experiment, the use of singly tagged reporters were used, Abp1-mCherry and Sla2-GFP (both *vps1* null KAY 1466 and 1459 respectively). Abp1 was chosen to again analyse the actin-dependent invagination stage of endocytosis, and Sla2 (mammalian Hip1R orthologue) was used as this protein binds actin and acts to initiate the endocytic coat invagination (Wesp et al. 1997; Ayscough et al. 1999). By analysing kymographs of Abp1-mCherry and Sla2-GFP accumulation in cells expressing Vps1 WT, RR-EE or in a *vps1* null strain three categories of patch movement were chosen. These were: 'invagination', where patches move into the cell as expected; 'no/short invagination', where patches arrive and either disappear quickly or disappear without inward movement; and 'aberrant scission' (figure 16A). This final category combined retractions of patches back to the membrane and delayed scission, where patches are seen to move inwards but are delayed in their disassembly. Visual examples of these categories are defined as patch tracks in figure 16D, which were created using ImageJ software (Schneider et al. 2012) by following the movement of a patch from one frame to the next through a time lapse movie. The X and Y coordinates were measured throughout these processes and were plotted using GraphPad Prism software in order to provide a visual guide of specific patches as they moved in to the cell.

Sla2-GFP kymographs were created by Dr. Iwona Smaczynska-de Rooji (figure 16A) these were analysed and categorised as described above. These data showed that, for the WT condition the majority of Sla2 patches invaginate as expected, whereas *vps1* null cells indicate a greater proportion of aberrant scission events and short/no invaginations of the Sla2-GFP marker, figure 16B (both found to be significant through use of t-test, p values for both <0.0001). These results reflects data previously published that reported an unusual accumulation of Sla2 at an endocytic site in the absence of Vps1 (Smaczynska-de Rooij et al. 2010). Cells expressing Vps1 RR-EE were also found to increase in aberrant scission events, in comparison to the WT condition and the null condition (t-test, both p values were <0.0001) figure 16B. This suggests that the RR-EE condition could be affecting the movement of Sla2-GFP at late stages of endocytosis (Palmer et al. 2015a).

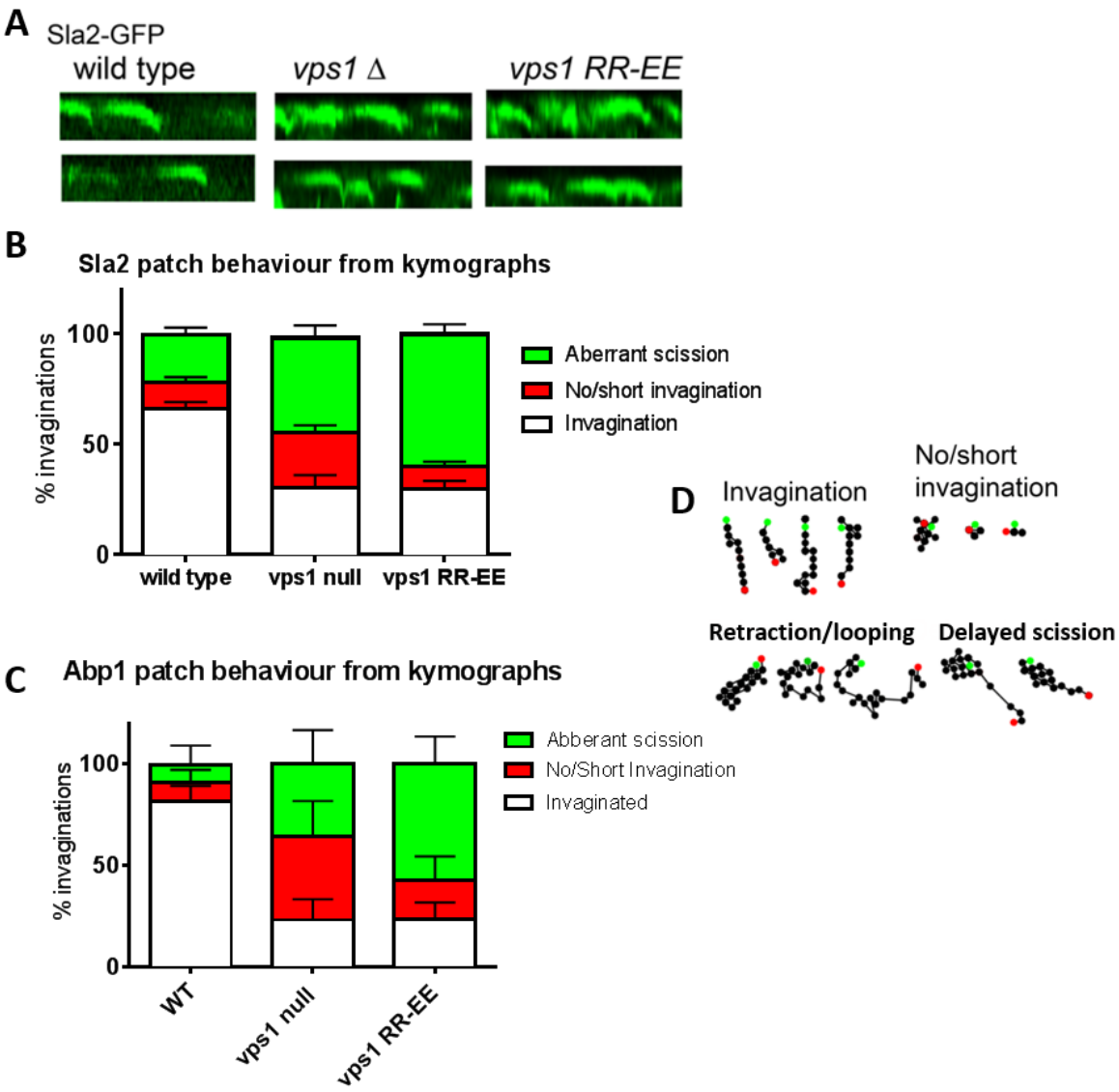

Figure 16. The effect of Vps1 RR-EE on Sla2 and Abp1 patch events A) Example kymographs by Dr. Iwona Smaczynska-de Rooij from Sla2 patches B) Quantified types of invagination from 22 different patches analysed from seven different cells and two independent experiments, error is SD. C) Analysis of 9 or more Abp1 patches from 17 cells and two independent experiments. Error is SD. D) examples of the different categories for patches analysed. Retraction, looping and delayed scission phenotypes were grouped as aberrant scission.

Abp1-mCherry kymographs were also analysed using the same descriptions of patch movements. Similar to the Sla2-GFP patch data the Vps1 RR-EE mutation seemed to significantly increase the number of aberrant and no/short scission events in comparison with both the WT (t-test p values <0.0001 and 0.0069 respectively) and the null condition (t-test p values 0.0003 and 0.0002 respectively) figure 16C. This again suggested that the expression of RR-EE could be affecting late stages of endocytosis. The results from the null Vps1 strain indicate that the deletion of *VPS1* causes an increase in the number of no/short invaginations as well as aberrant scission events (figure 16C). This may indicate a role for Vps1 at earlier stages of endocytosis, as well as during scission, which has been reported with mammalian

dynamin (Taylor et al. 2012; Grassart et al. 2014). The fact that Vps1 RR-EE expressing cells show an increase in the number of aberrant scission events in comparison with the *vsp1* null condition also suggests that the reduction in the ability of Vps1 to bind actin may cause a specific defect during scission.

4.4.3 RR457-8EE Vps1 and its effect on the lifetime and intensity of Rvs167 during endocytosis

The amphiphysin proteins Rvs167 and 161 bind to each other and were previously thought facilitate endocytic scission alone (Kaksonen et al. 2005). However, it has been discovered that Rvs167 interacts directly with Vps1 and that the two function together during scission (Smaczynska-de Rooij et al. 2012), similar to mammalian dynamin-1 binding amphiphysin-2 in neuronal cells (Meinecke et al. 2013). By using the amphiphysin Rvs167 as an endocytic marker, the effects of the Vps1 RR-EE mutation late stage endocytosis could be assessed. In order to do so, a yeast strain containing a GFP tagged Rvs167 (*vps1* null KAY 1337) was chosen and transfected with either plasmid born Vps1 WT, RR-EE, or an empty plasmid (thus retaining the *vps1* null condition). These cells were grown in culture to an OD_{600} of 0.7 before being imaged live by fluorescence microscopy. It was previously reported that the deletion of Vps1 reduces the lifetime and intensity of Rvs167-GFP at an endocytic site (Smaczynska-de Rooij et al. 2012). From the previous live cell data the RR-EE mutation appeared to have an effect on the later stages of endocytic invagination. This could suggest that the accumulation of Rvs167 was disrupted in some way causing defective scission. However Vps1 RR-EE does accumulate at an endocytic site to the same extent as the WT (figure 14). Therefore it was hypothesized that the RR-EE mutation would rescue the accumulation of Rvs167-GFP at an endocytic site and, if scission is delayed, prolong its lifetime at these sites.

By using live cell movies and ImageJ software (Schneider et al. 2012) the lifetime and peak intensities of Rvs167-GFP patches were recorded. As expected, there was a significant decrease in the overall lifetime (one way ANOVA $F=9.79$ d.f. 2,118 p 0.0001) and intensity (one way ANOVA $F= 4.59$ d.f. 2,114 p 0.0121) of Rvs167-GFP when Vps1 was not present (figure 17A). However, there was no significant difference in the lifetime or intensity of Rvs167-GFP patches between Vps1 WT and RR-EE conditions (Palmer et al. 2015a) (figure 17A,B). Therefore Vps1 RR-EE accumulates Rvs167-GFP to an endocytic site at the same levels as WT, as predicted, but also does not affect the lifetime of Rvs167-GFP at an endocytic site. This suggests that, whilst the accumulation of Rvs167-GFP and lifetime is rescued in comparison to *vps1* null cells there are still scission defects as seen in the kymograph analysis of Sla2-GFP and

Abp1-mCherry. Therefore, Rvs167 is recruited but is not sufficient to facilitate scission. Altogether these data suggest that the RR-EE mutation causes a defect at the scission stage of endocytosis, which cannot be rescued by Rvs167. As the RR-EE reduces the ability of Vps1 to bind actin, this suggests that the direct Vps1-actin interaction is required for scission during yeast endocytosis.

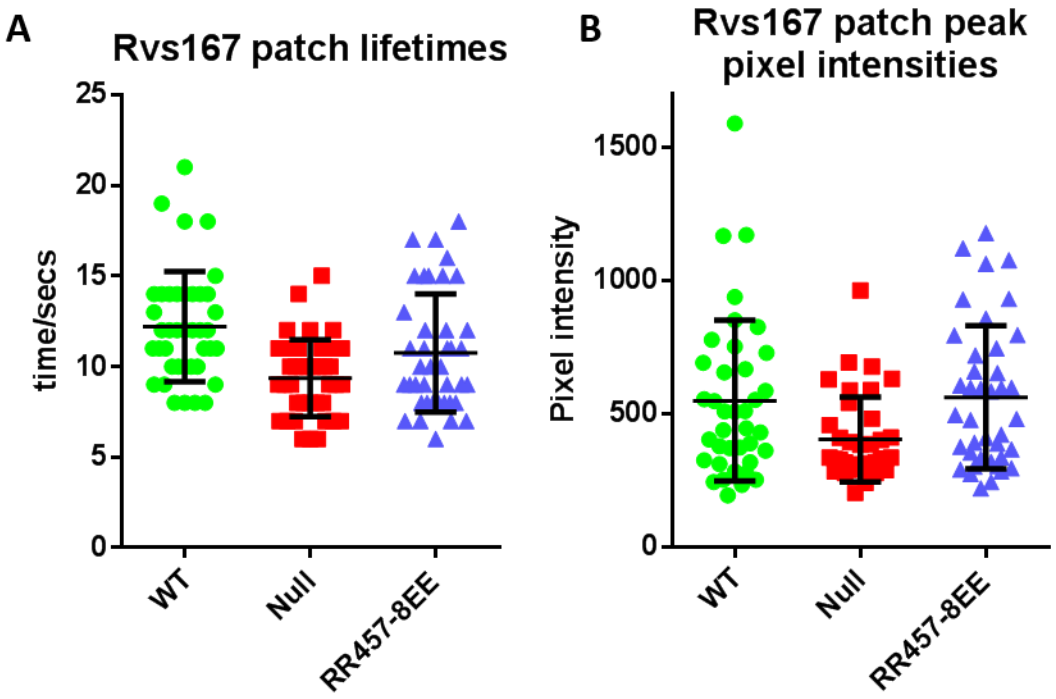

Figure 17. The effect of Vps1 RR-EE on Rvs167-GFP intensity and lifetime (Palmer et.al., 2015) A) Rvs 167 GFP lifetimes from ≥40 patches endocytic patches in ten cells for each strain were measured. Error is Standard Error (S.E.). By one way ANOVA the lifetime is significantly reduced between WT and null cells (one way ANOVA F=9.79 d.f. 2,118 p 0.0001) but not between WT and RR-EE. B) Rvs167 GFP patch intensity was measured as a maximum level of Rvs recruited to the site again from ≥40 patches endocytic patches in ten cells for each strain. One way ANOVA shows null cells to be significantly reduced in peak pixel intensity in comparison to WT (one way ANOVA F= 4.59 d.f. 2,114 p 0.0121) and this again is rescued in cells expressing Vps1 RR-EE.

4.5 The *in vivo* effects of integrated Vps1 mutations

The data reported so far for every *in vivo* experiment involved exogenous expression of Vps1 from a plasmid under its own promotor. Although Vps1 would be expressed at physiological levels from each plasmid, there is a chance that more than one plasmid was transfected into yeast cells, therefore increasing the production of Vps1 above physiological levels. This could have an impact on the results collected so far. In order to address this each of the mutations studied (RR-EE, KRR-EEE, E461K and E473K) were integrated into the genome. This offered an opportunity to check if the results from the plasmid study were caused by the overexpression of Vps1 or not. The integration of each mutation was performed by Laila

Moustaq and Dr. Iwona Smaczynska-de Rooij (Ayscough Lab) as this also lead into a separate investigation in to yeast endocytosis.

Yeast strains with the Vps1 mutations integrated into the genome (KAY 1756, 1793, 1794, 1806, 1807) were grown in liquid media to an OD_{600} of 0.7. Each culture was then plated onto solid media and grown at 37°C to test for temperature sensitivity. From the plasmid borne analysis (figure 8) yeast that were *vps1* null, or expressing the RR-EE, KRR-EEE and E473K mutations were expected to be temperature sensitive. As predicted, only the E461K mutation rescued growth at 37°C (figure 18). It has been shown that the plasmid borne RR-EE mutation rescues growth on sorbitol and therefore this was also tested with the integrated RR-EE. As seen in figure 18 the presence of sorbitol did rescue the growth of the RR-EE mutant but, this was to slightly lower levels than that seen with exogenous expression (figure 18). This could reflect a lower level of RR-EE expression in the integrated strains. Nevertheless, the integrated RR-EE mutation can still rescue growth at 37°C when sorbitol is present.

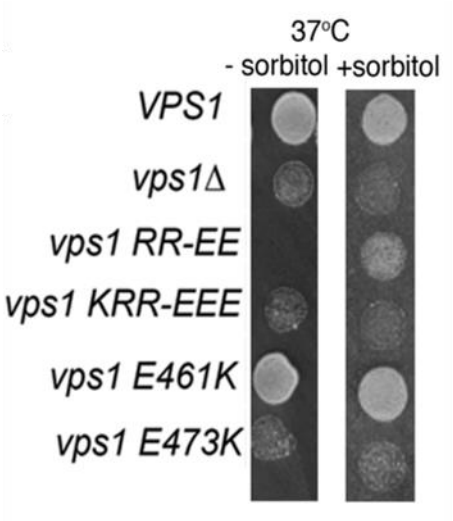

Figure 18. Testing temperature sensitivity of integrated Vps1 mutations. Integrated mutants grown on solid media are temperature sensitive at 37°C apart from E461K. Growth is rescued in RR-EE cells by the presence of sorbitol.

The temperature sensitivity test indicated the behaviour of the integrated mutations was similar to that of the exogenously expressed strains. Therefore the ability of the integrated strains to take up Lucifer yellow was repeated as a three point time course at 30°C at 10, 20 and 90 minutes. From the experiments with the plasmid borne strains it was predicted that the KRR-EEE and E473K would be defective in fluid phase uptake to the vacuole and the RR-EE and E461K mutations would reduce the speed of uptake in comparison to the WT, but not cause as much of a defect in endocytosis as the KRR-EEE and E473K mutations. As predicted, the KRR-EEE and E473K mutations did reduce uptake and act similarly to the *vps1* null strain (figure 19A). The E461K mutation did not significantly differ from the WT. Interestingly the integrated RR-EE mutation still exhibited a defect in uptake, although there were more cells with vacuolar staining at each time point in comparison to the *vps1* null strain (figure 19A). This indicated

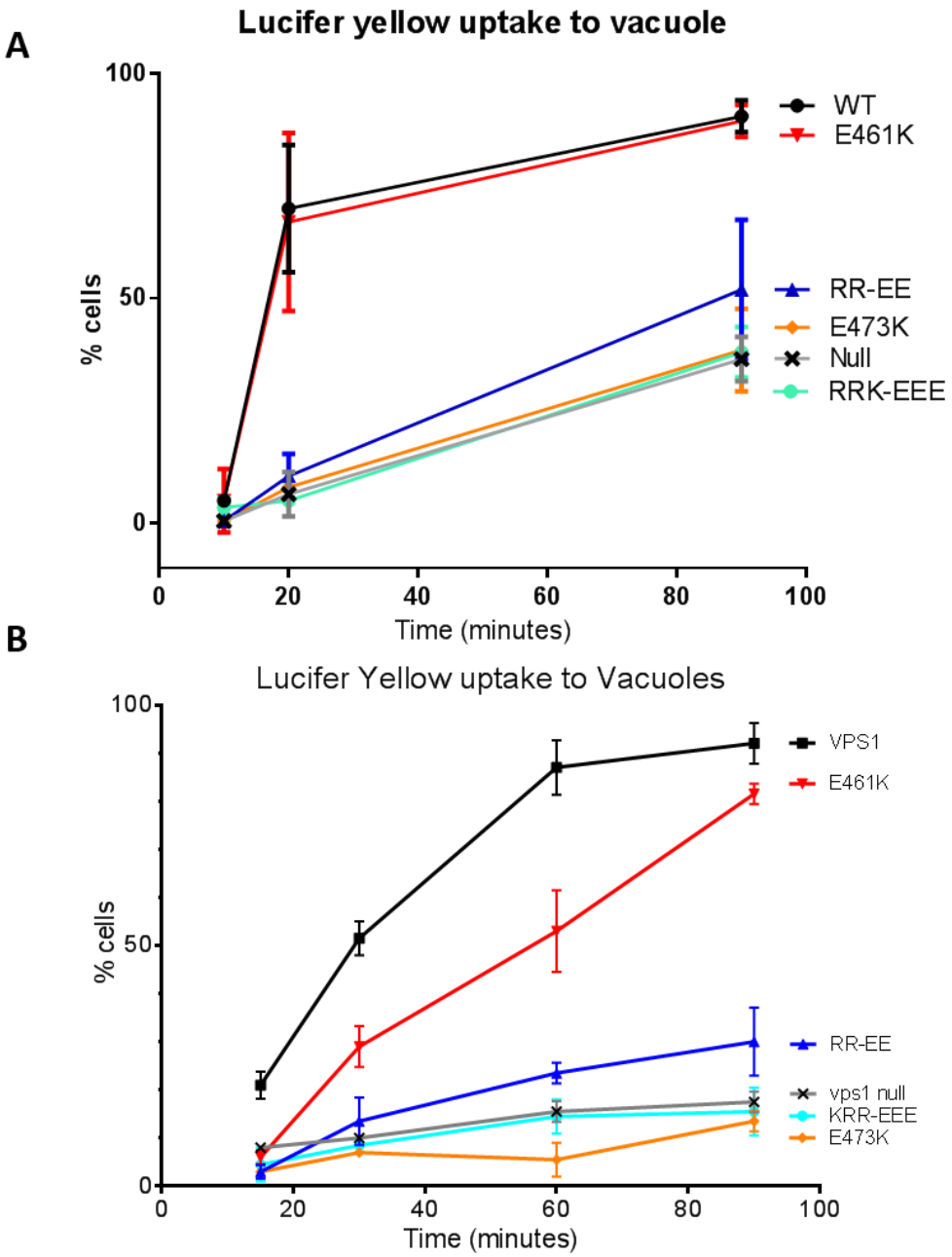

Figure 19. Integrated mutations in temperature sensitivity and Lucifer yellow uptake A) Lucifer yellow uptake analysed at 10, 20 and 90 minutes at 30ºC indicate slower uptake in all mutants and null strain other than E461K taken from 100 cells on two separate experiments B) more detailed analysis of Lucifer yellow uptake to vacuoles at RT and time points 10, 30 60 and 90 minutes. 100 cells counted in two independent experiments. This shows slight slowing in uptake in cells expressing E461K and a pronounced reduction in uptake in other Vps1 mutants and null cells.

that integrated RR-EE had a more marked reduction in Lucifer yellow uptake to the vacuole than plasmid borne RR-EE. This could be attributed to plasmid borne RR-EE expressing at a slightly higher level as explained above.

To compare the differences in uptake of this fluid phase marker more carefully, the temperature of the experiment was again dropped to RT (21°C) and time points included 10, 30, 60, and 90 minutes. The results in figure 19B (Palmer et al. 2015a) shows all Vps1

mutations reduce the vacuolar uptake of Lucifer yellow. This is a phenotype which is less well defined in cells expressing the E461K mutation, which was expected, as this may be due to its ability to rescue the null phenotype in all other cellular functions of Vps1 tested *in vivo*.

These two experiments suggest that the integrated strains containing KRR-EEE and E473K act similarly to that of plasmid borne strains, as both of these mutations are unable to rescue the *vps1* null phenotype. The E461K strain is still able to rescue the temperature sensitivity of *vps1* null strain when integrated into the genome or expressed from a plasmid, although the integrated mutation exhibits a very subtle defect in endocytosis, as assayed by vacuolar Lucifer yellow uptake. The plasmid borne E461K strain indicated that after 30 minutes at 30^{o}C 67% of cells were indicating Lucifer yellow staining in the vacuole which was lower than the WT strain where 94% of cells had taken Lucifer yellow dye into the vacuole (figure 13). However when E461K is integrated into the genome and tested for ability to uptake Lucifer yellow at 30^{o}C and average of 67% of cells have vacuole staining after just 20 minutes which is comparable to that of WT Vps1 (average 70%). This suggests that the integrated mutation is better at rescuing the *vps1* null phenotype than the plasmid borne strain. However it should be noted that the lack of repeats with the plasmid borne experiment performed at 30 minutes (30^{o}C) means this results is not as robust a result as it would ideally be. The integrated strain was tested not only at 30^{o}C, but also at 21^{o}C with four time points and over 100 cells counted on two separate occasions. This was a much more detailed experiment and showed a reproducible result whereby E461K was reducing the ability of Vps1 to take up Lucifer yellow dye. Therefore from this evidence it was concluded that the E461K mutation does reduce the ability of a cell to take up Lucifer yellow and traffic it to the vacuole which could indicate a defect in endocytosis.

The integration of the RR-EE mutation seemed to have increased the severity of temperature sensitivity due to the addition of sorbitol only partially rescuing this phenotype (figure 18). There seemed to also be a reduction in the cells ability to take up Lucifer yellow when compared to the plasmid borne RR-EE. This suggests that slight over-expression of the RR-EE mutants compensates for the detrimental effects of the mutation. Nevertheless, the RR-EE mutation whether integrated or plasmid borne, causes an endocytic defect in yeast cells as assayed by Lucifer yellow uptake. It should also be mentioned that the integrated RR-EE strain was also analysed by FM4-64 dye staining (data not shown) and it was found that the vacuole morphology was unaffected by this mutation (as seen with the plasmid borne RR-EE figure 9). In the future it would be prudent to check all functions of Vps1 with the integrated RR-EE however due to time limitations this was deemed beyond the scope of this project. Overall, this investigation suggested that the results gained with the plasmid borne Vps1 are comparable to that of the integrated Vps1 mutations.

4.6 The effects of RR-EE on the ability of Vps1 to bind and bundle actin

4.6.1 The affinity of actin for Vps1 RR457-8EE

High speed pelleting assays have shown that the Vps1 RR-EE mutation causes a significant reduction in the ability of Vps1 to bind actin (figure 4). Furthermore, *in vivo* data have indicated that Vps1 RR-EE mutation causes a defect at the scission stage of endocytosis (figures 16,17). However, in order to understand the mechanism by which a reduction in Vps1 actin binding could cause a scission defect, further investigation was required.

Before a more in-depth *in vitro* analysis of Vps1 WT and RR-EE was undertaken and the affinity of actin for Vps1 RR-EE was calculated for both rabbit and yeast F-actin. This was done to confirm the results of the high speed pelleting assay and provide a binding affinity to compare to the WT Vps1 data. This is included at this point in this chapter so as to more easily compare all aspects of the *in vitro* study into Vps1 RR-EE.

As described previously Vps1 RR-EE was purified from *E.coli* by his-trap column (HisTrap™ GE Healthcare) pre-spun, and incubated at concentrations ranging from 0.2-3 μM with 5 μM yeast F-actin. The samples were then spun at high speed (90,000 rpm TL100 rotor) for 15 minutes and supernatant and pellet fractions separated. These were run on an SDS-PAGE gel and analysed by densitometry (Image Lab software). By comparing the amount of Vps1 in the pellet a binding curve was created and a K_d estimated as 4.6 ± 2.6 μM for yeast actin figure 20A (in comparison to 1.9 ± 0.36 μM calculated for WT). This was also done with rabbit skeletal F-actin from which a comparable K_d was calculated of 1.6 ± 0.5 μM (WT 0.92 ± 0.31 μM) (Palmer et al. 2015a). This data indicates, in more detail, the reduction in affinity for actin that Vps1 has when the RR-EE mutation is present.

4.6.2 Vps1 bundles actin and this ability is perturbed by the RR-EE mutation

Dynamin-1 has been reported to bundle actin and charge mutations within the actin binding site prevented this bundling activity *in vitro* (Gu et al. 2010). If Vps1 is also able to bundle actin then this could indicate a mechanism by which bundled actin filaments are coupled to the scission stage of endocytosis. To investigate if the ability of dynamin to bundle actin is evolutionarily conserved a low speed centrifugation and falling ball assays were carried out.

Vps1 WT or RR-EE was purified from *E.coli* using a His-trap column (HisTrap™ GE Healthcare). Vps1 was then incubated with rabbit F-actin at a concentration of 1.5 μM and

3µM respectively. After incubation, the proteins were then spun at a low speed, 10,000 rpm (in TLA-100 rotor). At this speed single F-actin filaments are unable to pellet, however if these actin filaments are bundled together then they would be expected to sediment. At such a low speed Vps1 is unlikely to sediment, unless it binds to bundles of F-actin.

When spun at this low speed separately both Vps1 and F-actin were predicted to stay in the soluble supernatant fraction. However, if Vps1 can bundle actin, then both Vps1 and F-actin would be found in the pellet fraction after incubation. As expected, Vps1 WT, RR-EE and F-actin were found in the supernatant when spun separately (figure 20B). However, when Vps1 WT was incubated with F-actin there was a shift of both Vps1 and F-actin into the pellet fraction which suggested that Vps1 can bundle F-actin (figure 20B,C) (Palmer et al. 2015a). Interestingly, the presence of the mutation RR-EE prevented this and neither actin nor Vps1 were found in the pellet fraction after incubation (figure 20B,C). This suggests that the RR-EE mutation reduces actin binding to the extent that actin bundling cannot occur *in vitro* (Palmer et al. 2015a).

The ability of Vps1 to bundle actin was then tested with a second experimental approach, a falling ball assay (chapter 2 section 2.3.12). This assay tests the viscosity of a polymerised actin solution with and without Vps1 which can give an indication of actin bundling. Vps1 was purified, mixed with G-actin and additional salts to start the polymerisation of actin (KME, which contains Potassium chloride, Magnesium and EDTA). This solution was made up to a volume of at least 100 µl. This mixture was then taken up into a 100 µl capillary tube and sealed before being left at RT for 20 minutes for the actin to polymerise. This was the incubated overnight at 4^{o}C and then returned to RT the next day for analysis. Each capillary was placed in a holder and a stainless steel ball bearing was dropped into the top of the capillary and timed to see how long it takes for the ball to fall 6 cm through the solution. A dramatic increase of viscosity was seen when Vps1 concentration was increased from 0.5-1 µM in the presence of actin, and a slight decrease when combined with actin at 1.5 µM figure 20D (Palmer et al. 2015a). This result is indicative of actin bundling as the network of actin would increase viscosity, until at high concentrations many actin bundles are created forming channels through the actin causing a faster passage for the ball baring through the solution. The bundling ability of Vps1 was almost completely abolished in the RR-EE mutant suggesting again that the reduction of actin binding perturbs the ability of Vps1 RR-EE to bundle actin filaments.

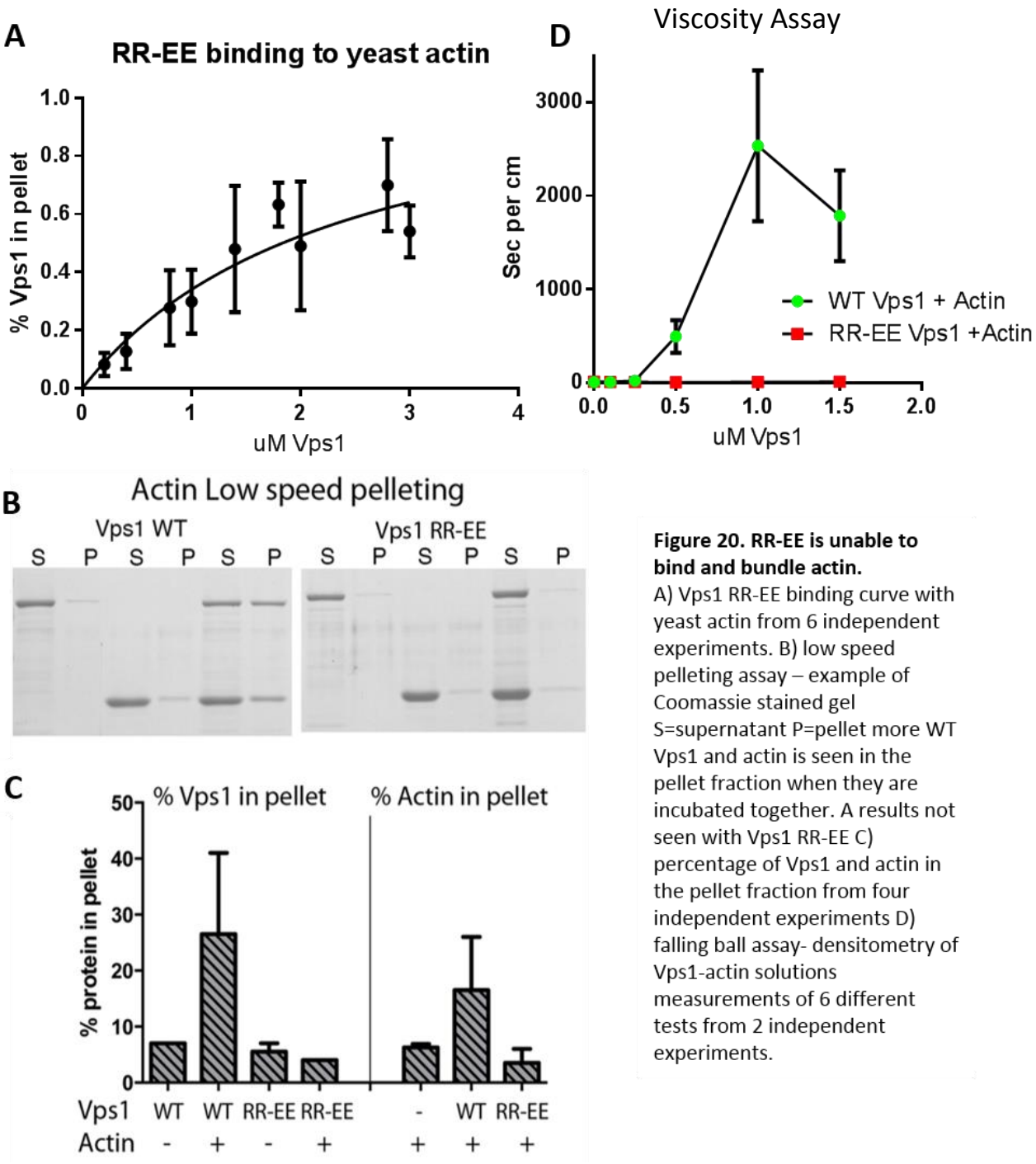

Figure 20. RR-EE is unable to bind and bundle actin.
A) Vps1 RR-EE binding curve with yeast actin from 6 independent experiments. B) low speed pelleting assay – example of Coomassie stained gel S=supernatant P=pellet more WT Vps1 and actin is seen in the pellet fraction when they are incubated together. A results not seen with Vps1 RR-EE C) percentage of Vps1 and actin in the pellet fraction from four independent experiments D) falling ball assay- densitometry of Vps1-actin solutions measurements of 6 different tests from 2 independent experiments.

4.7 Discussion

4.7.1 The direct Vps1-actin interaction

In this study the direct dynamin-actin interaction was found to be evolutionarily conserved and that a orthologous actin binding region described in mammalian dynamin-1 (amino acids 399-444) is found in the dynamin-like protein Vps1 (amino acids 438-483). This discovery, along with evidence that mutating these charged residues causes a defect in actin binding, suggests that these residues may be fundamental for the dynamin actin interaction, which is involved in several cellular functions in eukaryotic cells.

It has been reported that dynamin oligomerises in the presence of short actin filaments (Gu et al. 2010) and that the oligomerisation of dynamin stimulates its GTPase activity (Warnock et al. 1996). The effect of actin on Vps1 GTPase activity was tested during this study and there was found to be very little difference between GTP hydrolysis with or without the presence of actin, figure 3. Owing to experimental difficulties in running this assay this result is preliminary and would require further investigation, perhaps by using a continuous GTPase assay (Ingerman & Nunnari 2005).

4.7.2 Mutations in the actin binding site of Vps1

This study investigated the effects of four mutations in the actin binding region of Vps1, RR457-8EE, RR457-8EE+K453E, E461K and E473K. The actin binding site in dynamin sits within the middle alpha helical domain, which has also been attributed to the formation of dynamin dimers and olgiomers (Ramachandran et al. 2007). Interestingly amino acid residues which are known to be required for dynamin oligomerisation lie outside of the actin binding region (chapter 3 figure 2). Therefore these mutations to the actin binding site are unlikely to affect the ability of Vps1 to oligomerise. If the mutations were reducing the ability of Vps1 to oligomerise then they would have purified differently to the WT yielding higher concentrations of Vps1 after the pre-spinning step. This was not found to be the case with any of the mutations, suggesting that these mutations are not having a marked effect on the ability of Vps1 to oligomerise. To check this in the future, native gels could be run to analyse the oligomeric state of each mutation in comparison to WT Vps1.

It was predicted that the charge mutations which introduced a basic residue (E461K and E473K) would increase the affinity of Vps1 for actin and the introduction of acidic residues (RR-EE and KRR-EEE) would reduce this affinity, as described for human dynamin-1 (Gu et al. 2010). During this study neither E461K nor E473K mutations significantly increased binding between Vps1 and actin, as predicted, with the E473K mutation actually reducing the Vps1-actin interaction (figure 4). The reason why the E473K mutation reduces the affinity of actin

binding would require further *in vitro* analysis. When the mutation was modelled onto the dynamin-1 crystal structure it seemed to be angled away from the structure and this, along with the normal levels of expression *in vivo* (figure 7), suggests that this mutation is unlikely to reduce the ability of Vps1 to fold correctly. Nevertheless, further structural analyses by, for example circular dichroism (CD), may indicate that this mutation affects Vps1 structure, which could provide insight into the reason why this mutation causes a *vps1* null phenotype in all functions of Vps1 *in vivo.*

The mutation E461K does not increase the ability of Vps1 to bind actin nor does it affect the ability of Vps1 to hydrolyse GTP (figure 4,6). *In vivo* analyses has however, identified that the presence of E461K causes a single specific defect in fluid phase uptake (figure 13,19). This suggests that E461K affects the role of Vps1 in endocytosis but how it affects the Vps1-actin interaction requires further investigation. The role of this mutation in endocytosis is examined and discussed in more detail in chapter 5.

The final two mutations, RR-EE and KRR-EEE, were both predicted to reduce the ability of Vps1 to bind actin *in vitro*. The triple mutation, KRR-EEE, does not reduce the strength of the Vps1-actin interaction *in vitro* (figure 4), however it cannot express to the same level as WT Vps1 *in vivo* (figure 7), resulting in a *vps1* null phenotype in all functions of Vps1. The reduction in expression suggests that this mutation renders Vps1 unstable or vulnerable to proteolysis and degradation. As the RR-EE mutation is able to express to WT levels, this could suggest that the K453 residue is important for Vps1 structure or that the additional glutamic acid at this point forms unwanted associations with other proteins *in vivo* making it toxic resulting in its degradation. The reason why the additional K453E mutation does not reduce actin binding could also be to do with it causing a miss-folding of Vps1 which may expose actin binding regions of the protein which are usually inaccessible.

The creation of the RR-EE mutation in Vps1 caused a significant reduction in the ability of Vps1 to bind actin as predicted (figure 4) and did not affect the ability of Vps1 to hydrolyse GTP *in vitro*. *In vivo* expression of the Vps1 RR-EE mutation caused a temperature sensitive phenotype, which could be rescued by the addition of sorbitol (figures 8,18). This indicated that turgor pressure reduced the viability of cells expressing the Vps1 RR-EE mutation. Subsequently, the RR-EE mutation was found to cause a specific reduction in fluid phase uptake *in vivo* (figures 13,19). Yeast are known to require actin for endocytic events, a requirement which is reduced when turgor (and therefore membrane) pressure is reduced (Aghamohammadzadeh & Ayscough 2009). The reduction in actin binding ability caused by the RR-EE mutation and the specific effect on endocytosis suggests a link between the ability of Vps1 to bind actin and its role in endocytosis. This may suggest that the mammalian

orthologue of Vps1, dynamin-1 may also require its direct interaction with actin in order to perform efficient endocytosis in circumstances were membrane tension is increased.

4.7.3 RR457-8EE and its effect on endocytic invagination

In order to assess the role of RR-EE on endocytosis in more detail, early and late markers of endocytosis were utilised. By analysing the phenotypes of invaginations of both Sla2-GFP and Abp1-mCherry-positive endocytic sites, it was concluded that the Vps1 RR-EE mutation seemed to predominantly disrupt the scission stage of endocytosis. However, the recruitment and lifetime of Rvs167-GFP (a marker of the scission stage of endocytosis) was unchanged in comparison to Vps1 WT cells (figure 17). As with the Sla2-GFP and Abp1-mCherry analyses, it would be interesting to compare the phenotypes of the Rvs167-GFP patches to see if their inward movement is also affected and suggesting a defect during scission. Altogether this suggests that the scission stage of endocytosis is disrupted in yeast cells expressing Vps1 RR-EE however the Rvs167-GFP data did not rectify this, even though its accumulation is at normal levels, suggesting that Rvs167 is not sufficient for efficient endocytic scission. It should be noted that the RR-EE mutation is not lethal and therefore there may be other endocytic events taking place, such as the recently reported Abp1 dependent Vps1 independent endocytosis (Aghamohammadzadeh et al. 2014), which may be upregulated to counteract Vps1 mutations *in vivo*.

Alongside this study, an EM analysis of endocytic invaginations in cells expressing Vps1 WT and RR-EE was carried out by Dr. Martin Goldberg, Dr. Ritu Mishra and Dr. Simeon Johnson at Durham University. They discovered that the RR-EE mutation causes long invaginations to occur (some of which were well over 100 nm in length) which were significantly longer than invaginations analysed in WT cells (t-test p value ≤ 0.0001 n= 84 RR-EE and n= 64 WT) figure 21 (Palmer et al. 2015a). These long invaginations in the RR-EE condition were rescued by the presence of sorbitol (t-test p value 0.036) suggesting that this defect is linked to the requirement for actin, or force generation, during endocytosis. Other labs have reported the presence of long invaginations in cells where the formation of eisosomes has been disrupted (Moreira et al. 2012). To determine whether these long invaginations are eisosomes the eisosome localised protein Pil1-mRFP strain was created with both WT and RR-EE Vps1 (KAY 1849 and 1850 respectively). The size, shape and organisation of eisosomes in these cells were investigated by Dr. Iwona Smaczynska-de Rooij and they were found to be the same in the WT compared to the RR-EE cells suggesting the long invaginations seen in figure 21 are unlikely to be eisosomes. Nevertheless, by removing invaginations measured to be over 200 nm in length the average length of invaginations in RR-EE cells were still significantly longer than in WT cells

(75 nm average in RR-EE compared to 61 nm in WT $p \leq 0.01$). This provides *in vivo* evidence that the RR-EE mutation is indeed affecting scission and that this is linked to the requirement of actin during endocytosis. The fact that invagination can occur, but scission is delayed, provides evidence that actin is also required for the scission event and that it is coupled to scission by Vps1.

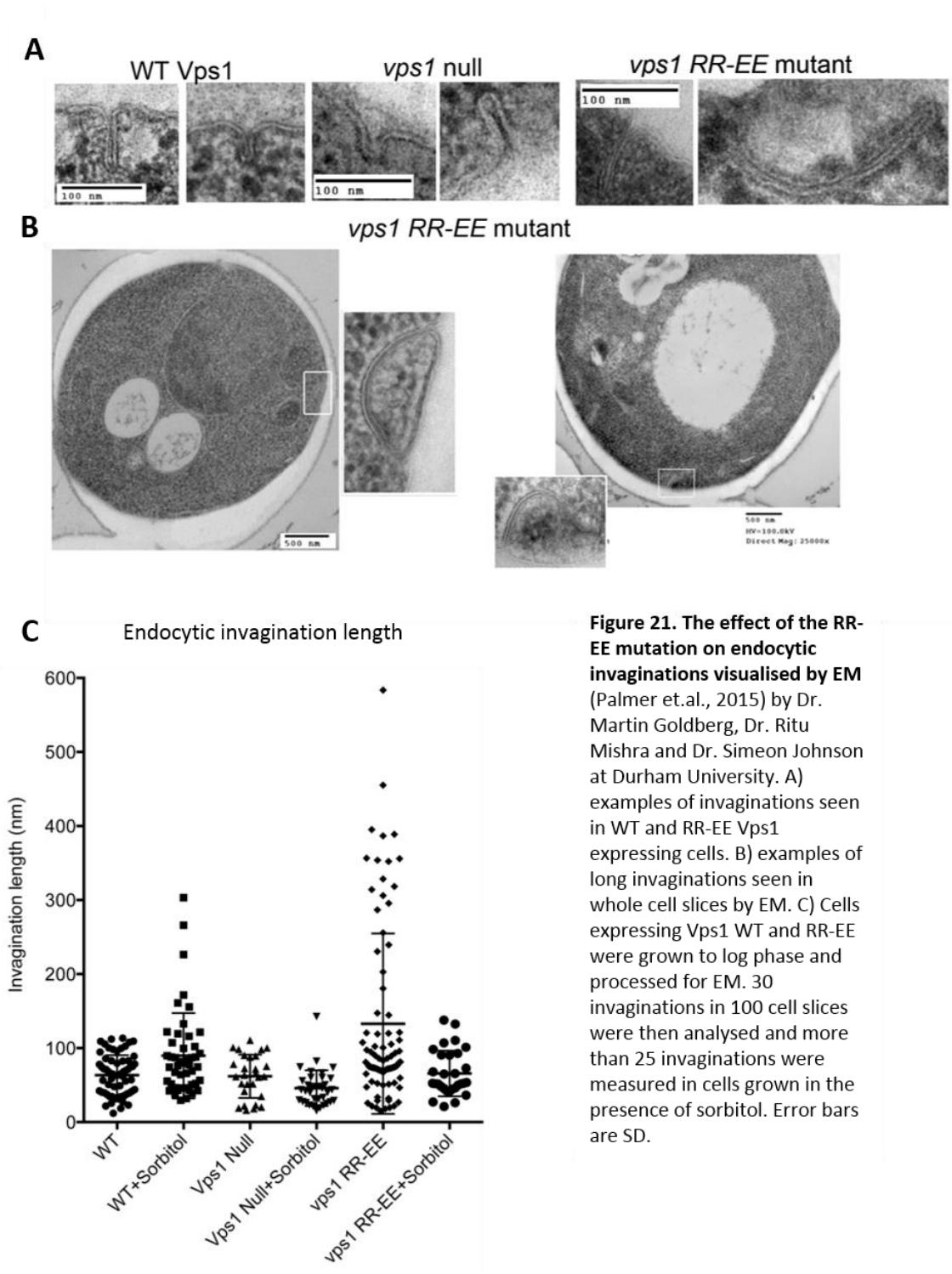

Figure 21. The effect of the RR-EE mutation on endocytic invaginations visualised by EM (Palmer et.al., 2015) by Dr. Martin Goldberg, Dr. Ritu Mishra and Dr. Simeon Johnson at Durham University. A) examples of invaginations seen in WT and RR-EE Vps1 expressing cells. B) examples of long invaginations seen in whole cell slices by EM. C) Cells expressing Vps1 WT and RR-EE were grown to log phase and processed for EM. 30 invaginations in 100 cell slices were then analysed and more than 25 invaginations were measured in cells grown in the presence of sorbitol. Error bars are SD.

4.7.4 The effects of RR457-8EE on the ring structure of Vps1 and actin bundling

During this study it was found that Vps1 can bundle actin filaments and actin bundling by Vps1 can be perturbed by the RR-EE mutation (figure 20). This could suggest that the coupling of actin to a scission event could be orchestrated by a re-organisation of actin bundles from invagination to the neck of an endocytic vesicle by Vps1. Dynamin-1 has been shown to be able to bundle actin (Gu et al. 2010) and the fact that this is also the case with the dynamin-like protein Vps1 provides further evidence that the function of these proteins is evolutionarily conserved. Despite the Vps1-actin interaction not being fully abolished by the RR-EE mutation the actin bundling ability is reduced significantly. This suggests that whilst Vps1 can still bind actin with the RR-EE mutation the reduction in affinity is enough to render Vps1 incapable of functioning with actin.

Mammalian dynamin is known to oligomerise into rings (Hinshaw & Schmid 1995) which form around lipids (Danino et al. 2004) stimulating its GTPase ability (Warnock et al. 1996) which results in ring constriction and vesicle scission (Cocucci et al. 2014). Whilst the knowledge that dynamin-1 can form rings is well established, the ability of Vps1 to form rings *in vitro* has not been investigated. During this study, Vps1 WT and RR-EE was purified and prepared without pre-spinning for electron microscopy. Dr. Chris Marklew carried out the loading and staining of Vps1 oligomers on carbon coated grids and Vps1 was then imaged by both Dr. Chris Marklew and Mr. Wesley Booth. This method, for the first time, showed that Vps1 can form rings like mammalian dynamin (Palmer et al. 2015a) and these rings have a distinctive morphology (figure 22A,B). The rings alone are 32 ± 3.7 nm in diameter which is smaller than that of dynamin rings (Hinshaw & Schmid 1995) reported to be around 43 nm in diameter and this difference may be due to Vps1 having a lower molecular mass than dynamin (~70 kDal in comparison to dynamin 100 kDal). Appearance of what has been described as 'double rings' can be seen which seem to surround the initial ring to create a larger 63 ± 8 nm ring structure of Vps1 (figure 22). This could indicate coiling of Vps1 as seen with in *in vitro* dynamin work (Hinshaw & Schmid 1995). Vps1 was also incubated with actin and Vps1 and actin structures were analysed by EM. The appearance of the double rings were counted for both WT with and without the presence of F-actin. It was discovered that there were more double rings present after incubation with actin suggesting that F-actin is having an effect on the oligomerisation of Vps1 (figure 22C).

The mutation RR-EE was also analysed by EM analysis with and without actin. Purified RR-EE oligomers were found to form rings but not as many double rings as the WT. This could suggest that the RR-EE changes the structure of Vps1 slightly, preventing it from forming

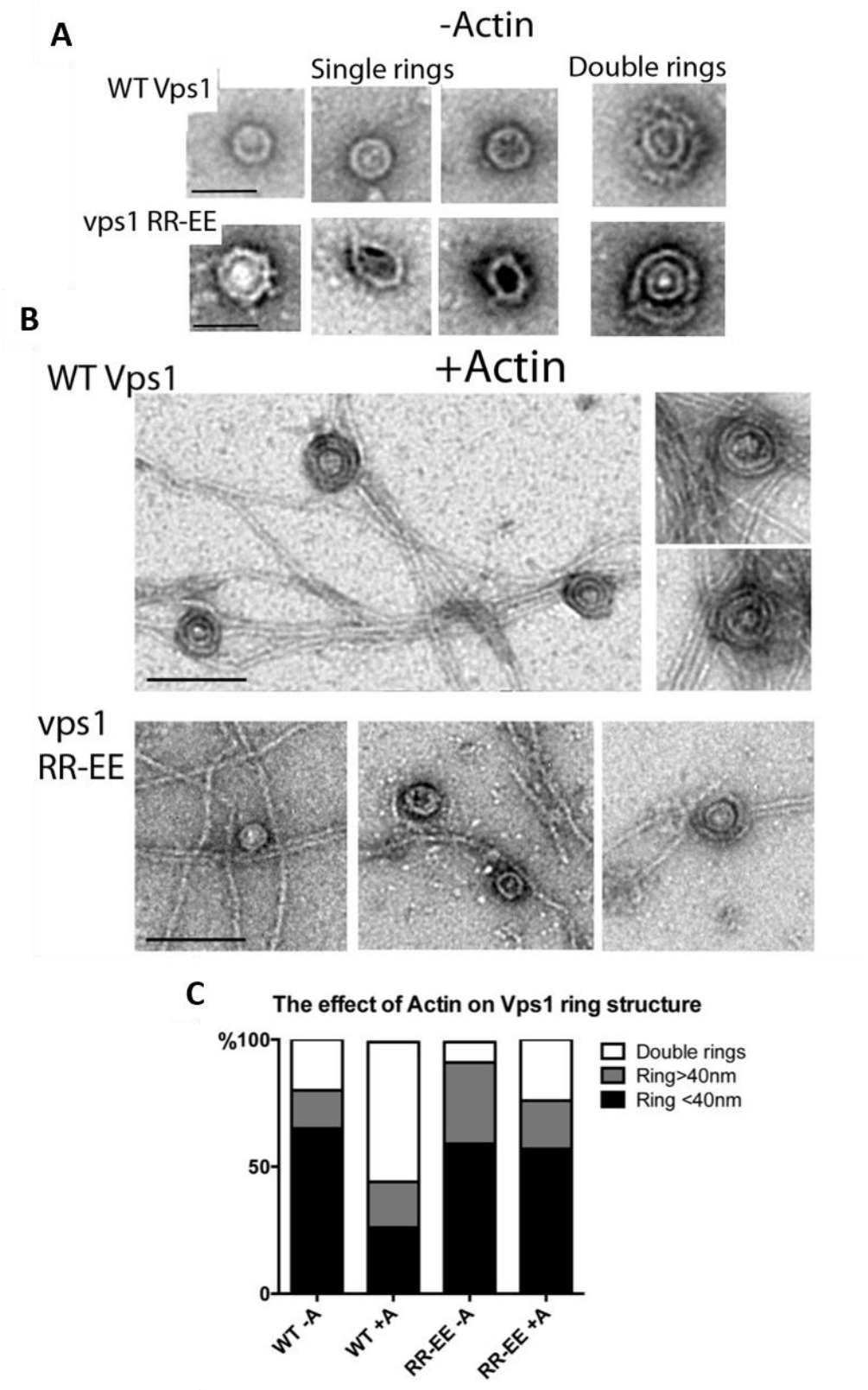

Figure 22. EM images of Vps1 rings with and without actin. (Palmer et.al., 2015) A) Vps1 was purified and visualised by EM (Dr. Chris Marklew) and found rings of Vps1 both single and double in WT and RR-EE purifications B) Rings of Vps1 after incubation with F-Actin. C) Quantification of the number of single and double rings of Vps1 WT and RR-EE alone and with actin (Prof. Kathryn Ayscough).

higher order oligomers. To check this, the secondary structure of both Vps1 WT and RR-EE was tested by CD. This suggested no structural difference between the WT and RR-EE (Palmer et al. 2015a). Therefore the lack of double rings could be due to changes in electrostatic interactions between Vps1 dimers by the addition of the acidic residues. The RR-EE may be indirectly affecting this oligomerisation slightly causing a change to the coiled structure however this is not causing a major effect enough to prevent oligomerisation completely. Vps1 RR-EE was then incubated with actin and the number of double rings analysed once more. This indicated an increase in the number of double rings in the presence of actin (figure 22C) but this was not as significant when compared to the WT condition. The slight increase in RR-EE double rings could reflect the fact that the RR-EE mutation does not abolish actin binding completely and therefore any effect that actin has on Vps1 oligomerisation will be reduced but not prevented with this condition. This also suggests that whatever effect the RR-EE mutation may be having on Vps1 structure it is mild, and would require further structural analysis to identify the subtle changes that could be happening to Vps1 which reduce double ring formation.

The *in vitro* data shows the RR-EE mutation to be reduced in actin binding and bundling. Therefore, taking this information along with the *in vivo* live cell and EM data the following model has been proposed see figure 23 (Palmer et al. 2015a). This suggests that Vps1 is recruited to the neck of an invaginated vesicle and promotes the bundling of actin. This bundling could re-direct actin force away from the tip of the invagination to the point at which scission should occur such that Vps1 GTPase action and the force of actin polymerisation work together to promote scission. In the case of the RR-EE Vps1 mutation there is still invagination and recruitment of Vps1 as well as proper recruitment of Rvs167. However, reduced actin binding prevents re-focusing of the actin polymerising force. This therefore uncouples the actin force from the Vps1 GTPase action causing a defect in scission. This could be the cause of the long invaginations into the cell that are unable to go through scission until other forces aid it (for example Brownian motion). This study provides evidence that the force of actin polymerisation is required during scission as well as invagination in yeast. Dynamin studies have identified *in vitro* that the force from the GTPase action of dynamin is not enough to facilitate scission and that other forces are required for scission to take place (Morlot et al. 2012). A redistribution of actin at the point of scission could be this extra force, something which is essential when there is high membrane tension and can be overcome by Vps1 alone when this membrane pressure is reduced.

It has been suggested that dynamin and actin recruitment functions in a feedback mechanism (Taylor et al. 2012) whereby actin monomers recruit dynamin monomers, then

dynamin monomers stimulate the polymerisation of actin which causes the oligomerisation of dynamin resulting in scission. If the mechanism in yeast relies on the Vps1-actin interaction then RR-EE may prevent accumulation of actin for polymerisation and actin polymers may be unable to stimulate Vps1 oligomerisation and therefore scission is delayed. This idea is supported by the reduced ability of RR-EE to form double rings in the presence of actin.

In conclusion, this study provides evidence for the requirement of the direct Vps1 and actin interaction in endocytic scission. This indicates an evolutionarily conserved role for dynamin and dynamin-like proteins in actin binding and bundling during membrane trafficking.

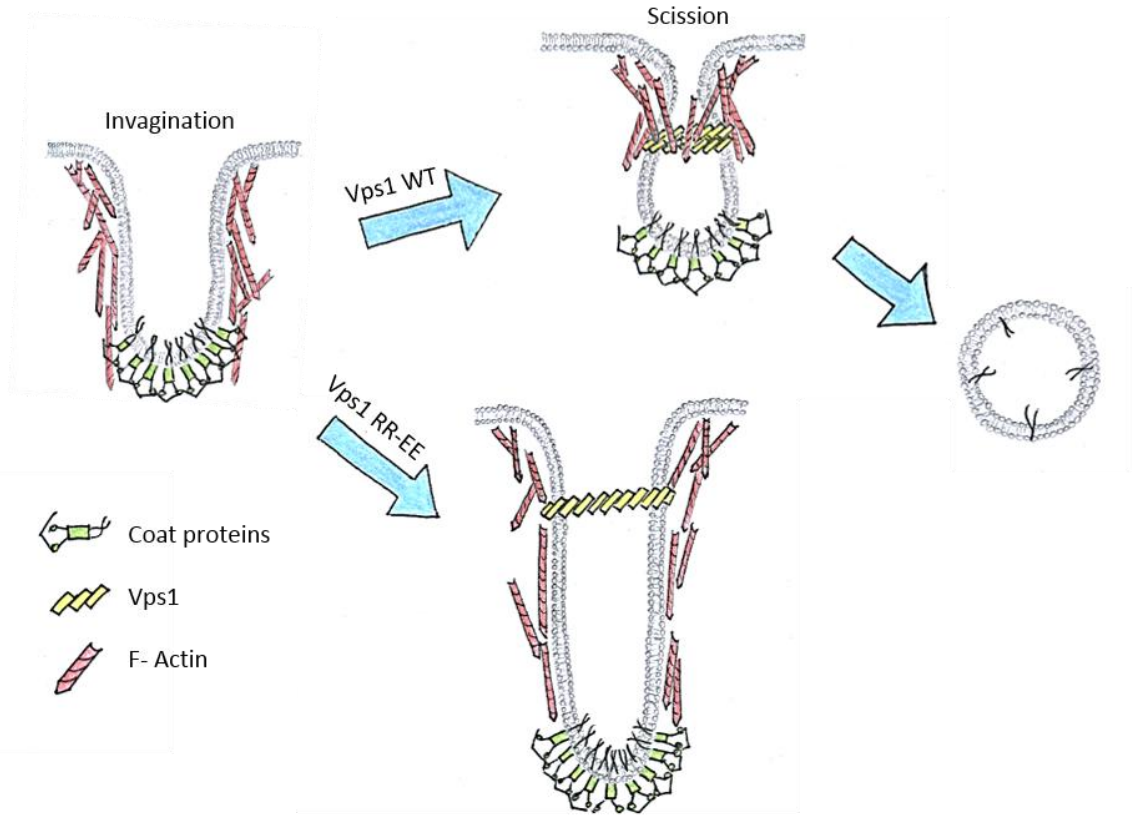

Figure 23. Vps1 actin binding is required for endocytic scission. This schematic depicts how the direct Vps1-actin interaction is required during scission. Actin overcoming turgor pressure, pushes the endocytic pit down into the cell. Vps1 WT oligomerises around the vesicle neck and bundles actin recruiting the force from actin polymerisation from tubulation to the vesicle neck. Using F-actin network and Vps1 GTPase action facilitates scission. In the case of Vps1 RR-EE Vps1 oligomerises around the vesicle next however is unable to bundle actin. Therefore the actin polymerisation is focused on invagination and stays uncoupled to the scission action of Vps1 which causes long endocytic tubules to form.

Chapter 5

Further analysis of the Vps1 E461K mutation in yeast endocytosis

5.1 Introduction

In the previous chapter, the mutation E461K in yeast Vps1 was shown to reduce fluid phase uptake suggesting an endocytic defect. In this chapter the endocytic defect caused by E461K is analysed in more detail so as to understand at which point during endocytosis E461K is affecting.

This single charge mutation has been analysed in chapter 4 and it was found to be highly conserved in mammalian dynamin-1 and 2 suggesting it to be an important residue for dynamin function. As previously discussed, the E422 residue (E461 in yeast) is not conserved in human, rat and mouse dynamin-3 where instead of a glutamic acid there is a glycine residue. By identifying how the E461K mutation affects endocytosis in Vps1 this could suggest a function or role of dynamin-1 and 2 in mammalian endocytosis which is different for dynamin-3 isoforms. This would be interesting as it could indicate new roles of the dynamin-3 isoform not yet tested. For instance, a difference in actin binding during cellular processes such as endocytosis.

Vps1 E461K has been shown to act similarly to the WT *in vitro* and only affect fluid phase uptake of Lucifer yellow dye *in vivo*. Therefore, to analyse this endocytic defect in more detail this chapter describes the specific effects of E461K on the lifetime and accumulation of the endocytic markers Sla1, Abp1, Sla2 and Rvs167 at an endocytic site. These data, along with EM analysis, from a collaborating laboratory at the University of Durham, suggests that the E461K mutation causes a defect in the early stage of endocytosis in yeast.

5.2 In vitro analysis of E461K

5.2.1 Vps1 E461K binds actin

In chapter 4 an *in vitro* analysis of the E461K mutation was undertaken. This included an ability of E461K to bind to actin. It was predicted that the introduction of a basic residue would increase the affinity between Vps1 and actin as was reported for dynamin-1 (Gu et al. 2010). The ability of Vps1 E461K to bind actin was shown by a high speed pelleting assay with rabbit F-actin in section 4.2.4 figure 4. Figure 1 shows that the same result was obtained with the use of yeast F-actin . As previously discussed, there was no significant increase in the amount of Vps1 E461K bound to yeast or rabbit F-actin after a high speed pelleting assay. There was however, a larger standard deviation between pelleting E461K Vps1 with yeast actin in comparison to the WT (figure 1). This could suggest that, in the presence of yeast actin, there is a slight increase in actin binding. However it is not shown here to be significantly more than that of the WT. Further analysis into this binding affinity would be required to test if there is a subtle increase in the affinity which this high speed pelleting assay may not be able to differentiate.

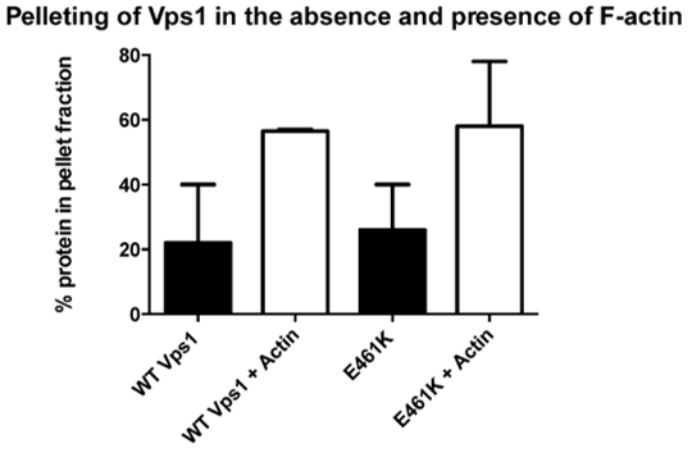

Figure 1. Vps1 E461K can bind directly to actin. Example of percentage Vps1 found in the pellet fraction from pelleting assay with or without the presence of yeast actin. Results show no significant difference (one way ANOVA) between the percentage in pellet between WT and E461K with or without actin error bars indicate SD.

5.2.2. Vps1 E461K can bind to lipids and hydrolyse GTP

The middle domain of dynamin sits between the GTPase domain and PH domain responsible for GTP hydrolysis and lipid binding respectively. Vps1 does not have a PH domain however is known to bind and tubulate lipids (Smaczynska-de Rooij et al. 2010). Any changes to the middle domain of Vps1 could affect these other functions of the protein, as previously discussed. Therefore these two functions were chosen and tested in Vps1 E461K. The lipid

binding ability was tested by a high speed pelleting assay with a mixed bovine fraction of lipids and it was found that the E461K can bind lipids as well as the WT (section 4.2.5 figure 5A). This suggests that this mutation is not affecting the ability of Vps1 to bind to lipids.

As a final test of Vps1 activity the ability of E461K to hydrolyse GTP was analysed. This GTPase assay is described in chapter 4 section 4.2.6 and indicates that the E461K mutation has the same rate of GTP hydrolysis to the WT. For clarity and comparison between Vps1 E461K and Vps1 WT the calculated GTP turnover (Kcat), rate, (Vmax) and GTP binding affinity (Km) is duplicated below.

0.5 µM protein in assay	**Vmax** µM Phosphate min^{-1}	**Km** µM	**Kcat** min^{-1}
WT	1.25 ± 0.13	0.18 ± 0.06	2.50 ± 0.26
E461K	0.99 ± 0.24	0.23 ± 0.19	1.98 ± 0.47

This suggests that the GTPase activity of Vps1 E461K is not affected and therefore the reduction in fluid phase uptake seen in section 4.3.7/4.5 figure 13/19B is unlikely to be due to a reduced GTPase activity of the protein.

5.3 Defects in endocytosis in cells expressing Vps1 E461K

5.3.1 The lifetime and intensity of Sla1-GFP and Abp1-mCherry in Vps1 E461K expressing cells

Having found that the E461K mutation reduces the fluid phase uptake of Lucifer yellow *in vivo* it was important to assess how this mutation may be affecting endocytic events specifically. The use of endocytic markers has been invaluable to the study of endocytosis in yeast and this method was utilised once again to study the effects of Vps1 E461K expression. This work was done alongside the analysis of the RR-EE mutation and therefore all the comparisons with WT and Null data are repeated in this section so as a comparison can be made solely with the E461K condition.

In order to assess the impact of the E461K mutation on early and invagination stages of endocytosis the cell line with both Sla1-GFP and Abp1-mCherry was used (KAY 1664). Sla1 is involved in the early coat stage of endocytosis, whereas Abp1 is an actin binding protein involved in invagination (Di Pietro et al. 2010; Kaksonen et al. 2005). These cells were transfected with Vps1 WT and E461K as well as an empty vector as a control. The transfected cells were then grown to on OD_{600} of 0.7 and placed on microscope slides for imaging. The live cell movies were taken by Dr. Iwona Smaczynska-de Rooji and they were subsequently analysed by ImageJ software (Schneider et al. 2012).

Given that the fluid phase uptake is reduced by the presence of Vps1 E461K, it was predicted that this mutation could be affecting the lifetime of endocytic reporter proteins at an endocytic site. To test this plasmids containing Vps1 and Vps1 E461K were transfected into the cell line KAY 1664 with Sla1-GFP and Abp1-mCherry integrated into the genome. This was compared with the same cell strain containing an empty plasmid- *vps1* null. The cells were then grown to an OD_{600} of 0.7 and imaged on a fluorescence microscope over time capturing both fluorophores in order to create live imaging movies of Sla1-GFP and Abp1-mCherry patches accumulating and invaginating into the cell. Analysing the lifetime of these fluorophores at an endocytic site provided an opportunity to see how the E461K mutation could be affecting the accumulation of the early stage endocytic marker Sla1 and the actin binding invagination marker Abp1. Vps1 is known to bind Sla1 (Yu & Cai 2004) and this is unlikely to be affected by the E461K mutation. Therefore the accumulation of Sla1-GFP at an endocytic site was hypothesised to be similar to the WT and that it would co-localise with Abp1-mCherry. As predicted, the movies showed clear co-localisation between Sla1-GFP and Abp1-mCherry (figure 2A). For each condition, five to six patches indicating clear endocytic events were then tracked throughout the movies. From these data the lifetime and intensity of both Sla1-GFP and Abp1-mCherry markers were normalised and plotted together over time. This created an intensity profile for both markers which indicted a reduction in lifetime for both Sla1-GFP and Abp1-mCherry patches in cells expressing Vps1 E461K (figure 2B). Sla1-GFP was found to accumulate before Abp1-mCherry as expected and this was also observed in the WT and null condition (figure 2C,D). When comparing the average lifetimes of both markers there was a significant reduction in the time both Sla1-GFP and Abp1-mCherry were found at endocytic sites when cells were expressing Vps1 E461K in comparison to the WT condition (calculated from at least 30 patches in each condition) (students t-test P value <0.0001) figure 2E (Palmer et al. 2015b). In order to analyse if the peak accumulation of these markers was also different when Vps1 contains the E461K mutation, each of the peak pixel intensities were analysed. The time at which the peak fluorescence intensities were observed were averaged and plotted with the mean lifetime indicated in the centre, flanked by the range of times within which the peak intensities were reached recorded (figure 2F). This indicated that the peak accumulation of both Sla1-GFP and Abl1-mCherry at an endocytic site occurs earlier on average than in cells expressing Vps1 WT. Overall this shows that there is a defect in Sla1 and Abp1 accumulation at an endocytic site in cells expressing Vps1 E461K and it results in a shorter lifetime for both these reporter proteins and this may suggest that the E461K mutation is effecting early stage endocytosis.

As previously discussed (chapter 4 section 4.4.2) this method of selecting few patches with clear endocytic events reduces the information that can be gained from this analysis.

Therefore the effects of Vps1 E461K was also analysed in two other ways with two different markers so as to verify this result and identify if indeed this mutation is affecting early stages of yeast endocytic events.

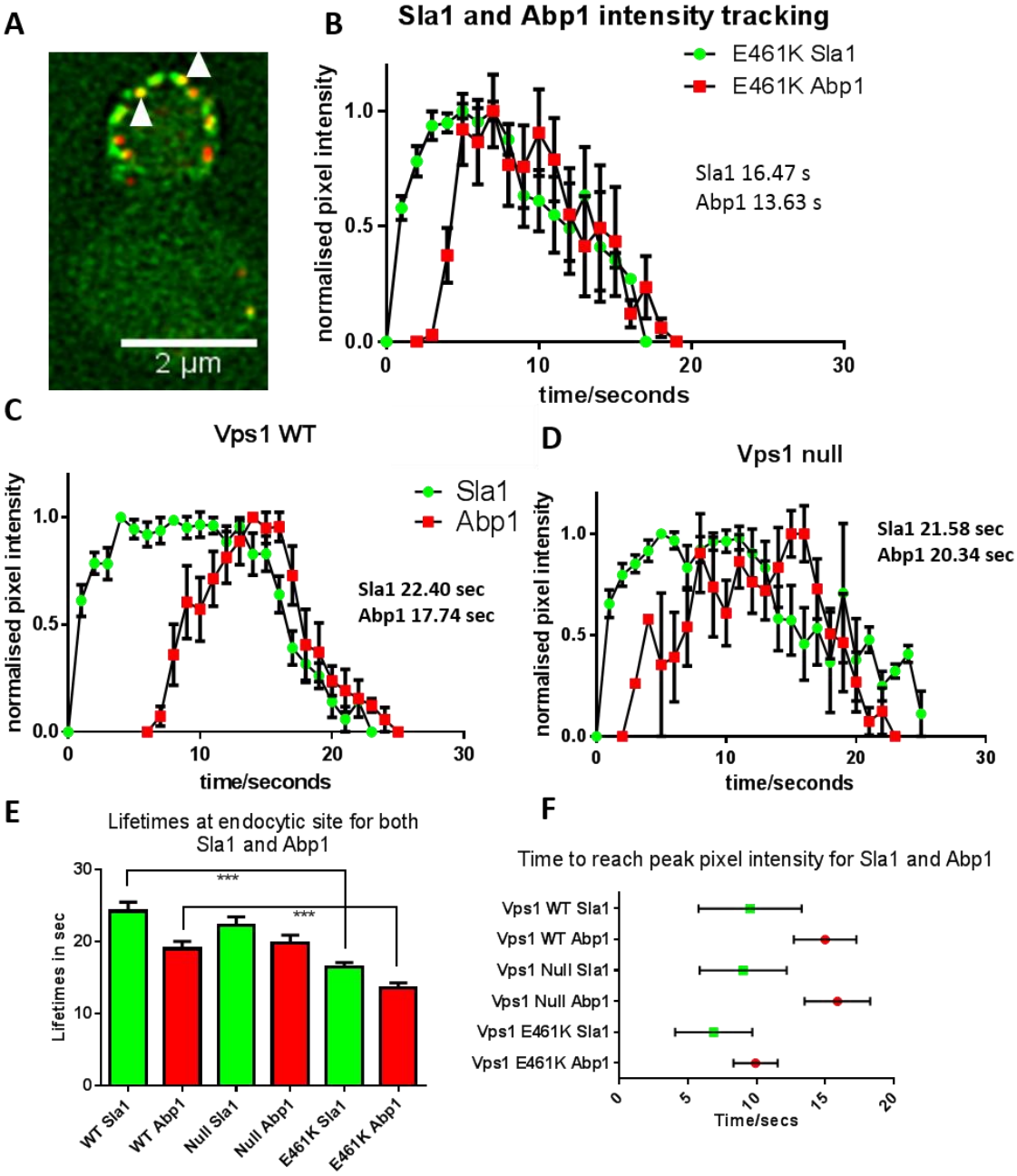

Figure 2. Sla1 and Abp1 accumulation and lifetime at an endocytic site in Vps1 E461K expressing cells . A) Example of co-localisation (indicated by white arrow heads) between Sla1 GFP and Abp1 mCherry in yeast cell expressing E461K. B-D) Intensity overlap graphs of Sla1 and Abp1 taken from dual colour movies. Normalised intensity graph is from 5-6 different patches of clear endocytic events. The average lifetime from the duel colour imaging is written along side the graph. E) The lifetimes of Sla1-GFP and Abp1-mCherry at an endocytic site was measured. There is a significant reduction in mean lifetime of Sla1-GFP and Abp1-mCherry in cells expressing Vps1 E461K mutation in comparison to the WT (student's t-test P value <0.001 error bars are SEM). F) This indicates the range of times for the peak pixel intensity for both Sla1 and Abp1 to appear in cells expressing Vps1, Vps1 null or Vps1 E461K. The green square or red spot indicates mean time for recruitment of these markers to an endocytic site.

5.3.2. The effects of Vps1 E461K on Sla2-GFP lifetime and behaviour

The endocytic marker Sla2 is an actin binding endocytic coat protein which acts to initiate invagination (Wesp et al. 1997). Sla2 is therefore involved in the early stages of yeast endocytosis and using this protein as a marker, this stage can be further analysed in cells expressing Vps1 E461K.

Plasmids containing Vps1 WT and Vps1 E461K were transfected into the cell line KAY 1459 with Sla2-GFP integrated into the genome. These cells were then grown to an OD_{600} of 0.7 and imaged on a fluorescence microscope over time to create live imaging movies of Sla2-GFP patches. It was hypothesised that if Vps1 E461K is affecting the early stages of endocytosis then the lifetime of Sla2-GFP will be reduced, similar to that of Sla1 and Abp1. After analysis of 30 separate patches it was found that the lifetime of Sla2-GFP in *vps1* null cells was significantly increased (one way ANOVA $F=19$ d.f. 2, 143 $p < 0.0001$) with an average of 38.4 ± 1.81 sec in comparison to WT 29.8 ± 0.91 (errors are SEM) as previously reported (Smaczynska-de Rooij et al. 2010). The average lifetime of Sla2 patches in Vps1 E461K expressing cells was 26.7 ± 1.3 sec which was a reduction in comparison to the WT however was not significant (figure 3A). The profiles of Sla2-GFP patches were then analysed by the creation of kymographs. Kymographs indicate the movement of the patches into the cell over time. From the kymographs it was observed that the *vps1* null cells indicate retractions back to the membrane and aberrant movements into the cell. Similarly the E461K cells show some short invaginations and some retractions (figure 3B). Finally, using patch tracking in ImageJ software (Schneider et al. 2012), the behaviour of 10 Sla2-GFP patches were tracked and their movement compared to a distance of 200 nm into the cell. 200 nm was chosen as this is thought to be the distance an endocytic vesicle is able to move into the cell before scission occurs (Kaksonen et al. 2003). As seen in figure 3B when patch tracking is utilised to see the movement of endocytic Sla2 there are fewer patches in E461K expressing cells that move past the 200 nm stage (figure 3B). This suggests that there is a reduction in the movement of Sla2-GFP into the cell, once again suggesting that the Vps1 E461K mutation is affecting early stage endocytosis (Palmer et al. 2015b). The lifetimes for Sla2-GFP were slightly reduced and the fact that this is not significant may reflect how this mutation is having a mild effect on endocytosis. As seen with the fluid phase uptake (section 4.3.7/4.5 figures 13/19B) there is a reduction in uptake in comparison to the WT condition but this is mild in comparison the Vps1 RR-EE or *vps1* null cells.

In the future it would be necessary to also assess the phenotypes of the invaginations by more detailed kymograph analysis. This was done in chapter 4 figure 16, to analyse how the patch movements were behaving in comparison to WT and could suggest further details in this analysis which would aid with understanding the mechanism by which Vps1 E461K affects early stage endocytosis.

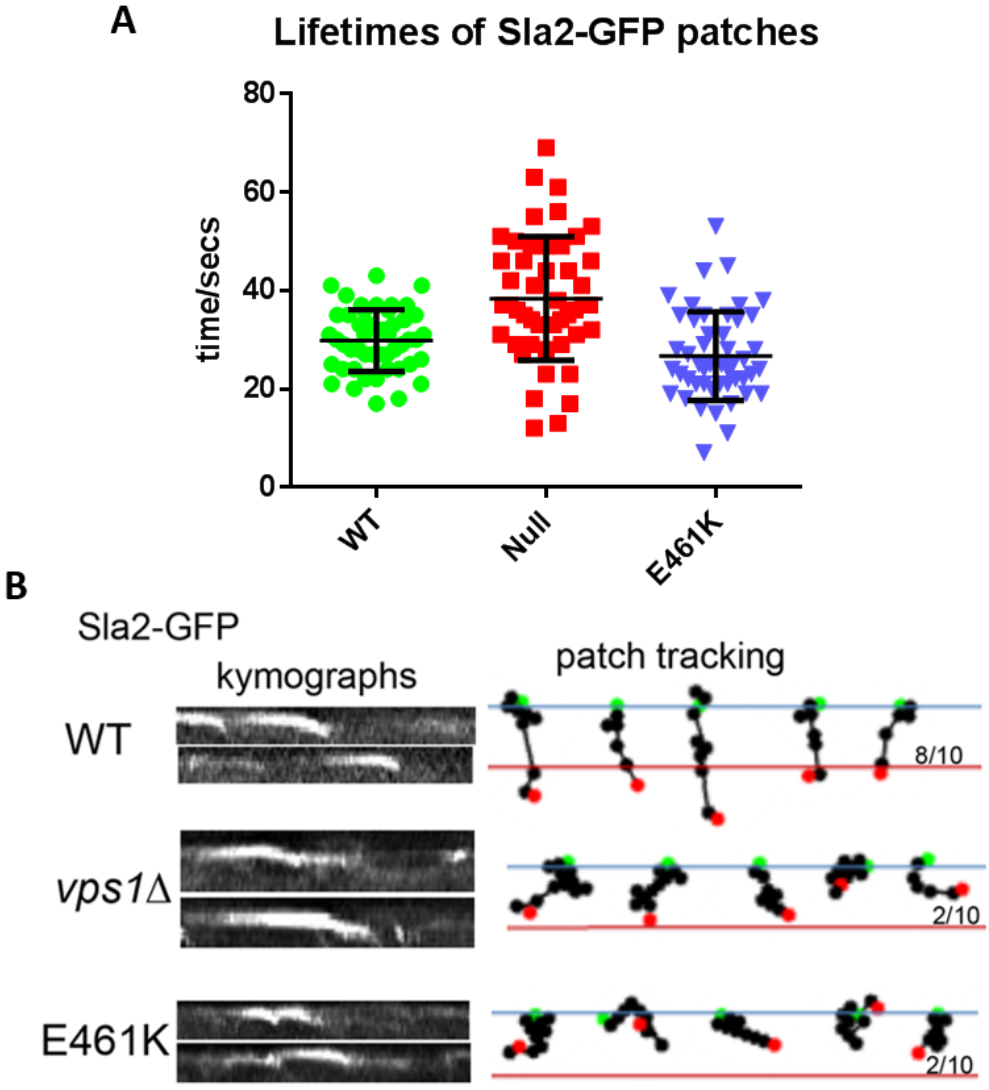

Figure 3. Sla2-GFP patch phenotype in cells expressing Vps1 E461K A) The lifetime of Sla2-GFP patches at the membrane. 30 individual patches were analysed and there is a significant increase in the lifetime of Sla2-GFP in *vps1* null cells (one way ANOVA F=19 d.f. 2, 143 $p < 0.0001$) but not between WT and E461K expressing cells. B) Live cell movies were analysed for Sla2 GFP patch accumulation. These were used to create kymographs of example patches on the left and patch tracks as seen on the right. Green and red spots indicative start and end of patch tracking respectively. The red line indicates 200 nm into the cell. 10 patches were analysed in this way and the number of patches passing this 200 nm mark are shown as a score out of 10.

5.3.3 The effects of Vps1 E461K on Rvs167-GFP lifetime and intensity

The protein Rvs167 has been reported to function with Rvs161 during the scission stage of endocytosis (Kaksonen et al. 2005). Rvs167 is an amphiphysin protein which can bind directly to Vps1 and these two proteins function together during endocytosis (Smaczynska-de Rooij et al. 2012). Using a GFP tagged Rvs167 the later stages of endocytosis can be analysed. As this mutation E461K has been found to shorten the lifetimes of Sla1-GFP, Abp1-mCherry and Sla2-GFP at an endocytic patch it was hypothesised that few patches would go on to scission and therefore a reduction in the lifetime and intensity of the late stage marker Rvs167-GFP should be observed.

Plasmids containing Vps1 WT, E461K and an empty control vector were transfected into the Rvs167-GFP expressing strain (KAY 1337). These were then grown to an OD_{600} of 0.7 and live cell imaged on a fluorescence microscope. From the movies collected the lifetime and peak pixel intensity of Rvs167-GFP patches were measured over time using ImageJ software (Schneider et al. 2012). As hypothesised there was a significant reduction in the overall lifetime of Rvs167-GFP in endocytic patches when cells are expressing Vps1 E461K rather than the WT (one way ANOVA F=21.80 d.f. 2,117 p<0.0001) (figure 4A). There was also a significant reduction in Rvs167-GFP average lifetime in *vps1* null cells as previously reported (Smaczynska-de Rooij et al. 2010). Moreover there was a significant reduction in the peak pixel intensity's of

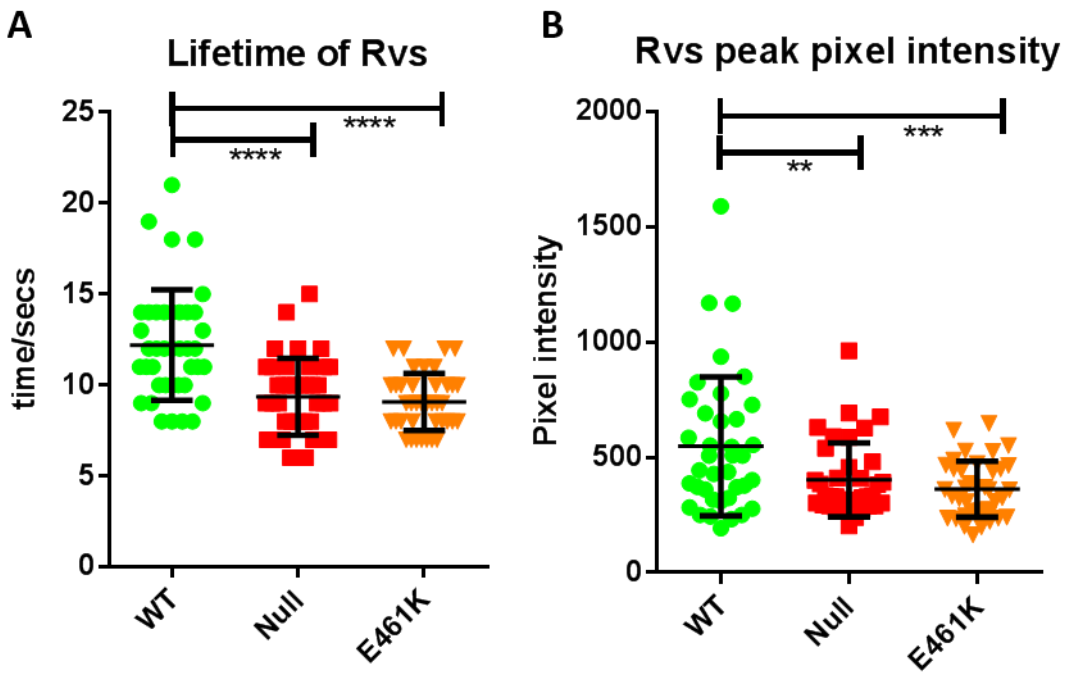

Figure 4. Rvs167-GFP lifetime and intensity in Vps1 E461K expressing cells. A) The lifetimes of over 30 Rvs167 GFP patches was recorded and there was a significant decrease in the lifetime of Rvs167 GFP between WT-Null and WT-E461K cells (one way ANOVA F=21.80 d.f. 2,117 p<0.0001). B) The peak pixel intensity of over 30 Rvs167 GFP patches was recorded and there was a significant decrease in the average pixel intensity between WT-Null and WT-E461K cells (one way ANOVA F=8.27 d.f. 2,112 p 0.0005) all error bars indicate SD.

Rvs167-GFP at endocytic sites in both E461K cells and *vps1* null cells in comparison to the WT (one way ANOVA F=8.27 d.f. 2,112 p 0.0005) (figure 4B) (Palmer et al. 2015b). These data indicate that the expression of Vps1 E461K is not rescuing the null phenotype of reduced Rvs167-GFP accumulation at an endocytic site. This provides evidence to support the hypothesis that E461K disrupts the early coat and invagination stages of endocytosis preventing them from continuing to scission and that Vps1 plays a role during the early stages of endocytosis.

5.4 Discussion

The role of dynamin in endocytosis has been thoroughly documented. However the vast majority of this work has focused on the action of dynamin at the scission stage of endocytosis. This study into the yeast dynamin Vps1 and the mutation E461K suggests that there may indeed be a role for dynamin and dynamin-like proteins in earlier stages of endocytosis including coat assembly and invagination. The E461K mutation was not found to affect the ability of Vps1 to bind actin or hydrolyse GTP however *in vivo* analysis suggests that Vps1 E461K has an effect in the early stages of endocytosis reducing the lifetimes of Sla1, Abp1, Sla2 and Rvs167. This data suggests that the use of the E461K mutation may be a way of identifying the different roles of Vps1 in endocytosis specifically to analyse the role of dynamin proteins in the early stages of endocytosis in contrast to their role in scission.

5.4.1 The in vitro analysis of Vps1 E461K

It was interesting to find that the E461K mutation does not increase the affinity between Vps1 and actin as predicted. However there seems to be more variety between the amount of Vps1 E461K that sediments in the high speed pelleting assay in comparison to the WT (figure 1). This could indicate actin has more of an effect on Vps1 E461K oligomerisation than the WT. In chapter 4 the morphology of Vps1 rings were analysed by EM for both WT and RR-EE proteins (figure 22). This was also done for the E416K condition by Dr. Chris Markew and Prof. Kathryn Ayscough. It was found that Vps1 E461K can form rings of a similar size in diameter to that of WT Vps1 (Vps1 E461K, 30.2 ± 4.9 nm n=44 Vps1 WT, 32 ± 3.7 nm n=49 error is SD) figure 5A,B (Palmer et al. 2015b). However, in the presence of actin there were no double ring structures seen in Vps1 E461K in comparison to the WT where 55% of structures in the presence of actin were double rings (figure 5B). This indicates that E461K can form rings however these may not be able to oligomerise further into double ring structures. Therefore the presence of more Vps1 E461K found in the pellet fractions sometimes during the pelleting assays may have been an artefact. Further investigation into the structure of these rings by 3-D

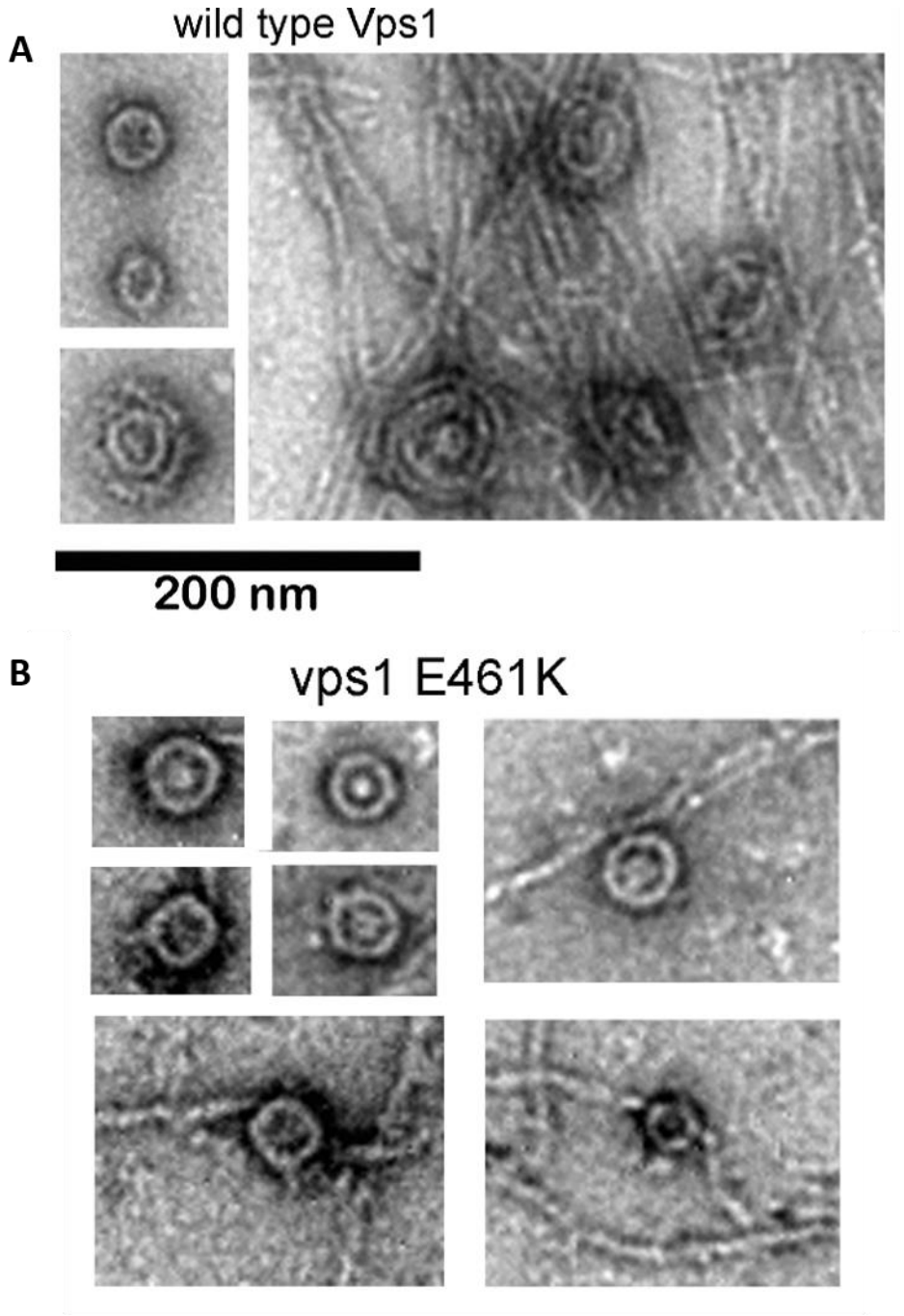

Figure 5. EM images of Vps1 WT and E461K rings with and without actin. A) Example of EM images of WT Vps1 rings and double rings in the presence of actin taken by Dr. Chris Marklew. B) Examples of Vps1 E461K EM images in the presence and absence of actin indicating the presence of single rings only.

reconstruction from EM images may indicate if these rings are lying flat or if they can form a spiral structure, as would be required to form around the vesicle neck. Hypothetically, the E461K mutation could be having a subtle effect on the structure of an oligomer such that the twist in a ring required for a spiral to occur cannot form. This would leave flat rings of Vps1 but would not be able to function as a WT Vps1 spiral therefore disrupting the ability of Vps1 E461K in endocytic fission.

During the EM analysis it was also apparent that the E461K single rings were not associated with as many actin filaments in comparison to the WT. This could indicate that the double ring structures are more able to bundle actin, perhaps due to the orientation of Vps1 molecules within the structure. This would have to be confirmed by further 3D EM reconstruction work and through solving the structure of a single Vps1 molecule. Moreover, a falling ball assay combined with low-speed pelleting assays would be required for conformation of whether the E461K mutation is less able to bundle actin than the WT.

5.4.2 The effects of Vps1 E461K on markers of endocytosis in vivo

There is a chance that the E461K mutation causes miss-localisation of Vps1 so that it is not present at an endocytic site. Due to the differences between endocytic reporter protein lifetimes in Vps1 E461K cells in comparison to *vps1* null (for example Sla2) this is unlikely. However to check the localisation of Vps1 E461K a biomolecular fluorescence complementation assay (BiFC) was carried out. This was done to see if Vps1 E461K and Rvs167 localise to the same area by the membrane. This has been shown to be the case for Vps1 WT and RR-EE (Palmer et al. 2015a). This experiment was carried out by Dr. Iwona Smaczynska-de Rooij who found that there was indeed fluorescence at the plasma membrane indicating localisation of Vps1 E461K with the endocytic scission stage protein Rvs167. An example image from this analysis can be seen in figure 6A (with controls figure 6B). The localisation of E461K at endocytic sites would ideally be tested using TIRF however time constraints meant this additional study could not be carried out during this project.

The expression of E461K was found to reduce the lifetime of Sla1-GFP and Abp1-mCherry in a dual labelled cell line (figure 2E). The limitations of this assay have previously been discussed however this was the first analysis which suggested that the E461K mutation was having an effect on the early stages of endocytosis. It was therefore interesting to find that the Sla2-GFP marker has a slightly reduced lifetime in E461K expressing cells but that this was not significant. This could suggest that the effect on these early stage endocytic markers are subtle which would be expected as the overall reduction in uptake (as tracked by the fluid phase marker Lucifer yellow) is only reduced and this is not as marked as in the *vps1* null or Vps1 RR-EE condition (chapter 4 sections 4.3.7/4.5).

The role of the Vps1 E461K mutation at the early stages of endocytosis was indicated once again by the reduction in both lifetime and intensity of Rvs167-GFP. Both the lifetime and intensity of this endocytic marker was similar to that of the null condition. This was interesting as it suggests some endocytic events are arrested before the scission stage, a phenotype reflected in the Sla2-GFP patches where few moved past 200 nm into the cell, indicating a defect before invagination and scission. This could be explained by the reduction in double ring

E461K structures, created in the presence of actin, in comparison to the WT. If Vps1 and actin act in a feedback loop during endocytosis, as described for dynamin and actin in mammalian cells (Taylor et al. 2012) then the higher order oligomers form after actin binding. If this leads to a defective single ring of Vps1 this could prevent invagination of a clathrin coated pit, potentially causing disassembly of endocytic proteins before scission can occur.

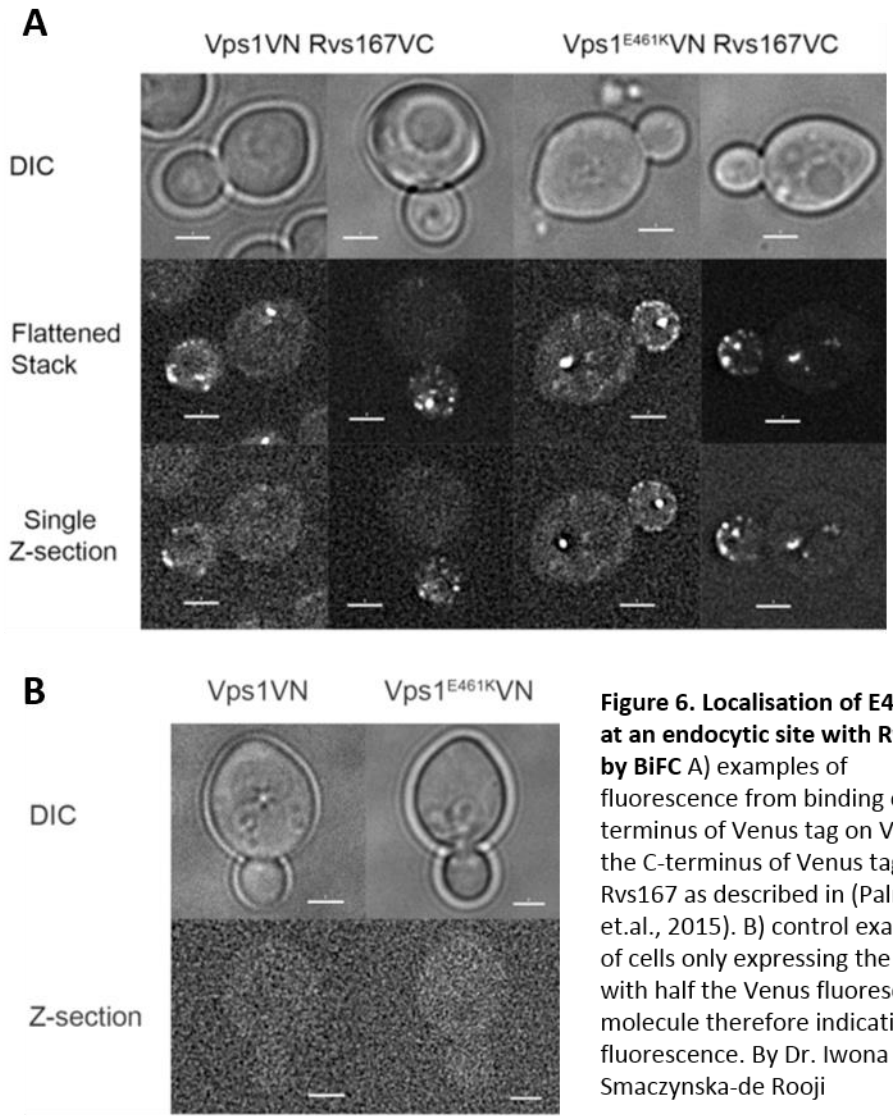

Figure 6. Localisation of E461K at an endocytic site with Rvs167 by BiFC A) examples of fluorescence from binding of N-terminus of Venus tag on Vps1 to the C-terminus of Venus tag on Rvs167 as described in (Palmer et.al., 2015). B) control example of cells only expressing the Vps1 with half the Venus fluorescence molecule therefore indicating no fluorescence. By Dr. Iwona Smaczynska-de Rooji

5.4.3 Vps1 E461K forms short endocytic invaginations

Along with the RR457-8EE mutation in the previous study, the effect of the E461K mutation on the formation of endocytic invaginations were tested by Dr. Martin Goldberg, Dr. Ritu Mishra and Dr. Simeon Johnson at Durham University. As seen in figure 7A it was found that cells expressing E461K formed short shallow invaginations (Palmer et al. 2015b). From 50 separate invaginations it was calculated that the average depth of these coated pits was 18 ± 7 nm in comparison to WT which averaged between 50-60 nm (figure 7A,B). This supports the rest of the in vivo data as it suggests that the E461K mutation is indeed affecting the early invagination stage, potentially causing an instability in the coat complex so invagination cannot continue. This mutation however does not prevent endocytosis and it has a very mild phenotype in cells overall. Without a temperature sensitive phenotype, like the *vps1* null condition, this suggests that even thought this EM data shows what would be predicted to cause a dramatic effect on endocytosis, E461K can in fact rescue the null phenotype to a great

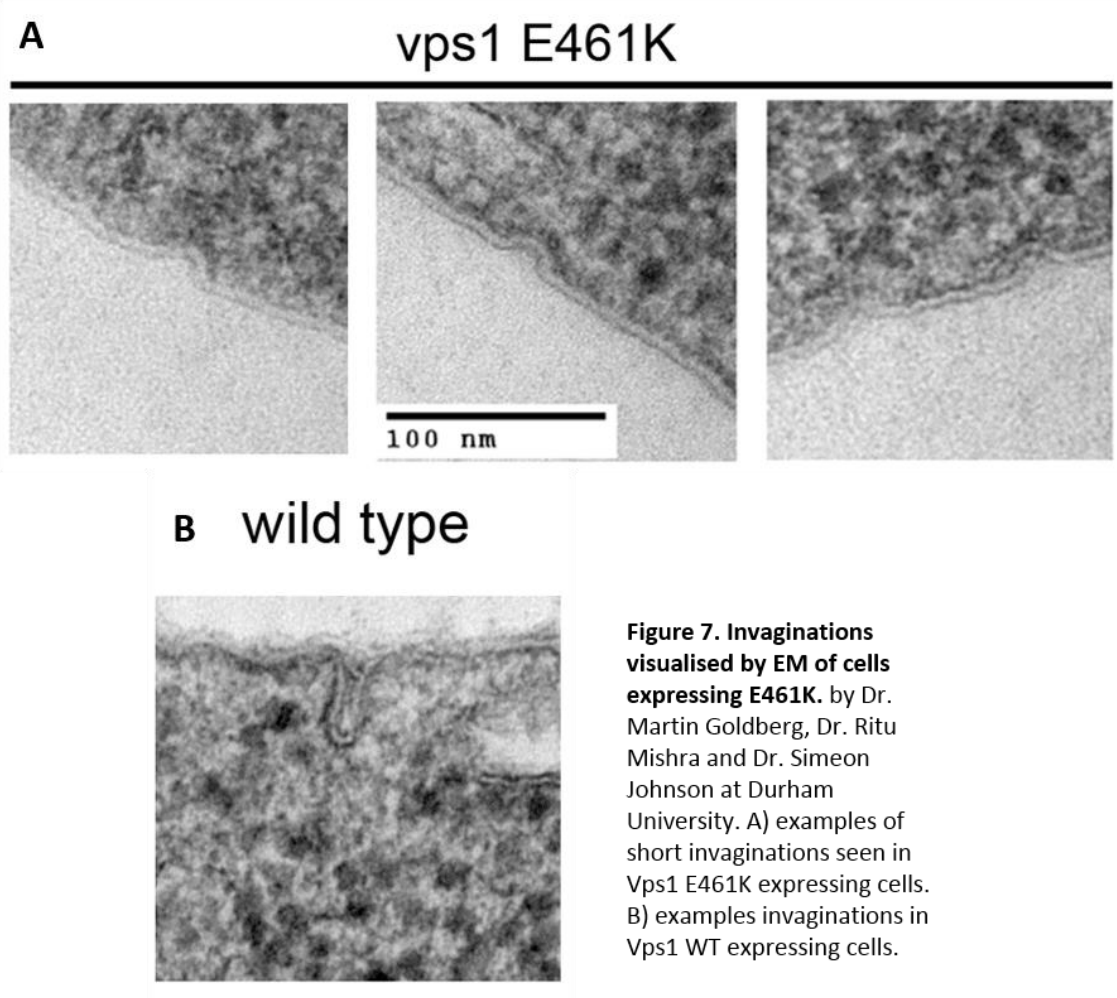

Figure 7. Invaginations visualised by EM of cells expressing E461K. by Dr. Martin Goldberg, Dr. Ritu Mishra and Dr. Simeon Johnson at Durham University. A) examples of short invaginations seen in Vps1 E461K expressing cells. B) examples invaginations in Vps1 WT expressing cells.

extent. This could be because the E461K mutation causes endocytic events to occur more frequently so where one is unstable and collapses another will form and this will happen over and over until the process is stable enough to continue through to scission. There are other types of endocytic uptake in yeast, described to function without Vps1 (Aghamohammadzadeh et al. 2014), which may act at a higher rate if the initial coat complexes for clathrin mediated endocytosis do not function properly. This may not overcome effects of the RR-EE mutation, as this has more of a detrimental effect later at scission, and therefore signals initiated by the coat complex would still take place.

In conclusion, the mutation E461K has a mild effect on the early stage of endocytosis causing a reduction in lifetime of Sla1, Sla2, Abp1 and Rvs167 markers as well as an increase in shallow invaginations seen by EM. Vps1 E461K is unable to bundle actin in comparison to the WT but may reduce the ability of Vps1 to form higher order structures in the presence of actin. Furthermore this mutation retains the ability of Vps1 to bind actin and hydrolyse GTP. Research into mammalian dynamin at an endocytic site suggests that there is a role for monomeric or non-oligomerised dynamin at early stages of endocytosis which act to stimulate the polymerisation of actin (Taylor et al. 2012). Vps1 E461K can form rings but not double rings suggestive of a system whereby actin stimulates E461K oligomerisation but this is blocked after single ring formation. This could lead to a block after initiation of endocytosis preventing invagination and scission events. Further biochemical analysis is required for this study, however this provides some further insight into the role of the amino acids in the middle domain of Vps1 and further evidence for the involvement of dynamin proteins at stages of endocytosis earlier than that of scission.

Chapter 6

Cellular and *in vitro* effects of actin binding site mutations in human dynamin-1

6.1 Introduction

In chapters 3 and 4 the use of *Saccharomyces cerevisiae* as a model organism was invaluable for this study, providing an easy way to manipulate the *VPS1* gene in a naturally occurring eukaryotic single cell system. Vps1, whilst known to function at the scission stage of endocytosis, was found to have two charged residues that are required for efficient actin binding and vesicle scission. This has provided new insights into the action of dynamin and actin at an endocytic site. Using this knowledge, there are potential impacts of these findings which go beyond the understanding of yeast endocytic function. In this chapter, the study moved on to test the orthologous charge mutations in dynamin-1 and investigate what impact they have on in vitro actin binding and cellular function.

The most well-characterised function of dynamin is its role during the scission stage of clathrin mediated endocytosis (CME) where it oligomersises around the vesicle neck and facilitates membrane scission in a GTPase dependent mechanism (Cocucci et al. 2014). In contrast to yeast, mammalian endocytosis does not always require actin, but actin is thought to play a role in most endocytic events that are modulated by dynamin (Ferguson et al. 2009; Taylor et al. 2012) and can overcome arrests in endocytosis due to high membrane tension caused, for example, by the polarisation of cells (Boulant et al. 2011).

Dynamin proteins also function in other cellular roles that require actin as described in chapter 1 section 1.5, including cell migration and invasion. Most, but not all, of these functions are thought to require dynamin-2 and this may be due to the ubiquitous expression of this isoform. Dynamin-2 is known to bind the actin regulatory protein cortactin in lamellipodia (McNiven et al. 2000), and charged residues in its actin binding site (as described by Gu et.al., 2010) were found to be required for actin organisation within the lamellipodia

(Menon et al. 2014). Interestingly it was recently reported that mutation of the charged residues in the dynamin-1 actin binding site prevented dynamin function during filopodia formation (Chou et al. 2014). As filopodia play an essential role in cell migration (Xue et al. 2010) a specific mutation within the actin binding site of dynamin may well also have an effect on cell migration. Similarly, the role of the direct dynamin-actin interaction has not been investigated in invadosome formation, however the interaction of dynamin-2 with actin-modulating proteins is known to be involved in the formation of invadosomes (Lee & De Camilli 2002; Baldassarre et al. 2003).

Cell functions that require both dynamin and actin, such as cell migration and invasion, can be utilised for tumour metastasis, and therefore understanding the direct interaction between these two proteins could lead to new therapeutic targets. Furthermore, there are other mutations which may affect the direct dynamin-actin interaction, that have been linked to other diseases. An example of this is the 'fitful' mutation (A408T in dynamin-1) (chapter 3 section 3.3.3) which produces an epileptic phenotype in mice (Boumil et al. 2010). This is intriguing as dynamin-1 is best known for its function in endocytosis in neuronal cells and it has been reported that polarised cells require actin for endocytosis where the membrane tension is highest (Boulant et al. 2011). Therefore, the direct dynamin-actin interaction could well be important during endocytosis in polarised neuronal cells, providing an explanation for why the A408T mutation causes the observed epileptic phenotype.

During this study the direct dynamin-actin interaction was tested with the mutations KK418-9EE and A408T in human dynamin-1. The KK418-9EE mutation (hereafter KK-EE) was then taken on for preliminary experiments into its effects on endocytosis, cell migration and invadosome formation. Future work would require further analyses of these tests as well as an investigation into homologous mutations in dynamin-2. This is due to relatively limited expression and reported functions of dynamin-1 compared with dynamin-2, which is reported to function in cellular processes beyond endocytosis, such as migration and invasion. Nevertheless the data presented in this chapter provide preliminary results for identifying the consequences of the direct dynamin-actin interaction, and set up new avenues for future research.

6.2 Purification of human dynamin-1

When first discovered, purified mammalian dynamin was obtained by way of affinity purification from rat brain extracts (Gout et al. 1993). This was then replaced with baculovirus expression in insect cell lines, such as SF9 or SF21, which can express mammalian proteins to a high concentration (Damke et al. 2001). This technique for recombinant mammalian dynamin expression has been superseded by transient transfection of the same insect cell lines with the Novagen vector backbone pIEX-6 (Chappie et al. 2009) and a 1:1 mix of the lipids, 1,2-dioleoyl-3-trimethylammonium-propane and 1,2-dioleoyl-*sn*-glycero-3-phosphoethanolamine (DOTAP:DOPE, Avanti). This transfection technique is used for dynamin expression in Sandra Schmid's laboratory (UT Southwestern Medical Centre) and she kindly gifted the use of the dynamin-1 pIEX-6 vector, along with the protocol for SF9 cell expression, for this study. In addition, SF21 cells (the clonal derivative of SF9) were kindly donated by Elizabeth Smythe (University of Sheffield). A slight modification to the protocol of note includes the use of a French Press to lyse the insect cells, as the nitrogen cavitation device specified in the Schmid laboratory protocol was not available.

The protocol exploits the interaction between dynamin-1 and amphiphysin-2 to affinity purify the protein, removing the need for a tag bound to dynamin. A recombinant fusion protein containing the SH3 domain of amphiphysin-2 and an N-terminal GST-tag is bound to glutathione-sepharose (GE Healthcare). The insect cell lysates were then mixed with the bound sepharose beads and dynamin was subsequently eluted with a high salt buffer (see chapter 2 section 2.3.7.2). The initial purifications yielded very little protein with a high level of contaminants (figure 1A arrowhead). Despite the purification technique not requiring a tag for affinity purification, the vector contained a 6-His tag, which was confirmed by western blotting figure 1B. The identity of the 100 kDa band on anti-his blots, as well as via Coomassie stained protein gels, was confirmed to be dynamin-1 by western blotting figure 1C. Several breakdown products of the protein were also visible on Coomassie stained protein electrophoresis gel and dynamin-1 western blots.

From the preliminary purifications it was clear that optimisation was required to increase the yield of full-length dynamin-1 and remove contaminants. In order to test how to remove these, some of the elutions (from the affinity purification in figure 1A) were exposed to a nickel affinity purification step, taking advantage of the His-tag on dynamin-1 in an attempt to remove the non-specific protein bands. As seen in figure 2A the initial protein purification had many contaminants, whereas elutions from the nickel beads by imidazole had fewer contaminants than before. Despite some loss of overall yield this method was added into the purification process as an initial step in the purification protocol. It was assumed that

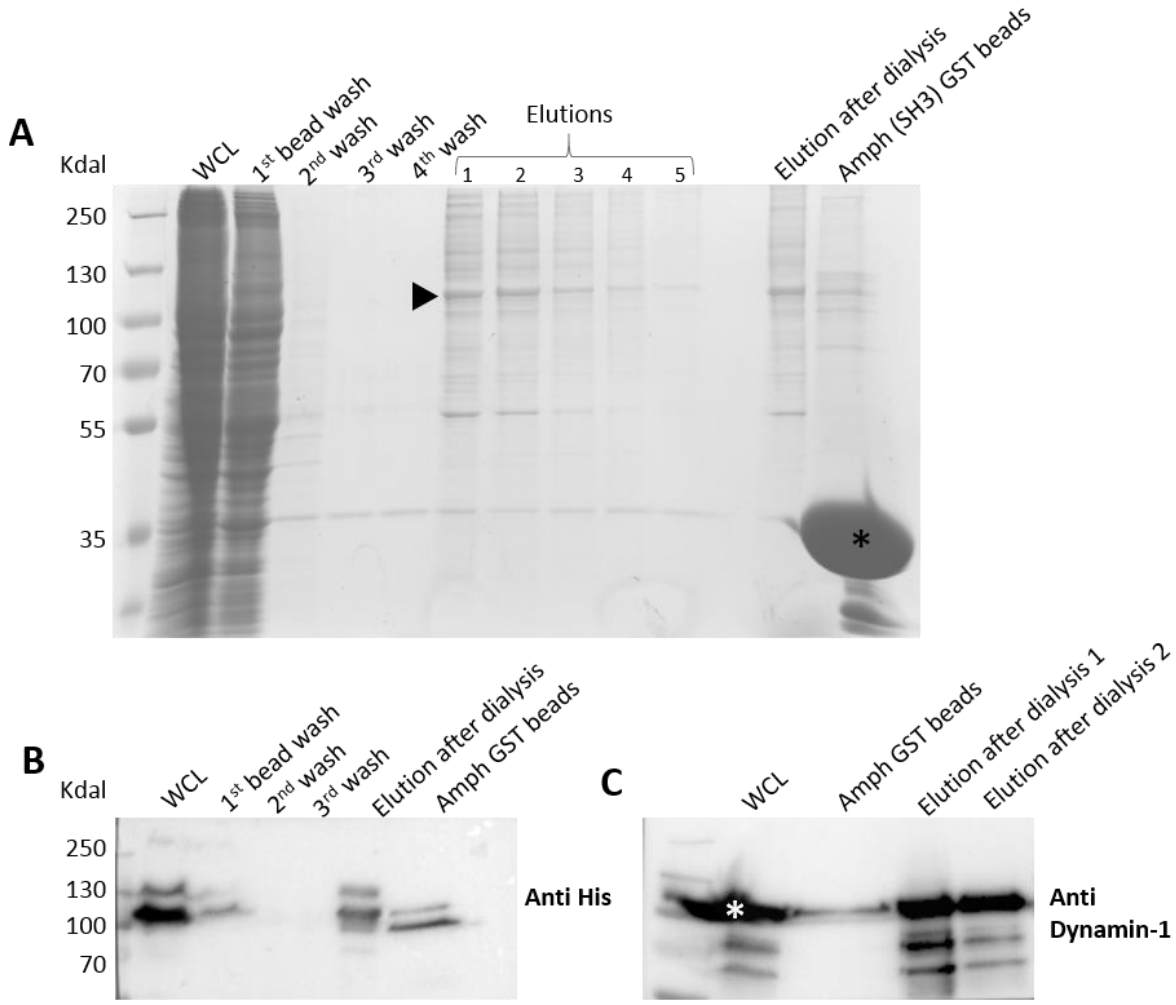

Figure 1. Purification of dynamin-1 from SF21 cells. A) Coomassie stained SDS-PAGE get of purification steps from SF21 cells to elutions of dynamin arrowhead indicates band at the size of dynamin-1. * is SH3 domain of amphiphysin-2. B) Western blot of samples used in `A' probed with anti His-tag antibody. C) Example of a western blot of purified dynamin, probed with anti dynamin-1 antibody. Elution number 1 is from the same prep in `A' and `B' and elution number 2 is from a similar prep. * Note that the first WCL band spilled into the protein marker lane, therefore the initial band, whilst looking like two lanes, is actually only the WCL sample.

the nickel bead affinity purification should precede amphiphysin-2 SH3 binding as the elution buffer containing imidazole was less likely to affect amphiphysin-2 SH3 binding, whereas the high salt elution from the GST beads would likely reduce nickel bead binding (figure 2B).

In addition to the purification step, another consideration was acted upon. Unlike SF9 cells, the SF21 cells used in this thesis require serum for optimum growth (Prof. Elizabeth Smythe laboratory personal communication). In Novagen's protocol for use of pIEX-6 vectors it is suggested that the presence of serum is only detrimental when mixing together the lipids and DNA prior to transfection. However, it has been published that the presence of serum at any point during transfection can reduce transfection efficiency (Kim et al. 2014). Therefore

SF21 cells were grown to an optimum density and then moved into serum free media before transfection and expression. The elutions subsequently not only yielded higher concentrations of protein, but also fewer contaminants (figure 2C). This method was repeated for further purifications of WT dynamin-1 as well as dynamin-1 KK-EE and A408T.

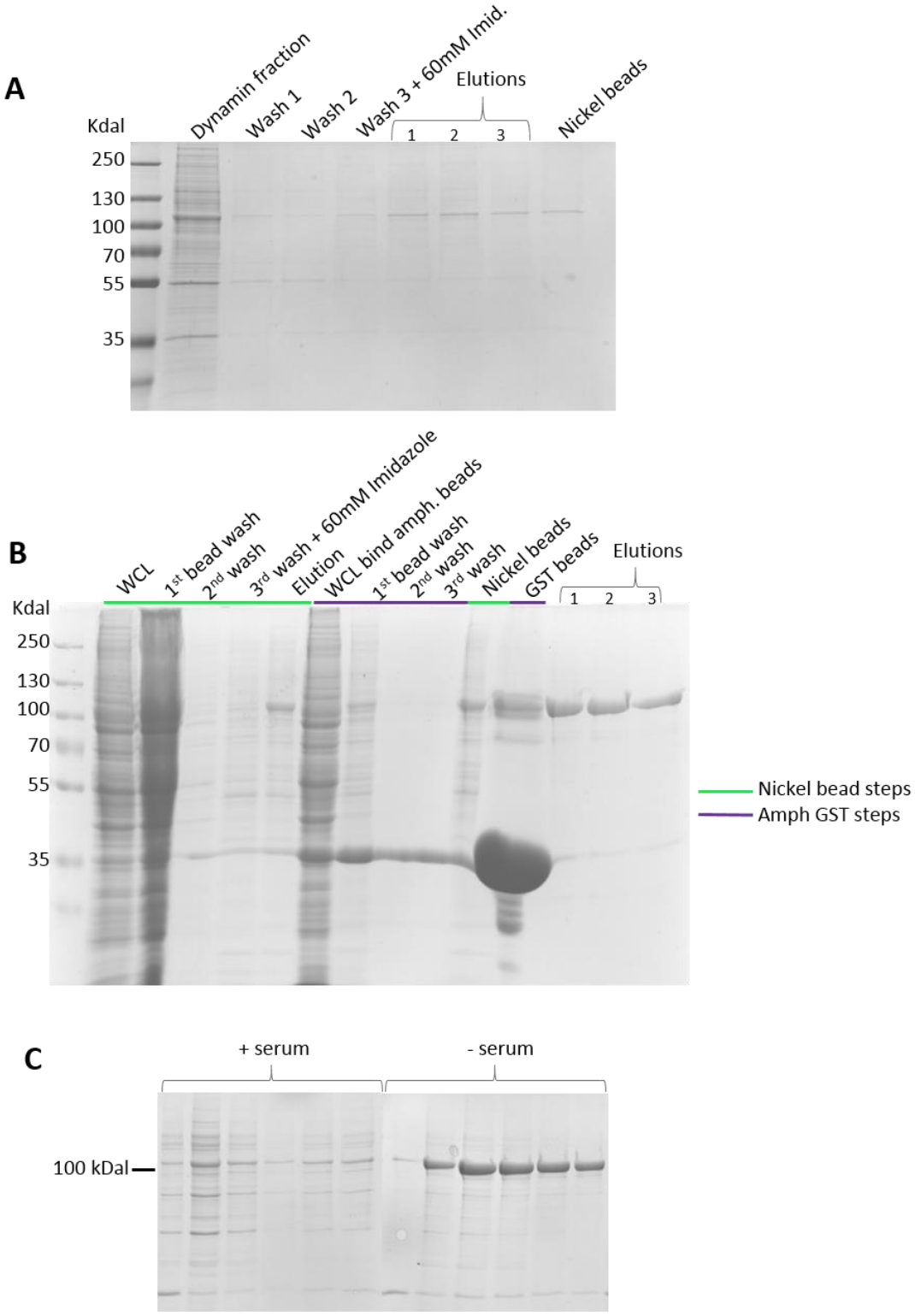

Figure 2. Optimisation of Dynamin-1 purification from SF21 cells A) Further purification of dynamin-1 elution fractions after purification from Amphiphysin GST beads. B) Example SDS-PAGE gel showing different stages of new purification protocol. Green bar denotes first nickel bead binding stage and final elution and purple bar indicates further amphiphysin-2 (Amph) GST binding and final elutions afterwards. C) Example of elutions if SF21 cells have been transfected with serum (left) or without serum (right).

6.3 Actin binding of human dynamin-1

It is known that human dynamin-1 binds directly to actin as shown using a co-sedimentation assay with F-actin (Gu et al. 2010). This method, as used in previous chapters 4 and 5, was repeated with the KK-EE and A408T mutations in dynamin-1 to investigate if they change the ability of dynamin to bind to actin. A pre-spinning step was required in the Vps1 study (chapter 2 section 2.3.11) to select for soluble protein (as well as remove insoluble or denatured protein). However, it has been reported that the oligomerisation of dynamin-1 is reduced in buffers containing physiological levels of salt (Warnock et al. 1997). Therefore this was taken into account and after dynamin purification the protein was dialysed into a low salt buffer to replace the pre-spinning step carried out during the Vps1 protocol. It was hypothesised that dynamin-1 would not pellet at high speed unless bound to F-actin. In order to test this, 1.5 µM dynamin-1 was incubated with 3 µM pre-polymerised F-actin and left at RT for 15 minutes. Following this incubation the dynamin-actin solution was spun at 90,000 rpm (Beckman rotor TL100) for 15 minutes, and the subsequent supernatant and pellet were separated. These fractions were run on an SDS-PAGE gel and stained with Coomassie safe stain to analyse the proportion of dynamin-1 that pelleted with F-actin, and hence the extent of binding between the two proteins.

As reported previously (Gu et al. 2010), a higher proportion of dynamin-1 was found in the pellet fraction after incubation with F-actin (figure 3A). In the low salt buffer without F-actin very little dynamin-1 oligomerises and therefore the majority of the protein remains in the soluble fraction after high speed centrifugation. This result demonstrates that dynamin-1 can bind F-actin *in vitro.*

The high speed pelleting experiment was repeated with dynamin-1 KK-EE and this, interestingly, indicated a greater propensity of the protein to sediment in the absence of actin. In comparison to WT dynamin-1, a greater proportion of the KK-EE mutant was found in the pellet fraction by gel densitometry calculations (average percentage in pellet without actin: WT 20.45% ± 2.91, KK-EE 54.7% ± 4.6 SEM). However, the presence of F-actin did not significantly change the proportion of dynamin-1 KK-EE observed in the pellet fraction (average percentage in pellet with actin: WT 38.9% ± 5.7, KK-EE 54.2% ± 5.1 SEM) (figure 3B). An additional band of lower molecular weight, thought to be a breakdown product of the dynamin KK-EE mutant, was consistently observed in these experiments, as seen with Vps1 protein (figure 3A). This additional band was present in the pellet fraction, both with and without actin, and was not observed on Coomassie stained SDS-PAGE gels immediately after purification, but was observed after the final overnight dialysis step. This suggested that, at some point during the 16 hours after purification, the KK-EE mutant is more susceptible to

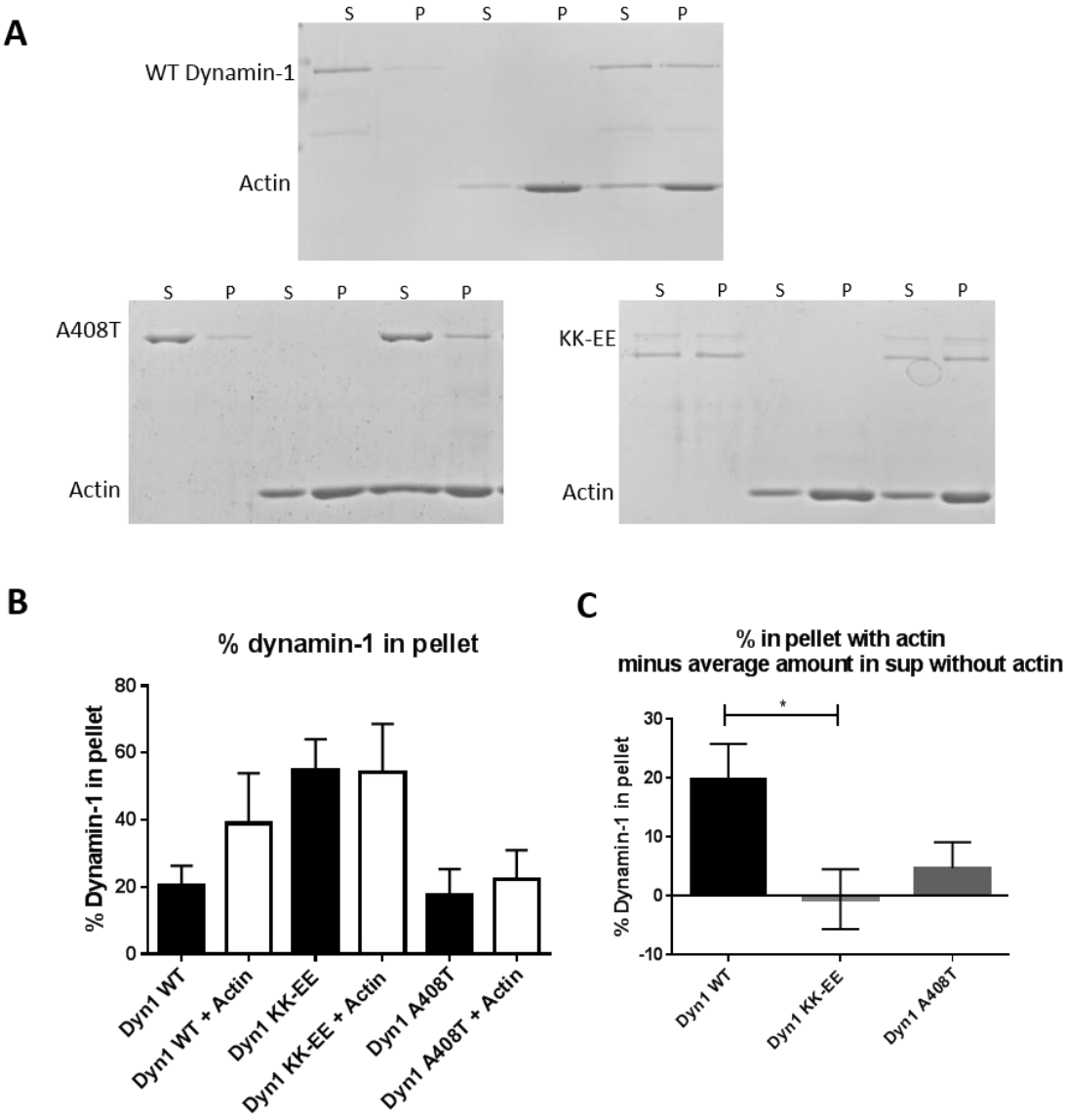

Figure 3. Dynamin-1 mutations KK-EE and A408T reduce its actin binding ability. A) example of co-sedimentary assays with WT dynamin-1 or dynamin with KK-EE or A408T mutations. Dynamin is at 1.5 µM and F-Actin 3 µM and mixes are centrifuged at 90K before being separated into supernatant (S) or pellet (P). Black arrow indicates breakdown from full length dynamin in dynamin KK-EE. B) percentages of dynamin found in the pellet determined by densitometry. WT n=4 WT+actin n=7, KK-EE n=4 KK-EE+actin n=8, A408T n=2 A408T + actin n=4. C) To compare differences in the amount of dynamin found only in the pellet when incubated with actin, percentages calculated without actin was subtracted. For each bar n= 2 for WT and KK-EE and n=3 for A408T.

breakdown *in vitro* than the WT protein. This was not found to be the case when dynamin-1 KK-EE was expressed in human epidermoid carcinoma cells, A431 (section 6.6 figure 5B).

The mutation A408T was found to reduce actin binding in comparison to WT in this assay with averages of 22% ± 4.4 (SEM) percent found in the pellet after incubation with actin and 17.5% ± 5.5 (SEM) percent without actin (figure 3A and B). In order to compare all these results, the background sedimentation of dynamin-1 independent of actin was removed for each condition. This was done by taking the average percentage of dynamin in the pellet without actin and subtracting this value from the percentage pelleting after incubation with actin. The results are shown in figure 3C and indicate a significant difference (one way ANOVA F=3.99 d.f. 2,18 p 0.0394) between WT dynamin-1 and KK-EE. The A408T mutations causes a small decrease in co-sedimentation with F-actin, however the reduction is not statistically significant. In the future this experiment would require further repeats for validation, due to variation in results arising from the experimental method. However, these data do indicate a significant reduction in the ability of dynamin-1 to bind actin when the KK-EE mutation is present.

The next part of the study was to investigate the effects of actin binding mutations on the ability of cells to endocytose, migrate and form invadosomes. The study into the cellular effects of the A408T mutation was planned, however due to unforeseen circumstances delaying the creation of the A408T mutation in cell expression plasmids, along with the short time frame for this part of the study, only the KK-EE mutation was taken on for further investigation.

6.4 Identification of cell lines and expression system for dynamin-1 KK-EE study

6.4.1 Identification of cell lines used for dynamin-1 study

It is understood that dynamin proteins can function in cell processes including endocytosis, cell migration and invasion. During the Vps1 study (Chapter 3) the effects of the actin binding mutations on all functions of Vps1 were tested in order to identify if these mutations had a global or specific effect on Vps1 function *in vivo*. The study identified the RR457-8EE mutation as having a specific effect on endocytosis, but the orthologous mutation in dynamin-1 (KK-EE) may have a more global effect on dynamin-1 functions, which are not required in yeast, such as in cell migration and invasion. Therefore three cellular processes that require dynamin and actin function were identified for analysis in mammalian cells. These

processes were endocytosis, cell migration and invadosome formation. In order to test these processes two cell lines were chosen; A431 and MDA-MB-231 cells.

A431 cells are derived from a human epidermoid carcinoma (Giard et al. 1973) and are known to require actin for endocytosis when grown in solution (Fujimoto et al. 2000). Therefore these cells were chosen to investigate whether the KK-EE mutation effects actin-dependent endocytosis. Furthermore, A431 cells are known to be able to migrate and invade through tissues (Kao et al. 2008). This provides an opportunity to test the ability of these cells to migrate and invade when expressing the KK-EE mutation, and therefore further the understanding of the direct dynamin-actin interaction in cancer cell metastasis.

MDA-MB-231 cells are a breast cancer cell line (Cailleau et al. 1978) that have been previously used for 2D cell migration assays (Spence et al. 2012). This cell line is also known to form invadosomes when stimulated with Phorbol 12,13-dibutyrate (PDBu) a protein kinase C activator, unlike other breast cancer cell lines, such as MCF-7 (Goicoechea et al. 2009). Hence MDA-MB-231 cells were used to test the effect of the KK-EE mutation on single cell migration and invadosome formation experiments in the presence of dynamin-1 WT and KK-EE.

6.4.2 Overexpression of dynamin-1 in A431 and MDA-MB-231 cells

In order to address the effects of the dynamin-1 KK-EE mutation in cells, a transient overexpression system was used so that the overexpression of dynamin-1 dominates over the effects of dynamin-2 and 3 already present in the cell lines. This method was beneficial due to the speed in which cells could be analysed after transfection and the overexpression GFP plasmid (Pietro De Camilli, Addgene 22163) has also commonly used in other studies into dynamin-1 function in cells (Lee & De Camilli 2002). In future work the use of a double or triple dynamin knockout cell line would ideally be used, however this was deemed beyond the scope of this project.

6.5 Optimising the transient transfection of A431 cells

The electroporation method was selected for the transient transfection A431 cells, using the Neon® Transfection System, for its ease and reported high transfection efficiency (Brees & Fransen 2014). The correct electroporation conditions for A431 cells required selection and optimisation. In order to determine this, a test vector eGFP-N1 was utilised, following the 24 well optimisation protocol for adherent cells in the Invitrogen manual. As described in the protocol, the electroporation efficiency of 24 different conditions (see table figure 4) were tested and analysed. Following transfection, the cells were fixed and stained to allow counting of cells expressing GFP by fluorescence microscopy, and therefore the levels of

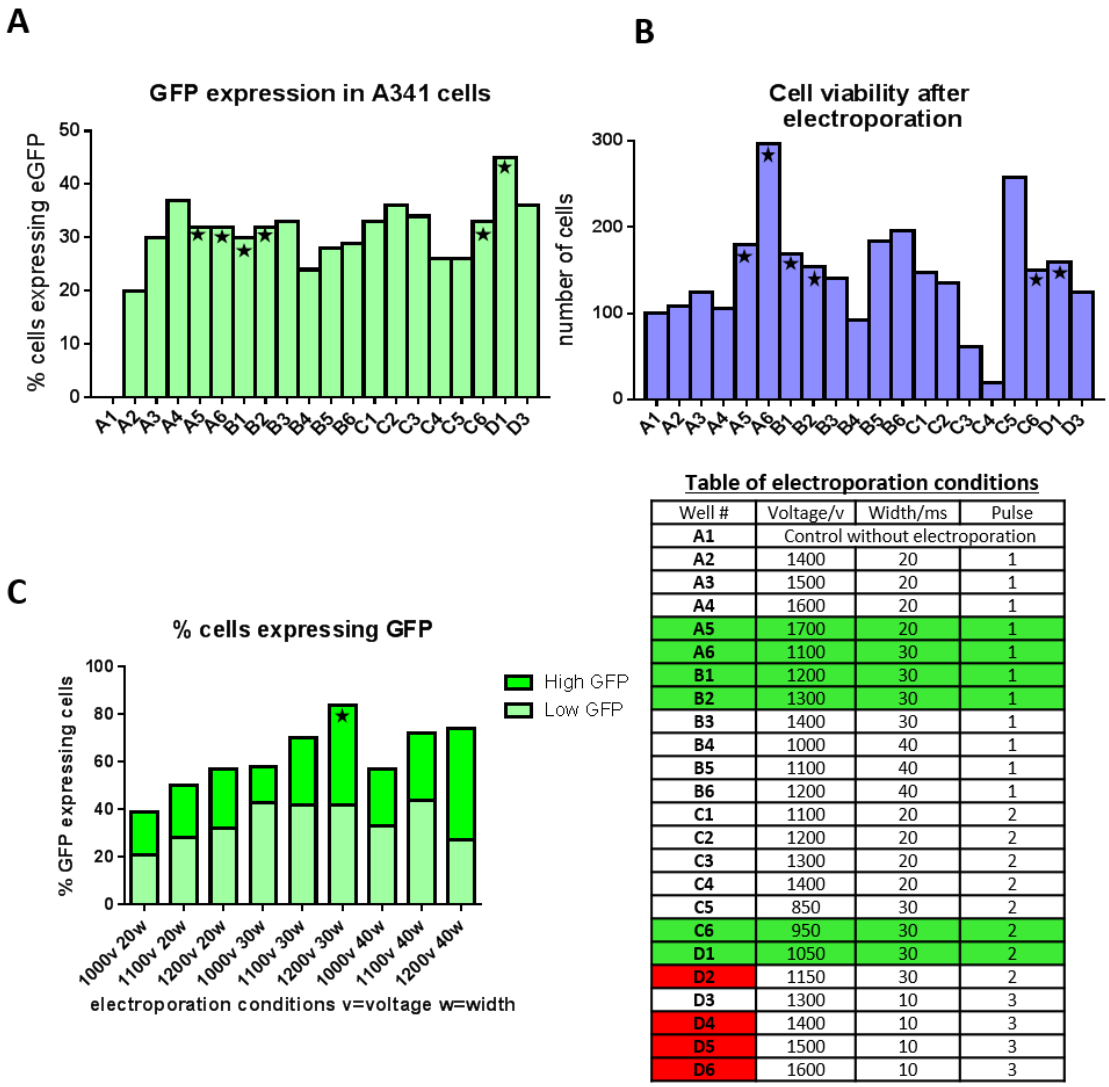

Table of electroporation conditions

Well #	Voltage/v	Width/ms	Pulse
A1	Control without electroporation		
A2	1400	20	1
A3	1500	20	1
A4	1600	20	1
A5	1700	20	1
A6	1100	30	1
B1	1200	30	1
B2	1300	30	1
B3	1400	30	1
B4	1000	40	1
B5	1100	40	1
B6	1200	40	1
C1	1100	20	2
C2	1200	20	2
C3	1300	20	2
C4	1400	20	2
C5	850	30	2
C6	950	30	2
D1	1050	30	2
D2	1150	30	2
D3	1300	10	3
D4	1400	10	3
D5	1500	10	3
D6	1600	10	3

Figure 4. Optimisation of electroporation conditions for A431 cells A) The percentage of GTP expressing cells in different condition. B) The total number of cells counted. Stars in A/B indicate conditions where over 150 cells were counted and the expression of GFP was over 30%. C) Further optimisation using a range of voltages and pulse width all with 1 pulse. Star indicates the chosen condition where over 80% of cells are expressing GFP. Table of conditions: favourable conditions are shaded green and correspond to stars in both figure A graphs. Conditions shaded in red indicate where very few cells survived electroporation and so were not included in the analysis.

transfection efficiency by fluorescence microscopy (figure 4A). Conditions D2 and D4-6 (see table figure 4) had very few live cells following electroporation and so were not included in the analysis as these would not be viable electroporation conditions for A431 cells. For all other conditions, over 150 cells were counted in 20-30 fields of view. In some conditions more cells were found per field of view in comparison to others and therefore the total number of cells counted for all conditions is also shown in figure 4B. The total number of cells indicates the toxicity of the conditions and the percentage of these cells expressing GFP indicates the transfection efficiency.

From the initial optimisation protocol, conditions that gave more than 30% GFP expression and at least 150 countable cells were considered. Upon comparison the selected conditions varied in efficiency but the highest GFP expression (marked as * figure 4A,B) was observed after electroporation with voltages in the range of 1000-1200, with 1 pulse, and pulse widths between 20-40 ms.

Using this data a subsequent round of optimisation was carried out in order to further identify the best electroporation condition for these cells. This re-tested the conditions selected in figure 4A and from this the most efficient condition was observed as 1200 v, 30 ms and 1 pulse, which gave a transfection efficiency of 80% (figure 4C). Interestingly, the highest percentage of cells expressing GFP in the first set of analyses was only 45%. This may be due to the experimental conditions, as with 24 different sets of electroporation conditions, cells would have been kept in solution for much longer before seeding onto a plate. The first analysis of all 24 wells also focused initially on brighter cells, owing to a high level of GFP expression (figure 4A) which could have resulted in missing cells expressing low levels of GFP which were taken into consideration during the second round of optimisation. In conclusion, after optimisation, the condition 1200 v 30 w and 1 pulse was selected for the transfection of A431 cells in subsequent experiments.

6.6 Expression of dynamin-1 WT and KK-EE GFP in A431 cells

Using the conditions selected in 6.5, WT and KK-EE human dynamin-1 in the eGFP-N1 vector (here after GFP-tagged dynamin-1 will be referred to as either WT or KK-EE) were transfected into A431 cells. After testing the electroporation of these constructs it was found that overexpression of dynamin-1 (WT and KK-EE) resulted in a large proportion of cell death in comparison to the empty GFP vector. This is expected with an overexpression system, although this has not been reported in other studies using the overexpression of dynamin proteins (Lee & De Camilli 2002; Altschuler et al. 1998), which may be due to differences in transfection technique. Future work would include additional optimisations of electroporation conditions for each construct separately.

A431 cells overexpressing GFP vector, WT dynamin-1 and dynamin-1 KK-EE GFP were live cell sorted with a flow cytometer (chapter 2 section 2.6.5). This was done in order to select for transfected cells only to carry out a scratch wound assay (section 6.9.1) however it also gave an indication of the proportion of cells that were transfected with dynamin-1 WT and KK-EE. In each case 1-2x10^6 cells were electroporated for A431 untransfected and GFP vector and at least 4x10^6 cells with WT or KK-EE. As seen in figure 5A there are very few sorted cells that

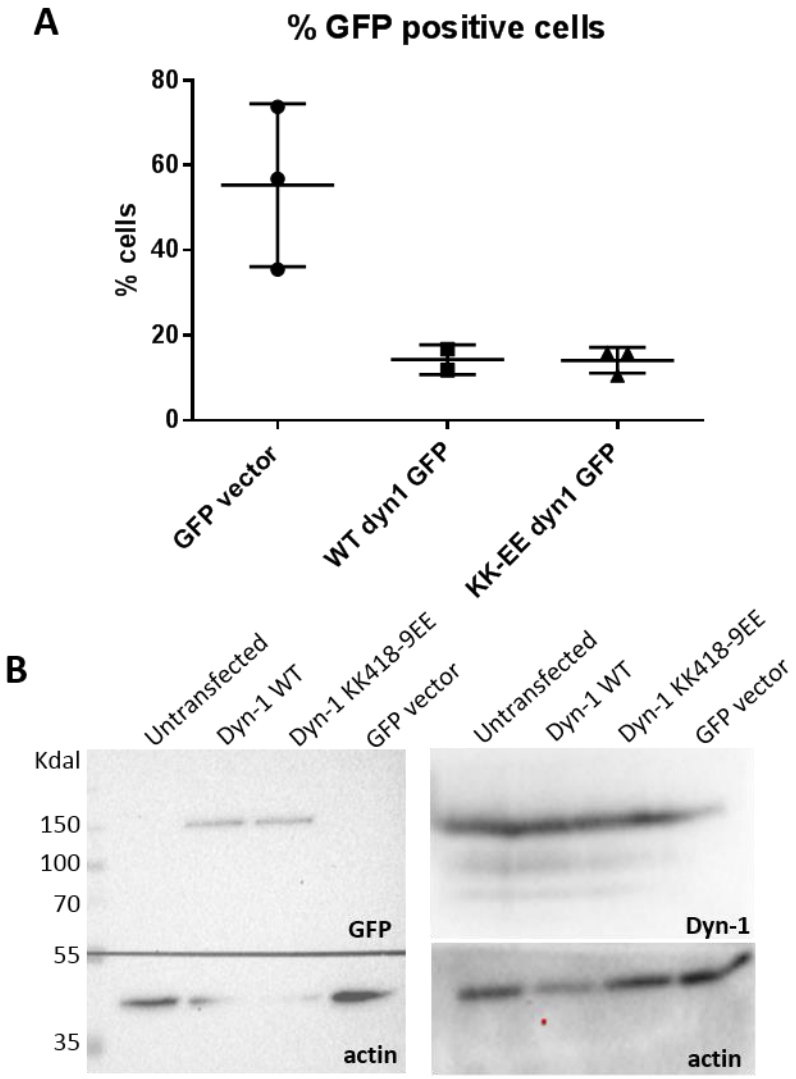

Figure 5. The expression of GFP tagged Dynamin-1 in transfected A431 cells. A) The percentage of cells expressing GFP was recorded after a live cell sort of transfected A431 cells. Error is SD. Each point indicates one experiment n=3 for GFP and KK-EE and n=2 for WT. B) The western blot on left shows whole cell lysates of A431 with or without transfection with GFP vector Dyn-1 WT or Dyn-1 KK-EE probed with anti GFP antibodies. Below is actin loading control and note less actin probed in middle two lanes probably due to defective transfer or antibody probing. The same samples were run again for the western on the right which was probed with anti dynamin-1 antibodies and below actin is the loading control. Note higher exposure for actin than dynamin antibodies as the latter are more sensitive and the signal became overexposed rapidly.

are expressing the dynamin-1 GFP vectors in comparison to the vector alone. For A431 cells transfected with the GFP vector, the mean percentage of cells expressing GFP was 55.36 % from three sorts, compared with 14.27 % for WT (2 sorts) and 14.11 % for KK-EE (3 sorts). From these data it was clear that very few cells survive transfection with dynamin-1 constructs, and this would have an impact on future experiments.

A separate observation to also note is that, in some cases, the A431 cells overexpressing dynamin-1 WT seemed to be less viable than cells overexpressing KK-EE. This is perhaps due to a loss of activity caused by the KK-EE mutation (which could be linked to a reduced actin binding ability) which may impact the cells less than the overexpression of fully functional dynamin-1 WT. The *in vitro* work (figure 3A) suggested that the KK-EE mutation causes dynamin-1 to become more susceptible to proteolysis, as indicated by the presence of truncated bands after the purification. Therefore, the reason that KK-EE may be less toxic to A431 cells could also be because it breaks down in the cells as readily as *in vitro*. To test this, a western blot of transfected A431 whole cell lysates was analysed with both anti-GFP antibodies and anti-dynamin-1 antibodies. As seen in figure 5B a band is present at the 150 kDa position in both anti-GFP and dynamin blots, indicating that the GFP is fused to the dynamin constructs. These results indicate that any breakdown of dynamin-1 is not enhanced by the presence of the KK-EE mutation, suggesting that breakdown of the KK-EE dynamin-1 seen *in vitro* is not taking place in A431 cells. Therefore any potential reduction in overexpression toxicity may be due to a reduced actin binding ability of the protein.

6.7 Rhodamine phalloidin staining of A431 cells

Despite the low viability of A431 cells expressing dynamin-1 WT and KK-EE, this project continued with the assessment of the effects of the KK-EE mutation in cells. To begin with, the organisation of the actin cytoskeleton was assessed. This was chosen as a previously published study into the direct dynamin-actin interaction reported that the abrogation of actin binding by dynamin caused a reduction in the number of stress fibres in podocyte cells (Gu et al. 2010). Therefore, there was a possibility that the actin cytoskeleton in A431 cells would be affected by the charge mutation KK-EE.

In order to visualise the actin cytoskeleton, transfected A431 cells were fixed and stained with rhodamine-phalloidin (chapter 2 section 2.6.6). Initial investigations indicated that mock-transfected A431 cells do not have a well-defined stress fibre morphology but do show strong cortical actin staining (arrows figure 6). When compared with cells overexpressing dynamin-1 WT and KK-EE, there seemed to be little observable difference between the actin morphologies and this may be due to the cell type. A431 cells can migrate and are invasive and this requires a dynamic actin cytoskeleton. It could be that the formation of stress fibres in A431 cells are more transient than in other cell types that require stress fibres for function, such as kidney podocytes. Podocytes have well-defined actin stress fibres to aid in withstanding pressure surrounding the kidney glomerulus. In future investigations the use of non-cancer cell lines, such as podocyte cells should also be used to address any changes in

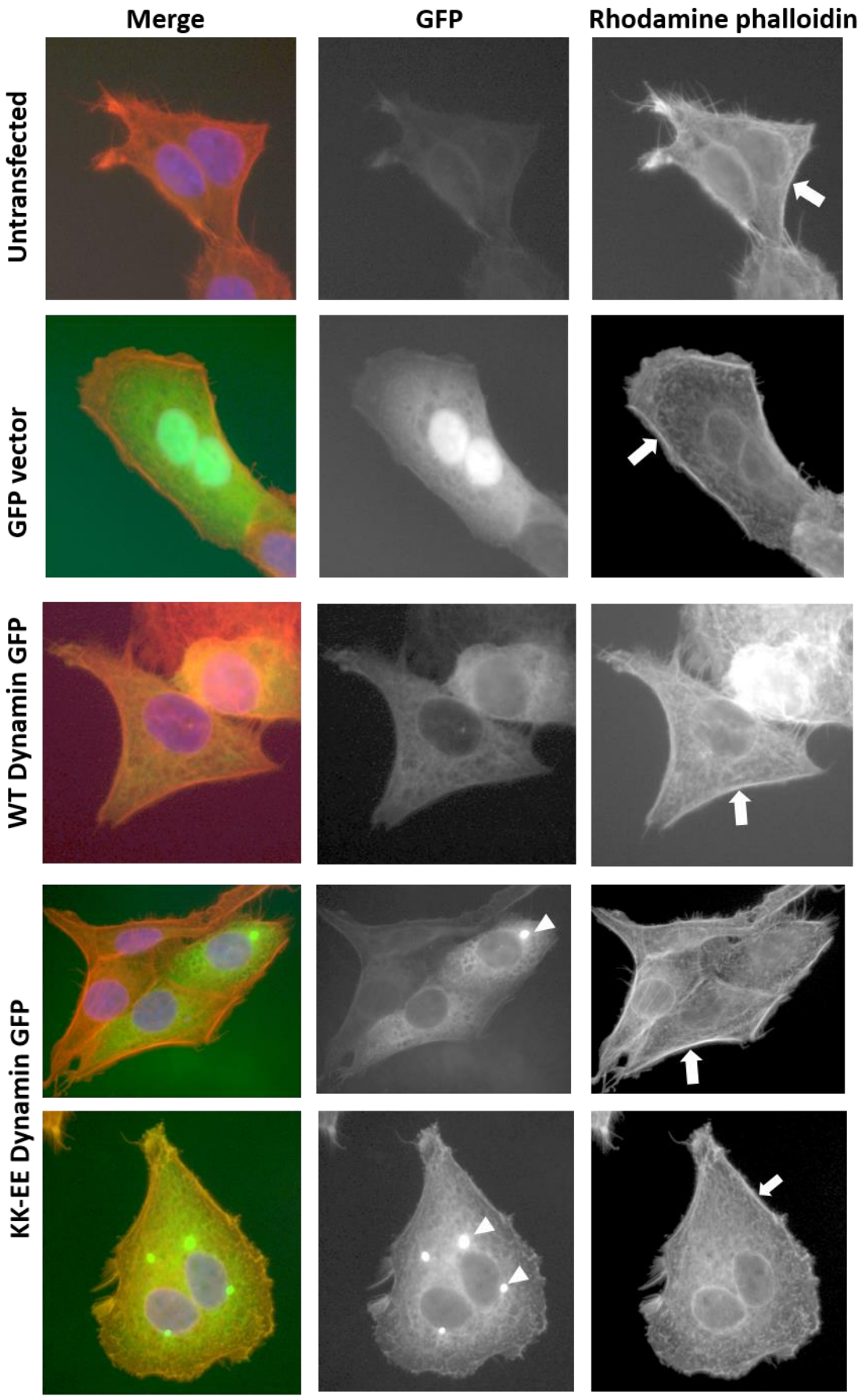

Figure 6. Rhodamine Phalloidin staining in transfected A431 cells. These images show examples of transfected A431 cells measured for size and area. Arrows indicate cortical actin staining, arrow heads indicate accumulations of dynamin-1-GFP.

actin stress fibre morphology caused by the KK-EE mutation. There were some bright accumulations observed in cells expressing dynamin-1 WT and KK-EE and these were assumed to be caused by accumulation and degradation of the proteins in the lysosome in response to overexpression (arrowheads figure 6). In order to test this possibility, these cells could be co-stained with a lysosomal marker, such as LysoTracker® (Thermo Fisher), in future experiments to see if the overexpression is causing dynamin-1-GFP to be trafficked to the lysosome for degradation.

Whilst imaging the A431 cells the appearance of larger cells seemed to be more prevalent in cells overexpressing the dynamin-1 KK-EE mutation. Therefore, the average cell size and longest cell length were also assessed for each transfection condition. Interestingly, the average cell area in cells expressing WT and KK-EE was significantly larger than mock-transfected A431 cells or cells expressing the empty GFP vector (one way ANOVA $F=11.98$ d.f. 3,132 $p<0.0001$) (figure 7A). There was, however, no difference between the averages of longest cell length measurements (p 0.1236) (figure 7B). Therefore the overexpression of WT and KK-EE dynamin-1 increases the average cell size but this does not increase cell length. This suggests that the overexpression of dynamin-1 may have an effect on cell spreading or cell adhesion.

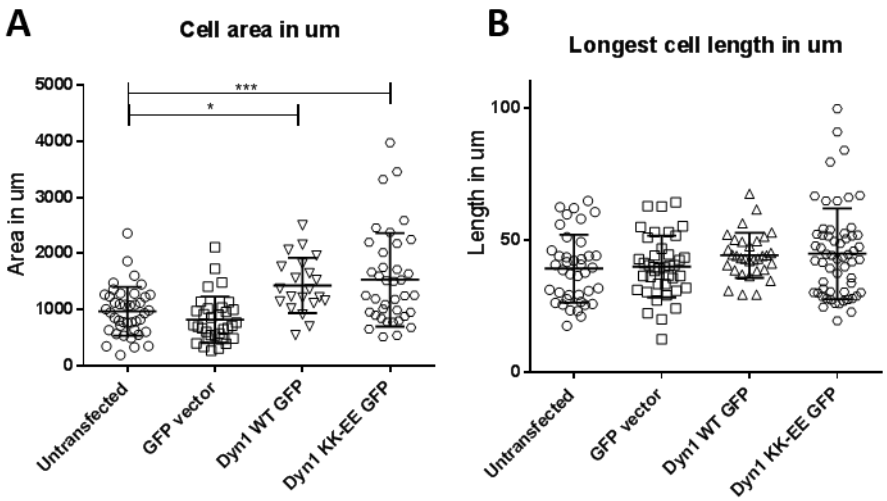

Figure 7. A431 cell morphology. A) Graph indicates total cell area data collected from ImageJ pixel analysis. There is a significant increase in the total cell area between Untransfected and WT as well as between untransfected and KK-EE expressing cells (one way ANOVA $F=11.98$ d.f. 3,132 $p<0.0001$). B) Graph indicates longest cell length in these cells. This shows no significant difference between the cell types (one way ANOVA p value 0.1236).

6.8 Transferrin uptake in A431 cells overexpressing dynamin-1

It is reported that A431 cells require actin for endocytosis when grown in suspension (Fujimoto et al. 2000). Therefore an uptake assay was undertaken with a fluorescently-labelled transferrin to analyse the effects of the dynamin-1 KK-EE overexpression on endocytosis.

Traditional transferrin uptake assays investigate the uptake of a fluorescently-labelled transferrin over time. The easiest way to do this is via an ELISA assay (Hopkins & Trowbridge 1983; Smythe et al. 1994). This assay was tested but the total number of transfected cells after live cell sorting was not high enough for this method of large scale transferrin uptake analysis (personal communication Prof. Elizabeth Smythe laboratory). Similarly, as endocytosis in A431 cells has only been found to require actin when the cells are in solution, a microscopy experiment would also not be a high enough throughput method to assess a predicted reduction, rather than prevention, of transferrin uptake. Therefore fluorescence-activated cell sorting (FACS) analysis was utilised to examine large numbers of cells, and therefore changes in levels of fluorescence, that would be difficult to quantify by traditional microscopy techniques.

Adherent transfected cells were removed from the plate surface, washed, and then incubated with fluorescently labelled transferrin for 10 minutes in suspension. The cells were then washed in a low pH glycine buffer to remove surface bound transferrin (Semerdjieva et al. 2008), (chapter 2 section 2.6.4) so as to only assess transferrin uptake into the cell cytosol. Cells were first sorted and analysed for cell size and granularity and the data was gated to remove doublet, dead and degraded cells. Next the transferrin-568 conjugate (Molecular probes) fluorescence and GFP fluorescence were gated separately and the cells analysed. An example of the fluorescence captured in the red channel, including gating parameters, is shown in figure 8. This was repeated on two separate occasions and the median fluorescence of transferrin-568 conjugate plotted in figure 9A,B. The median fluorescence is always chosen over the mean due to the results being collected in Log_{10}. The median transferrin fluorescence was also tested on two separate occasions in untransfected A431 cells and these data were combined with the gated untransfected populations measured during the GFP, WT and KK-EE FACS analyses. As seen in figure 9B there is very little difference between transferrin uptake in GFP, WT and KKEE dynamin-1 expressing cells and any differences between them are not significant (p 0.3821). For all conditions the GFP-positive cells are higher in transferrin fluorescence than untransfected cells (one way ANOVA F=17.19 d.f. 3,12 p 0.0005). One possibility for this is that there is bleed through of the GFP fluorescence into the red channel

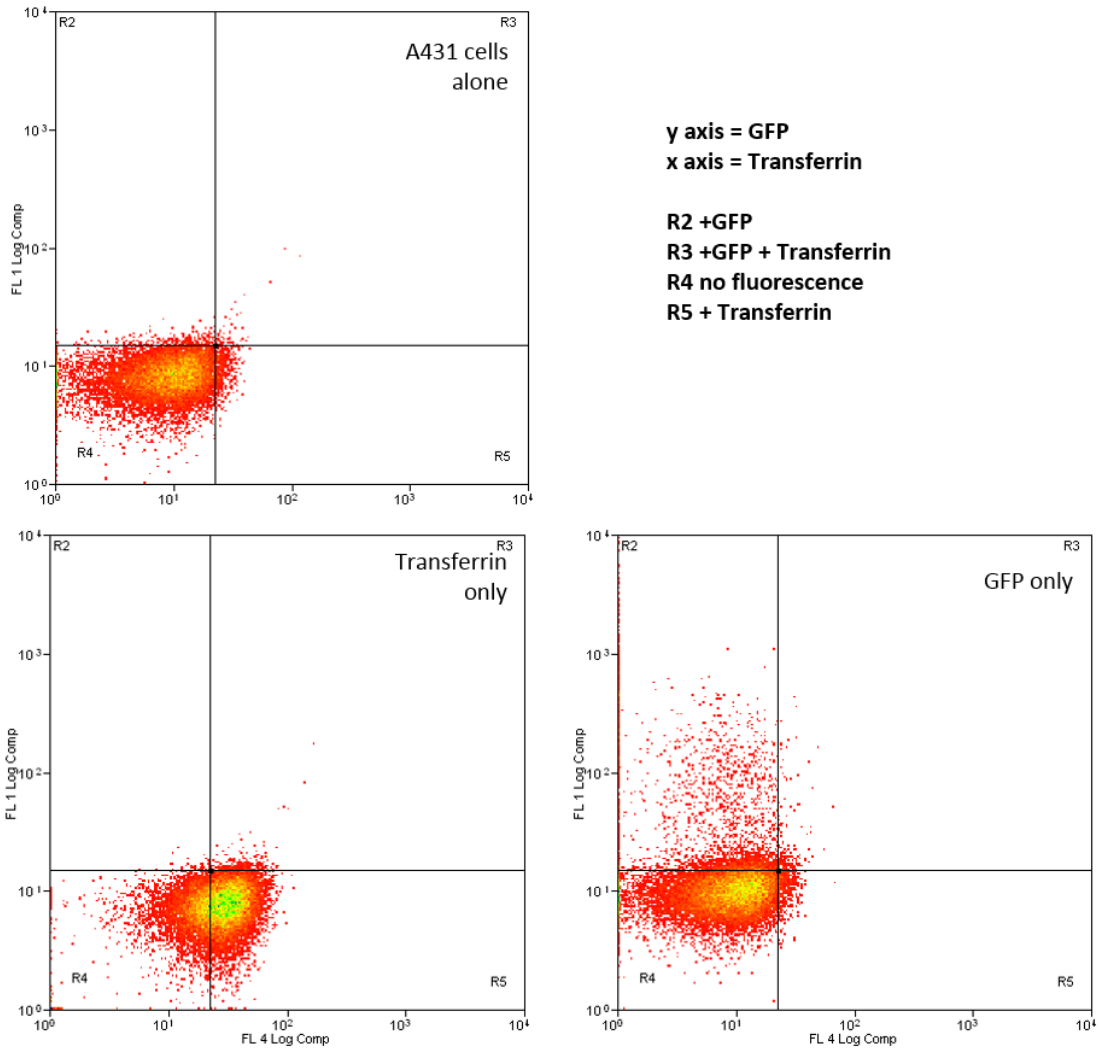

Figure 8. Example of gates for transferrin uptake analysis by FACs. After removal of small or doublet cells A431 cells are gated for fluorescence. As the key suggest x axis is red transferrin fluorescence and y axis is green GFP fluorescence. From these red and green have been gated for further analysis of the effects of overexpression dynamin-1 constructs.

causing a higher fluorescence readout. Otherwise the cells may have a higher metabolic rate and take up more transferrin due to the overexpression of GFP or dynamin-1.

Future work would require further repeats of these experiments to be carried out with repeats at earlier and later time points to follow the course of transferrin uptake. Furthermore, by reducing the temperature of the assay, endocytic uptake in the cells would be slowed down and therefore any differences in transferrin uptake may be more accurately assessed. These results suggest that transferrin uptake is not affected by the presence of the KK-EE mutation in dynamin-1. Transferrin is classically thought of as a marker of CME (Harding et al. 1983) however there are other methods of endocytosis as described in the introduction (section 1.1). Further investigations into the effects on the uptake of other receptors such as G-protein coupled receptors (GPCR) receptors and epidermal growth factor receptor (EGFR)

would be interesting in order to fully characterise the effects of the KK-EE mutation on endocytosis. Due to time constraints these assays were deemed beyond the scope of this project.

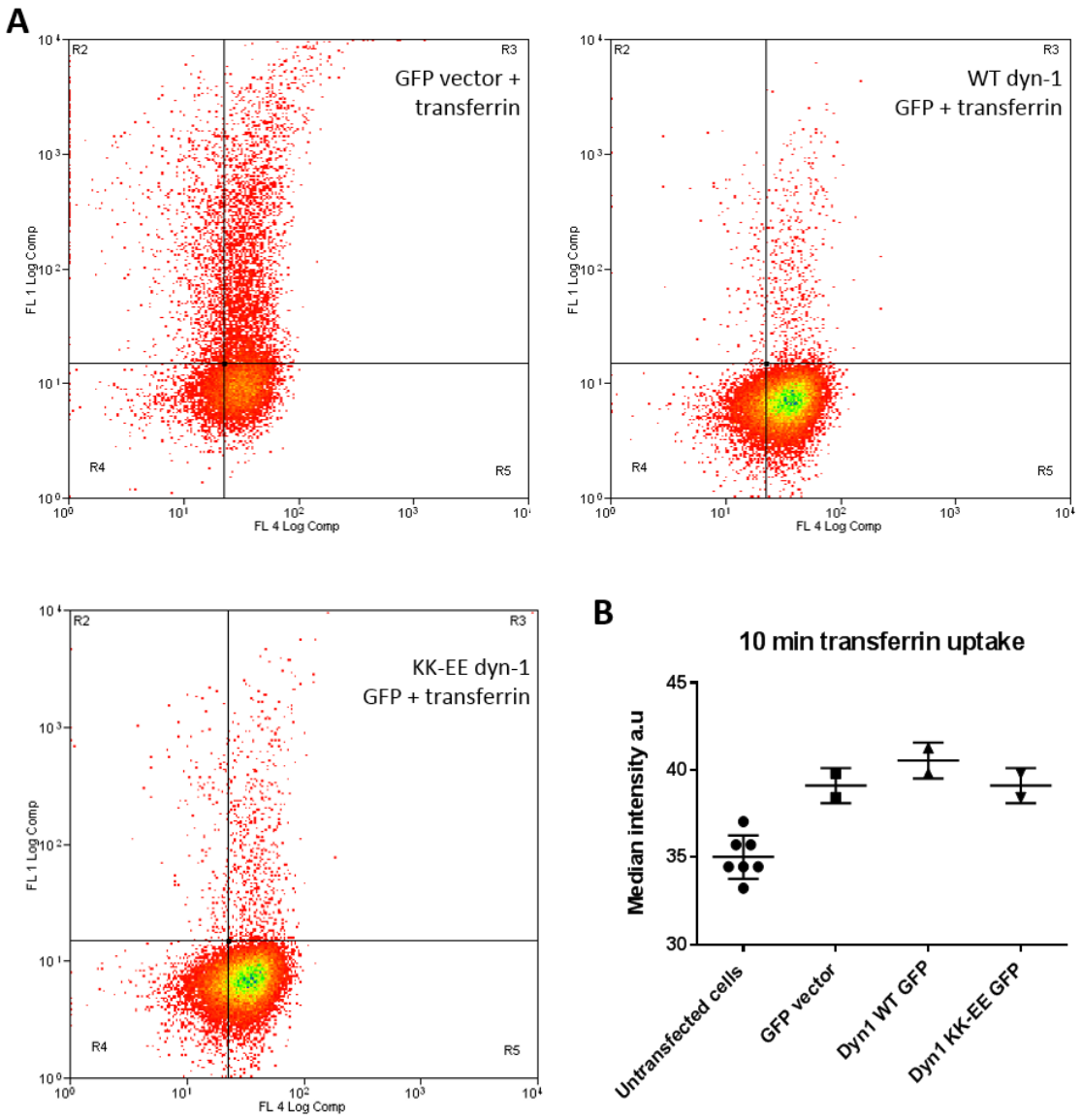

Figure 9. Overexpression of dynamin-1 on transferrin uptake in A431 cells A) Examples of FACs readouts for transferrin and GFP fluorescence with GFP vector, Dyn-1 WT GFP and Dyn-1 KK-EE GFP. X and y axis are red and green fluorescence respectively. R2 is green fluorescence R3 green and red, R4 non fluorescent cells and R5 green fluorescence only. B) Read out for median fluorescence after 10 minutes transferrin uptake in solution.

6.9 Testing the effects of overexpressing dynamin-1 WT and KK-EE on cell migration

6.9.1 A431 scratch wound cell migration assay

Dynamin is thought to function in a number of different cellular processes directly or indirectly with actin to modulate migration. Most studies to date have focused on dynamin-2 for example, dynamin-2 can indirectly interact with actin through binding cortactin to regulate actin filaments and growth factor induced circular ruffles which are involved in advancing the leading edge (Mooren et al. 2009; Schafer et al. 2002; McNiven et al. 2000). This could be orchestrated by a direct dynamin-2-actin interaction, and it has been shown that mutations to the actin binding site reduce the ability of dynamin-2 to function in the formation of lamellipodia and cell spreading (Menon et al. 2014). The inhibition of dynamin-1 and -2 by siRNA depletion and inhibitors, such as dynasore (Macia et al. 2006) and myristyl trimethyl ammonium bromide (miTMAB™ Abcam), has been reported to reduce 2D migration and transwell Matrigel® (Corning) invasion in cancer cells (Eppinga et al. 2011; Yamada et al. 2009). Interestingly, by mutating the region involved in the direct interaction between dynamin-1 and actin it was found that filopodia formation was reduced in murine NIE 155 neuroblastoma cells (Chou et al. 2014) suggesting a direct role for the dynamin-1-actin interaction in cell migration.

Therefore, with the KK-EE mutation reducing actin binding *in vitro* and modulating A431 cell size, it was considered appropriate to test if this mutation, and indeed the overexpression of WT dynamin-1, has an effect on cell migration. To do so, a scratch wound assay was chosen as this has been analysed previously with A431 cells (Draper et al. 2003). A scratch wound assay is a pseudo-chemoattractant assay where a confluent monolayer of cells are grown and then a scratch is made within the layer of cells creating a 'wound' into which cells migrate over time. In order to achieve this, transfected A431 cells were live cell sorted and GFP-expressing cells were seeded at a density to form a confluent cell layer. Cells were then allowed to fully adhere and spread before the start of the assay. As the cells were still mitotically active in this monolayer, cell division reduced the number of transfected cells more significantly than was expected (figure 10A).

Despite these difficulties, the speed of wound closure was analysed as it was hypothesised that the mixed populations of cells would still exhibit altered rates of wound closure despite the low numbers of transfected cells. For each experiment five different areas along the leading edge were taken as a starting point from which the movement of the cells was measured and calculated as a speed of movement per μm distance. In the mixed population movies the areas selected were as close to transfected cells along the leading edge

as possible. There was a significant decrease in cell front movement speed between the untransfected and dynamin-1 WT overexpressing populations seen in figure 10B, however this was also found in the population of cells expressing GFP vector (one way ANOVA $F=10.14$ d.f. 3,49 $p<0.0001$). This difference may indicate that the overexpression of both GFP and WT dynamin-1 have a negative impact on cell migration. The overexpression of dynamin-1 has been found to be toxic to cells and this may be due to its effect on critical cell functions involving the actin cytoskeleton. This negative effect on cell migration seems to be reduced when the KK-EE dynamin-1 mutation is expressed. This could be due to its inability to bind actin, thus diminishing the negative effects of overexpression during cell migration. However this reduction in movement is also seen with the GFP tag expressed alone. As GFP is unlikely to affect cell migration in this way, it is possible that this result is due to the low number of technical repeats, owing to time limitations and further repeats would be required to elucidate if these speculations are true.

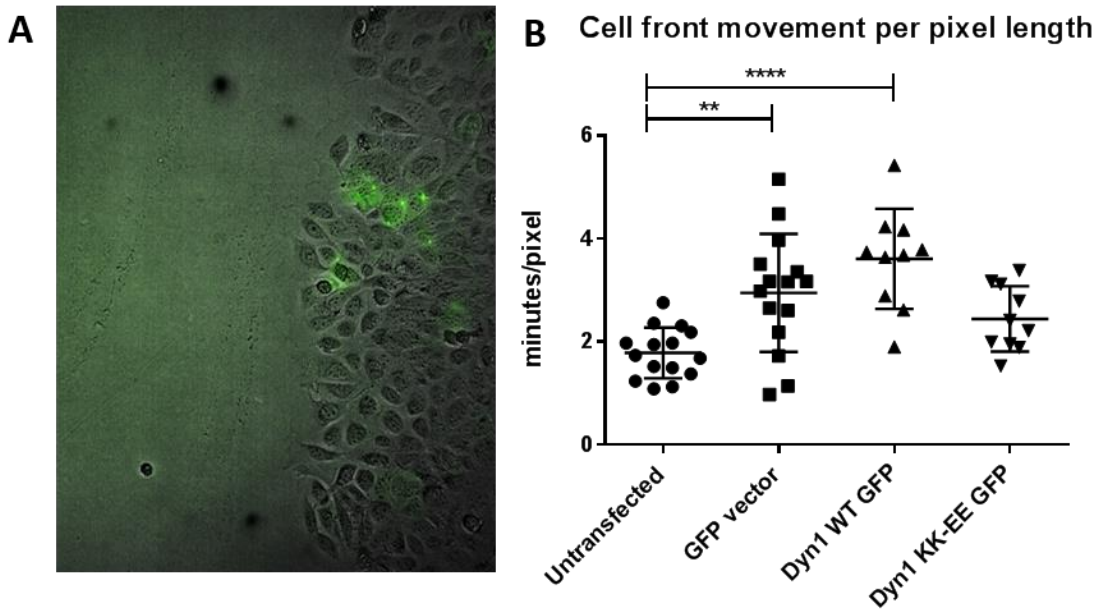

Figure 10. Scratch wound assay with transfected A431 cells A) Example of an image of view at the start of the assay with only a small percentage transfected with dynamin-1 WT GFP. B) Calculated cell speed of the leading edge of cells. Five measurements were taken per movie and they show an in increase in speed when cells have dynamin-1 WT overexpressed or GFP vector.

There is a chance that, within the monolayer, the transfected cells are moving differently towards the leading edge which, if tracked, could provide evidence for how the overexpression of dynamin-1 WT and KK-EE are affecting cell migration. Therefore, selected single cells were tracked and plotted to analyse the overall directionality of movement, as well as average velocity and overall distance travelled. When the tracked cell movements are plotted with the wound as the y axis the vast majority of cells move towards the left side of the graph (figure 11A) as expected. When compared, none of the conditions showed any significant differences in distance travelled (figure 11C) (one way ANOVA p value 0.7817) or velocity of movement (data not shown, one way ANOVA p value 0.0817). However, A431 cells transfected with GFP or KK-EE have a significantly reduced directionality of movement compared with untransfected cells (figure 11B) (one way ANOVA F=5.438, d.f. 3,54 p 0.0025). Indicating that the overexpression of dynamin-1 KK-EE causes cells to be less able to move consistently in one direction. However, this is also seen when GFP is overexpressed which may indicate that this is an artefact or that high expressions of GFP also reduce a cells directionality of movement. The WT single cell tracks seem to show a more varied cell movement (figure 11A) suggesting the overexpression of WT may have more of a detrimental effect overall in cells in comparison to the KK-EE mutation. It is tempting to speculate that the KK-EE which reduces actin binding may negatively impact lamellipodia formation specifically, however the toxicity of the WT overexpression has a more global effect. The plotted tracks of A431 cells expressing dynamin-1 WT seem to move in more random directions than untransfected cells, however this observation is not reflected in the average directionality of these tracked cells. It should also be noted that many of the tracked cells were behind the leading edge and their movement may well be affected by the untransfected cells that surround them. These results may be different if the cells were in a monolayer of transfected cells only. This experiment requires further experiments and repeats to verify any of the observations made at this stage however they do suggest that the overexpression of the KK-EE mutation is affecting A431 cell migration.

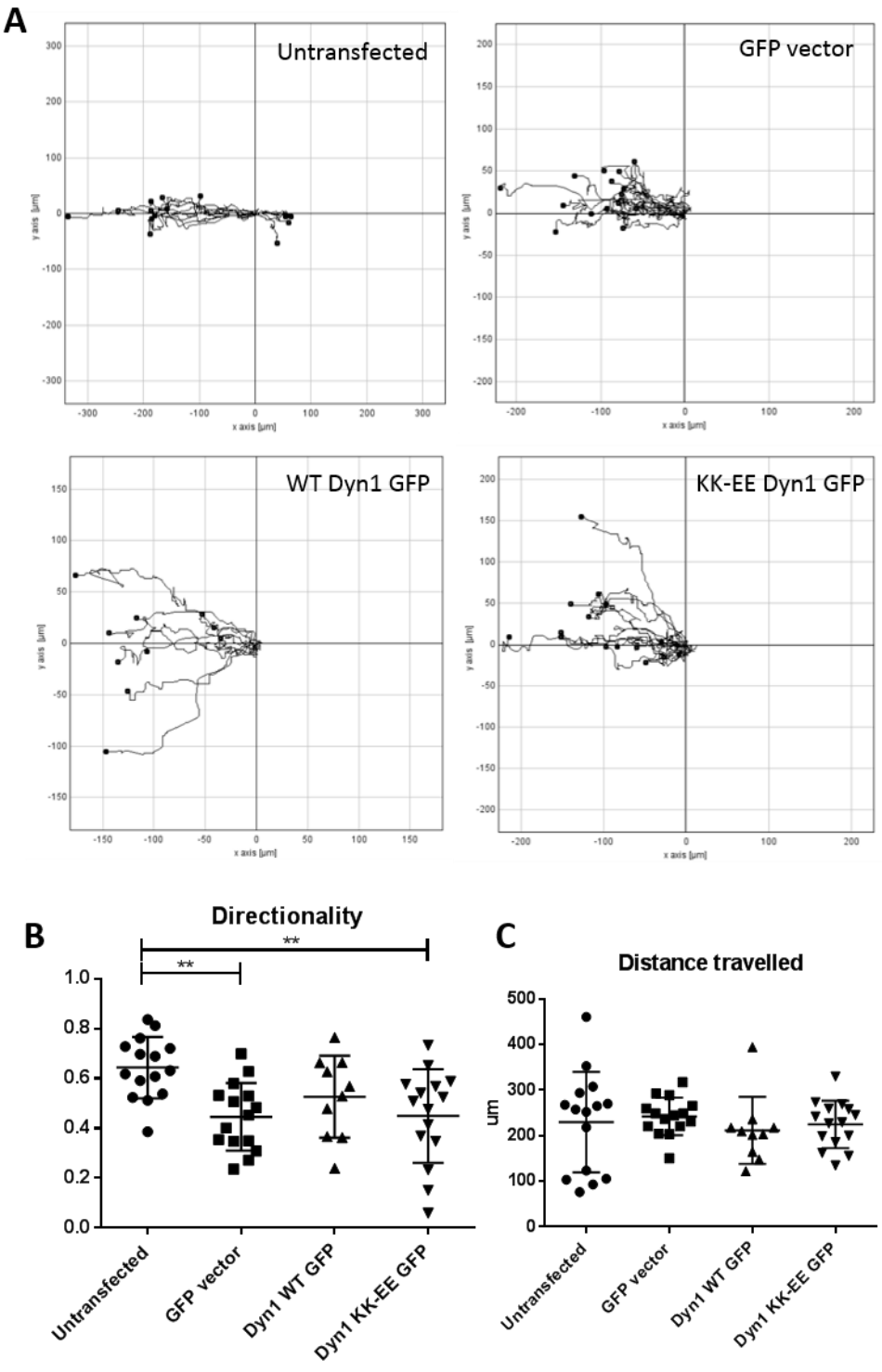

Figure 11. Single cell analysis from scratch wound assay data. A) Single A431 migrations overexpressing GFO, WT and KK-EE. Negative x value indicates movement towards the wound. B) Directionality of single cell movements with significance calculated via one way ANOVA test. C) distance of all tracked single cells and any differences in total distances travelled are not significant overall.

6.9.2 MDA-MB-231 single cell migration assay

During this part of the study the use of the A431 cell line came into question. A431 cells were selected for their requirement for actin during endocytosis. As A431 cells are also cancer cells it made sense to analyse them in a migration assay as well as for their ability to take up transferrin. During these analyses it became clear that this cell line harbours some multinucleated cells which could affect the formation of invadosomes in these cells making them difficult to study. Secondly when tested in single cell migration assays (data not shown) A431 cells did not migrate far enough for the cell movements to be effectively tracked. There is a possibility that the migration of these cells require a chemo-attractant or that this migration assay requires further optimisation, however it was deemed more time efficient to select a cell line that was well documented in its ability to migrate in a 2D migration assay. Therefore the MDA-MB-231 cell line was used for the remaining assays during this project.

The scratch wound assay gives an indication as to how the overexpression of WT and KK-EE effects the wound closure of a monolayer of cells. However, in this pseudo-attractant assay it was difficult to analyse single cell movements due to there only being a small number of transfected cells within the confluent monolayer. In order to test how the WT and KK-EE affects the movement of single cells a migration assay was chosen in which sparsely seeded and transfected MDA-MB-231 cells were tracked over time. MDA-MB-231 cells were transfected by electroporation and seeded on to fibronectin covered dishes at least six hours before live cell imaging. The cells were then transferred to a heated microscope chamber and cell images were recorded every 5 minutes for 16 hours. The movies were then analysed by tracking individual cells and plotting their movement on a graph with each starting point normalised to zero (figure 12A). Analysis and graph creation was carried out using the chemotaxis tool in ImageJ (Ibidi). This experiment analysed cells from three technical repeats, and therefore a more detailed analysis with at least three more independent experiments would be required for a more robust study of the effects of dynamin-1 KK-EE on single cell migration.

MDA-MB-231 cells did migrate as expected on the fibronectin covered plate (chapter 2 section 2.6.10) and could be tracked easily. However, the overexpression of dynamin-1 WT and KK-EE was toxic to many cells, similar to what was observed when using the A431 cell line. Due to time limitations the full optimisation of the MDA-MB-231 cell transfection was unable to take place however the experiment did yield a number of transfected cells that were able to migrate and these were tracked and analysed.

Observation of the plotted cell migration paths (figure 12A) suggest some differences between the cell conditions. For example, the tracked cells overexpressing dynamin-1 WT seem to cover a smaller area than untransfected, KK-EE or GFP expressing cells which is similar

to the A431 results. This could suggest that the WT is having more of a detrimental effect on MDA-MB-231 cell migration than the KK-EE. This indicates that the overexpression of dynamin-1 WT reduces the ability of cells to migrate whereas the overexpressed dynamin-1 KK-EE, due to a loss of actin binding ability, has less of a detrimental effect on MDA-MB-231 cell migration.

If the migration of MDA-MB-231 cells was being hindered by the overexpression of dynamin-1 WT the overall distance each cell has travelled and their velocity should be reduced in comparison to untransfected cells. To test this, the total distance each cell moved was analysed using the chemotaxis tool (Ibidi). This indicated that cells expressing GFP vector, dynamin-1 WT and KK-EE move significantly further than untransfected cells (figure 12B, one way ANOVA F=6.091 d.f. 3,39 p 0.0018). This suggested that the overexpression of dynamin-1 WT and KK-EE were both increasing the ability of cells to migrate despite the pattern of cell tracks for dynamin-1 WT suggesting a reduction in area covered by the cells. There was also an unexpected increase in the total distance travelled by MDA-MB-231 cells overexpressing GFP. This was reflected, as expected, in the overall velocity of cells where overexpression of dynamin-1 WT, KK-EE and GFP vector had a significantly higher velocity than that of untransfected MDA-MB-231 cells (data not shown, one way ANOVA F=6.045 d.f. 3,39 p 0.0019). This may suggest that an overexpression of a GFP tag alone affects MDA-MB-231 cell migration. Other explanations include the fact that this experiment wasn't fully optimised to double check how many cells survived the transfection and therefore were alive during the live cell imaging. It is probable that there were more untransfected cells per well and the cell density may well reduce single cell migration distance and therefore overall distance and velocity. This experiment would have to be repeated and optimised for a more thorough investigation into the effects of dynamin-1 KK-EE on MDA-MB-231 cell migration.

Overall, cells migrating in this assay would have infrequently come into contact with other cells and no chemo-attractants were present in the media. Therefore, it makes sense that cells would not always travel in one direction, but move randomly around the space. As a result any increase in directionality (Euclidean distance divided by total distance accumulated) may suggest an inability of a cell to change direction. MDA-MB-231 cells transfected with KK-EE have a significantly higher directionality of movement in comparison to GFP vector alone (figure 12C, one way ANOVA F=3.49 d.f. 3.39 p 0.0253). As the effect of KK-EE was only significant when compared to cells overexpressing GFP, it suggests the GFP is having an unexpected effect on the ability of MDA-MB-231 cells to migrate in a single direction. This result seems to suggest an anomaly arising due to the low number of repeats that were collected. However, if this is indeed a result that can be verified, it may suggest that the ability of dynamin to bind actin is required for investigative cell movements into new areas resulting

in a direction change. This hypothesis is supported by a recent report suggesting that mutations to the actin binding site of dynamin-1 can impair the formation of filopodia (Chou et al. 2014).

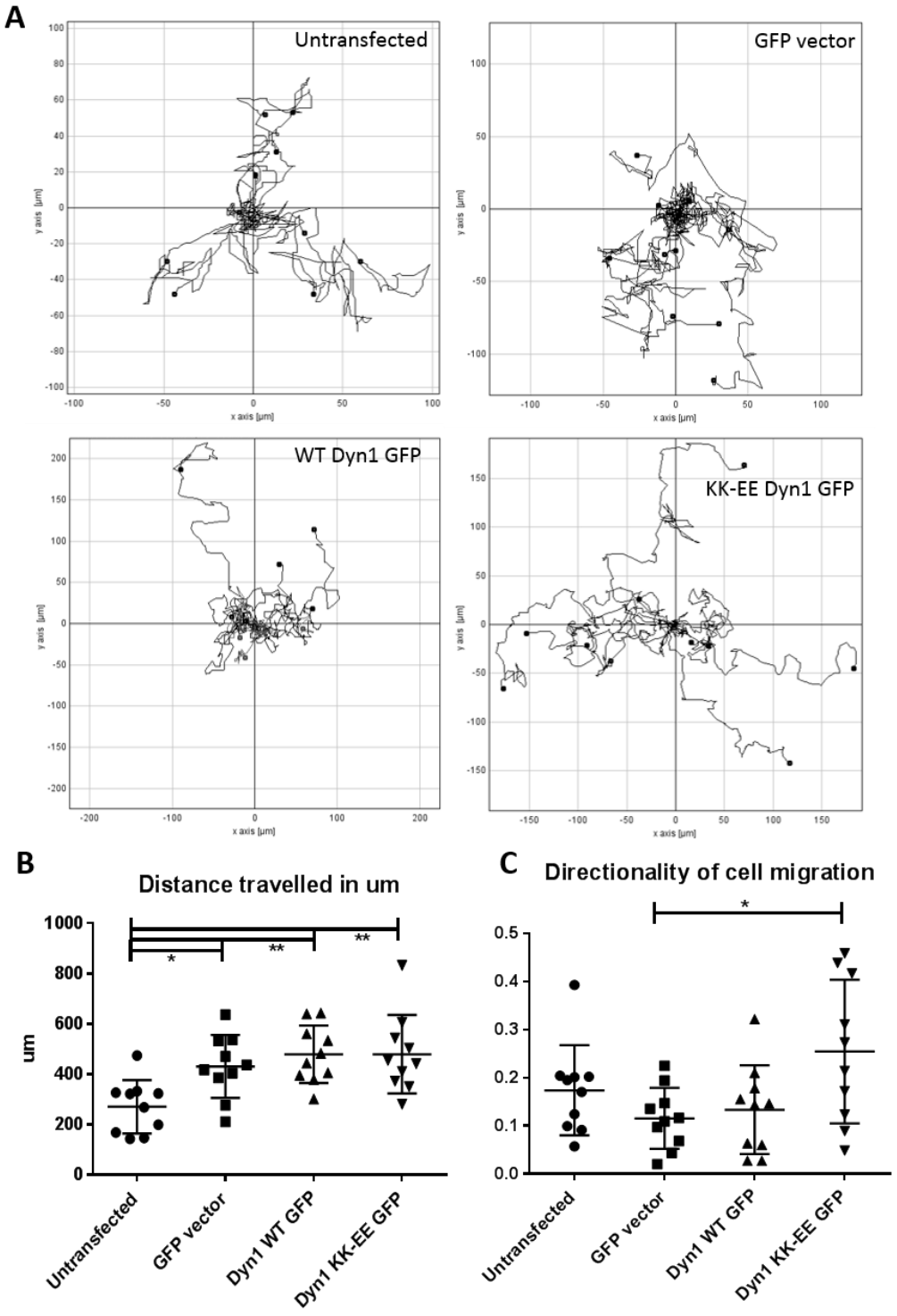

Figure 12. MDA MB 231 single cell migration assay A) Single cell migrations plotted with each starting point normalised to zero. B) Indicates the distance each cell track covered. This indicates a significant increase in overall distance covered by cells expressing GFP vector, Dyn-1 WT and Dyn-1 KK-EE in comparison to untransfected cells (ANOVA F=6.091 d.f. 3,39 p 0.0018).C) Directionality from the migration patterns shown in A indicating the Dyn-1 KK-EE has a significant increase in directionality than GFP expressing cells (ANOVA F=3.494 d.f. 3,39 p 0.0253). Both B and C were calculated using ImageJ plugin Chemotaxis tool (Ibidi).

6.10 MDA-MB-231 PDBu stimulated invadosome formation

A final part to this investigation was to test the ability of MDA-MB-231 cells to form podosomes and invadopodia (collectively named 'invadosomes') in the presence of dynamin-1 KK-EE. Invadosomes are actin rich structures created for the adhesion to and degradation of extracellular matrix. They can form alone or combine to form actin rosettes (reviewed in Linder 2009) therefore actin rich puncta are thought to be associated with the presence of invadosomes. In order to study these structures, MDA-MB-231 cells were transfected with each construct and then stimulated with PDBu to form invadosomes. The cells were then fixed and stained for actin with rhodamine phalloidin. Dual staining of actin with cortactin, used as a marker of invadosomes (Génot & Gligorijevic 2014), was attempted to confirm that the observed actin puncta were indeed invadosomes. However, due to technical issues this approach could not be sufficiently optimised. In future studies it will be imperative to analyse the co-staining of actin with invadosome markers to confirm that the observed actin puncta are indeed invasive cellular structures. It would also be important to verify the invasiveness of these structures either by analysing the breakdown of a fluorescent form of Matrigel, or by testing the invasion of the cells through Matrigel using a Boyden chamber (Kao et al. 2008).

The staining of actin by rhodamine phalloidin indicated co-localisation between actin puncta and dynamin-GFP constructs thought to be invadosome structures (figure 13). For all conditions there are no differences in the number of cells displaying actin puncta or rings (figure 14) suggesting that the overexpression of dynamin-1 WT or KK-EE has no effect on the formation of invadosomes. Whilst preliminary, these data suggest that both dynamim-1 WT and KK-EE mutation localise to actin rich structures which are likely to indicate invadosomes. The KK-EE mutation may not affect the formation of these structures but could affect the ability of invadosomes to invade, a distinction which requires further analysis in future work (as described above), which was unfortunately beyond the scope of this project.

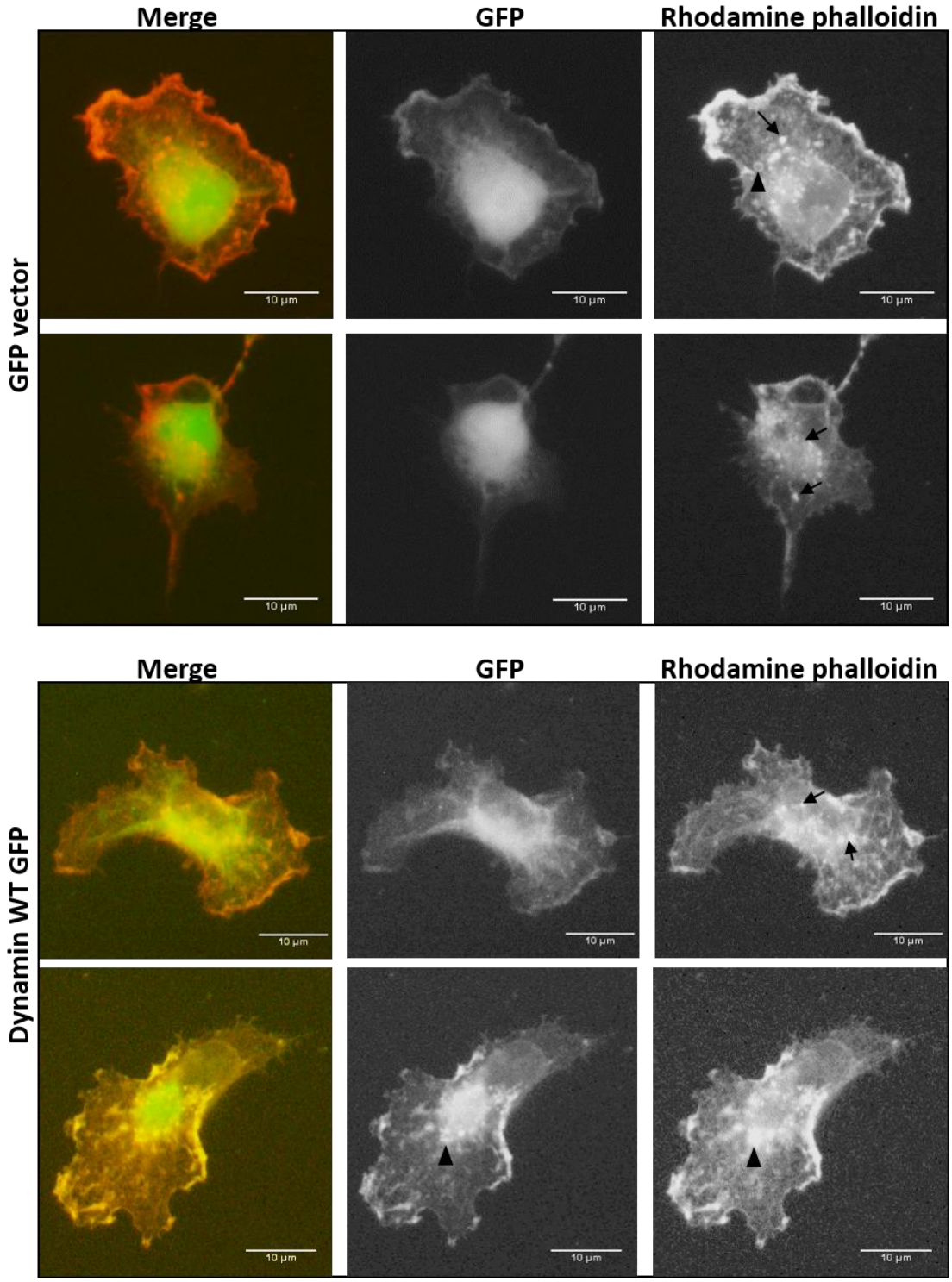
Merge
GFP
Rhodamine phalloidin
GFP vector
Dynamin WT GFP
10 µm

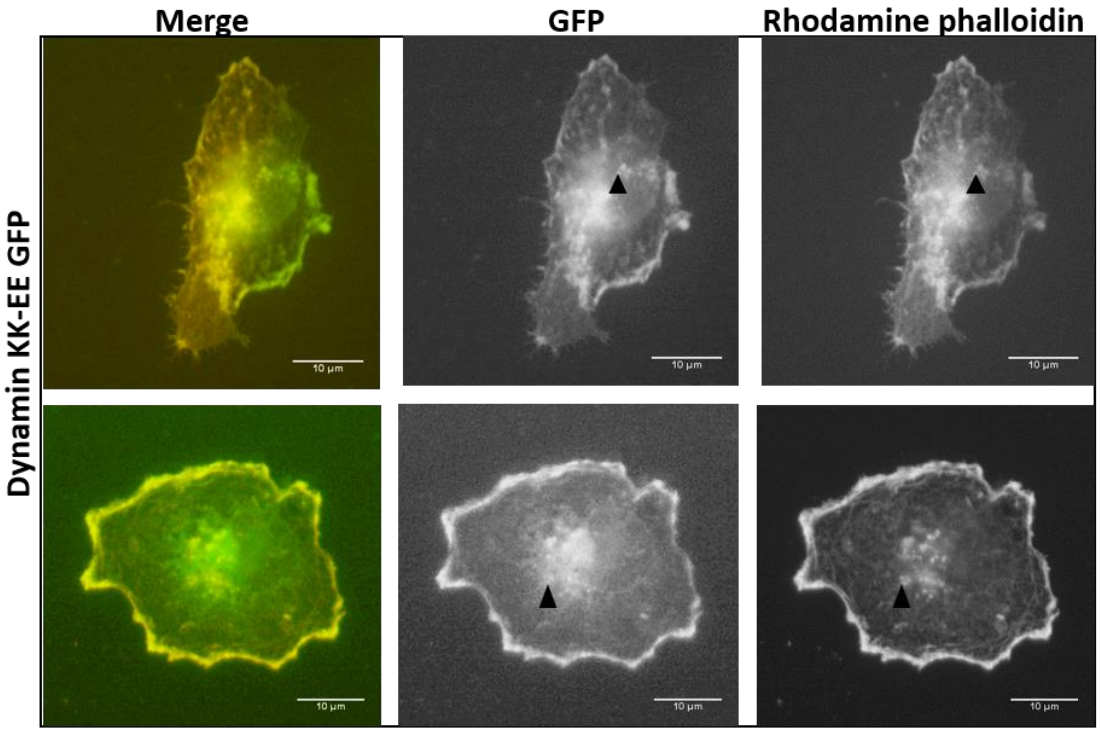

Figure 13. Podosome formation in MDA MB 231 cells A) Examples of cells overexpressing GFP. Arrows indicate actin puncta and arrow head indicates rings of actin B) In cells overexpressing dynamin WT arrows indicate actin puncta and arrow heads indicate co-localisation between dynamin WT fluorescence and actin puncta. C) In cells overexpressing dynamin KK-EE arrow heads indicate co-localisation.

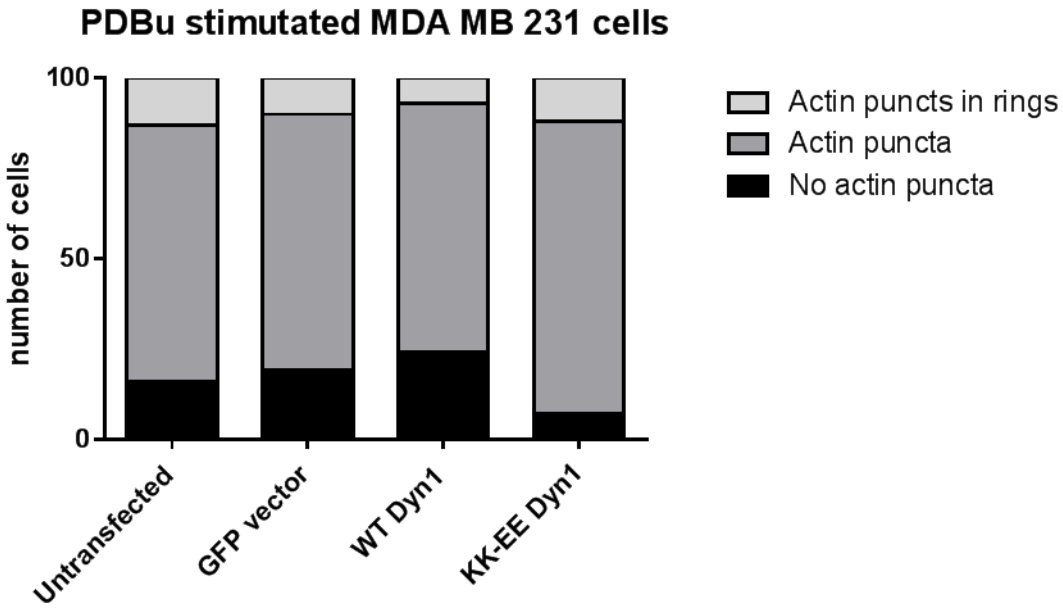

Figure 14. Actin puncta in PDBu stimulated MDA MB 231 cells Graph to show the number of actin puncta and actin rings observed in 100 PDBu stimulated MDA MB 231 cells analysed.

6.11 Discussion

6.11.1 Mutations A408T and KK-EE compromise dynamin-1 actin binding ability

Dynamin-1 is best characterised as functioning at the scission stage of endocytosis in neuronal cells (reviewed in Saheki & De Camilli 2012). There is also evidence supporting the involvement of dynamin-1 in cell functions such as filopodial formation (Yamada et al. 2013; Chou et al. 2014), the formation of actin comets (Lee & De Camilli 2002) and the regulation of stress fibres (Gu et al. 2010). With this in mind, the study of the direct dynamin-1-actin interaction may indicate links between these other cell functions and the actin cytoskeleton, in neuronal tissues and beyond.

In this study the role of the direct dynamin-actin interaction was analysed using the specific charge mutation KK-EE, as identified in the preceding yeast dynamin (Vps1) investigation. An *in vitro* analysis of human dynamin-1 suggested that the KK-EE mutation (and to a lesser degree the A408T mutation) does indeed reduce the ability of dynamin to bind actin as predicted. Subsequent analyses in mammalian cell lines have indicated that the KK-EE mutation does not affect the uptake of transferrin in A431 cells nor the formation of invadosome-like structures in MDA-MB-231 cells. However, it does cause an increase in the overall cell size of A431 cells and may have an effect on cell migration in both cell lines. Despite the preliminary nature of the cellular data this project has created a starting block for future investigations in to the direct dynamin-actin interaction and its role in cell processes.

Initially, the A408T mutation was included in this study as it is a rare example of a disease mutation found within the described actin binding site of dynamin-1. This murine mutation caused an epileptic phenotype (Boumil et al. 2010) and may well cause structural changes to the tertiary structure of dynamin-1 due to the single change of a hydrophobic alanine to a polar, phosphorylatable threonine. This mutation was found to slightly reduce actin binding and it would be interesting to see if this affects the oligomerisation of dynamin. Previous research has found the A408T mutation reduces transferrin uptake in COS-7 cells (Boumil et al. 2010) a cell type reported to not require actin for transferrin endocytosis (Fujimoto et al. 2000). Therefore, the A408T mutation could be effecting both the ability of dynamin to oligomerise or to hydrolyse GTP as well as effecting actin binding during its endocytic role. Nevertheless the reduction in actin binding may well play a pivotal role in exacerbating this epileptic phenotype and it would be fascinating to see if this is directly linked to the role of dynamin-1 in neuronal endocytosis.

The main focus for this chapter was the KK-EE mutation which was found to significantly reduce actin binding *in vitro*. This is interesting as it confirms that these specific

amino acids are involved in the direct actin interaction. This mutation, like the orthologous RR-EE mutation in Vps1, does not abolish actin binding completely, indicating that the interaction is dependent on other residues, possibly within this region of the protein. It has been shown that human dynamin-1 can bundle actin and that bundling is reduced when mutations in its actin binding site are mutated from basic to acidic (Gu et al. 2010). It would be interesting in future studies to see if the dynamin-1 KK-EE mutation also reduces the ability of dynamin to bundle actin *in vitro:* perhaps by using a low speed pelleting or falling ball assay alongside electron microscopy (EM) analysis of dynamin oligomers with F-actin structures.

The mutation KK-EE was found to breakdown readily *in vitro* indicating that its introduction causes a structural change to dynamin-1. To test if this is the case, future studies would include an investigation of dynamin-1 KK-EE structure by EM or circular dichroism. This would suggest whether the structure of dynamin-1 has been compromised or not and could indicate if dynamin-1 KK-EE was still able to form higher order oligomers. The middle domain of dynamin is known to be the area in which dynamin forms dimers and higher order oligomers. Further investigation into the actin binding site and residues involved in oligomerisation could give an indication as to how actin is assembled with dynamin at an endocytic site. This could provide new evidence for understanding how the force from actin polymerisation could be linked to endocytic invagination and scission in cases where it is required to overcome membrane tension (Aghamohammadzadeh & Ayscough 2009).

6.11.2 Preliminary study into the effects of the KK-EE mutation in cellular functions of dynamin-1

This project used an overexpression system to transiently transfect two cancer cell lines with dynamin WT and KK-EE mutant constructs. Predominantly, the data from these experiments have indicated that the overexpression of these constructs are toxic to A431 and MDA-MB-231 cells. Future studies would require the use of dynamin expressed at normal levels in cell lines where the levels of endogenous dynamin isoforms are reduced or removed entirely. This would provide a better experimental system for analysing the effects of the dynamin-1 KK-EE mutation on cell function without the difficulties arising from the overexpression of dynamin-1.

The role of the direct dynamin-actin interaction in endocytosis has not been investigated fully. The initial study into dynamin actin binding indicated that, in HeLa cells, transferrin uptake was not affected by the dynamin-1 actin binding mutation K/E (Gu et al. 2010). However this cell line does not require actin for endocytic uptake. Other studies into dynamin-2 in lamellipodial formation indicated differences in the localisation of WT dynamin-1

puncta in comparison to the dynamin-1 K/E mutants deficient for actin binding (Menon et al. 2014). The authors suggested that this could indicate differences in endocytic uptake, however this still requires more detailed analysis. Furthermore, the role of the dynamin-actin interaction could also be linked to other types of endocytic uptake distinct from CME such as clathrin independent pathways and ultrafast endocytosis. Closer analyses of these pathways may indicate some instances when the direct dynamin-actin interaction is required for endocytosis, potentially in membrane regions where the lipid composition is such that invagination requires a higher input of energy. For example, in adherent A431 cells it was observed that clathrin coated pits did not have actin filaments associated with them, but caveolar structures (which can require dynamin function) were associated with actin (Fujimoto et al. 2000) suggesting different types of invagination will require different amounts of stabilisation and energy for their production.

The involvement of dynamin-1 in cell migration and invasion has not been well documented. Most research into the role of dynamin in cell migration has focused on dynamin-2, which is found ubiquitously in cells. In this study the KK-EE mutation in dynamin-1 seemed to increase directionality in MDA-MB-231 2D single cell migration assays, suggesting that the dynamin-actin interaction may be affecting the ability of these cells to change direction. This investigation would have to be continued for a further in-depth analysis of this preliminary finding however it does suggest that there are some migratory mechanisms that could require the actin binding ability of dynamin-1. These could involve the bundling of actin in the formation of filopodia (Chou et al. 2014), or the stabilisation of actin filaments (Gu et al. 2010), or indeed in the recycling of receptors from the cell surface. It is known that dynamin and actin are required separately for cell migration and most recently these investigations have been expanded into a 3D matrix system. This research utilised Ryngo 1-23® (Previously Bis-T-23, Odell et al. 2009) which blocks dynamin GTPase activity *in vitro* and actually enhances actin-dependent dynamin oligomerisation in cells (Gu et al. 2014). Ryngo 1-23® was found to reduce the ability of some cancer cell lines to migrate indicating that the actin dependent polymerisation of dynamin may require tight regulation during cell migration for the formation of the actomyosin network to be utilised (Lees et al. 2015).

Finally this study included an investigation into how the overexpression of dynamin-1 WT and KK-EE affected invadosome structures in MBA-MB-231 cells. It was found that the overexpression had a negligible impact on the formation of invadosome-like structures. However, this would need to be repeated in a cell system in which other isoforms of dynamin have been knocked down to leave only dynamin-1. Then when creating actin binding mutations in dynamin-1 their effect in cells can be more precisely analysed. If the ability of dynamin to bundle actin is diminished it would be interesting to see if this does affect the

formation or stability of invadosomes as this may indicate new avenues for therapeutic targets to overcome cancer cell metastasis.

Whilst preliminary, these results indicate areas of study which could impact our current understanding of human diseases such as cancer and epilepsy, and therefore this study has great potential for future investigations. Furthermore this chapter supports the idea that there is a direct interaction between dynamin-1 and actin which is comparable to the Vps1-actin interaction. By perturbing the dynamin-1-actin interaction in a similar way to the Vps1 study, changes to the way cells migrate have been found, supporting the idea that dynamin-1 binding to actin may have a role in the reorganisation of the actin cytoskeleton *in vivo*.

Chapter 7

Discussion

7.1 Introduction

The aim of this study was to determine whether the dynamin-actin interaction is evolutionarily conserved, to see if this interaction is required for yeast dynamin (Vps1) function *in vivo* and to more specifically define the residues required for dynamin-actin binding. Using yeast as a model organism, these data have provided evidence for a Vps1-actin interaction that can be impaired by the mutation RR457-8EE. The reduction in actin binding causes a specific endocytic defect at the point of scission, indicating a novel role for actin during scission which is distinct from membrane invagination. A separate point mutation E461K was found to affect early stage endocytosis which implies that Vps1 is also required during early initiation of endocytosis. Finally, creating the equivalent mutation for RR-EE in human dynamin-1 (KK418-9EE) has indicated that this mutation alone could be affecting dynamin-1 function in cell migration.

7.2 The Vps1-actin interaction

7.2.1 Vps1 bundles F-actin

This study identified that the Vps1-actin interaction was required for endocytic events in yeast. Vps1 was, for the first time, shown to form oligomeric rings *in vitro* which bind and bundle actin. Using EM analysis human dynamin-1 has been shown to bundle actin filaments (Gu et al. 2010) (figure 1A). From these images it was suggested that dynamin-1 rings can either bind alongside F-actin filaments or form a ring surrounded by perpendicular actin filaments (see insert figure 1A). The results from the Vps1 study indicated that Vps1 rings can form alongside actin filaments rather than inside them (figure 2B). The idea that dynamin rings may be surrounded by actin filaments, as suggested by Gu and colleagues, doesn't quite fit with the observation that the actin binding residues are found in the middle of the ring with the GTPase domains around the outside (figure 1B). When analysing the EM images it can

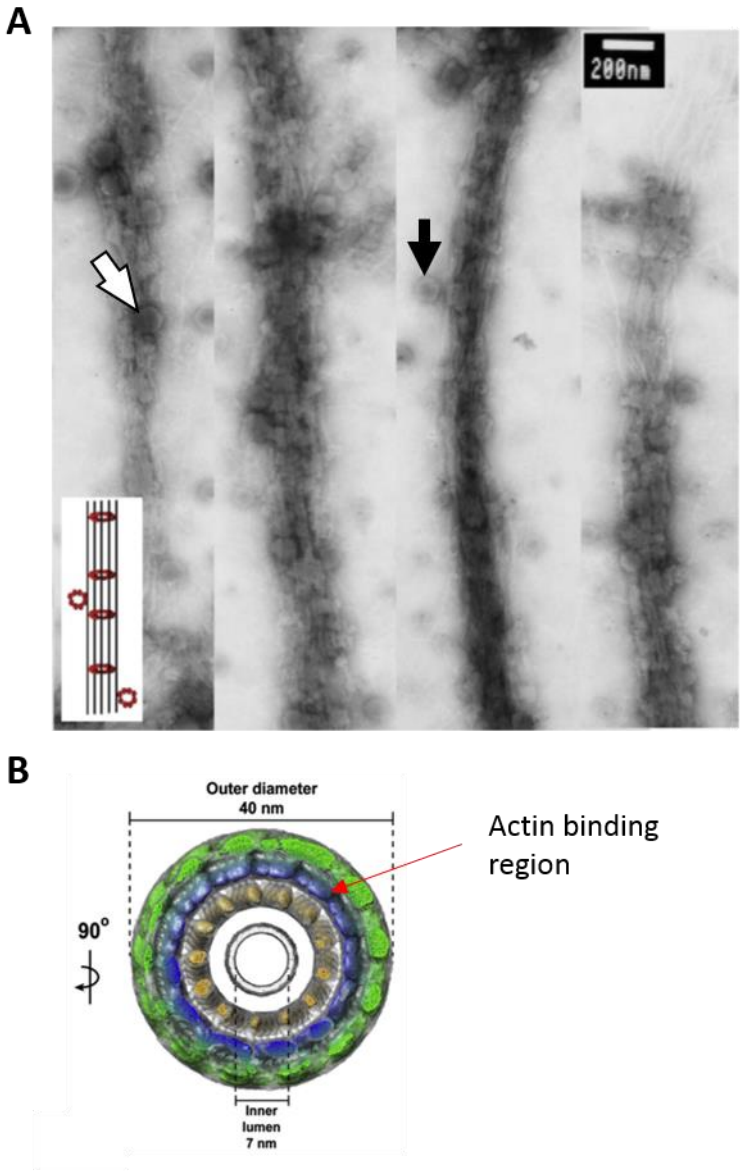

Figure 1. Dynamin bundles F-actin A) EM images of bundles F-actin with dynamin-1. Gu et al., 2010, reproduced with permission from John Wiley and Sons. Insert shows a diagram of how dynamin rings may arrange actin. White arrow indicates a dynamin ring surrounded by actin filaments, the black arrow shows an example of a dynamin ring associated alongside F-actin. B) Diagram as seen in figure 12 chapter 3, added here for clarity. This indicates the position of the actin binding region within a dynamin ring (Chappie et al., 2011).

been seen that there are a few filaments held straight within the structure (figure 1A). This could be to do with the resolution of the images or may indicate that actin is held at a slight angle to a dynamin ring which may suggest that dynamin rings are not perpendicular inside actin filament bundles as suggested in the diagram (see insert figure 1A).

As shown in figure 1B, investigations have identified the structure of a dynamin ring by EM 3D reconstruction (Chappie et al. 2011; Hinshaw & Schmid 1995). These rings were held in place by the addition of a non-hydrolysable GTP molecule; which allowed the rings to be stably imaged, as a snap shot of a structure which *in vivo* is transient. Therefore it was thought that

there were many dynamin rings which have to form around a vesicle neck before scission, inspiring different theories as to how this spiral structure can change to bring the lipids together at the vesicle neck (reviewed in Faelber et al. 2012). As seen in chapter 3 and figure 1B, if there are many rings of dynamin stacked together then the actin binding site would be partially protected from actin by the GTPase domains around the outside of the ring. However, it is now understood that a single dynamin ring alone can facilitate scission (Grassart et al. 2014; Cocucci et al. 2014), thus there is the possibility that actin binding can occur around the top of the dynamin ring during assembly, or alongside dynamin dimers as they form around lipids. Either way it is possible that the middle domain re-organises to be able to bind actin and to facilitate oligomerisation although how this occurs throughout the different stages of dynamin function in a cell has yet to be investigated.

In addition to the middle domain binding actin, there is also the possibility that the GTPase domain of dynamin is involved in actin binding. Blocking dynamin GTPase activity through the mutation K44A is known to reduce actin-dependent oligomerisation of dynamin in a cell (Gu et al. 2014) suggesting that the hydrolysis of GTP is required for the actin interaction or that there is an actin binding site within the GTPase domain. The K44A mutation has been shown to affect actin dynamics in invadosomes, actin comet formation and filopodia, which implies a close relationship between the GTPase domain and actin binding (Chou et al. 2014; Lee & De Camilli 2002; Ochoa et al. 2000). An additional actin binding site would not be unexpected as mutations to the known actin binding site of both dynamin-1 and Vps1 do not fully abolish their interaction with actin. Basic amino acids are known to facilitate actin binding for a number of different proteins (Amann et al. 1998; Tang et al. 1997; Friederich et al. 1992) and it is known that Vps1 contains an insert A region in its GTPase domain which contains basic amino acids, such as the sequence RRPKK. Thus through these residues, insert A may have actin binding ability, although this has not yet been investigated. If this is the case then Vps1-actin binding could happen in two stages during endocytosis. First actin could be bound by the middle domain of Vps1 dimers and trimers stimulating its polymerisation and subsequent bundling. This could be then directed to the scission stage of an endocytic pit whereby the GTPase domain could facilitate further actin binding to continue the affinity between Vps1 and actin throughout the scission process.

7.2.2 Vps1 double ring formation

Vps1 WT was found to form oligomeric rings as seen by EM which were found to exist as either single or double rings, the latter of which were more numerous in the presence of actin (figure 2A,B). This suggests that actin can stimulate higher order ring oligomerisation of Vps1 which is supported by the fact that the actin binding mutation RR-EE does not form as

many double ring structures in the presence of actin. Furthermore, in the original dynamin-1-actin study it was shown that the presence of actin can increase dynamin oligomerisation, as indicated by an increase in GTPase activity and ring formation seen using EM (Gu et al. 2010). Vps1 was not found to increase its GTPase activity in the presence of actin however, these results were carried out in the presence of F-actin filaments rather than short capped F-actin as described in the original report. This result could be repeated with the use of capped short F-actin to analyse whether this increases Vps1 GTPase activity which may indicate higher order oligomerisation.

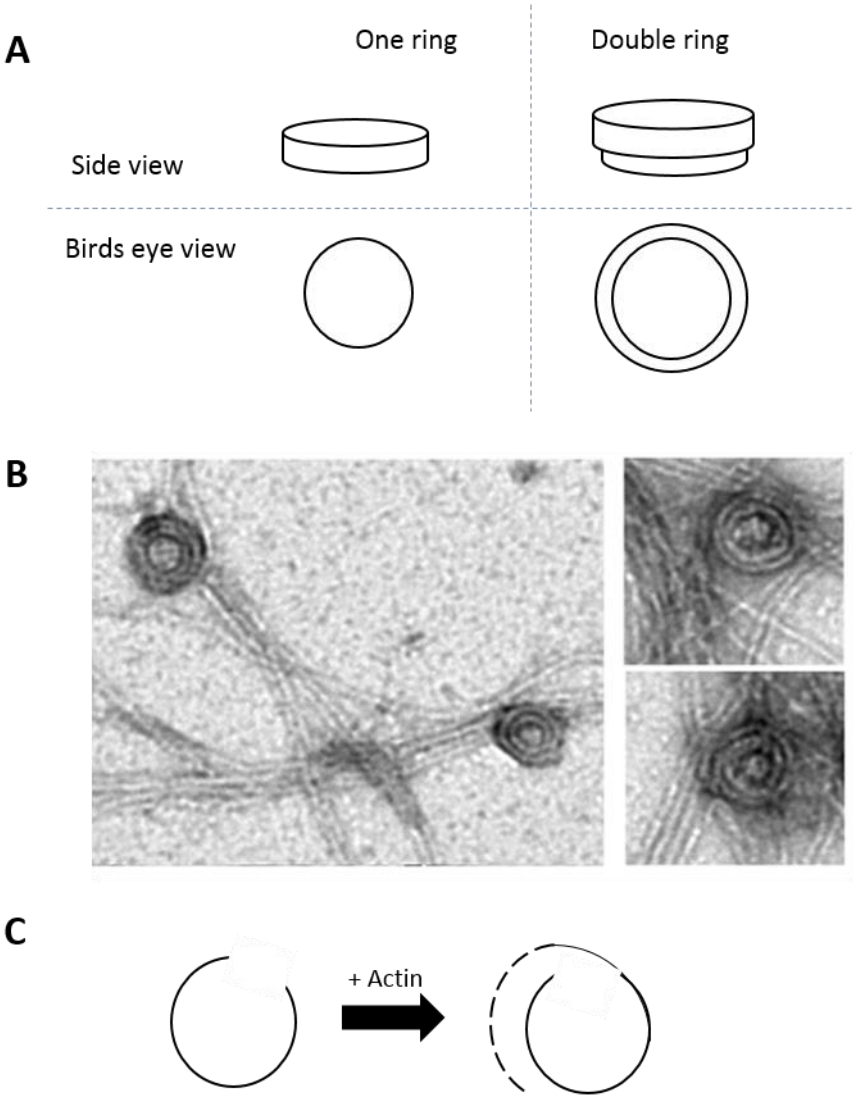

Figure 2. Vps1 double rings A) A diagram of what the double ring structure may show. When two rings coil together the first is smaller than the first and therefore could be seen from the top as two rings B) Image from Palmer et al., 2015a, shows WT Vps1 double rings with filamentous actin. C) Diagram to represent the theory that a ring of Vps1 is stimulated to wrap a second ring around itself in the presence of actin.

The Vps1 oligomers seemed to show an initial ring with an additional outer ring. These images would require 3-D reconstruction to fully analyse how these double rings could form from single Vps1 oligomers. Analysis of the double rings found that the inside rings had a similar diameter to single Vps1 rings. Therefore the outer larger ring seems to oligomerise around the first with the first ring being visible through the second (figure 2A). This suggests that the presence of actin causes a change in Vps1 structure to create a larger diameter ring around the initial one.

From the *in vitro* work it was found that Vps1 RR-EE can form single rings but that there was a reduction in the number of double ring structures seen in the presence of F-actin. If this mutation is affecting the structure of Vps1 it may also affect its ability to oligomerise into double rings which could be causing the defects observed during endocytosis. However, single ring formation was not prevented by this mutation and was not seen to reduce the overall amount of Vps1 that can pellet in a high speed pelleting assay. Therefore these findings are more likely to support the theory that the interaction between Vps1 and actin initiates higher order double ring formation *in vitro*.

The mutation E461K also prevented the creation of oligomeric double rings as can be seen in the EM analysis (Palmer et al. 2015b). As the E461K mutation does not affect actin binding ability, this cannot be due to a lack of actin binding, as is seen with the RR-EE mutation. Instead the E461K mutation may be affecting higher order Vps1 ring structures so that the effect of actin on the oligomerisation of Vps1 is impaired.

In order to understand the oligomerisation stages of Vps1 and how they affect actin binding it would be important to find a way in which Vps1 can be de-oligomerised and re-oligomerised *in vitro*. Dynamin-1 oligomerisation is known to be reduced in buffers containing physiological levels of salt (Warnock et al. 1997) whilst increasing salt levels promotes oligomerisation. However for Vps1, so far, no chemical conditions have been identified that stimulate a change in oligomerisation state and therefore to analyse oligomerisation and actin binding, both separately and combined will be a challenge. One way in which this could be achieved is through the use of multiple point mutations such as the mutation I649K or G436D which are known to reduce oligomerisation (Mishra et al. 2011). The latter mutation prevents Vps1 oligomerisation (data not shown here) and is orthologous to the G397D mutation created in rat dynamin-1 to prevent oligomerisation for crystallisation studies (Ford et al. 2011). Combining either of these mutations with the actin binding mutations RR-EE or E461K could help elucidate the effects caused by differences in actin binding in comparison to those due to oligomerisation defects. However, this would still leave questions unanswered about how these mechanisms change during the process of scission, where a Vps1 molecule is predicted

to change conformation just like the dynamin power stroke, in order to facilitate scission (Chappie et al. 2011; Cocucci et al. 2014).

Dynamin is known to form spirals around lipids (Chappie et al. 2011). The presence of Vps1 double rings could also indicate that actin stimulates the oligomerisation of Vps1 from a single complete ring into a spiral (figure 2C). If this is the case then actin may promote the creation of Vps1 spirals after they form a ring around lipids which may be more conducive to facilitating scission. It will be imperative to repeat these experiments in the presence of lipids, which may indicate whether Vps1 rings and double rings form around lipids in different ways depending on the presence of actin.

7.2.3 Vps1 RR-EE indicates a role for the Vps1-actin interaction during endocytic scission

During this study it was found that the RR-EE mutation reduced the ability of Vps1 to bind and bundle actin. *In vivo* this mutation causes an endocytic defect at the point of scission indicating that the direct Vps1-actin interaction is required for efficient scission during CME. This study has identified that endocytic scission is impaired by reducing the Vps1-actin interaction, causing long invaginations to appear which can stretch over 200 nm into the cell (Palmer et al. 2015a). By reducing turgor pressure, the need for the Vps1-actin interaction was seemingly reduced and invagination length returned to normal, suggesting that even after invagination, turgor pressure has to be overcome to re-arrange the lipids for vesicle release into the cytoplasm. This suggests that actin function in yeast endocytosis occurs in two stages; firstly to form an invagination linked to the lipids by endocytic proteins such as Sla2 and Ent1 (Skruzny et al. 2012), and secondly to link the force of actin polymerisation away from invagination and towards facilitating scission (Palmer et al. 2015a). An EM study of the localisation of endocytic proteins in yeast provides further evidence in support of this theory. By immuno-electron microscopy the actin regulatory protein Las17 was discovered to localise to the tip of short invaginations. When observed on long invaginations (presumably before a scission event) Las17 was seen to shift its localisation from the tip to the middle of an endocytosed tubule (Idrissi et al. 2008; Idrissi et al. 2012). This supports the idea that actin polymerisation is first linked to the tip of a vesicle to facilitate invagination and this then changes to localise actin nucleation and polymerisation to the point of scission.

7.2.4 Vps1 E461K indicates a role for Vps1 in the early stages of CME

It was hypothesised that introducing a positively charged lysine into the actin binding site of Vps1 would increase the affinity between Vps1 and actin. This point mutation E461K did

not increase this affinity, perhaps due to it being a single mutation rather than multiple, as tested in the original dynamin-1 study (Gu et al. 2010). The role of dynamin in the early stages of mammalian endocytosis has yet to be fully elucidated. It is understood that in mammalian cell culture a few dynamin-2 molecules are found at a site of endocytosis before invagination, suggesting that dynamin aids in the recruitment of actin to this site (Cocucci et al. 2014; Grassart et al. 2014; Taylor et al. 2012). The Vps1 study identified that Vps1 E461K seems to arrest endocytosis at the early stages of endocytosis. It is possible that actin is involved in this process however, how this creates shallow invaginations that have seemingly not gone through to full invagination is not yet clear. Due to the poor temporal resolution of EM techniques, there is a possibility that the short invaginations seen in cells with the E461K mutation by EM are not indicating an arrest but rather an increase in the speed of endocytosis, where a snapshot of the process leaves a small number of invagination's where CME has progressed to scission much more quickly than in the WT cell system. This idea, whilst it is possible, is unlikely due to the observed reduction in fluid phase uptake seen when Vps1 E461K is present. However there is only a small decrease in fluid phase uptake seen when Vps1 E461K is expressed which may indicate a different uptake mechanism functioning in yeast that could override CME function when it is perturbed. Other mechanisms of endocytic uptake include Rho dependent endocytic events and Abp1 dependent pathways which may not depend on the Vps1-actin interaction (Aghamohammadzadeh et al. 2014; Prosser et al. 2011), although this has yet to be confirmed.

7.3 Mammalian dynamin-actin interaction

7.3.1 Dynamin middle domain: actin binding verses oligomerisation

The actin binding site within dynamin-1 has been identified as being within the middle coiled-coil region (Gu et al. 2010). This region shares orthology with that of Vps1 as shown in chapter 3 figure 4. It is unclear how, or if, residues which are required for actin binding are also involved in dynamin oligomerisation. This would require a more thorough structural investigation in order to understand how these two functions can take place within the same area of the protein. As described in chapter 3, the specific amino acid residues, which have been defined as being important for dimerisation, surround but are not within, the actin binding site (section 3.1.1). Therefore this suggests that the residues required for oligomerisation are distinct from those which bind actin. It has long been known that dynamin oligomers do not stay in one structural orientation but go through a power stroke mechanism to facilitate scission (Chappie et al. 2011; Cocucci et al. 2014). This could suggest that the actin binding mechanism could function in both actin binding and oligomerisation at different stages

of dynamin function. Or that different structures of dynamin may influence actin binding and bundling in different ways.

Recently, these dynamin structural studies have been followed up by an investigation into the dynamin tetramer crystal structure. This report indicated in more detail how interfaces 1 and 3 (chapter 3 section 3.1.1) were involved in the tetrameric structure of four dynamin monomers (Reubold et al. 2015). The actin binding region has been described to fall between residues 399 and 444 in dynamin-1 and from the initial studies only residue 399 was suggested to be involved in dimer formation (Faelber et al. 2011). Interestingly, residues 399, 402, 403 and 410 seem to all play a role in the tetramerisation of dynamin. A dynamin tetramer requires residue 399 to form a salt bridge with residues 410 and 345 in two separate molecules of the adjacent dimer. Similarly the residues 402 and 403 were found to create salt bridges across the two dimers (Reubold et al. 2015). This either indicates a dual role for these residues in both actin binding and oligomerisation or suggests that the actin binding region may lie further upstream in the primary structure encompassing a smaller area than previously thought. The latter suggestion is supported by the fact that the actin binding point mutations studied in this thesis lie outside of the region described to be required for tetramer formation (KK418-419 and E422 in dynamin-1, RR457-8 E461 in Vps1).

7.3.2 Conserved actin binding residues between dynamin-1 and dynamin-like proteins

In chapter 3 the actin binding sites of Vps1 were compared to classical dynamin proteins 1,2 and 3, from humans, rats and mice. There are other dynamin-like proteins in mammalian cells and yeast which have other cellular functions, such as during the fission and fusion of mitochondria. It is known that Vps1 is similar to the MxA anti-viral protein with 31% identical amino acids (Obar et al. 1990; Rothman et al. 1990), and the human dynamin-like protein Drp1 which is 58% identical (Imoto et al. 1998). As Vps1 can also bind to actin, then it is possible that other dynamin-like proteins also contain charged residues in their middle domains which could be involved in an interaction with actin. Conversely actin binding may be restricted to dynamin proteins which are involved in endocytosis and therefore dynamin-like proteins may not have actin binding residues in their middle domain. To test this idea, the canonical sequences from human MxA and MxB antiviral proteins were compared to the dynamin-1 actin binding site, along with the mitochondrial scission proteins OPA1 and Drp1. As seen in figure 3 the actin binding site in dynamin-1 has some similarity with the MxA protein middle domain, with some similar charge residues selected for the Vps1 study. This is not too surprising as the MxA protein has been described to have similar amino acid orthology

to Vps1 (Obar et al. 1990; Rothman et al. 1990). The MxB protein however holds little resemblance to that of the dynamin-1 actin binding site. This could suggest very different roles for these two proteins and perhaps that MxA is more likely to be able to bind actin. The mitochondrial protein OPA1 does not have similar charged residues in the region selected for the Vps1 study. This could suggest that the role of OPA1 does not rely on actin for mitochondrial fission. However Drp1 has similarly positioned charged residues within this area to both dynamin-1 and Vps1. Vps1 and Drp1 are known to share similarities in structure (Imoto et al. 1998) and therefore it may also bind to actin in the same way as Vps1. This is interesting as it could suggest that Drp1 requires actin for mitochondrial and peroxisomal fission in mammalian cells and could indicate other dynamin-like proteins which interact with actin in a similar way to dynamin-1.

```
DYN1_HUMAN        -------RTGLFTPDMAFETIVKKQVKKIREPCLKCVDMVISELISTVRQCTK-------
DYN2_HUMAN        -------RTGLFTPDLAFEAIVKKQVVKLKEPCLKCVDLVIQELINTVRQCTS-------
DYN3_HUMAN        -------RTGLFTPDMAFEAIVKKQIVKLKGPSLKSVDLVIQELINTVKKCTK-------
MX1(A)_HUMAN      ENQYRGRELPGFVNYRTFETIVKQQIKALEEPAVDMLHTVTDMVRLAFT---DVSIKNFE
MX2(B)_HUMAN      EKQYRGKELLGFVNYKTFEIIVHQYIQQLVEPALSMLQKAMEIIQQAFI---NVAKKHFG
OPA1_HUMAN        LKQWTDKQLPNKAVEVAWETLQEEFSRFMTEPKGKEHDDIFDKLKEAVKEESI-KRHKWN
DNM1L_HUMAN       IRNATGPRPALFVPEVSFELLVKRQIKRLEEPSLRCVELVHEEMQRIIQHCSNYSTQELL
VPS1_YEAST        MYNSSGSAPSLFVGTEAFEVLVKQQIRRFEEPSLRLVTLVFDELVRMLKQIIS--QPKYS
                             .   ::* : ..    :  *        . :   .
```

Figure 3. A comparison between middle domain residues in human dynamin proteins and dynamin-like proteins. The actin binding region of the canonical dynamin-1,2 and 3 proteins (399-444) was compared with homologues regions in human dynamin-like proteins Mx1,2 OPA1 Dnm1 and with the yeast Vps1. * Indicates the same amino acid. : Indicates strong similarity between amino acids and . Indicates weak similarity. Key Blue= acidic Purple = basic Red= small/hydrophobic Green =hydroxyl/sulphydryl/amine/glycine

7.3.3 Dynamin binding to actin filaments

In mammals there are six different isoforms of actin which have slight variations in their amino acid sequence which are all greater than 93% identical (reviewed in Perrin & Ervasti 2010). Four of these isoforms are muscle specific and two are cytosolic (β_{cyto}actin, γ_{cyto}actin) and therefore ubiquitously expressed. It is known that different actin binding proteins bind specifically to β and γ cytosolic actin such as cofilin and profilin (Larsson & Lindberg 1988; De La Cruz 2005). Therefore there is a chance that actin binding proteins could differentially bind these two types of cytosolic actin and thus modulate their function in different ways. Dynamin is known to act in actin regulatory processes throughout the cell and there is a possibility that dynamin can bind varying actin isoforms differently in order to orchestrate different mechanisms; from endocytosis, to the formation of actin comets, and invadopodia. In the future it would be interesting to see if dynamin proteins do bind actin isoforms in different ways and whether this causes a change in actin dynamics. Such evidence may point to specific functions for each of the dynamin isoforms when binding to actin *in vivo*

however, the binding affinities between rabbit and yeast actin to Vps1 were shown to be very similar. In yeast there is only one actin gene and due to the high level of similarity between mammalian and yeast actin (85%) it is unlikely to have affected the results gained in this study. Studying the differences between different actin isoforms and dynamin function will afford a fascinating insight into the modulation of the actin-dynamin interaction and indicate how these may have been fine-tuned during evolution.

Mammals contain three dynamin genes 1,2 and 3 which have variable sequence in the actin binding region (chapter 3 section 3.3.1). Each gene can produce different splice variants making over 25 different possible forms of dynamin (Cao et al. 1998). It has been published that dynamin-1 expression occurs mainly in neuronal cells (Nakata et al. 1991), dynamain-2 is ubiquitously expressed (Cook et al. 1994) and dynamin-3 is found at high levels in the brain and testis (Cook et al. 1996; Nakata et al. 1993). These studies do not suggest that there is a reduction of dynamin-2 expression in the brain for example, but that tissues will probably require all three dynamin proteins and regulate their expression depending on the cells requirements at that time. Understanding what requirements a neuronal cell has for dynamin-1 expression predominantly for example, has yet to be fully elucidated. It has been shown that for synaptic vesicle recycling, dynamin isoforms 1, 2 and 3 are required to work together. Dynamin-1 functions during fast uptake when the neuron was undergoing high frequency firing (Tanifuji et al. 2013) and both dynamin-1 and 3 functioning in bulk endocytic uptake (Wu et al. 2014). Dynamin-2 has been found to act in a slower more constitutive form of endocytosis in neuronal cells (Liu et al. 2011b; Tanifuji et al. 2013). Dynamin-3 has also been found to be involved in regulating platelet volume with certain splice variants giving rise to different sized platelets (Nürnberg et al. 2012). Clearly there are a number of different roles that each dynamin play in different cell types and discovering how this may be facilitated along with actin dynamics would be an important advancement in this field.

Certain actin binding proteins are known to interact with F-actin and modulate the twist of actin molecules within a filament. For example, cofilin de-polymerises actin doing so through changing the twist in an actin filament (McGough et al. 1997). Therefore the way in which actin regulatory proteins bind and affect F-actin structure could have an effect on actin regulation within the cell. This could be to make actin more stable, less stable or perhaps more flexible, potentially providing new surfaces for other actin regulatory proteins to bind. The three isoforms of dynamin could affect actin filaments in different ways depending upon which one was bound and what level of oligomerisation it was at. For example, dynamin-1 may bind actin to make it more stable and less likely to depolymerise whilst bundling filaments together for either actin stress fibres in podocytes or actin force during neuronal ultrafast endocytosis.

Differences between dynamin proteins and their interaction with actin could also shed light on why different splice variants are expressed.

7.3.4 Dynamin-1 binding actin to create mechanical forces

Dynamin-1 has been found to be highly expressed in podocyte cells which are part of the kidney filtration system (Gu et al. 2010). Podocytes are under a lot pressure as they filter toxins from the blood to be excreted. Therefore actin stress fibres are extremely important for maintaining their structure. It was fascinating to see that the original dynamin-1 actin binding study investigated the formation of the stress fibres in podocytes and that this indicated that dynamin may function to allow actin to overcome pressure from the cell's surroundings. Dynamin-1 is understood to function in neuronal endocytosis, it can bend membranes and functions during ultrafast endocytosis which also requires actin (Liu et al. 2011b; Watanabe et al. 2013). Neuronal cells are polarised and therefore are predicted to require actin for endocytosis (Boulant et al. 2011). It could be that dynamin-1 is required to aid cells in overcoming membrane tension as a whole. Dynamin-1 could be required both to function with actin at endocytosis in polarised cells (such as in neurons) and to interact and orchestrate strong stress fibres when cells are under pressure (such as in the kidney nephron). The role of dynamin-1 may therefore in some cases be linked to protecting the cell when external pressure is exerted on it, i.e. during podocyte function for example. One way to test this would be to put cells that do not usually over-express dynamin-1 under pressure mechanically and see if they start to increase dynamin-1 expression over dynamin-2/3.

7.4 Potential impacts of researching the dynamin-actin interaction

There are implications to this study which go beyond the further understanding of yeast endocytic function in that cell functions that use both dynamin and actin, such as during cell migration and cell invasion, can be utilised for cancer cell growth and proliferation. Moreover, there are naturally occurring point mutations in dynamin that are linked to diseases such as centronuclear myopathy, Charcot-Marie-Tooth disease and epilepsy. Dynamin and actin, are both required for cell migration and invasion. Therefore these mechanisms could also be involved in cancer cell metastasis. By understanding the functions of dynamin and actin there is potential for the development of new therapeutic targets to prevent cancer cell metastasis and other genetic disorders.

Dynamin is known to function in lamellipodia formation (Menon et al. 2014; McNiven et al. 2000) and during cell invasion in the stability of podosomes and invadsomes (Lee & De Camilli 2002; Baldassarre et al. 2003). By blocking the ability of dynamin to hydrolyse GTP with the K44A mutation it was found that F-actin turnover at podosomes was reduced (Ochoa et al. 2000). This suggested that the GTPase function of dynamin in these processes is intrinsically linked to dynamin function at podosomes. It has also been found that, unlike lipid stimulated oligomerisation, dynamin's actin-dependent ability to oligomerise also requires its GTPase action (Gu et al. 2014), therefore this direct actin interaction may well play a role in the formation and stabilisation of podosomes and invadosomes.

7.4.1 Genetic disorders

Point mutations naturally occurring in the dynamin-2 gene are known to lead to diseases such as centronuclear myopathy (CNM) and Charcot-Marie-Tooth (CMT). CNM describes congenital disorders leading to muscle wasting phenotypes caused by centralised nuclei in muscle fibres. CMT is a disorder of the peripheral nervous system resulting in loss of motor and sensory function over time as well as muscle wasting. Most mutations of dynamin-2 associated with CMT are found in the PH domain, reviewed in (Tanabe & Takei 2012), whereas mutations associated with CNM are mainly found in the middle domain of dynamin and some are known to increase dynamin oligomerisation *in vitro* (Wang et al. 2010) and *in vivo* (James et al. 2014). However this is not a simple case, as a CNM mutation found in the PH domain of dynamin-2 affects the GTPase action of the protein (Kenniston & Lemmon 2010) and there has been a reported CMT associated mutation in the middle domain of the protein (Gallardo et al. 2008). CNM and CMT mutations in dynamin-2 cause a reduction in its ability to both act in clathrin independent endocytosis and traffic vesicles from the Golgi (Liu et al. 2011a), which provides some insight into how the mutations could be affecting cellular processes. However it is still unclear how a dominant mutation in the dynamin-2 gene that is required for embryonic development can cause progressive diseases. There are a growing number of mutations linked to these disorders that occur in the middle domain of dynamin-2 and have been found to affect dynamin oligomerisation however it has not been tested whether the same mutations affect actin binding. Understanding how these mutations affect the direct dynamin-actin interaction could aid in the discovery of new therapeutic targets and the identification of the causes of these diseases.

7.4.2 Infection

As previously discussed, actin is likely to be involved in endocytosis in mammalian cells either as a scaffold or force generator at early stages through to scission. Thus understanding this interaction with dynamin may provide new therapeutic targets for reducing the uptake of bacterial or viral infection in cells (reviewed in Harper et al. 2013; Weissmann 2015). The role of dynamin in actin comets, such as in Listeria infection, has been well documented (Lee & De Camilli 2002) indicating its role in propagating this pathogen. The MxA protein shares orthology with Vps1 middle domain (figure 3) and therefore may also bind and function with actin. If this is the case then this could lead to a greater understanding of the role that dynamin-like proteins play with actin in anti-viral cellular processes.

7.4.3 Epilepsy

Finally the 'fitful' missense mutation (A408T) in the dynamin-1 gene which causes an epileptic phenotype in mice (Boumil et al. 2010) falls within dynamin-1's actin binding region. As described in chapter 6 section 6.3, this mutation was found to slightly reduce actin binding. Epilepsy is caused by a misfiring of synapses which is intrinsically linked to membrane trafficking. Therefore finding a mutation within the actin binding site of dynamin-1 linked to this sort of disorder may well provide a new lead to understanding the function of the direct actin-dynamin interaction in neurons.

7.5 Future directions

Yeast cells always require actin during endocytosis to overcome turgor pressure. This mechanism may well be required in mammalian cells *in vivo* (such as in polarised neuronal cells) so as to overcome membrane tension and facilitate scission. Therefore the next direction that this study could take is to investigate this in more detail. During this study we used tissue cultured A431 cells as they have been described to require actin for endocytosis when grown in solution (Fujimoto et al. 2000). However there are ways of mechanically and osmotically pressurising the plasma membrane of a cell so as to induce actin dependent endocytosis. By swelling cells osmotically it was shown that actin was then recruited to overcome membrane tension (Boulant et al. 2011). This could be repeated in future experiments to see if dynamin-1 with the actin binding mutation KK-EE prevents endocytic uptake in this system. Cells can also be grown under agar or mechanically stretched to induce membrane tension. Each of these mechanisms could be used to test if the ability of dynamin to bind actin is required during CME which would provide evidence that the involvement of actin in scission may be evolutionarily conserved. Indeed, an experiment carried out by Dr. Katja Vogt (Prof. Kathryn Ayscough Lab)

found that osmotically swelled epithelial MDCK (Madin-Darby Canine Kidney) cells were less able to endocytose transferrin when dynamin-1 KK-EE was overexpressed. This was not the case when WT dynamin-1 was overexpressed in the same cells indicating that the direct dynamin-1-actin interaction is indeed important when cells require actin during endocytosis when membrane tension is increased osmotically.

Vps1 is known to function with actin during endocytic scission, where it binds Sla1 and Rvs167 (Smaczynska-de Rooij et al. 2012; Yu & Cai 2004). Investigating the E461K mutation has suggested that Vps1 may function during the beginning of CME. This raises questions about whether an early function for Vps1 during patch accumulation may be linked to its oligomerisation state. Further research could indicate a mechanism whereby oligomerisation is regulated to create rings of Vps1 required both during patch accumulation and during scission. Furthermore, the interaction between Vps1, Rvs167 and actin at scission requires clarification. It has been suggested that Rvs167 stimulates the disassembly of Vps1 (Smaczynska-de Rooij et al. 2012). Modelling work has suggested that the disassembly of BAR proteins during CME may also induce the energy transfer required for scission (Walani et al. 2015) however, this work was done without considering the role of dynamin proteins. Nevertheless, if Rvs167 disassembles Vps1 after it is oligomerised at a vesicle neck then this, along with actin remodelling, may contribute to scission.

The overexpression of the dynamin-1 KK-EE mutation was found to affect the cell migration of MDA-MB-231 cancer cells*. In vitro* this mutation caused a reduction in dynamin-1 actin binding ability which may have implications upon how the dynamin-actin interaction may be utilised in different cell types. For example, how the dynamin-actin interaction is regulated and required during neuronal growth cone dynamics. Neuronal growth cones are elongated extensions which act as neuronal appendages during development. They respond to the guidance chemicals or cues in their environment to orchestrate the growth of neurons to create the right connections and linkages during development. These extensions are known to be actin dependent. Furthermore, dynamin-1 is understood to act with cortactin to regulate growth cone filopodia, and dynamin-2 has been found to regulate growth cone spreading, again functioning with cortactin to localise α-actinin (actin binding and bundling protein) to the leading edge (Kurklinsky et al. 2011; Yamada et al. 2013). This suggests that dynamin-2 may have a larger role to play in growth cone morphology however the data was collected from neurons grown in a 2D culture. In a developing embryo there will be more of an impact from surrounding cells and perhaps in a more physiological environment dynamin-1 may have a more defined role to play in membrane dynamics and actin regulation. This could be tested using 3D matrices of varying densities and discovering how dynamin-1 WT and KK-EE localisation may change with actin. This research could also overlap with investigations into

the dynamin-actin interaction in endocytosis in a high membrane tension environment, again with the use of the KK-EE mutation.

Finally, these data have provided details about how the KK-EE and A408T mutations affect dynamin-1 function with actin *in vitro*. This leads to questions about how these mutations affect other aspects of dynamin-1 function, such as its GTPase ability and oligomerisation, both of which could be tested using the malachite green GTPase assay and EM analyses, respectively. Furthermore, exactly how dynamin molecules bind to actin has not been clarified. There is a chance that different dynamin isoforms may bind actin in different regions, and this could be tested using a yeast two hybrid screen with single mutations to the actin gene, as described in Urbanek et al. (2013). This could provide more detail as to which region of G-actin dynamin can bind to, or it may expose dynamin isoforms which can only bind to F-actin. The dynamin-actin interaction may also be affected by the way in which F-actin filaments are formed in a cell. For example the tension on an actin filament has been suggested to affect the way in which the actin severing protein cofilin acts. It was found that by holding actin taut with optical tweezers, cofilin was less able to facilitate filament severing therefore this prevents severing of stress fibres (Hayakawa et al. 2011). By repeating this with different fluorescently bound dynamin isoforms the specificity or differences between dynamin isoforms binding taut actin could be revealed. This could also be repeated with different actin isoforms so as to identify which isoforms more readily associate with dynamin. The optical tweezer technique could also be utilised to twist actin filaments which may also affect the association between dynamin and actin. This altogether would provide a more in depth analysis of how dynamin structures associate with actin filaments. These methods could stimulate new ideas and theories into how the orientation and structure of dynamin and actin molecules may facilitate scission during endocytosis or orchestrate actin dynamics during cell migration.

Overall this project has shown that the direct yeast dynamin Vps1-actin interaction is required for vesicle scission during endocytosis. This has revealed that the direct dynamin-actin interaction is evolutionarily conserved and that this mechanism may be required in situations where mammalian cell membrane tension requires actin for endocytosis. The specific point mutation RR-EE in yeast causes a reduction in actin binding in dynamin-1 (KK-EE) and this provides a more specific mutation to further test the dynamin-actin interaction in mammalian endocytosis, cell migration and invasion. These data have set the path for future investigations into the yeast dynamin-actin interaction during endocytosis and has produced preliminary data to show how dynamin-1 may require direct actin binding in mammalian cell processes.

References

Abutbul-Ionita, I., Rujiviphat, J., Nir, I., McQuibban, G.A. & Danino, D., 2012. Membrane tethering and nucleotide-dependent conformational changes drive mitochondrial genome maintenance (Mgm1) protein-mediated membrane fusion. *The Journal of biological chemistry*, 287(44), pp.36634–8.

Achiriloaie, M., Barylko, B. & Albanesi, J.P., 1999. Essential role of the dynamin pleckstrin homology domain in receptor-mediated endocytosis. *Molecular and cellular biology*, 19(2), pp.1410–5.

Adams, A.E., Botstein, D. & Drubin, D.G., 1991. Requirement of yeast fimbrin for actin organization and morphogenesis in vivo. *Nature*, 354(6352), pp.404–8.

Adams, A.E. & Pringle, J.R., 1984. Relationship of actin and tubulin distribution to bud growth in wild-type and morphogenetic-mutant Saccharomyces cerevisiae. *The Journal of cell biology*, 98(3), pp.934–45.

Aderem, A. & Underhill, D.M., 1999. Mechanisms of phagocytosis in macrophages. *Annual review of immunology*, 17, pp.593–623.

Aghamohammadzadeh, S. & Ayscough, K.R., 2009. Differential requirements for actin during yeast and mammalian endocytosis. *Nature cell biology*, 11(8), pp.1039–42.

Aghamohammadzadeh, S. & Ayscough, K.R., 2010. The yeast actin cytoskeleton and its function in endocytosis. *Fungal Biology Reviews*, 24(1-2), pp.37–46.

Aghamohammadzadeh, S., Smaczynska-de Rooij, I.I. & Ayscough, K.R., 2014. An Abp1-dependent route of endocytosis functions when the classical endocytic pathway in yeast is inhibited. *PLoS ONE*, 9(7), pp.1–11.

Aguet, F., Antonescu, C.N., Mettlen, M., Schmid, S.L. & Danuser, G., 2013. Advances in analysis of low signal-to-noise images link dynamin and AP2 to the functions of an endocytic checkpoint. *Developmental cell*, 26(3), pp.279–91.

Alexander, C., Votruba, M., Pesch, U.E., Thiselton, D.L., Mayer, S., Moore, A., Rodriguez, M., Kellner, U., Wissinger, B. et al, 2000. OPA1, encoding a dynamin-related GTPase, is mutated in autosomal dominant optic atrophy linked to chromosome 3q28. *Nature genetics*, 26(2), pp.211–5.

Alberts. B., Johnson. A., Lewis. J., Raff. M., Roberts. K., Walter. P., 2008. Molecular biology of the Cell 5th edition. *Garland Science.*

Alpadi, K., Kulkarni, A., Namjoshi, S., Srinivasan, S., Sippel, K.H., Ayscough, K., Zieger, M., Schmidt, A., Peters, C. et al, 2013. Dynamin-SNARE interactions control trans-SNARE formation in intracellular membrane fusion. *Nature communications*, 4, p.1704.

Altschuler, Y., Barbas, S.M., Terlecky, L.J., Tang, K., Hardy, S., Mostov, K.E. & Schmid, S.L., 1998. Redundant and distinct functions for dynamin-1 and dynamin-2 isoforms. *The Journal of cell biology*, 143(7), pp.1871–81.

Amann, K.J., Renley, B.A. & Ervasti, J.M., 1998. A Cluster of Basic Repeats in the Dystrophin Rod Domain Binds F-actin through an Electrostatic Interaction. *Journal of Biological Chemistry*, 273(43), pp.28419–28423.

Amberg, D.C., 1998. Three-dimensional imaging of the yeast actin cytoskeleton through the budding cell cycle. *Molecular biology of the cell*, 9(12), pp.3259–62.

Andersson, F., Löw, P. & Brodin, L., 2010. Selective perturbation of the BAR domain of endophilin impairs synaptic vesicle endocytosis. *Synapse (New York, N.Y.)*, 64(7), pp.556–60.

Anggono, V., Smillie, K.J., Graham, M.E., Valova, V.A., Cousin, M.A. & Robinson, P.J., 2006. Syndapin I is the phosphorylation-regulated dynamin I partner in synaptic vesicle endocytosis. *Nature neuroscience*, 9(6), pp.752–60.

Arnold, A.M., Anderson, G.W., McIver, B. & Eberhardt, N.L., 2003. A novel dynamin III isoform is up-regulated in the central nervous system in hypothyroidism. *International journal of developmental neuroscience,* 21(5), pp.267–75.

Artym, V. V, Matsumoto, K., Mueller, S.C. & Yamada, K.M., Dynamic membrane remodeling at invadopodia differentiates invadopodia from podosomes. *European journal of cell biology*, 90(2-3), pp.172–80.

Asinof, S.K., Sukoff Rizzo, S.J., Buckley, A.R., Beyer, B.J., Letts, V.A., Frankel, W.N. & Boumil, R.M., 2015. Independent Neuronal Origin of Seizures and Behavioral Comorbidities in an Animal Model of a Severe Childhood Genetic Epileptic Encephalopathy. *PLoS genetics*, 11(6), p.e1005347.

Ausubel, F., editors; R. Brent, R. Kingston, D. Moore, J. Seidman, J. Smith, & K. Struhl, 1993. Short protocols in molecular biology, 2nd ed. Wiley and sons.

Avinoam, O., Schorb, M., Beese, C.J., Briggs, J.A.G. & Kaksonen, M., 2015. Endocytic sites mature by continuous bending and remodeling of the clathrin coat. *Science*, 348(6241), pp.1369–1372.

Ayscough, K.R., Eby, J.J., Lila, T., Dewar, H., Kozminski, K.G. & Drubin, D.G., 1999. Sla1p is a functionally modular component of the yeast cortical actin cytoskeleton required for correct localization of both Rho1p-GTPase and Sla2p, a protein with talin homology. *Molecular biology of the cell*, 10(4), pp.1061–75.

Baldassarre, M., Pompeo, A., Beznoussenko, G., Castaldi, C., Cortellino, S., McNiven, M.A., Luini, A. & Buccione, R., 2003. Dynamin participates in focal extracellular matrix degradation by invasive cells. *Molecular biology of the cell*, 14(3), pp.1074–84.

Bankaitis, V.A., Johnson, L.M. & Emr, S.D., 1986. Isolation of yeast mutants defective in protein targeting to the vacuole. *Proceedings of the National Academy of Sciences of the United States of America*, 83(23), pp.9075–9.

Banta, L.M., Robinson, J.S., Klionsky, D.J. & Emr, S.D., 1988. Organelle assembly in yeast: characterization of yeast mutants defective in vacuolar biogenesis and protein sorting. *The Journal of cell biology*, 107(4), pp.1369–83.

Barlow, L.D., Dacks, J.B. & Wideman, J.G., 2014. From all to (nearly) none: Tracing adaptin evolution in Fungi. *Cellular logistics*, 4(1), p.e28114.

Bethoney, K.A., King, M.C., Hinshaw, J.E., Ostap, E.M. & Lemmon, M.A., 2009. A possible effector role for the pleckstrin homology (PH) domain of dynamin. *Proceedings of the National Academy of Sciences of the United States of America*, 106(32), pp.13359–64.

Bleazard, W., McCaffery, J.M., King, E.J., Bale, S., Mozdy, A., Tieu, Q., Nunnari, J. & Shaw, J.M., 1999. The dynamin-related GTPase Dnm1 regulates mitochondrial fission in yeast. *Nature cell biology*, 1(5), pp.298–304.

van der Bliek, A.M. & Meyerowitz, E.M., 1991. Dynamin-like protein encoded by the Drosophila shibire gene associated with vesicular traffic. *Nature*, 351(6325), pp.411–4.

Böcking, T., Aguet, F., Harrison, S.C. & Kirchhausen, T., 2011. Single-molecule analysis of a molecular disassemblase reveals the mechanism of Hsc70-driven clathrin uncoating. *Nature structural & molecular biology*, 18(3), pp.295–301.

Boettner, D.R., Chi, R.J. & Lemmon, S.K., 2012. Lessons from yeast for clathrin-mediated endocytosis. *Nature cell biology*, 14(1), pp.2–10.

Boettner, D.R., D'Agostino, J.L., Torres, O.T., Daugherty-Clarke, K., Uygur, A., Reider, A., Wendland, B., Lemmon, S.K. & Goode, B.L., 2009. The F-BAR protein Syp1 negatively regulates WASp-Arp2/3 complex activity during endocytic patch formation. *Current biology,* 19(23), pp.1979–87.

Bon, E., Recordon-Navarro, P., Durrens, P., Iwase, M., Toh-E, A. & Aigle, M., 2000. A network of proteins around Rvs167p and Rvs161p, two proteins related to the yeast actin cytoskeleton. *Yeast*, 16(13), pp.1229–41.

Boucrot, E., Ferreira, A.P. a, Almeida-souza, L., Debard, S., Vallis, Y., Howard, G., Bertot, L., Sauvonnet, N. & Mcmahon, H.T., 2014. Endophilin marks and controls a clathrin-independent endocytic pathway . *Nature*.

Boulant, S., Kural, C., Zeeh, J.-C., Ubelmann, F. & Kirchhausen, T., 2011. Actin dynamics counteract membrane tension during clathrin-mediated endocytosis. *Nature cell biology*, 13(8), pp.1124–1131.

Boumil, R.M., Letts, V.A., Roberts, M.C., Lenz, C., Mahaffey, C.L., Zhang, Z.-W., Moser, T. & Frankel, W.N., 2010. A missense mutation in a highly conserved alternate exon of dynamin-1 causes epilepsy in fitful mice. *PLoS genetics*, 6(8).

Brach, T., Godlee, C., Moeller-Hansen, I., Boeke, D. & Kaksonen, M., 2014. The initiation of clathrin-mediated endocytosis is mechanistically highly flexible. *Current biology*, 24(5), pp.548–54.

Brees, C. & Fransen, M., 2014. A cost-effective approach to microporate mammalian cells with the Neon Transfection System. *Analytical Biochemistry*, 466, pp.49–50.

Brinkley, B.R., Beall, P.T., Wible, L.J., Mace, M.L., Turner, D.S. & Cailleau, R.M., 1980. Variations in cell form and cytoskeleton in human breast carcinoma cells in vitro. *Cancer research*, 40(9), pp.3118–29.

Burston, H., Maldonado-Báez, L., Davey, M., Montpetit, B., Schluter, C., Wendland, B. & Conibear, E., 2009. Regulators of yeast endocytosis identified by systematic quantitative analysis. *The Journal of cell biology*, 185(6), pp.1097–110.

Cailleau, R., Olivé, M. & Cruciger, Q. V, 1978. Long-term human breast carcinoma cell lines of metastatic origin: preliminary characterization. *In vitro*, 14(11), pp.911–5.

Cantor, A.B., 2012. Dynamin 3 and platelet size variation. *Blood*, 120(24), pp.4666–7.

Cao, H., Garcia, F. & McNiven, M.A., 1998. Differential distribution of dynamin isoforms in mammalian cells. *Molecular biology of the cell*, 9(9), pp.2595–609.

Carlier, M.F., 1990. Actin polymerization and ATP hydrolysis. *Advances in biophysics*, 26, pp.51–73.

Carr, J.F. & Hinshaw, J.E., 1997. Dynamin assembles into spirals under physiological salt conditions upon the addition of GDP and gamma-phosphate analogues. *The Journal of biological chemistry*, 272(44), pp.28030–5.

Carroll, S.Y., Stimpson, H.E.M., Weinberg, J., Toret, C.P., Sun, Y. & Drubin, D.G., 2012. Analysis of yeast endocytic site formation and maturation through a regulatory transition point. *Molecular biology of the cell*, 23(4), pp.657–68.

Carroll, S.Y., Stirling, P.C., Stimpson, H.E.M., Giesselmann, E., Schmitt, M.J. & Drubin, D.G., 2009. A yeast killer toxin screen provides insights into a/b toxin entry, trafficking, and killing mechanisms. *Developmental cell*, 17(4), pp.552–60.

Chapa-y-Lazo, B., Allwood, E.G., Smaczynska-de Rooij, I.I., Snape, M.L. & Ayscough, K.R., 2014. Yeast endocytic adaptor AP-2 binds the stress sensor Mid2 and functions in polarized cell responses. *Traffic,* 15(5), pp.546–57.

Chappie, J.S., Acharya, S., Leonard, M., Schmid, S.L. & Dyda, F., 2010. G domain dimerization controls dynamin's assembly-stimulated GTPase activity. *Nature*, 465(7297), pp.435–440.

Chappie, J.S., Acharya, S., Liu, Y.-W., Leonard, M., Pucadyil, T.J. & Schmid, S.L., 2009. An intramolecular signaling element that modulates dynamin function in vitro and in vivo. *Molecular biology of the cell*, 20(15), pp.3561–71.

Chappie, J.S., Mears, J. a., Fang, S., Leonard, M., Schmid, S.L., Milligan, R. a., Hinshaw, J.E. & Dyda, F., 2011. A pseudoatomic model of the dynamin polymer identifies a hydrolysis-dependent powerstroke. *Cell*, 147(1), pp.209–222.

Chen, D.C., Yang, B.C. & Kuo, T.T., 1992. One-step transformation of yeast in stationary phase. *Current genetics*, 21(1), pp.83–4.

Chen, M.S., Obar, R.A., Schroeder, C.C., Austin, T.W., Poodry, C.A., Wadsworth, S.C. & Vallee, R.B., 1991. Multiple forms of dynamin are encoded by shibire, a Drosophila gene involved in endocytosis. *Nature*, 351(6327), pp.583–6.

Chi, R.J., Liu, J., West, M., Wang, J., Odorizzi, G. & Burd, C.G., 2014. Fission of SNX-BAR-coated endosomal retrograde transport carriers is promoted by the dynamin-related protein Vps1. *The Journal of cell biology*, 204(5), pp.793–806.

Chou, A.M., Sem, K.P., Wright, G.D., Sudhaharan, T. & Ahmed, S., 2014. Dynamin1 is a novel target for IRSp53 and works with Mena and Eps8 to regulate filopodial dynamics. *The Journal of biological chemistry*, pp.30.

Clark, E.S., Whigham, A.S., Yarbrough, W.G. & Weaver, A.M., 2007. Cortactin is an essential regulator of matrix metalloproteinase secretion and extracellular matrix degradation in invadopodia. *Cancer research*, 67(9), pp.4227–35.

Clayton, E.L., Sue, N., Smillie, K.J., O'Leary, T., Bache, N., Cheung, G., Cole, A.R., Wyllie, D.J., Cousin, M.A. et al, 2010. Dynamin I phosphorylation by GSK3 controls activity-dependent bulk endocytosis of synaptic vesicles. *Nature neuroscience*, 13(7), pp.845–51.

Cocucci, E., Aguet, F., Boulant, S. & Kirchhausen, T., 2012. The first five seconds in the life of a clathrin-coated pit. *Cell*, 150(3), pp.495–507.

Cocucci, E., Gaudin, R. & Kirchhausen, T., 2014. Dynamin recruitment and membrane scission at the neck of a clathrin-coated pit. *Molecular biology of the cell*, 25(22), pp.3595–609.

Colwill, K., Field, D., Moore, L., Friesen, J. & Andrews, B., 1999. In vivo analysis of the domains of yeast Rvs167p suggests Rvs167p function is mediated through multiple protein interactions. *Genetics*, 152(3), pp.881–93.

Cook, T., Mesa, K. & Urrutia, R., 1996. Three dynamin-encoding genes are differentially expressed in developing rat brain. *Journal of neurochemistry*, 67(3), pp.927–31.

Cook, T.A., Urrutia, R. & McNiven, M.A., 1994. Identification of dynamin 2, an isoform ubiquitously expressed in rat tissues. *Proceedings of the National Academy of Sciences of the United States of America*, 91(2), pp.644–8.

Cope, M.J., Yang, S., Shang, C. & Drubin, D.G., 1999. Novel protein kinases Ark1p and Prk1p associate with and regulate the cortical actin cytoskeleton in budding yeast. *The Journal of cell biology*, 144(6), pp.1203–18.

Damke, H., Muhlberg, A.B., Sever, S., Sholly, S., Warnock, D.E. & Schmid, S.L., 2001. Expression, purification, and functional assays for self-association of dynamin-1. *Methods in enzymology*, 329, pp.447–57.

Danino, D., Moon, K.-H. & Hinshaw, J.E., 2004. Rapid constriction of lipid bilayers by the mechanochemical enzyme dynamin. *Journal of structural biology*, 147(3), pp.259–67.

Daumke, O., Roux, A. & Haucke, V., 2014. BAR domain scaffolds in dynamin-mediated membrane fission. *Cell*, 156(5), pp.882–92.

David, C., Solimena, M. & De Camilli, P., 1994. Autoimmunity in stiff-Man syndrome with breast cancer is targeted to the C-terminal region of human amphiphysin, a protein similar to the yeast proteins, Rvs167 and Rvs161. *FEBS letters*, 351(1), pp.73–9.

Derman, A.I., Becker, E.C., Truong, B.D., Fujioka, A., Tucey, T.M., Erb, M.L., Patterson, P.C. & Pogliano, J., 2009. Phylogenetic analysis identifies many uncharacterized actin-like proteins (Alps) in bacteria: regulated polymerization, dynamic instability and treadmilling in Alp7A. *Molecular microbiology*, 73(4), pp.534–52.

Destaing, O., Ferguson, S.M., Grichine, A., Oddou, C., De Camilli, P., Albiges-Rizo, C. & Baron, R., 2013. Essential function of dynamin in the invasive properties and actin architecture of v-Src induced podosomes/invadosomes. *PLoS ONE*, 8(12).

Di, A., 2003. Dynamin Regulates Focal Exocytosis in Phagocytosing Macrophages. *Molecular Biology of the Cell*, 14(5), pp.2016–2028.

Donaldson, J.G., Porat-Shliom, N. & Cohen, L.A., 2009. Clathrin-independent endocytosis: a unique platform for cell signaling and PM remodeling. *Cellular signalling*, 21(1), pp.1–6.

Draper, B.K., Komurasaki, T., Davidson, M.K. & Nanney, L.B., 2003. Epiregulin is more potent than EGF or TGFalpha in promoting in vitro wound closure due to enhanced ERK/MAPK activation. *Journal of cellular biochemistry*, 89(6), pp.1126–37.

Drubin, D.G., Miller, K.G. & Botstein, D., 1988. Yeast actin-binding proteins: evidence for a role in morphogenesis. *The Journal of cell biology*, 107(6), pp.2551–61.

Ehrlich, M., Boll, W., Van Oijen, A., Hariharan, R., Chandran, K., Nibert, M.L. & Kirchhausen, T., 2004. Endocytosis by random initiation and stabilization of clathrin-coated pits. *Cell*, 118(5), pp.591–605.

Engqvist-Goldstein, A.E., Kessels, M.M., Chopra, V.S., Hayden, M.R. & Drubin, D.G., 1999. An actin-binding protein of the Sla2/Huntingtin interacting protein 1 family is a novel component of clathrin-coated pits and vesicles. *The Journal of cell biology*, 147(7), pp.1503–18.

Engqvist-Goldstein, A.E., Warren, R.A., Kessels, M.M., Keen, J.H., Heuser, J. & Drubin, D.G., 2001. The actin-binding protein Hip1R associates with clathrin during early stages of endocytosis and promotes clathrin assembly in vitro. *The Journal of cell biology*, 154(6), pp.1209–23.

Engqvist-Goldstein, A.E.Y., Zhang, C.X., Carreno, S., Barroso, C., Heuser, J.E. & Drubin, D.G., 2004. RNAi-mediated Hip1R silencing results in stable association between the endocytic machinery and the actin assembly machinery. *Molecular biology of the cell*, 15(4), pp.1666–79.

Eppinga, R.D., Krueger, E.W., Weller, S.G., Zhang, L., Cao, H. & McNiven, M.A., 2011. Increased expression of the large GTPase dynamin 2 potentiates metastatic migration and invasion of pancreatic ductal carcinoma. *Oncogene*, 31(10), pp.1228–1241.

Eyster, C.A., Higginson, J.D., Huebner, R., Porat-Shliom, N., Weigert, R., Wu, W.W., Shen, R.-F. & Donaldson, J.G., 2009. Discovery of new cargo proteins that enter cells through clathrin-independent endocytosis. *Traffic,* 10(5), pp.590–9.

Faelber, K., Held, M., Gao, S., Posor, Y., Haucke, V., Noé, F. & Daumke, O., 2012. Structural insights into dynamin-mediated membrane fission. *Structure*, 20(10), pp.1621–8.

Faelber, K., Posor, Y., Gao, S., Held, M., Roske, Y., Schulze, D., Haucke, V., Noé, F. & Daumke, O., 2011. Crystal structure of nucleotide-free dynamin. *Nature*, 477, pp.556–560.

Ferguson, S., Raimondi, A., Paradise, S., Shen, H., Mesaki, K., Ferguson, A., Destaing, O., Ko, G., De Camilli, P. et al, 2009. Coordinated Actions of Actin and BAR Proteins Upstream of Dynamin at Endocytic Clathrin-Coated Pits. *Developmental Cell*, 17(6), pp.811–822.

Ferguson, S.M. & De Camilli, P., 2012. Dynamin, a membrane-remodelling GTPase. *Nature reviews. Molecular cell biology*, 13(2), pp.75–88.

Fiserova, J. & Goldberg, M.W., 2010. Immunoelectron microscopy of cryofixed freeze-substituted Saccharomyces cerevisiae. *Methods in molecular biology*, 657, pp.191–204.

Ford, M.G.J., Jenni, S. & Nunnari, J., 2011. The crystal structure of dynamin. *Nature*, 477(7366), pp.561–566.

Freeman, S.A. & Grinstein, S., 2014. Phagocytosis: receptors, signal integration, and the cytoskeleton. *Immunological reviews*, 262(1), pp.193–215.

Friederich, E., Vancompernolle, K., Huet, C., Goethals, M., Finidori, J., Vandekerckhove, J. & Louvard, D., 1992. An actin-binding site containing a conserved motif of charged amino acid residues is essential for the morphogenic effect of villin. *Cell*, 70(1), pp.81–92.

Friesen, H., Humphries, C., Ho, Y., Schub, O., Colwill, K. & Andrews, B., 2006. Characterization of the yeast amphiphysins Rvs161p and Rvs167p reveals roles for the Rvs heterodimer in vivo. *Molecular biology of the cell*, 17(3), pp.1306–21.

Fujimoto, L.M., Roth, R., Heuser, J.E. & Schmid, S.L., 2000. Actin assembly plays a variable, but not obligatory role in receptor-mediated endocytosis in mammalian cells. *Traffic*, 1(6), pp.161–171.

Gabaldón, T., 2010. Peroxisome diversity and evolution. *Philosophical transactions of the Royal Society of London.* 365(1541), pp.765–73.

Gagny, B., Wiederkehr, A., Dumoulin, P., Winsor, B., Riezman, H. & Haguenauer-Tsapis, R., 2000. A novel EH domain protein of Saccharomyces cerevisiae, Ede1p, involved in endocytosis. *Journal of cell science*, 113, pp.3309–19.

Galkin, V.E., Orlova, A., Vos, M.R., Schröder, G.F. & Egelman, E.H., 2015. Near-Atomic Resolution for One State of F-Actin. *Structure*, 23(1), pp.173–182.

Gallardo, E., Claeys, K.G., Nelis, E., García, A., Canga, A., Combarros, O., Timmerman, V., De Jonghe, P. & Berciano, J., 2008. Magnetic resonance imaging findings of leg musculature in Charcot-Marie-Tooth disease type 2 due to dynamin 2 mutation. *Journal of neurology*, 255(7), pp.986–92.

Galletta, B.J., Chuang, D.Y. & Cooper, J.A., 2008. Distinct roles for Arp2/3 regulators in actin assembly and endocytosis. *PLoS biology*, 6(1), p.e1.

Geli, M.I. & Riezman, H., 1996. Role of type I myosins in receptor-mediated endocytosis in yeast. *Science*, 272(5261), pp.533–5.

Génot, E. & Gligorijevic, B., 2014. Invadosomes in their natural habitat. *European journal of cell biology*, 93(10-12), pp.367–79.

Gheorghe, D.M., Aghamohammadzadeh, S., Smaczynska-de Rooij, I.I., Allwood, E.G., Winder, S.J. & Ayscough, K.R., 2008. Interactions between the yeast SM22 homologue Scp1 and actin demonstrate the importance of actin bundling in endocytosis. *The Journal of biological chemistry*, 283(22), pp.15037–46.

Giard, D.J., Aaronson, S.A., Todaro, G.J., Arnstein, P., Kersey, J.H., Dosik, H. & Parks, W.P., 1973. In vitro cultivation of human tumors: establishment of cell lines derived from a series of solid tumors. *Journal of the National Cancer Institute*, 51(5), pp.1417–23.

Goicoechea, S.M., Bednarski, B., García-Mata, R., Prentice-Dunn, H., Kim, H.J. & Otey, C.A., 2009. Palladin contributes to invasive motility in human breast cancer cells. *Oncogene*, 28(4), pp.587–98.

Gold, E.S., Underhill, D.M., Morrissette, N.S., Guo, J., McNiven, M.A. & Aderem, A., 1999. Dynamin 2 Is Required for Phagocytosis in Macrophages. *Journal of Experimental Medicine*, 190(12), pp.1849–1856.

Goode, B.L., 2002. Purification of yeast actin and actin-associated proteins. *Methods in enzymology*, 351, pp.433–41.

Goode, B.L., Wong, J.J., Butty, A.C., Peter, M., McCormack, A.L., Yates, J.R., Drubin, D.G. & Barnes, G., 1999. Coronin promotes the rapid assembly and cross-linking of actin filaments and may link the actin and microtubule cytoskeletons in yeast. *The Journal of cell biology*, 144(1), pp.83–98.

Goodman, A., 2003. The Saccharomyces cerevisiae Calponin/Transgelin Homolog Scp1 Functions with Fimbrin to Regulate Stability and Organization of the Actin Cytoskeleton. *Molecular Biology of the Cell*, 14(7), pp.2617–2629.

Goodson, H. V, Anderson, B.L., Warrick, H.M., Pon, L.A. & Spudich, J.A., 1996. Synthetic lethality screen identifies a novel yeast myosin I gene (MYO5): myosin I proteins are required for polarization of the actin cytoskeleton. *The Journal of cell biology*, 133(6), pp.1277–91.

Gourlay, C.W., Dewar, H., Warren, D.T., Costa, R., Satish, N. & Ayscough, K.R., 2003. An interaction between Sla1p and Sla2p plays a role in regulating actin dynamics and endocytosis in budding yeast. *Journal of cell science*, 116, pp.2551–64.

Gout, I., Dhand, R., Hiles, I.D., Fry, M.J., Panayotou, G., Das, P., Truong, O., Totty, N.F., Booker, G.W., et al. 1993. The GTPase dynamin binds to and is activated by a subset of SH3 domains. *Cell*, 75(1), pp.25–36.

Grabs, D., Slepnev, V.I., Songyang, Z., David, C., Lynch, M., Cantley, L.C. & De Camilli, P., 1997. The SH3 domain of amphiphysin binds the proline-rich domain of dynamin at a single site that defines a new SH3 binding consensus sequence. *The Journal of biological chemistry*, 272(20), pp.13419–25.

Grassart, A., Cheng, A.T., Hong, S.H., Zhang, F., Zenzer, N., Feng, Y., Briner, D.M., Davis, G.D., … Drubin, D.G., 2014. Actin and dynamin2 dynamics and interplay during clathrin-mediated endocytosis. *Journal of Cell Biology*, 205, pp.721–735.

Gray, N.W., Fourgeaud, L., Huang, B., Chen, J., Cao, H., Oswald, B.J., Hémar, A. & McNiven, M.A., 2003. Dynamin 3 is a component of the postsynapse, where it interacts with mGluR5 and Homer. *Current biology*, 13(6), pp.510–5.

Greener, T., Zhao, X., Nojima, H., Eisenberg, E. & Greene, L.E., 2000. Role of cyclin G-associated kinase in uncoating clathrin-coated vesicles from non-neuronal cells. *The Journal of biological chemistry*, 275(2), pp.1365–70.

Gross, S.R., 2013. Actin binding proteins: their ups and downs in metastatic life. *Cell adhesion & migration*, 7(2), pp.199–213.

Gu, C., Chang, J., Shchedrina, V.A., Pham, V.A., Hartwig, J.H., Suphamungmee, W., Lehman, W., Hyman, B.T., Sever, S. et al, 2014. Regulation of dynamin oligomerization in cells: the role of dynamin-actin interactions and its GTPase activity. *Traffic*, 15(8), pp.819–38.

Gu, C., Yaddanapudi, S., Weins, A., Osborn, T., Reiser, J., Pollak, M., Hartwig, J. & Sever, S., 2010. Direct dynamin-actin interactions regulate the actin cytoskeleton. *The EMBO journal*, 29(21), pp.3593–3606.

Harding, C., Heuser, J. & Stahl, P., 1983. Receptor-mediated endocytosis of transferrin and recycling of the transferrin receptor in rat reticulocytes. *The Journal of cell biology*, 97(2), pp.329–39.

Harper, C.B., Popoff, M.R., McCluskey, A., Robinson, P.J. & Meunier, F.A., 2013. Targeting membrane trafficking in infection prophylaxis: dynamin inhibitors. *Trends in Cell Biology*, 23(2), pp.90–101.

Hasilik, A. & Tanner, W., 1978. Biosynthesis of the vacuolar yeast glycoprotein carboxypeptidase Y. Conversion of precursor into the enzyme. *European journal of biochemistry / FEBS*, 85(2), pp.599–608.

Hayakawa, K., Tatsumi, H. & Sokabe, M., 2011. Actin filaments function as a tension sensor by tension-dependent binding of cofilin to the filament. *The Journal of cell biology*, 195(5), pp.721–7.

Hayden, J., Williams, M., Granich, A., Ahn, H., Tenay, B., Lukehart, J., Highfill, C., Dobard, S. & Kim, K., 2013. Vps1 in the late endosome-to-vacuole traffic. *Journal of biosciences*, 38(1), pp.73–83.

Henley, J.R., Krueger, E.W., Oswald, B.J. & McNiven, M.A., 1998. Dynamin-mediated internalization of caveolae. *The Journal of cell biology*, 141(1), pp.85–99.

Henmi, Y., Tanabe, K. & Takei, K., 2011. Disruption of Microtubule Network Rescues Aberrant Actin Comets in Dynamin2-Depleted Cells T. Spielmann, ed. *PLoS ONE*, 6(12), p.e28603.

Henne, W.M., Boucrot, E., Meinecke, M., Evergren, E., Vallis, Y., Mittal, R. & McMahon, H.T., 2010. FCHo proteins are nucleators of clathrin-mediated endocytosis. *Science*, 328(5983), pp.1281–4.

Hettema, E.H., Ruigrok, C.C., Koerkamp, M.G., van den Berg, M., Tabak, H.F., Distel, B. & Braakman, I., 1998. The cytosolic DnaJ-like protein djp1p is involved specifically in peroxisomal protein import. *The Journal of cell biology*, 142(2), pp.421–34.

Hinshaw, J.E. & Schmid, S.L., 1995. Dynamin self-assembles into rings suggesting a mechanism for coated vesicle budding. *Nature*, 374(6518), pp.190–2.

Hirst, J., Irving, C. & Borner, G.H.H., 2013. Adaptor protein complexes AP-4 and AP-5: new players in endosomal trafficking and progressive spastic paraplegia. *Traffic*, 14(2), pp.153–64.

Hoepfner, D., van den Berg, M., Philippsen, P., Tabak, H.F. & Hettema, E.H., 2001. A role for Vps1p, actin, and the Myo2p motor in peroxisome abundance and inheritance in Saccharomyces cerevisiae. *The Journal of cell biology*, 155(6), pp.979–90.

Holmes, K.C., Popp, D., Gebhard, W. & Kabsch, W., 1990. Atomic model of the actin filament. *Nature*, 347(6288), pp.44–9.

Holtzman, D.A., Yang, S. & Drubin, D.G., 1993. Synthetic-lethal interactions identify two novel genes, SLA1 and SLA2, that control membrane cytoskeleton assembly in Saccharomyces cerevisiae. *The Journal of cell biology*, 122(3), pp.635–44.

Hopkins, C.R. & Trowbridge, I.S., 1983. Internalization and processing of transferrin and the transferrin receptor in human carcinoma A431 cells. *The Journal of cell biology*, 97(2), pp.508–21.

Howard, L., Nelson, K.K., Maciewicz, R.A. & Blobel, C.P., 1999. Interaction of the metalloprotease disintegrins MDC9 and MDC15 with two SH3 domain-containing proteins, endophilin I and SH3PX1. *The Journal of biological chemistry*, 274(44), pp.31693–9.

Huang, K.M., Gullberg, L., Nelson, K.K., Stefan, C.J., Blumer, K. & Lemmon, S.K., 1997. Novel functions of clathrin light chains: clathrin heavy chain trimerization is defective in light chain-deficient yeast. *Journal of cell science*, 110, pp.899–910.

Huckaba, T.M., Gay, A.C., Pantalena, L.F., Yang, H.-C. & Pon, L.A., 2004. Live cell imaging of the assembly, disassembly, and actin cable-dependent movement of endosomes and actin patches in the budding yeast, Saccharomyces cerevisiae. *The Journal of cell biology*, 167(3), pp.519–30.

Idrissi, F.-Z., Blasco, A., Espinal, A. & Geli, M.I., 2012. Ultrastructural dynamics of proteins involved in endocytic budding. *Proceedings of the National Academy of Sciences of the United States of America*, 109(39), pp.E2587–94.

Idrissi, F.-Z., Grötsch, H., Fernández-Golbano, I.M., Presciatto-Baschong, C., Riezman, H. & Geli, M.-I., 2008. Distinct acto/myosin-I structures associate with endocytic profiles at the plasma membrane. *The Journal of cell biology*, 180(6), pp.1219–32.

Imoto, M., Tachibana, I. & Urrutia, R., 1998. Identification and functional characterization of a novel human protein highly related to the yeast dynamin-like GTPase Vps1p. *Journal of cell science*, 111, pp.1341–9.

Ingerman, E. & Nunnari, J., 2005. A continuous, regenerative coupled GTPase assay for dynamin-related proteins. *Methods in Enzymology*, 404(1995), pp.611–619.

Ireton, K., Rigano, L.A., Polle, L. & Schubert, W.-D., 2014. Molecular mechanism of protrusion formation during cell-to-cell spread of Listeria. *Frontiers in cellular and infection microbiology*, 4, p.21.

Jackson, L.P., Kelly, B.T., McCoy, A.J., Gaffry, T., James, L.C., Collins, B.M., Höning, S., Evans, P.R. & Owen, D.J., 2010. A large-scale conformational change couples membrane recruitment to cargo binding in the AP2 clathrin adaptor complex. *Cell*, 141(7), pp.1220–9.

James, N.G., Digman, M.A., Ross, J.A., Barylko, B., Wang, L., Li, J., Chen, Y., Mueller, J.D., Jameson, D.M., et al. 2014. A mutation associated with centronuclear myopathy enhances the size and stability of dynamin 2 complexes in cells. *Biochimica et biophysica acta*, 1840(1), pp.315–21.

Jones, L.J., Carballido-López, R. & Errington, J., 2001. Control of cell shape in bacteria: helical, actin-like filaments in Bacillus subtilis. *Cell*, 104(6), pp.913–22.

Jost, M., Simpson, F., Kavran, J.M., Lemmon, M.A. & Schmid, S.L., 1998. Phosphatidylinositol-4,5-bisphosphate is required for endocytic coated vesicle formation. *Current biology*, 8(25), pp.1399–402.

Kabsch, W., Mannherz, H.G., Suck, D., Pai, E.F. & Holmes, K.C., 1990. Atomic structure of the actin:DNase I complex. *Nature*, 347(6288), pp.37–44.

Kadota, K. & Kadota, T., 1973. Isolation of coated vesicles, plain synaptic vesicles, and flocculent material from a crude synaptosome fraction of guinea pig whole brain. *The Journal of cell biology*, 58(1), pp.135–51.

Kaksonen, M., Sun, Y. & Drubin, D.G., 2003. A pathway for association of receptors, adaptors, and actin during endocytic internalization. *Cell*, 115(4), pp.475–487.

Kaksonen, M., Toret, C.P. & Drubin, D.G., 2005. A modular design for the clathrin- and actin-mediated endocytosis machinery. *Cell*, 123(2), pp.305–20.

Kamioka, Y., Fukuhara, S., Sawa, H., Nagashima, K., Masuda, M., Matsuda, M. & Mochizuki, N., 2004. A novel dynamin-associating molecule, formin-binding protein 17, induces tubular membrane invaginations and participates in endocytosis. *The Journal of biological chemistry*, 279(38), pp.40091–9.

Kao, W.-T., Lin, C.-Y., Lee, L.-T., Lee, P.-P.H., Hung, C.-C., Lin, Y.-S., Chen, S.-H., Ke, F.-C., Lee, M.-T., et al. 2008. Investigation of MMP-2 and -9 in a highly invasive A431 tumor cell sub-line selected from a Boyden chamber assay. *Anticancer research*, 28(4B), pp.2109–20.

Kenniston, J.A. & Lemmon, M.A., 2010. Dynamin GTPase regulation is altered by PH domain mutations found in centronuclear myopathy patients. *The EMBO journal*, 29(18), pp.3054–67.

Kessels, M.M., Engqvist-Goldstein, A.E. & Drubin, D.G., 2000. Association of mouse actin-binding protein 1 (mAbp1/SH3P7), an Src kinase target, with dynamic regions of the cortical actin cytoskeleton in response to Rac1 activation. *Molecular biology of the cell*, 11(1), pp.393–412.

Kessels, M.M., Engqvist-Goldstein, A.E., Drubin, D.G. & Qualmann, B., 2001. Mammalian Abp1, a signal-responsive F-actin-binding protein, links the actin cytoskeleton to endocytosis via the GTPase dynamin. *The Journal of cell biology*, 153(2), pp.351–66.

Kilmartin, J. V & Adams, A.E., 1984. Structural rearrangements of tubulin and actin during the cell cycle of the yeast Saccharomyces. *The Journal of cell biology*, 98(3), pp.922–33.

Kim, B.-K., Seu, Y.-B., Bae, Y.-U., Kwak, T.-W., Kang, H., Moon, I.-J., Hwang, G.-B., Park, S.-Y. & Doh, K.-O., 2014. Efficient delivery of plasmid DNA using cholesterol-based cationic lipids containing polyamines and ether linkages. *International journal of molecular sciences*, 15(5), pp.7293–312.

Kirchhausen, T., 2000. Clathrin. *Annual review of biochemistry*, 69, pp.699–727.

Kirchhausen, T., Owen, D. & Harrison, S.C., 2014. Molecular structure, function, and dynamics of clathrin-mediated membrane traffic. *Cold Spring Harbor perspectives in biology*, 6(5), p.a016725.

van der Klei, I.J. & Veenhuis, M., 1997. Yeast peroxisomes: function and biogenesis of a versatile cell organelle. *Trends in microbiology*, 5(12), pp.502–9.

Klein, D.E., Lee, A., Frank, D.W., Marks, M.S. & Lemmon, M.A., 1998. The pleckstrin homology domains of dynamin isoforms require oligomerization for high affinity phosphoinositide binding. *The Journal of biological chemistry*, 273(42), pp.27725–33.

Konopka, C.A., Schleede, J.B., Skop, A.R. & Bednarek, S.Y., 2006. Dynamin and cytokinesis. *Traffic*, 7(3), pp.239–47.

Korn, E.D., Carlier, M.F. & Pantaloni, D., 1987. Actin polymerization and ATP hydrolysis. *Science*, 238(4827), pp.638–44.

Kosaka, T. & Ikeda, K., 1983. Reversible blockage of membrane retrieval and endocytosis in the garland cell of the temperature-sensitive mutant of Drosophila melanogaster, shibirets1. *The Journal of cell biology*, 97(2), pp.499–507.

Kowalski, J.R., Egile, C., Gil, S., Snapper, S.B., Li, R. & Thomas, S.M., 2005. Cortactin regulates cell migration through activation of N-WASP. *Journal of cell science*, 118, pp.79–87.

Kreitzer, G., Marmorstein, A., Okamoto, P., Vallee, R. & Rodriguez-Boulan, E., 2000. Kinesin and dynamin are required for post-Golgi transport of a plasma-membrane protein. *Nature cell biology*, 2(2), pp.125–7.

Krueger, E.W., Orth, J.D., Cao, H. & McNiven, M.A., 2003. A dynamin-cortactin-Arp2/3 complex mediates actin reorganization in growth factor-stimulated cells. *Molecular biology of the cell*, 14(3), pp.1085–96.

Kübler, E. & Riezman, H., 1993. Actin and fimbrin are required for the internalization step of endocytosis in yeast. *The EMBO journal*, 12(7), pp.2855–62.

Kuhn, J.R. & Pollard, T.D., 2005. Real-time measurements of actin filament polymerization by total internal reflection fluorescence microscopy. *Biophysical journal*, 88(2), pp.1387–402.

Kukulski, W., Schorb, M., Kaksonen, M. & Briggs, J.A.G., 2012. Plasma membrane reshaping during endocytosis is revealed by time-resolved electron tomography. *Cell*, 150(3), pp.508–20.

Kulkarni, A., Alpadi, K., Sirupangi, T. & Peters, C., 2014. A dynamin homolog promotes the transition from hemifusion to content mixing in intracellular membrane fusion. *Traffic*, 15(5), pp.558–71.

Kuravi, K., Nagotu, S., Krikken, A.M., Sjollema, K., Deckers, M., Erdmann, R., Veenhuis, M. & van der Klei, I.J., 2006. Dynamin-related proteins Vps1p and Dnm1p control peroxisome abundance in Saccharomyces cerevisiae. *Journal of cell science*, 119, pp.3994–4001.

Kurklinsky, S., Chen, J. & McNiven, M.A., 2011. Growth cone morphology and spreading are regulated by a dynamin-cortactin complex at point contacts in hippocampal neurons. *Journal of neurochemistry*, 117(1), pp.48–60.

De La Cruz, E.M., 2005. Cofilin binding to muscle and non-muscle actin filaments: isoform-dependent cooperative interactions. *Journal of molecular biology*, 346(2), pp.557–64.

Lamaze, C., Dujeancourt, A., Baba, T., Lo, C.G., Benmerah, A. & Dautry-Varsat, A., 2001. Interleukin 2 receptors and detergent-resistant membrane domains define a clathrin-independent endocytic pathway. *Molecular cell*, 7(3), pp.661–71.

Lappalainen, P., Kessels, M.M., Cope, M.J. & Drubin, D.G., 1998. The ADF homology (ADF-H) domain: a highly exploited actin-binding module. *Molecular biology of the cell*, 9(8), pp.1951–9.

Larsson, H. & Lindberg, U., 1988. The effect of divalent cations on the interaction between calf spleen profilin and different actins. *Biochimica et biophysica acta*, 953(1), pp.95–105.

Lee, A., Frank, D.W., Marks, M.S. & Lemmon, M.A., 1999. Dominant-negative inhibition of receptor-mediated endocytosis by a dynamin-1 mutant with a defective pleckstrin homology domain. *Current biology*, 9(5), pp.261–4.

Lee, D.-W., Wu, X., Eisenberg, E. & Greene, L.E., 2006. Recruitment dynamics of GAK and auxilin to clathrin-coated pits during endocytosis. *Journal of cell science*, 119, pp.3502–12.

Lee, E. & De Camilli, P., 2002. Dynamin at actin tails. *Proceedings of the National Academy of Sciences of the United States of America*, 99, pp.161–166.

Lees, J.G., Gorgani, N.N., Ammit, A.J., McCluskey, A., Robinson, P.J. & O'Neill, G.M., 2015. Role of dynamin in elongated cell migration in a 3D matrix. *Biochimica et biophysica acta*, 1854(3), pp.611–8.

Leonard, M., Song, B.D., Ramachandran, R. & Schmid, S.L., 2005. Robust colorimetric assays for dynamin's basal and stimulated GTPase activities. *Methods in enzymology*, 404, pp.490–503.

Lewis, M.J., Nichols, B.J., Prescianotto-Baschong, C., Riezman, H. & Pelham, H.R., 2000. Specific retrieval of the exocytic SNARE Snc1p from early yeast endosomes. *Molecular biology of the cell*, 11(1), pp.23–38.

Li, R., 1997. Bee1, a yeast protein with homology to Wiscott-Aldrich syndrome protein, is critical for the assembly of cortical actin cytoskeleton. *The Journal of cell biology*, 136(3), pp.649–58.

Lim, J.P. & Gleeson, P.A., 2011. Macropinocytosis: an endocytic pathway for internalising large gulps. *Immunology and cell biology*, 89(8), pp.836–43.

Linder, S., 2009. Invadosomes at a glance. *Journal of cell science*, 122, pp.3009–13.

Linder, S., Wiesner, C. & Himmel, M., 2011. Degrading devices: invadosomes in proteolytic cell invasion. *Annual review of cell and developmental biology*, 27, pp.185–211.

Liu, H.P. & Bretscher, A., 1989. Disruption of the single tropomyosin gene in yeast results in the disappearance of actin cables from the cytoskeleton. *Cell*, 57(2), pp.233–42.

Liu, Y.-W., Lukiyanchuk, V. & Schmid, S.L., 2011a. Common membrane trafficking defects of disease-associated dynamin 2 mutations. *Traffic*, 12(11), pp.1620–33.

Liu, Y.-W., Neumann, S., Ramachandran, R., Ferguson, S.M., Pucadyil, T.J. & Schmid, S.L., 2011b. Differential curvature sensing and generating activities of dynamin isoforms provide opportunities for tissue-specific regulation. *Proceedings of the National Academy of Sciences of the United States of America*, 108(26), pp.E234–42.

Liu, Y.-W., Surka, M.C., Schroeter, T., Lukiyanchuk, V. & Schmid, S.L., 2008. Isoform and splice-variant specific functions of dynamin-2 revealed by analysis of conditional knock-out cells. *Molecular biology of the cell*, 19(12), pp.5347–59.

Liu, Z., Pan, Q., Ding, S., Qian, J., Xu, F., Zhou, J., Cen, S., Guo, F. & Liang, C., 2013. The interferon-inducible MxB protein inhibits HIV-1 infection. *Cell host & microbe*, 14(4), pp.398–410.

Lukehart, J., Highfill, C. & Kim, K., 2013. Vps1, a recycling factor for the traffic from early endosome to the late Golgi. *Biochemistry and cell biology*, 91(6), pp.455–65.

Lundmark, R. & Carlsson, S.R., 2004. Regulated membrane recruitment of dynamin-2 mediated by sorting nexin 9. *The Journal of biological chemistry*, 279(41), pp.42694–702.

Lundmark, R. & Carlsson, S.R., 2009. SNX9 - a prelude to vesicle release. *Journal of cell science*, 122, pp.5–11.

Lundmark, R. & Carlsson, S.R., 2003. Sorting nexin 9 participates in clathrin-mediated endocytosis through interactions with the core components. *The Journal of biological chemistry*, 278(47), pp.46772–81.

Luxenburg, C., Geblinger, D., Klein, E., Anderson, K., Hanein, D., Geiger, B. & Addadi, L., 2007. The architecture of the adhesive apparatus of cultured osteoclasts: from podosome formation to sealing zone assembly. *PloS one*, 2(1), p.e179.

Macia, E., Ehrlich, M., Massol, R., Boucrot, E., Brunner, C. & Kirchhausen, T., 2006. Dynasore, a cell-permeable inhibitor of dynamin. *Developmental cell*, 10(6), pp.839–50.

MacLean-Fletcher, S.D. & Pollard, T.D., 1980. Viscometric analysis of the gelation of Acanthamoeba extracts and purification of two gelation factors. *The Journal of cell biology*, 85(2), pp.414–28.

Mannherz, H.G., Goody, R.S., Konrad, M. & Nowak, E., 1980. The interaction of bovine pancreatic deoxyribonuclease I and skeletal muscle actin. *European journal of biochemistry / FEBS*, 104(2), pp.367–79.

Mayor, S. & Pagano, R.E., 2007. Pathways of clathrin-independent endocytosis. *Nature reviews. Molecular cell biology*, 8(8), pp.603–12.

McCann, R.O. & Craig, S.W., 1997. The I/LWEQ module: a conserved sequence that signifies F-actin binding in functionally diverse proteins from yeast to mammals. *Proceedings of the National Academy of Sciences of the United States of America*, 94(11), pp.5679–84.

McGough, A., Pope, B., Chiu, W. & Weeds, A., 1997. Cofilin changes the twist of F-actin: implications for actin filament dynamics and cellular function. *The Journal of cell biology*, 138(4), pp.771–781.

McNiven, M.A., 1998. Dynamin: a molecular motor with pinchase action. *Cell*, 94(2), pp.151–4.

McNiven, M.A., Kim, L., Krueger, E.W., Orth, J.D., Cao, H. & Wong, T.W., 2000. Regulated interactions between dynamin and the actin-binding protein cortactin modulate cell shape. *The Journal of cell biology*, 151(1), pp.187–98.

McWilliam, H., Li, W., Uludag, M., Squizzato, S., Park, Y.M., Buso, N., Cowley, A.P. & Lopez, R., 2013. Analysis Tool Web Services from the EMBL-EBI. *Nucleic acids research*, 41, pp.597–600.

Mears, J.A., Lackner, L.L., Fang, S., Ingerman, E., Nunnari, J. & Hinshaw, J.E., 2011. Conformational changes in Dnm1 support a contractile mechanism for mitochondrial fission. *Nature structural & molecular biology*, 18(1), pp.20–6.

Meglei, G. & McQuibban, G.A., 2009. The dynamin-related protein Mgm1p assembles into oligomers and hydrolyzes GTP to function in mitochondrial membrane fusion. *Biochemistry*, 48(8), pp.1774–84.

Mehrotra, N., Nichols, J. & Ramachandran, R., 2014. Alternate pleckstrin homology domain orientations regulate dynamin-catalyzed membrane fission. *Molecular biology of the cell*, 25(6), pp.879–90.

Meinecke, M., Boucrot, E., Camdere, G., Hon, W.-C.C., Mittal, R. & McMahon, H.T., 2013. Cooperative recruitment of dynamin and BIN/Amphiphysin/Rvs (BAR) domain-containing proteins leads to GTP-dependent membrane scission. *Journal of Biological Chemistry*, 288(9), pp.6651–61.

Menon, M., Askinazi, O.L. & Schafer, D., 2014. Dynamin2 organizes lamellipodial actin networks to orchestrate lamellar actomyosin. *PloS one*, 9(4), p.e94330.

Menon, M. & Schafer, D., 2013. Dynamin: Expanding Its Scope to the Cytoskeleton, *International Review of Molecular and Cell biology,* 302, pp. 187

Merrifield, C.J., Feldman, M.E., Wan, L. & Almers, W., 2002. Imaging actin and dynamin recruitment during invagination of single clathrin-coated pits. *Nature cell biology*, 4, pp.691–8.

Merrifield, C.J. & Kaksonen, M., 2014. Endocytic accessory factors and regulation of clathrin-mediated endocytosis. *Cold Spring Harbor perspectives in biology*, 6(11), pp 16733.

Merrifield, C.J., Perrais, D. & Zenisek, D., 2005. Coupling between clathrin-coated-pit invagination, cortactin recruitment, and membrane scission observed in live cells. *Cell*, 121(4), pp.593–606.

Merrifield, C.J., Qualmann, B., Kessels, M.M. & Almers, W., 2004. Neural Wiskott Aldrich Syndrome Protein (N-WASP) and the Arp2/3 complex are recruited to sites of clathrin-mediated endocytosis in cultured fibroblasts. *European journal of cell biology*, 83(1), pp.13–8.

Mishra, R., Smaczynska-de Rooij, I.I., Goldberg, M.W. & Ayscough, K.R., 2011. Expression of Vps1 I649K a self-assembly defective yeast dynamin, leads to formation of extended endocytic invaginations. *Communicative & integrative biology*, 4, pp.115–117.

Mooren, O.L., Galletta, B.J. & Cooper, J.A., 2012. Roles for actin assembly in endocytosis. *Annual review of biochemistry*, 81, pp.661–86.

Mooren, O.L., Kotova, T.I., Moore, A.J. & Schafer, D., 2009. Dynamin2 GTPase and cortactin remodel actin filaments. *Journal of Biological Chemistry*, 284(36), pp.23995–4005.

Moreau, V., Galan, J.M., Devilliers, G., Haguenauer-Tsapis, R. & Winsor, B., 1997. The yeast actin-related protein Arp2p is required for the internalization step of endocytosis. *Molecular biology of the cell*, 8(7), pp.1361–75.

Moreira, K.E., Schuck, S., Schrul, B., Fröhlich, F., Moseley, J.B., Walther, T.C. & Walter, P., 2012. Seg1 controls eisosome assembly and shape. *The Journal of cell biology*, 198(3), pp.405–20.

Morlot, S., Galli, V., Klein, M., Chiaruttini, N., Manzi, J., Humbert, F., Dinis, L., Lenz, M., … Roux, A., 2012. Membrane shape at the edge of the dynamin helix sets location and duration of the fission reaction. *Cell*, 151(3), pp.619–29.

Motley, A.M. & Hettema, E.H., 2007. Yeast peroxisomes multiply by growth and division. *Journal of Cell Biology*, 178(3), pp.399–410.

Mukherjee, S., Ghosh, R.N. & Maxfield, F.R., 1997. Endocytosis. *Physiological reviews*, 77(3), pp.759–803.

Munn, A.L., Stevenson, B.J., Geli, M.I. & Riezman, H., 1995. end5, end6, and end7: mutations that cause actin delocalization and block the internalization step of endocytosis in Saccharomyces cerevisiae. *Molecular biology of the cell*, 6(12), pp.1721–42.

Nakata, T., Iwamoto, A., Noda, Y., Takemura, R., Yoshikura, H. & Hirokawa, N., 1991. Predominant and developmentally regulated expression of dynamin in neurons. *Neuron*, 7(3), pp.461–9.

Nakata, T., Takemura, R. & Hirokawa, N., 1993. A novel member of the dynamin family of GTP-binding proteins is expressed specifically in the testis. *Journal of cell science*, 105, pp.1–5.

Nannapaneni, S., Wang, D., Jain, S., Schroeder, B., Highfill, C., Reustle, L., Pittsley, D., Maysent, A., Kim, K., et al. 2010. The yeast dynamin-like protein Vps1:vps1 mutations perturb the internalization and the motility of endocytic vesicles and endosomes via disorganization of the actin cytoskeleton. *European journal of cell biology*, 89(7), pp.499–508.

Navarro, P., Durrens, P. & Aigle, M., 1997. Protein-protein interaction between the RVS161 and RVS167 gene products of Saccharomyces cerevisiae. *Biochimica et biophysica acta*, 1343(2), pp.187–92.

Newpher, T.M. & Lemmon, S.K., 2006. Clathrin is important for normal actin dynamics and progression of Sla2p-containing patches during endocytosis in yeast. *Traffic*, 7(5), pp.574–88.

Newpher, T.M., Smith, R.P., Lemmon, V. & Lemmon, S.K., 2005. In vivo dynamics of clathrin and its adaptor-dependent recruitment to the actin-based endocytic machinery in yeast. *Developmental cell*, 9(1), pp.87–98.

Nothwehr, S.F., Conibear, E. & Stevens, T.H., 1995. Golgi and vacuolar membrane proteins reach the vacuole in vps1 mutant yeast cells via the plasma membrane. *The Journal of cell biology*, 129(1), pp.35–46.

Nürnberg, S.T., Rendon, A., Smethurst, P.A., Paul, D.S., Voss, K., Thon, J.N., Lloyd-Jones, H., Sambrook, J.G., Ouwehand, W.H., et al. 2012. A GWAS sequence variant for platelet volume marks an alternative DNM3 promoter in megakaryocytes near a MEIS1 binding site. *Blood*, 120(24), pp.4859–68.

Obar, R.A., Collins, C.A., Hammarback, J.A., Shpetner, H.S. & Vallee, R.B., 1990. Molecular cloning of the microtubule-associated mechanochemical enzyme dynamin reveals homology with a new family of GTP-binding proteins. *Nature*, 347(6290), pp.256–61.

Ochoa, G.C., Slepnev, V.I., Neff, L., Ringstad, N., Takei, K., Daniell, L., Kim, W., Cao, H., De Camilli, P., et al. 2000. A functional link between dynamin and the actin cytoskeleton at podosomes. *Journal of Cell Biology*, 150(2), pp.377–389.

Oda, T., Iwasa, M., Aihara, T., Maéda, Y. & Narita, A., 2009. The nature of the globular- to fibrous-actin transition. *Nature*, 457(7228), pp.441–5.

Odell, L.R., Chau, N., Mariana, A., Graham, M.E., Robinson, P.J. & McCluskey, A., 2009. Azido and diazarinyl analogues of bis-tyrphostin as asymmetrical inhibitors of dynamin GTPase. *ChemMedChem*, 4(7), pp.1182–8.

Okamoto, P.M., Herskovits, J.S. & Vallee, R.B., 1997. Role of the basic, proline-rich region of dynamin in Src homology 3 domain binding and endocytosis. *The Journal of biological chemistry*, 272(17), pp.11629–35.

Orth, J.D., Krueger, E.W., Cao, H. & McNiven, M.A., 2002. The large GTPase dynamin regulates actin comet formation and movement in living cells. *Proceedings of the National Academy of Sciences*, 99(1), pp.167–172.

Oser, M., Yamaguchi, H., Mader, C.C., Bravo-Cordero, J.J., Arias, M., Chen, X., Desmarais, V., van Rheenen, J., Condeelis, J., 2009. Cortactin regulates cofilin and N-WASp activities to control the stages of invadopodium assembly and maturation. *The Journal of cell biology*, 186(4), pp.571–87.

Ozyamak, E., Kollman, J., Agard, D.A. & Komeili, A., 2013. The bacterial actin MamK: in vitro assembly behavior and filament architecture. *The Journal of biological chemistry*, 288(6), pp.4265–77.

Palmer, S.E., Smaczynska-de Rooij, I.I., Marklew, C.J., Allwood, E.G., Mishra, R., Goldberg, M.W. & Ayscough, K.R., 2015a. A Charge Swap mutation E461K in the yeast dynamin Vps1 reduces endocytic invagination. *Communicative & Integrative Biology*, 8(4), p.e1051274.

Palmer, S.E., Smaczynska-de Rooij, I.I., Marklew, C.J., Allwood, E.G., Mishra, R., Johnson, S., Goldberg, M.W. & Ayscough, K.R., 2015b. A Dynamin-Actin Interaction Is Required for Vesicle Scission during Endocytosis in Yeast. *Current Biology*, 25(7), pp.868–78.

Park, R.J., Shen, H., Liu, L., Liu, X., Ferguson, S.M. & De Camilli, P., 2013. Dynamin triple knockout cells reveal off target effects of commonly used dynamin inhibitors. *Journal of cell science*, 126, pp.5305–12.

Parton, R.G. & Simons, K., 2007. The multiple faces of caveolae. *Nature reviews. Molecular cell biology*, 8(3), pp.185–94.

Payne, G.S. & Schekman, R., 1985. A test of clathrin function in protein secretion and cell growth. *Science*, 230(4729), pp.1009–14.

Pearse, B.M., 1976. Clathrin: a unique protein associated with intracellular transfer of membrane by coated vesicles. *Proceedings of the National Academy of Sciences of the United States of America*, 73(4), pp.1255–1259.

Pearse, B.M. & Bretscher, M.S., 1981. Membrane recycling by coated vesicles. *Annual review of biochemistry*, 50, pp.85–101.

Pelkmans, L., Kartenbeck, J. & Helenius, A., 2001. Caveolar endocytosis of simian virus 40 reveals a new two-step vesicular-transport pathway to the ER. *Nature cell biology*, 3(5), pp.473–83.

Perrin, B.J. & Ervasti, J.M., 2010. The actin gene family: function follows isoform. *Cytoskeleton*, 67(10), pp.630–4.

Peter, B.J., Kent, H.M., Mills, I.G., Vallis, Y., Butler, P.J.G., Evans, P.R. & McMahon, H.T., 2004. BAR domains as sensors of membrane curvature: the amphiphysin BAR structure. *Science*, 303(5657), pp.495–9.

Di Pietro, S.M., Cascio, D., Feliciano, D., Bowie, J.U. & Payne, G.S., 2010. Regulation of clathrin adaptor function in endocytosis: novel role for the SAM domain. *The EMBO journal*, 29(6), pp.1033–44.

Poincloux, R., Lizárraga, F. & Chavrier, P., 2009. Matrix invasion by tumour cells: a focus on MT1-MMP trafficking to invadopodia. *Journal of cell science*, 122, pp.3015–24.

Popp, D. & Robinson, R.C., 2011. Many ways to build an actin filament. *Molecular Microbiology*, 80(2), pp.300–308.

Praefcke, G.J.K. & McMahon, H.T., 2004. The dynamin superfamily: universal membrane tubulation and fission molecules? *Nature reviews. Molecular cell biology*, 5(2), pp.133–47.

Prosser, D.C., Drivas, T.G., Maldonado-Báez, L. & Wendland, B., 2011. Existence of a novel clathrin-independent endocytic pathway in yeast that depends on Rho1 and formin. *The Journal of cell biology*, 195(4), pp.657–71.

Pruyne, D.W., Schott, D.H. & Bretscher, A., 1998. Tropomyosin-containing actin cables direct the Myo2p-dependent polarized delivery of secretory vesicles in budding yeast. *The Journal of cell biology*, 143(7), pp.1931–45.

Pucadyil, T.J. & Schmid, S.L., 2008. Real-time visualization of dynamin-catalyzed membrane fission and vesicle release. *Cell*, 135(7), pp.1263–75.

Qualmann, B., Roos, J., DiGregorio, P.J. & Kelly, R.B., 1999. Syndapin I, a synaptic dynamin-binding protein that associates with the neural Wiskott-Aldrich syndrome protein. *Molecular biology of the cell*, 10(2), pp.501–13.

Ramachandran, R., 2011. Vesicle scission: Dynamin. *Seminars in Cell and Developmental Biology*, 22(1), pp.10–17.

Ramachandran, R., Pucadyil, T.J., Liu, Y.-W., Acharya, S., Leonard, M., Lukiyanchuk, V. & Schmid, S.L., 2009. Membrane insertion of the pleckstrin homology domain variable loop 1 is critical for dynamin-catalyzed vesicle scission. *Molecular biology of the cell*, 20(22), pp.4630–9.

Ramachandran, R., Surka, M., Chappie, J.S., Fowler, D.M., Foss, T.R., Song, B.D. & Schmid, S.L., 2007. The dynamin middle domain is critical for tetramerization and higher-order self-assembly. *The EMBO journal*, 26(2), pp.559–66.

Rapoport, I., Miyazaki, M., Boll, W., Duckworth, B., Cantley, L.C., Shoelson, S. & Kirchhausen, T., 1997. Regulatory interactions in the recognition of endocytic sorting signals by AP-2 complexes. *The EMBO journal*, 16(9), pp.2240–50.

Raths, S., Rohrer, J., Crausaz, F. & Riezman, H., 1993. end3 and end4: two mutants defective in receptor-mediated and fluid-phase endocytosis in Saccharomyces cerevisiae. *The Journal of cell biology*, 120(1), pp.55–65.

Raymond, C.K., Howald-Stevenson, I., Vater, C.A. & Stevens, T.H., 1992. Morphological classification of the yeast vacuolar protein sorting mutants: evidence for a prevacuolar compartment in class E vps mutants. *Molecular biology of the cell*, 3(12), pp.1389–402.

Reems, J.-A., Wang, W., Tsubata, K., Abdurrahman, N., Sundell, B., Tijssen, M.R., van der Schoot, E., Di Summa, F., Gilligan, D.M., et al. 2008. Dynamin 3 participates in the growth and development of megakaryocytes. *Experimental hematology*, 36(12), pp.1714–27.

Reider, A., Barker, S.L., Mishra, S.K., Im, Y.J., Maldonado-Báez, L., Hurley, J.H., Traub, L.M. & Wendland, B., 2009. Syp1 is a conserved endocytic adaptor that contains domains involved in cargo selection and membrane tubulation. *The EMBO journal*, 28(20), pp.3103–16.

Reis, C.R., Chen, P.-H., Srinivasan, S., Aguet, F., Mettlen, M. & Schmid, S.L., 2015. Crosstalk between Akt/GSK3β signaling and dynamin-1 regulates clathrin-mediated endocytosis. *The EMBO journal*.

Renard, H.-F., Simunovic, M., Lemière, J., Boucrot, E., Garcia-Castillo, M.D., Arumugam, S., Chambon, V., Lamaze, C., Johannes, L., et al. 2014. Endophilin-A2 functions in membrane scission in clathrin-independent endocytosis. *Nature*, 517, pp. 493-496.

Reubold, T.F., Faelber, K., Plattner, N., Posor, Y., Ketel, K., Curth, U., Schlegel, J., Anand, R., Eschenburg, S., et al. 2015. Crystal structure of the dynamin tetramer. *Nature*, 525(7569), pp.404–8.

Robertson, A.S., Smythe, E. & Ayscough, K.R., 2009. Functions of actin in endocytosis. *Cellular and molecular life sciences*, 66(13), pp.2049–65.

Robinson, J.S., Klionsky, D.J., Banta, L.M. & Emr, S.D., 1988. Protein sorting in Saccharomyces cerevisiae: isolation of mutants defective in the delivery and processing of multiple vacuolar hydrolases. *Molecular and cellular biology*, 8(11), pp.4936–48.

Robinson, M.S., 2004. Adaptable adaptors for coated vesicles. *Trends in cell biology*, 14(4), pp.167–74.

Robinson, M.S., 2015. Forty Years of Clathrin-coated Vesicles. *Traffic,* 16(12) pp. 1210-38.

Rodal, A.A., Sokolova, O., Robins, D.B., Daugherty, K.M., Hippenmeyer, S., Riezman, H., Grigorieff, N. & Goode, B.L., 2005. Conformational changes in the Arp2/3 complex leading to actin nucleation. *Nature structural & molecular biology*, 12(1), pp.26–31.

van Rossum, A.G.S.H., de Graaf, J.H., Schuuring-Scholtes, E., Kluin, P.M., Fan, Y.-X., Zhan, X., Moolenaar, W.H. & Schuuring, E., 2003. Alternative splicing of the actin binding domain of human cortactin affects cell migration. *The Journal of biological chemistry*, 278(46), pp.45672–9.

Roth, T.F. & Porter, K.R., 1964. Yolk protein uptake in the oocyte of the mosquito aedes aegypti. *The Journal of cell biology*, 20, pp.313–32.

Rothman, J.E. & Schmid, S.L., 1986. Enzymatic recycling of clathrin from coated vesicles. *Cell*, 46(1), pp.5–9.

Rothman, J.H., Howald, I. & Stevens, T.H., 1989. Characterization of genes required for protein sorting and vacuolar function in the yeast Saccharomyces cerevisiae. *The EMBO journal*, 8(7), pp.2057–2065.

Rothman, J.H., Raymond, C.K., Gilbert, T., O'Hara, P.J. & Stevens, T.H., 1990. A putative GTP binding protein homologous to interferon-inducible Mx proteins performs an essential function in yeast protein sorting. *Cell*, 61(6), pp.1063–74.

Rothman, J.H. & Stevens, T.H., 1986. Protein sorting in yeast: mutants defective in vacuole biogenesis mislocalize vacuolar proteins into the late secretory pathway. *Cell*, 47(6), pp.1041–51.

Roux, A., Uyhazi, K., Frost, A. & De Camilli, P., 2006. GTP-dependent twisting of dynamin implicates constriction and tension in membrane fission. *Nature*, 441(7092), pp.528–31.

Rozelle, A.L., Machesky, L.M., Yamamoto, M., Driessens, M.H.E., Insall, R.H., Roth, M.G., Luby-Phelps, K., Marriott, G., Yin, H.L., et al. 2000. Phosphatidylinositol 4,5-bisphosphate induces actin-based movement of raft-enriched vesicles through WASP-Arp2/3. *Current Biology*, 10(6), pp.311–320.

Saheki, Y. & De Camilli, P., 2012. Synaptic vesicle endocytosis. *Cold Spring Harbor perspectives in biology*, 4(9), p.a005645.

Saint-Pol, A., Yélamos, B., Amessou, M., Mills, I.G., Dugast, M., Tenza, D., Schu, P., Antony, C., Johannes, L., et al. 2004. Clathrin adaptor epsinR is required for retrograde sorting on early endosomal membranes. *Developmental cell*, 6(4), pp.525–38.

Salim, K., Bottomley, M.J., Querfurth, E., Zvelebil, M.J., Gout, I., Scaife, R., Margolis, R.L., Gigg, R., Panayotou, G., et al. 1996. Distinct specificity in the recognition of phosphoinositides by the pleckstrin homology domains of dynamin and Bruton's tyrosine kinase. *The EMBO journal*, 15(22), pp.6241–50.

Salisbury, J.L., Condeelis, J.S. & Satir, P., 1980. Role of coated vesicles, microfilaments, and calmodulin in receptor-mediated endocytosis by cultured B lymphoblastoid cells. *The Journal of cell biology*, 87(1), pp.132–41.

Santolini, E., Salcini, A.E., Kay, B.K., Yamabhai, M. & Di Fiore, P.P., 1999. The EH network. *Experimental cell research*, 253(1), pp.186–209.

Schafer, D., Weed, S., Binns, D., Karginov, A. V., Parsons, J.T. & Cooper, J. A., 2002. Dynamin2 and cortactin regulate actin assembly and filament organization. *Current Biology*, 12(02), pp.1852–1857.

Schiffer, M., Teng, B., Gu, C., Shchedrina, V.A., Kasaikina, M., Pham, V.A., Hanke, N., Rong, S., Sever, S., et al. 2015. Pharmacological targeting of actin-dependent dynamin oligomerization ameliorates chronic kidney disease in diverse animal models. *Nature medicine*, 21(6), pp.601–9.

Schneider, C.A., Rasband, W.S. & Eliceiri, K.W., 2012. NIH Image to ImageJ: 25 years of image analysis. *Nature methods*, 9(7), pp.671–5.

Scott, C.C., Vacca, F. & Gruenberg, J., 2014. Endosome maturation, transport and functions. *Seminars in cell & developmental biology*, 31, pp.2–10.

Sekiya-Kawasaki, M., Groen, A.C., Cope, M.J.T. V, Kaksonen, M., Watson, H.A., Zhang, C., Shokat, K.M., Wendland, B., Drubin, D.G., et al. 2003. Dynamic phosphoregulation of the cortical actin cytoskeleton and endocytic machinery revealed by real-time chemical genetic analysis. *The Journal of cell biology*, 162(5), pp.765–72.

Semerdjieva, S., Shortt, B., Maxwell, E., Singh, S., Fonarev, P., Hansen, J., Schiavo, G., Grant, B.D. & Smythe, E., 2008. Coordinated regulation of AP2 uncoating from clathrin-coated vesicles by rab5 and hRME-6. *The Journal of cell biology*, 183(3), pp.499–511.

Sever, S., Muhlberg, A.B. & Schmid, S.L., 1999. Impairment of dynamin's GAP domain stimulates receptor-mediated endocytosis. *Nature*, 398(6727), pp.481–6.

Sever, S., Skoch, J., Newmyer, S., Ramachandran, R., Ko, D., McKee, M., Bouley, R., Ausiello, D., Bacskai, B.J., et al. 2006. Physical and functional connection between auxilin and dynamin during endocytosis. *The EMBO journal*, 25(18), pp.4163–74.

Shin, N., Ahn, N., Chang-Ileto, B., Park, J., Takei, K., Ahn, S.-G., Kim, S.-A., Di Paolo, G. & Chang, S., 2008. SNX9 regulates tubular invagination of the plasma membrane through interaction with actin cytoskeleton and dynamin 2. *Journal of cell science*, 121, pp.1252–63.

Shpetner, H.S., Herskovits, J.S. & Vallee, R.B., 1996. A binding site for SH3 domains targets dynamin to coated pits. *The Journal of biological chemistry*, 271(1), pp.13–6.

Shpetner, H.S. & Vallee, R.B., 1989. Identification of dynamin, a novel mechanochemical enzyme that mediates interactions between microtubules. *Cell*, 59(3), pp.421–32.

Singer-Krüger, B., Nemoto, Y., Daniell, L., Ferro-Novick, S. & De Camilli, P., 1998. Synaptojanin family members are implicated in endocytic membrane traffic in yeast. *Journal of cell science*, 111, pp.3347–56.

Siverira, L., Wong, D., Masiarz, F. & Schekman, R., 1990. Yeast clathrin has a distinctive light chain that is important for cell growth. *The Journal of Cell Biology*, 111(4), p.1437.

Skruzny, M., Brach, T., Ciuffa, R., Rybina, S., Wachsmuth, M. & Kaksonen, M., 2012. Molecular basis for coupling the plasma membrane to the actin cytoskeleton during clathrin-mediated endocytosis. *Proceedings of the National Academy of Sciences of the United States of America*, 109(38), pp.2533–42.

Skruzny, M., Desfosses, A., Prinz, S., Dodonova, S.O., Gieras, A., Uetrecht, C., Jakobi, A.J., Abella, M., Kaksonen, M., et al. 2015. An Organized Co-assembly of Clathrin Adaptors Is Essential for Endocytosis. *Developmental cell*, 33(2), pp.150–62.

Smaczynska-de Rooij, I.I., Allwood, E.G., Aghamohammadzadeh, S., Hettema, E.H., Goldberg, M.W. & Ayscough, K.R., 2010. A role for the dynamin-like protein Vps1 during endocytosis in yeast. *Journal of cell science*, 123, pp.3496–3506.

Smaczynska-de Rooij, I.I., Allwood, E.G., Mishra, R., Booth, W.I., Aghamohammadzadeh, S., Goldberg, M.W. & Ayscough, K.R., 2012. Yeast Dynamin Vps1 and Amphiphysin Rvs167 Function Together During Endocytosis. *Traffic*, 13, pp.317–328.

Smirnova, E., Griparic, L., Shurland, D.L. & van der Bliek, A.M., 2001. Dynamin-related protein Drp1 is required for mitochondrial division in mammalian cells. *Molecular biology of the cell*, 12(8), pp.2245–56.

Smirnova, E., Shurland, D.L., Ryazantsev, S.N. & van der Bliek, A.M., 1998. A human dynamin-related protein controls the distribution of mitochondria. *The Journal of cell biology*, 143(2), pp.351–8.

Smythe, E. & Ayscough, K.R., 2006. Actin regulation in endocytosis. *Journal of cell science*, 119, pp.4589–4598.

Smythe, E. & Ayscough, K.R., 2003. The Ark1/Prk1 family of protein kinases. Regulators of endocytosis and the actin skeleton. *EMBO reports*, 4(3), pp.246–51.

Smythe, E., Smith, P.D., Jacob, S.M., Theobald, J. & Moss, S.E., 1994. Endocytosis occurs independently of annexin VI in human A431 cells. *The Journal of cell biology*, 124(3), pp.301–6.

Song, B.D., Yarar, D. & Schmid, S.L., 2004. An assembly-incompetent mutant establishes a requirement for dynamin self-assembly in clathrin-mediated endocytosis in vivo. *Molecular biology of the cell*, 15(5), pp.2243–52.

Soulet, F., Yarar, D., Leonard, M. & Schmid, S.L., 2005. SNX9 regulates dynamin assembly and is required for efficient clathrin-mediated endocytosis. *Molecular biology of the cell*, 16(4), pp.2058–67.

Spence, H.J., Timpson, P., Tang, H.R., Insall, R.H. & Machesky, L.M., 2012. Scar/WAVE3 contributes to motility and plasticity of lamellipodial dynamics but not invasion in three dimensions. *The Biochemical journal*, 448(1), pp.35–42.

Spudich, J.A. & Watt, S., 1971. The regulation of rabbit skeletal muscle contraction. I. Biochemical studies of the interaction of the tropomyosin-troponin complex with actin and the proteolytic fragments of myosin. *The Journal of biological chemistry*, 246(15), pp.4866–71.

Srinivasan, S., Seaman, M., Nemoto, Y., Daniell, L., Suchy, S.F., Emr, S., De Camilli, P. & Nussbaum, R., 1997. Disruption of three phosphatidylinositol-polyphosphate 5-phosphatase genes from Saccharomyces cerevisiae results in pleiotropic abnormalities of vacuole morphology, cell shape, and osmohomeostasis. *European journal of cell biology*, 74(4), pp.350–60.

Stamenova, S.D., Dunn, R., Adler, A.S. & Hicke, L., 2004. The Rsp5 ubiquitin ligase binds to and ubiquitinates members of the yeast CIN85-endophilin complex, Sla1-Rvs167. *The Journal of biological chemistry*, 279(16), pp.16017–25.

Stefan, C.J., Audhya, A. & Emr, S.D., 2002. The yeast synaptojanin-like proteins control the cellular distribution of phosphatidylinositol (4,5)-bisphosphate. *Molecular biology of the cell*, 13(2), pp.542–57.

Steinmetz, M.O., Goldie, K.N. & Aebi, U., 1997. A correlative analysis of actin filament assembly, structure, and dynamics. *The Journal of cell biology*, 138(3), pp.559–74.

Stevenson, R.P., Veltman, D. & Machesky, L.M., 2012. Actin-bundling proteins in cancer progression at a glance. *Journal of cell science*, 125, pp.1073–9.

Stimpson, H.E.M., Toret, C.P., Cheng, A.T., Pauly, B.S. & Drubin, D.G., 2009. Early-arriving Syp1p and Ede1p function in endocytic site placement and formation in budding yeast. *Molecular biology of the cell*, 20(22), pp.4640–51.

Sun, Y., Carroll, S., Kaksonen, M., Toshima, J.Y. & Drubin, D.G., 2007. PtdIns(4,5)P2 turnover is required for multiple stages during clathrin- and actin-dependent endocytic internalization. *The Journal of cell biology*, 177(2), pp.355–67.

Sun, Y. & Drubin, D.G., 2012. The functions of anionic phospholipids during clathrin-mediated endocytosis site initiation and vesicle formation. *Journal of cell science*, 125, pp.6157–65.

Sun, Y., Kaksonen, M., Madden, D.T., Schekman, R. & Drubin, D.G., 2005. Interaction of Sla2p's ANTH domain with PtdIns(4,5)P2 is important for actin-dependent endocytic internalization. *Molecular biology of the cell*, 16(2), pp.717–30.

Sun, Y., Martin, A.C. & Drubin, D.G., 2006. Endocytic internalization in budding yeast requires coordinated actin nucleation and myosin motor activity. *Developmental cell*, 11(1), pp.33–46.

Sweitzer, S.M. & Hinshaw, J.E., 1998. Dynamin undergoes a GTP-dependent conformational change causing vesiculation. *Cell*, 93(6), pp.1021–9.

Szent-Györgyi, A.G., 2004. The early history of the biochemistry of muscle contraction. *The Journal of general physiology*, 123(6), pp.631–41.

Takei, K., Haucke, V., Slepnev, V., Farsad, K., Salazar, M., Chen, H. & De Camilli, P., 1998. Generation of coated intermediates of clathrin-mediated endocytosis on protein-free liposomes. *Cell*, 94(1), pp.131–41.

Tanabe, K. & Takei, K., 2012. Dynamin 2 in Charcot-Marie-Tooth disease. *Acta medica Okayama*, 66(3), pp.183–90.

Tang, H.Y. & Cai, M., 1996. The EH-domain-containing protein Pan1 is required for normal organization of the actin cytoskeleton in Saccharomyces cerevisiae. *Molecular and cellular biology*, 16(9), pp.4897–914.

Tang, H.Y., Xu, J. & Cai, M., 2000. Pan1p, End3p, and S1a1p, three yeast proteins required for normal cortical actin cytoskeleton organization, associate with each other and play essential roles in cell wall morphogenesis. *Molecular and cellular biology*, 20(1), pp.12–25.

Tang, J.X., Szymanski, P.T., Janmey, P.A. & Tao, T., 1997. Electrostatic Effects of Smooth Muscle Calponin on Actin Assembly. *European Journal of Biochemistry*, 247(1), pp.432–440.

Tanifuji, S., Funakoshi-Tago, M., Uedas, F., Kasaharas, T. & Mochida, S., 2013. Dynamin isoforms decode action potential firing for synaptic vesicle recycling. *Journal of Biological Chemistry*, 288, pp.19050–19059.

Tarone, G., Cirillo, D., Giancotti, F.G., Comoglio, P.M. & Marchisio, P.C., 1985. Rous sarcoma virus-transformed fibroblasts adhere primarily at discrete protrusions of the ventral membrane called podosomes. *Experimental cell research*, 159(1), pp.141–57.

Taylor, M.J., Lampe, M. & Merrifield, C.J., 2012. A feedback loop between dynamin and actin recruitment during clathrin-mediated endocytosis. *PLoS Biology*, 10(4).

Taylor, M.J., Perrais, D. & Merrifield, C.J., 2011. A high precision survey of the molecular dynamics of mammalian clathrin-mediated endocytosis. *PLoS Biology*, 9(3).

Thompson, H.M., Skop, A.R., Euteneuer, U., Meyer, B.J. & McNiven, M.A., 2002. The large GTPase dynamin associates with the spindle midzone and is required for cytokinesis. *Current biology*, 12(24), pp.2111–7.

Toret, C.P., Lee, L., Sekiya-Kawasaki, M. & Drubin, D.G., 2008. Multiple pathways regulate endocytic coat disassembly in Saccharomyces cerevisiae for optimal downstream trafficking. *Traffic*, 9(5), pp.848–59.

Tse, S.M.L., Furuya, W., Gold, E., Schreiber, A.D., Sandvig, K., Inman, R.D. & Grinstein, S., 2003. Differential role of actin, clathrin, and dynamin in Fc gamma receptor-mediated endocytosis and phagocytosis. *The Journal of biological chemistry*, 278(5), pp.3331–8.

Tsuboi, S., Takada, H., Hara, T., Mochizuki, N., Funyu, T., Saitoh, H., Terayama, Y., Yamaya, K., Ochs, H.D., et al. 2009. FBP17 Mediates a Common Molecular Step in the Formation of Podosomes and Phagocytic Cups in Macrophages. *The Journal of biological chemistry*, 284(13), pp.8548–56.

Tsujita, K., Takenawa, T. & Itoh, T., 2015. Feedback regulation between plasma membrane tension and membrane-bending proteins organizes cell polarity during leading edge formation. *Nature cell biology*, 17(6), pp.749-58.

Uezu, A., Horiuchi, A., Kanda, K., Kikuchi, N., Umeda, K., Tsujita, K., Suetsugu, S., Araki, N., Nakanishi, H., et al. 2007. SGIP1alpha is an endocytic protein that directly interacts with phospholipids and Eps15. *The Journal of biological chemistry*, 282(36), pp.26481–9.

Umeda, A., Meyerholz, A. & Ungewickell, E., 2000. Identification of the universal cofactor (auxilin 2) in clathrin coat dissociation. *European journal of cell biology*, 79(5), pp.336–42.

Ungewickell, E., Ungewickell, H., Holstein, S.E., Lindner, R., Prasad, K., Barouch, W., Martin, B., Greene, L.E. & Eisenberg, E., 1995. Role of auxilin in uncoating clathrin-coated vesicles. *Nature*, 378(6557), pp.632–5.

Urbanek, A.N., Smith, A.P., Allwood, E.G., Booth, W.I. & Ayscough, K.R., 2013. A novel actin-binding motif in Las17/WASP nucleates actin filaments independently of Arp2/3. *Current biology,* 23(3), pp.196–203.

Vaid, K.S., Guttman, J.A., Babyak, N., Deng, W., McNiven, M.A., Mochizuki, N., Finlay, B.B. & Vogl, A.W., 2007. The role of dynamin 3 in the testis. *Journal of cellular physiology*, 210(3), pp.644–54.

Vallis, Y., Wigge, P., Marks, B., Evans, P.R. & McMahon, H.T., 1999. Importance of the pleckstrin homology domain of dynamin in clathrin-mediated endocytosis. *Current biology*, 9(5), pp.257–60.

Vater, C.A., Raymond, C.K., Ekena, K., Howald-Stevenson, I. & Stevens, T.H., 1992. The VPS1 protein, a homolog of dynamin required for vacuolar protein sorting in Saccharomyces cerevisiae, is a GTPase with two functionally separable domains. *The Journal of cell biology*, 119(4), pp.773–86.

Veiga, E., Guttman, J.A., Bonazzi, M., Boucrot, E., Toledo-Arana, A., Lin, A.E., Enninga, J., Pizarro-Cerdá, J., Cossart, P., et al. 2007. Invasive and adherent bacterial pathogens co-Opt host clathrin for infection. *Cell host & microbe*, 2(5), pp.340–51.

Vetter, I.R. & Wittinghofer, A., 2001. The guanine nucleotide-binding switch in three dimensions. *Science*, 294(5545), pp.1299–304.

Wakita, Y., Kakimoto, T., Katoh, H. & Negishi, M., 2011. The F-BAR protein Rapostlin regulates dendritic spine formation in hippocampal neurons. *The Journal of biological chemistry*, 286(37), pp.32672–83.

Walani, N., Torres, J. & Agrawal, A., 2015. Endocytic proteins drive vesicle growth via instability in high membrane tension environment. *Proceedings of the National Academy of Sciences of the United States of America*, 112(12), pp.1423–32.

Wang, H., Robinson, R.C. & Burtnick, L.D., 2010a. The structure of native G-actin. *Cytoskeleton*, 67(7), pp.456–65.

Wang, L., Barylko, B., Byers, C., Ross, J.A., Jameson, D.M. & Albanesi, J.P., 2010b. Dynamin 2 mutants linked to centronuclear myopathies form abnormally stable polymers. *The Journal of biological chemistry*, 285(30), pp.22753–7.

Warnock, D.E., Baba, T. & Schmid, S.L., 1997. Ubiquitously expressed dynamin-II has a higher intrinsic GTPase activity and a greater propensity for self-assembly than neuronal dynamin-I. *Molecular biology of the cell*, 8(12), pp.2553–62.

Warnock, D.E., Hinshaw, J.E. & Schmid, S.L., 1996. Dynamin self-assembly stimulates its GTPase activity. *Journal of Biological Chemistry*, 271, pp.22310–22314.

Warnock, D.E. & Schmid, S.L., 1996. Dynamin GTPase, a force-generating molecular switch. *BioEssays : news and reviews in molecular, cellular and developmental biology*, 18(11), pp.885–93.

Warren, D.T., Andrews, P.D., Gourlay, C.W. & Ayscough, K.R., 2002. Sla1p couples the yeast endocytic machinery to proteins regulating actin dynamics. *Journal of cell science*, 115, pp.1703–15.

Watanabe, S., Rost, B.R., Camacho-Pérez, M., Davis, M.W., Söhl-Kielczynski, B., Rosenmund, C. & Jorgensen, E.M., 2013. Ultrafast endocytosis at mouse hippocampal synapses. *Nature*, 504, pp.242–7.

Weaver, A.M., Karginov, A. V, Kinley, A.W., Weed, S.A., Li, Y., Parsons, J.T. & Cooper, J.A., 2001. Cortactin promotes and stabilizes Arp2/3-induced actin filament network formation. *Current biology*, 11(5), pp.370–4.

Weber, K. & Osborn, M., 1969. The reliability of molecular weight determinations by dodecyl sulfate-polyacrylamide gel electrophoresis. *The Journal of biological chemistry*, 244(16), pp.4406–12.

Weinberg, J. & Drubin, D.G., 2012. Clathrin-mediated endocytosis in budding yeast. *Trends in cell biology*, 22(1), pp.1–13.

Weissmann, G., 2015. Ebola, dynamin, and the cordon sanitaire of Dr. Adrien Proust. *FASEB journal : official publication of the Federation of American Societies for Experimental Biology*, 29(1), pp.1–4.

Welch, M.D. & Way, M., 2013. Arp2/3-mediated actin-based motility: a tail of pathogen abuse. *Cell host & microbe*, 14(3), pp.242–55.

Wendland, B. & Emr, S.D., 1998. Pan1p, yeast eps15, functions as a multivalent adaptor that coordinates protein-protein interactions essential for endocytosis. *The Journal of cell biology*, 141(1), pp.71–84.

Wendland, B., McCaffery, J.M., Xiao, Q. & Emr, S.D., 1996. A novel fluorescence-activated cell sorter-based screen for yeast endocytosis mutants identifies a yeast homologue of mammalian eps15. *The Journal of cell biology*, 135(6), pp.1485–500.

Wendland, B., Steece, K.E. & Emr, S.D., 1999. Yeast epsins contain an essential N-terminal ENTH domain, bind clathrin and are required for endocytosis. *The EMBO journal*, 18(16), pp.4383–93.

Wesp, A., Hicke, L., Palecek, J., Lombardi, R., Aust, T., Munn, A.L. & Riezman, H., 1997. End4p/Sla2p interacts with actin-associated proteins for endocytosis in Saccharomyces cerevisiae. *Molecular biology of the cell*, 8(11), pp.2291–306.

Williams, M. & Kim, K., 2014. From membranes to organelles: Emerging roles for dynamin-like proteins in diverse cellular processes. *European Journal of Cell Biology*, 93(7), pp.267-77.

Wilsbach, K. & Payne, G.S., 1993. Vps1p, a member of the dynamin GTPase family, is necessary for Golgi membrane protein retention in Saccharomyces cerevisiae. *The EMBO journal*, 12(8), pp.3049–59.

Winder, S.J., Hemmings, L., Maciver, S.K., Bolton, S.J., Tinsley, J.M., Davies, K.E., Critchley, D.R. & Kendrick-Jones, J., 1995. Utrophin actin binding domain: analysis of actin binding and cellular targeting. *Journal of cell science*, 108, pp.63–71.

Winder, S.J., Jess, T. & Ayscough, K.R., 2003. SCP1 encodes an actin-bundling protein in yeast. *The Biochemical journal*, 375, pp.287–95.

Winter, D., Lechler, T. & Li, R., 1999. Activation of the yeast Arp2/3 complex by Bee1p, a WASP-family protein. *Current biology*, 9(9), pp.501–4.

Winter, D., Podtelejnikov, A. V., Mann, M. & Li, R., 1997. The complex containing actin-related proteins Arp2 and Arp3 is required for the motility and integrity of yeast actin patches. *Current Biology*, 7(7), pp.519–529.

Witke, W., Podtelejnikov, A. V, Di Nardo, A., Sutherland, J.D., Gurniak, C.B., Dotti, C. & Mann, M., 1998. In mouse brain profilin I and profilin II associate with regulators of the endocytic pathway and actin assembly. *The EMBO journal*, 17(4), pp.967–76.

Wong, W.T., Schumacher, C., Salcini, A.E., Romano, A., Castagnino, P., Pelicci, P.G. & Di Fiore, P.P., 1995. A protein-binding domain, EH, identified in the receptor tyrosine kinase substrate Eps15 and conserved in evolution. *Proceedings of the National Academy of Sciences of the United States of America*, 92(21), pp.9530–4.

Wu, H. & Parsons, J.T., 1993. Cortactin, an 80/85-kilodalton pp60src substrate, is a filamentous actin-binding protein enriched in the cell cortex. *The Journal of cell biology*, 120(6), pp.1417–26.

Wu, H., Reynolds, A.B., Kanner, S.B., Vines, R.R. & Parsons, J.T., 1991. Identification and characterization of a novel cytoskeleton-associated pp60src substrate. *Molecular and cellular biology*, 11(10), pp.5113–24.

Wu, Y., O'Toole, E.T., Girard, M., Ritter, B., Messa, M., Liu, X., McPherson, P.S., Ferguson, S.M. & De Camilli, P., 2014. A dynamin 1-, dynamin 3- and clathrin-independent pathway of synaptic vesicle recycling mediated by bulk endocytosis. *eLife*, 3, pp.01621.

Xing, Y., Böcking, T., Wolf, M., Grigorieff, N., Kirchhausen, T. & Harrison, S.C., 2010. Structure of clathrin coat with bound Hsc70 and auxilin: mechanism of Hsc70-facilitated disassembly. *The EMBO journal*, 29(3), pp.655–65.

Xue, F., Janzen, D.M. & Knecht, D.A., 2010. Contribution of Filopodia to Cell Migration: A Mechanical Link between Protrusion and Contraction. *International journal of cell biology*, 2010, p.507821.

Yamada, H., Abe, T., Li, S.-A., Masuoka, Y., Isoda, M., Watanabe, M., Nasu, Y., Kumon, H., Takei, K., et al. 2009. Dynasore, a dynamin inhibitor, suppresses lamellipodia formation and cancer cell invasion by destabilizing actin filaments. *Biochemical and biophysical research communications*, 390(4), pp.1142–8.

Yamada, H., Abe, T., Satoh, A., Okazaki, N., Tago, S., Kobayashi, K., Yoshida, Y., Oda, Y., Takei, K., et al. 2013. Stabilization of actin bundles by a dynamin 1/cortactin ring complex is necessary for growth cone filopodia. *The Journal of neuroscience*, 33(10), pp.4514–26.

Yang, H.-C. & Pon, L.A., 2002. Actin cable dynamics in budding yeast. *Proceedings of the National Academy of Sciences of the United States of America*, 99(2), pp.751–6.

Yarar, D., Waterman-Storer, C.M. & Schmid, S.L., 2005. A dynamic actin cytoskeleton functions at multiple stages of clathrin-mediated endocytosis. *Molecular biology of the cell*, 16(2), pp.964–75.

Yin, H., Pruyne, D., Huffaker, T.C. & Bretscher, A., 2000. Myosin V orientates the mitotic spindle in yeast. *Nature*, 406(6799), pp.1013–5.

Young, B.A., Buser, C. & Drubin, D.G., 2010. Isolation and partial purification of the Saccharomyces cerevisiae cytokinetic apparatus. *Cytoskeleton*, 67(1), pp.13–22.

Young, M.E., Cooper, J.A. & Bridgman, P.C., 2004. Yeast actin patches are networks of branched actin filaments. *The Journal of cell biology*, 166(5), pp.629–35.

Yu, X. & Cai, M., 2004. The yeast dynamin-related GTPase Vps1p functions in the organization of the actin cytoskeleton via interaction with Sla1p. *Journal of cell science*, 117, pp.3839–3853.

Zechel, K., 1980. Dissociation of the DNAse-I . actin complex by formamide. *European journal of biochemistry / FEBS*, 110, pp.337–341.

Zechel, K., 1981. Effects of formamide on the polymerization and depolymerization of muscle actin. *European journal of biochemistry / FEBS*, 119(1), pp.209–13.

Zheng, J., Cahill, S.M., Lemmon, M.A., Fushman, D., Schlessinger, J. & Cowburn, D., 1996. Identification of the binding site for acidic phospholipids on the pH domain of dynamin: implications for stimulation of GTPase activity. *Journal of molecular biology*, 255(1), pp.14–21.

Appendix 1.

A Dynamin-Actin Interaction Is Required for Vesicle Scission during Endocytosis in Yeast

Current Biology, 25(7), pp.868–78

Palmer, S.E., Smaczynska-de Rooij, I.I., Marklew, C.J., Allwood, E.G., Mishra, R., Johnson, S., Goldberg, M.W. & Ayscough, K.R., 2015a.

Appendix 2.

A Charge Swap mutation E461K in the yeast dynamin Vps1 reduces endocytic invagination

Communicative & Integrative Biology, 8(4), p.e1051274

Palmer, S.E., Smaczynska-de Rooij, I.I., Marklew, C.J., Allwood, E.G., Mishra, R., Goldberg, M.W. & Ayscough, K.R., 2015b.